ANDRÉ HERKENHOFF GOMES

SOME CONTRIBUTIONS TO THE STUDY OF A QUANTUM ELECTRODYNAMICS WITH LORENTZ SYMMETRY VIOLATION

Thesis presented before the *Universidade Federal de Viçosa* in partial fulfillment of the requirements of the *Programa de Pós-Graduação em Física* for the degree of *Doctor Scientiae.*
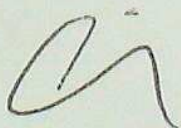
VIÇOSA
MINAS GERAIS - BRAZIL
2014

ANDRÉ HERKENHOFF GOMES

SOME CONTRIBUTIONS TO THE STUDY OF A QUANTUM ELECTRODYNAMICS
WITH LORENTZ SYMMETRY VIOLATION

Thesis presented at the Universidade Federal de Viçosa in partial fulfillment of the requirements of the Programa de Pós-Graduação em Física for the degree of *Doctor Scientiae.*
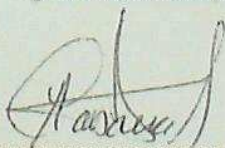
APPROVED: july 9th, 2014.
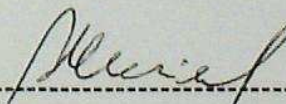
Olivier Piguet
(Co-adviser)
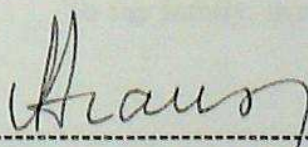
Oswaldo Monteiro Del Cima
(Co-adviser)

Rodolfo Alvan Casana Sifuentes

Arthur Kos Antunes Maciel

Daniel Heber Theodoro Franco
(Adviser)

To my family, my lovely girlfriend, and my friends.

"What we know is a drop, what we ignore is an ocean."

Acknowledgements

I wish to thank, first and foremost, my family — my father, José Pedro, my mother, Maria Augusta, and my sister, Karine — for their never-ending support on the paths I have chosen for my life. Without them I would have never come to this moment and hardly been as happy as I am to do what I do.

To my lovely girlfriend, Maria Inês, who I have met after this thesis was already written, but has given me since then — at such an important moment in my life — much more than I could have ever asked for. You are the most beautiful thing that has ever happened to me.

To my advisor, professor Daniel, for giving me support along the four years of my doctorate, and trusting my skills and choices.

To professor Alan Kostelecký, for advising me during my stay at the Indiana University Bloomington and for his wise advices. Additionally, I would also like to thank him for giving me the opportunity of a joint work as it has given invaluable contribution to my formation as a physicist.

To all my friends, for their support, but in special for those from the physics department — for the always pleasant daily company — and my longtime friends from the (now extinct) *Clube de Astronomia de Viçosa*. To the friends I met in Bloomington, for they were essential to my social health during my time outside Brazil. I am also specially grateful to Newton — who is truly like a brother to me — for his continuous support. I would be much less capable of anything without those people.

To the professors who have helped building my formation as a physicist and all staff from the *Departamento de Física* of the *Universidade Federal de Viçosa* for making this a pleasant workplace.

Contents

List of Figures

List of Tables

Resumo

GOMES, André Herkenhoff, D.Sc., Universidade Federal de Viçosa, Julho de 2014. **Algumas contribuições ao estudo de uma eletrodinâmica quântica com violação da simetria de Lorentz.** Orientador: Daniel Heber Theodoro Franco. Co-orientadores: Olivier Piguet e Oswaldo Monteiro Del Cima.

Nesta tese, estudamos diferentes aspectos de uma eletrodinâmica quântica (EDQ) para um único férmion com violação da simetria de Lorentz baseada no arcabouço teórico do Modelo Padrão Estendido, onde a quebra da simetria de Lorentz é controlada por coeficientes com índices de Lorentz — campos de fundo que selecionam direções preferenciais no espaçotempo — acoplados a campos convencionais. Desenvolvemos dois estudos separados, o primeiro motivado pelos aspectos teóricos do modelo e o outro pela busca experimental de sinais da violação da simetria de Lorentz.

A renormalizabilidade da extensão mínima da EDQ com quebra da simetria de Lorentz — no sentido de ser renormalizável por contagem de potências — é primeiramente investigada. Empregamos o método algébrico de renormalização para enfatizar a procura por anomalias de calibre. Observamos que a quebra da simetria de Lorentz introduz novas possíveis estruturas anômalas além das convencionais. Na prática, identidades de calibre convencionais são estendidas para incluir efeitos da perda da invariância de Lorentz e não são mais automaticamente satisfeitas pois recebem correções que violam a simetria de Lorentz, sendo cada uma dessas correções controladas pelos chamados coeficientes de anomalia, que devem ser explicitamente calculados para uma resposta definitiva sobre esses candidatos a anomalia serem características reais do modelo ou não. Em primeira ordem na expansão em loops, verificamos que o modelo é livre de anomalias e fornecemos argumentos sugerindo que ao menos alguns desses

coeficientes devem ser nulos a todas as ordens, mas ainda há a questão sobre os coeficientes restantes desenvolverem valores não-nulos ou não devido a correções de vários loops. Por outro lado, encontramos modelos mais restritos, onde a simetria C ou PT é exigida, que são completamente livres de anomalias de calibre a todas as ordens em teoria de perturbação.

Uma vez que nenhuma anomalia é encontrada — o que vimos ser garantido ao menos para os casos invariantes sob C ou PT — a prova da renormalizabilidade do modelo a todas as ordens é concluída se os parâmetros livres introduzidos pela renormalização puderem ser fixados por condições de renormalização adequadas. Análise explícita deste último ponto exige a determinação das correções radiativas finitas dos diagramas divergentes e nós apresentamos resultados preliminares baseados na análise a um loop da autoenergia do férmion. Contra as nossas expectativas, contribuções de alguns coeficientes que violam a simetria de Lorentz parecem falhar em ser renormalizadas adequadamente uma vez que os parâmetros livres que estas introduzem aparentemente não podem ser consistentemente fixados pelas condições de renormalização. Por outro lado, encontramos coeficientes, cujas contribuições são adequadamente renormalizadas, que geram novos fenômenos físicos onde, em específico, suas correções radiativas modificam a propagação livre de férmions — um efeito ausente na EDQ convencional — e discutimos as consequências para medições experimentais conforme observamos existir a possibilidade de efeitos radiativos serem tão relevantes quanto efeitos em nível de árvore dados ajustes experimentais adequados.

Passando de uma análise motivada por questões teóricas da extensão mínima da EDQ para uma investigação orientada por questões experimentais, estendemos nosso modelo para incluir contribuições não-mínimas — motivadas pelo *status* de teoria efetiva do Modelo Padrão Estendido — e o aplicamos no contexto de experimentos medindo $g - 2$ de muons. Após uma breve revisão destes experimentos que proveem medidas de alta precisão do momento magnético anômalo do muon, usamos um ferramental adequado à descrição de férmions com operadores de dimensões arbitrárias que violam a simetria de Lorentz para discutir sinais da quebra de simetria a serem procurados experimentalmente — especificamente, comparações entre a frequência anômala de

muons e antimuons, assim como variações siderais e anuais desta quantidade. Usando dados disponíveis na literatura, apresentamos limites inéditos em coeficientes de quebra de simetria e também estimamos a sensibilidade aos efeitos da violação da simetria de Lorentz de futuros experimentos.

Abstract

GOMES, André Herkenhoff, D.Sc., Universidade Federal de Viçosa, July, 2014. **Some contributions to the study of a quantum electrodynamics with Lorentz symmetry violation.** Adviser: Daniel Heber Theodoro Franco. Co-advisers: Olivier Piguet and Oswaldo Monteiro Del Cima.

In this thesis, we study different aspects of a single-fermion Lorentz-violating quantum electrodynamics (QED) based on the framework of the Standard Model Extension, where Lorentz symmetry breaking is controlled by coefficients with Lorentz indices — constant background fields selecting preferred directions in spacetime — coupled to conventional fields. We develop two separate studies, the first motivated by theoretical aspects of the model and the other by the experimental search of Lorentz-violating signals.

Renormalizability of the minimal Lorentz-violating QED extension — in the sense the model is power-counting renormalizable — is first investigated. We employ the algebraic approach of renormalization to emphasize the search for gauge quantum anomalies. The breaking of Lorentz symmetry is found to introduce new possible anomalous structures besides the conventional ones. In practice, conventional gauge identities are extended to include effects of Lorentz violation and are no longer automatically satisfied as they receive Lorentz-violating corrections, each of them controlled by so-called anomaly coefficients which have to be explicitly calculated for a definite answer as to whether these candidate anomalies are real features of the model or not. To one-loop order, we verify the model is free of anomalies and we provide arguments suggesting at least some of the anomaly coefficients may vanish to all orders, but there is still the question as to whether or not the remaining coefficients can develop nonva-

nishing value under multiloop radiative corrections. On the other hand, we find more restricted models, where C or PT symmetry is enforced, are completely free of gauge anomalies to all orders in perturbation theory.

Once no anomaly is found — which we verified it is the case at least for the C or PT invariant models — proof of renormalizability to all orders is concluded if free parameters introduced by renormalization can be fixed by suitable renormalization conditions. Explicit analysis of this last point demands determination of finite radiative corrections from divergent diagrams and we present preliminary results based on analysis of the one-loop fermion self-energy. Against our expectations, contribution from specific Lorentz-violating coefficients appear to fail to be properly renormalized once their introduced free parameters apparently cannot be consistently fixed by renormalization conditions. On the other hand, we find coefficients, whose contributions are adequately renormalized, that can lead to new physical phenomena, namely, their radiative corrections modify the free propagation of fermions — an effect absent in conventional QED — and implications for experimental measurements are discussed as we find there is the possibility of radiative effects may be as relevant as tree-level ones under adequate experimental set up.

Departing from a theory-motivated analysis of the minimal Lorentz-violating QED and moving on to an experiment-oriented investigation, we then extend our framework to include nonminimal contributions — motivated by the status of the SME as an effective field theory — and apply it in the context of muon $(g-2)$ experiments. After a brief overview of such experiments providing high precision measurements of the muon anomalous magnetic moment, we use a framework suitable for fermions with Lorentz-violating operators of arbitrary dimension to discuss Lorentz-violating signatures to be experimentally searched for — namely, comparisons between muon and antimuons anomaly frequency, as well as sidereal and annual variations of this quantity. Using data available in the literature, we present new bounds on coefficients controlling the symmetry breaking and also estimate the sensitivity of upcoming experiments to Lorentz violation.

Introduction

One of the deepest currently open problems of particle physics deals with the nature of spacetime itself and how fundamental particles feel it at extremely high energies — possibly of the Planck scale $E_P \sim 10^{19}\,\mathrm{GeV}$ — where gravitational interaction is expected to play a fundamental role even for quantum phenomena.

In our comparatively low energy world, considering currently attainable energies, at the microscopic scale where a quantum-based description of Nature is required, the Standard Model (SM) has achieved unprecedented success in describing the way fundamental particles behave and interact. At the macroscopic scale, the classical framework of General Relativity (GR) describes in a beautiful way how spacetime and massive bodies influence each other. Both theories are paramount in describing what they were initially conceived for. Nevertheless, as we understand it, Nature has one continuum, seamless line connecting *principles* governing microscopic and macroscopic universes. Our description of Nature is then expected to reflect this behavior. However, our two best approaches, the principles underlying the SM and GR, seem to be incompatible with each other. A long sought and yet unknown consistent quantum description of gravity — or maybe a unified model describing all physical interactions — insists in frustrating our expectations. Several attempts have been devised — string theory and loop quantum gravity, to name two current popular approaches — but none of them are fully developed or well-understood to the point of making unique, definite testable predictions.

Although a "top to bottom" approach to the search for fundamental models pushes our creativity to the extreme — usually leading to highly interesting new ideas and to the development of formidable new mathematical tools — we are in a period in

Introduction

the history of physics where experimental access to natural energy scales where those models play dominant roles is not expected for any near future. Nevertheless, we may expect that any new physics beyond Standard Model originating in higher energy scales would leave *accessible clues* in our current low energy Universe. Discovery of such clues would inevitably lead to drastic paradigm changes in our understanding of Nature.

Standard Model and General Relativity physics work extremely well, nevertheless so far their principles seem to be incompatible with each other. Changing focus from a top-down search for fundamental models to a bottom-up approach may be rewarding. As our expectations dictate something new — possibly radically different from our conventional principles — may reveal itself as we approach the Planck scale, the match of a so far unknown fundamental physics to our conventional low energy description of Nature may suggest some pillars of modern physics could be only approximately valid in the low energy limit. Lorentz and CPT symmetries, for instance, are so fundamental to our conventional description of Nature that they have to be tested. If any deviation from exact invariance were ever found, our whole conception of fundamental physics would drastically change. Testing the very basic building blocks, in the search for any minuscule deviation, can teach us a lot about paths to follow for more fundamental descriptions of Nature.

It turns out, an "anti-CPT" theorem [1] states, under mild hypotheses, that violation of CPT symmetry has to be accompanied by Lorentz symmetry violation — although the converse is not true. Therefore, tests of Lorentz invariance may also test CPT symmetry. So far, no experiment has ever found any deviation from exact Lorentz symmetry. Violations of Lorentz invariance, if realized in Nature at (currently) attainable energy scales, are expected to be suppressed by the ratio of the characteristic energy of the experiment and the Planck energy, therefore they should be dimmingly small. For instance, at the electroweak scale $E_{\mathrm{EW}} \approx 246\,\mathrm{GeV}$, signals of Lorentz noninvariance may become weaker by a factor of 10^{17}. The fact that current high precision experiments can achieve such sensitivity (or even better ones [2]) opens up an amazing perspective for probing Lorentz and CPT violation away from the Planck scale.

Introduction

A natural question arises as how to investigate consequences of the hypothesis that Lorentz symmetry is not exact in Nature but rather may be broken by tiny contributions outside conventional SM and GR physics? Without the aid of any known viable underlying theory, a reasonable approach is to build a framework as general as possible and possibly independent of details of an underlying model. A fundamental feature must be the inclusion of all known Lorentz invariant physics. As the "bottom to top" idea suggests, availability of connection to present or near-future experimental techniques where the hypothesis of Lorentz violation can be tested is another cornerstone of this approach.

A powerful framework for systematic investigations of Lorentz symmetry violation is the Standard Model Extension (SME). In flat spacetime, this framework is based on the quantum field theory formalism for point particles in four dimensions and is devised as the most general Lorentz-violating extension of the Standard Model [3,4]. Inclusion of gravitational phenomena further extends this framework by a Lorentz-violating generalization of General Relativity in Riemann-Cartan geometries [5]. Formulated in the Lagrangian formalism, the SME comprises all possible coordinate scalars involving Standard Model fields, gravitation, and Lorentz-violating background fields — coefficients with Lorentz indices, selecting preferred spacetime directions — controlling the extent to which Lorentz symmetry is broken. Among other possibilities, these background fields could emerge after spontaneous breaking of Lorentz symmetry as vacuum expectation values of tensorial degrees of freedom in string models [6,7], for instance. Although the SME framework is independent of the underlying fundamental physics, the existence of different mechanisms leading to Lorentz symmetry violation further motivates its study.

The SME's comprehensive framework allows for construction of realistic submodels such that theoretical issues — such as causality, stability, and renormalizability, for example — can be fully investigated, and precise Lorentz-violating signals can be predicted in a formalism suitable for experimental search. As the SME encompasses all conventional physics, its framework can be used to reanalyse data of a variety of already performed high precision experiments while focusing on what it tells about

Introduction

Lorentz violation, therefore placing bounds on SME coefficients — for instance, comparison between masses of meson particle and antiparticle [8] — and, naturally, to the analysis of experiments specifically devised to test Lorentz invariance — resonant cavities aboard the International Space Station [9] is an example. A great advantage of the SME framework is that it reveals several accessible ways of testing Lorentz invariance [10]. As a considerable amount of Lorentz violating coefficients remain unbounded, there exists the possibility of Lorentz symmetry violation may be lurking at plain sight, but invisible to our eyes as long as particular experiments have not been performed yet.

The main scope of this thesis is twofold. First, we investigate the theoretical consistency of Lorentz symmetry violation under quantum corrections, namely, we study the renormalizability of a single-fermion (minimal) QED limit of the SME. Although the SME can be regarded as an effective field theory, the importance of this study lies in the fact that it could nevertheless indicate when the effective theory approach breaks down — whether due to a loss of renormalizability at some loop order or because of quantum anomalies. Our second aim concerns the application of this framework to the experimental search of Lorentz violation. We employ the (nonminimal) QED limit of the SME for muons in the context of $(g-2)$ experiments. Measurement of the muon $g-2$ is accomplished to enormous precision, and the natural high sensitivity of the muon $g-2$ to effects from high energy scales makes this type of experiment a valuable venue for testing Lorentz symmetry. Although, our two main goals seem to be unrelated at first, an intermediate link between them is pursued — and here is presented as preliminary results. Investigation of radiative corrections to the fermion self-energy reveals that Lorentz-violating corrections alter the physics of fermion free propagation — an effect not present in the conventional QED — and implications of this result may be experimentally searched, for instance, in muon $g-2$ physics.

This thesis is divided as follows. In Chapter 1, we give a brief introduction to the ideas behind the Standard Model Extension and Lorentz symmetry violation, introducing some of its general features, implementation of Lorentz violation, model construction and typical experimental signals. Chapter 2 will be based on Refs. [11,12]

where we investigated the renormalizability of the minimal Lorentz-violating QED extension coming from the SME framework, with main focus on the issue of gauge anomalies. In Chapter 3, as a natural continuation of the previous chapter, we start an investigation of one-loop finite radiative corrections to this extended QED — in particular, those coming from the fermion self-energy. The chapter is based on preliminary results, and provides a link between the theoretical aspects investigated in Chapter 2 and the experimental search for Lorentz violation in the last chapter. Accordingly, the last chapter is based in Ref. [13], where we investigated the nonminimal QED sector of the SME for muons in the context of $(g-2)$ experiments. An overall summary of the works composing this thesis is presented at the Conclusion, along with perspectives for future works. Additionally, Appendix A is devoted to the transformations between Earth-based laboratory frames and nonrotating Sun-centered frames, which were fundamental for deriving the results of Chapter 4.

Chapter 1

A very brief overview of the SME

Aiming at a better understanding of the Standard Model Extension (SME) and Lorentz symmetry violation itself, in this chapter we give a very brief overview of this topic. To the reader, we suggest Refs. [14,15] for an excellent introduction on the subject. In what follows, we first discuss what we ean by "Lorentz noninvariance" of a model, and how this can be implemented. Afterwards, we mention possible mechanisms for breaking Lorentz symmetry, with emphasis on spontaneous symmetry breaking, and the following sections deal with construction of the SME. We close this chapter by presenting some experimental tests of Lorentz noninvariance in different SME sectors.

1.1   Lorentz Violation and the SME

As briefly mentioned in the Introduction, a framework suitable for systematic investigations of Lorentz and CPT symmetry violation called the *Standard Model Extension* has been devised by Colladay and Kostelecký in 1997 and 1998 [3,4] as a Lorentz-violating extension of the Standard Model (SM), and further extended in 2004 to include General Relativity [5]. It is constructed, by definition, as the most general Lorentz-violating effective model based on the framework of quantum field theory for point particles in four dimensions. It was initially motivated by former results on string-based models featuring the possibility of spontaneous breaking of Lorentz and CPT symmetry [6,7] and further motivated by the high precision to what CPT symmetry could be tested at that time [8]. Spontaneous breaking of Lorentz symmetry

leads to a nontrivial vacuum permeated by background tensorial-like fields which select preferred directions and positions in spacetime, breaking its isotropy and homogeneity. Nevertheless, Lorentz and CPT symmetries are observed as exact in Nature to a great degree of precision in a number of experiments, therefore deviations from these symmetries, if any, should be dimmingly small, requiring high precision tests to be observed. Such high precision requirement is naturally desirable as it may lead to sensitivity to Planck-suppressed phenomena — indeed, muon experiments, for instance, do achieve such sensitivities [2] — representing a formidable venue for the search of new physics. To date, no Lorentz violation has been observed in Nature [10], but the question whether it really occurs in accessible energy scales or not can only be answered by means of experimental search, and thus even from a theoretical point of view, we need realistic models to predict where and how to look for it, and the SME provides an adequate framework for that.

1.2   What is meant by Lorentz symmetry violation?

In the SME framework — in flat spacetime, for simplicity — Lorentz symmetry is broken in the sense that *coordinate scalars* in its action are not invariant under *particle* Lorentz transformation. Coordinate transformations, also called *observer* Lorentz transformations, implement changes among *coordinate systems* describing the same physical situation and, in this sense, they carry no physical meaning, as illustrated in Fig. 1.1. On the other hand *particle* Lorentz transformations have physical meaning as they probe the way *particles* and *fields* behave along different directions and positions in spacetime, as in Fig. 1.2. If spacetime is isotropic and homogeneous, both transformations are symmetries of the model, and the two are (inversely) related. If Lorentz symmetry[1] is broken, this relation is lost as a consequence, and particle transformations are expected to reveal the inequivalence of physical phenomena in different directions or positions in spacetime, independently of the coordinate system used.

---

[1]When the context allows no confusion, we may omit the word "particle" when referring to *particle* Lorentz transformations or symmetry. On the other hand, *observer* Lorentz transformations will be mostly referred as *coordinate* transformations.

1. A very brief overview of the SME
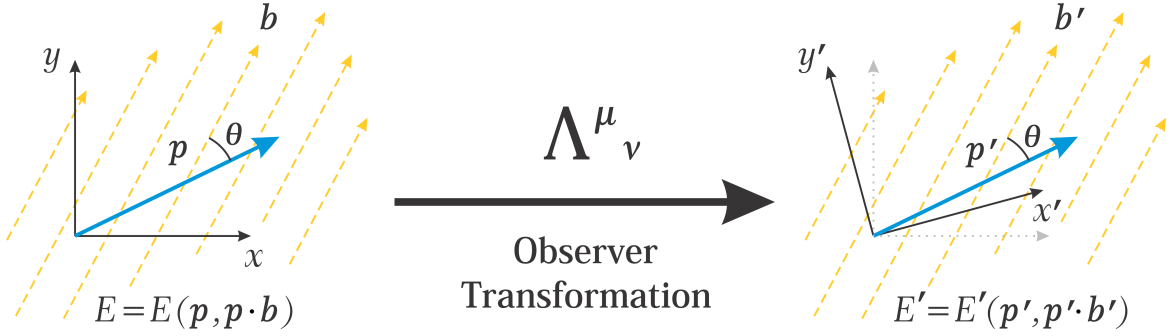
Figure 1.1: Coordinate (or observer) transformations. There is no change in the physics observed as the coupling angle θ between the particle momentum $\boldsymbol{p}$ and the background field $\boldsymbol{b}$ remains the same after the transformation.
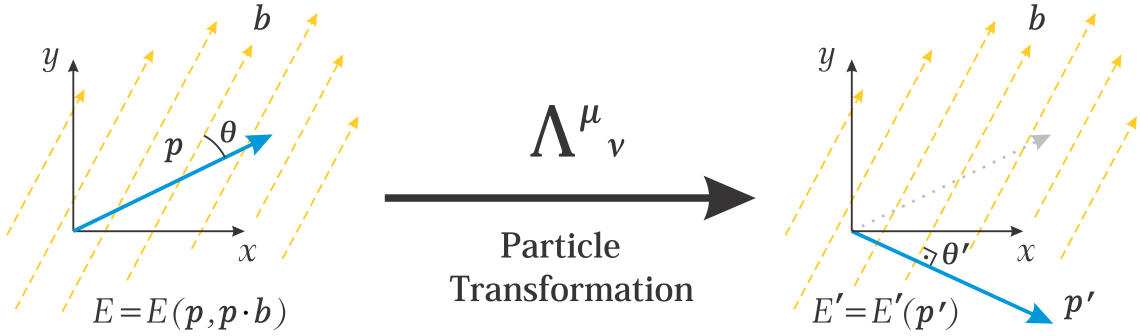
Figure 1.2: Particle transformations. Different spacetime directions are probed as the coupling angle θ between the particle momentum $\boldsymbol{p}$ and the background field $\boldsymbol{b}$ changes after the transformation.

Construction of coordinate scalars are based on how we connect different reference frames. As coordinate systems *per se* have no physical significance, invariance under changes among those are fundamental. Adopting a structure to spacetime, *i.e.*, specifying the way we measure spacetime intervals between different events, allows construction of transformation operations to connect different frames. Describing physical quantities as geometrical structures — like tensors and spinors — and looking at how they behave under such transformations tell us how to construct quantities that do not feel those transformations — invariants, scalars under such transformations.

The SME is based on a Lorentzian spacetime structure, global for Minkowski spacetime [3,4] and local for the Riemann-Cartan geometrical framework used to consider violations of local Lorentz symmetry in the context of gravity [5]. Nevertheless,

although the spacetime structure is conventional, the SME vacuum is nontrivial in the sense that locally it has preferred spacetime directions as it is permeated by Lorentz-violating background fields. Therefore, coordinate and particle transformations are both implemented by means of conventional Lorentz boosts and spatial rotations — locally implemented for the case of curved spacetimes — but particle Lorentz symmetry is no longer a feature of our description.

Formulated on the basis of quantum field theory for point particles in four dimensions, the SME action contains all conventional Lorentz invariant physics, and is additionally constructed by coordinate scalars that are not invariant under Lorentz transformations. Background fields are described by particle Lorentz scalars represented by coefficients with Lorentz indices, which we call Lorentz-violating coefficients, SME coefficients, or just "coefficients" when the context allows no confusion. To illustrate this point, consider a *coordinate* transformation acting on the 4-momentum p_μ as $p'_\mu = \Lambda_\mu{}^\nu p_\nu$ and a *particle* transformation acting as $p''_\mu = \Lambda_\mu{}^\nu p_\nu$. Considering a Lorentz-violating coefficient $b^\mu = (b_0; \boldsymbol{b})$, it transforms as a coordinate vector, $b'^\mu = \Lambda^\mu{}_\nu b^\nu$, but it behaves as set of 4 scalars under particle transformations, $b''^\mu = b^\mu$. In this sense, the contraction $p \cdot b \equiv p_\mu b^\mu$ is a coordinate scalar, $p' \cdot b' = p \cdot b$, but it is not invariant under particle transformations, $p'' \cdot b = p \cdot b$, thus violating Lorentz symmetry.

1.3   A mechanism for Lorentz symmetry violation

As will be made clear soon, construction of the SME is independent of fundamental models originating Lorentz symmetry violations. Nevertheless, existence of such models is an extra factor to motivate investigation of this possibility and further testify on its plausibility. Known approaches allowing for breaking of Lorentz symmetry include strings, spacetime-foam models, nontrivial spacetime topology, loop quantum gravity, noncommutative field theory, cosmologically varying scalars, among others — see Ref. [16] for a brief overview of such possibilities. In particular, a surprising result adds extra interest in models allowing for spontaneous breaking of Lorentz symmetry. In Ref. [5], it was shown that *explicit* Lorentz symmetry breaking — when SME coef-

1. A very brief overview of the SME

ficients are externally prescribed — is not compatible with either Riemann geometry or General Relativity nor its extension to Riemann-Cartan geometry, but *spontaneous* breaking of Lorentz symmetry is. This result further opens up two questions: (i) what other geometries can be made compatible with explicit Lorentz violation? Pseudo-Riemann-Finsler geometries in the context of Lorentz violation [17,18] is a newborn research field and looks promising as it was discovered that fermions experiencing explicit Lorentz violation follow geodesics in this geometry instead of pseudo-Riemann ones; and (ii) in the case of spontaneous breaking, what is the fate of Nambu-Goldstone bosons? Interesting results [19–22] show gravitons and photons can be interpreted as Nambu-Goldstone bosons originating from spontaneous breaking of Lorentz invariance.

Due to the popularity and desirable features of spontaneous symmetry breaking — and the mentioned result suggesting it is the sole mechanism for Lorentz violation compatible with General Relativity — it is worth a brief explanation in the context of Lorentz violation (restricted to flat spacetime, for simplicity).

The central idea is that the vacuum in Lorentz-violating models is no longer trivial, i.e, it is permeated by nonvanishing vacuum expectation values (VEV) of tensorial fields, as this is the energetically most favorable field configuration instead of a symmetric state with vanishing field VEV. The underlying Hamiltonian is still Lorentz invariant — Nambu-Goldstone bosons are generated so as to restore the spontaneously broken symmetry — but the vacuum is no longer.

Differently from the spontaneous breaking of gauge symmetry in the electroweak model, where the VEV of a scalar field (the Higgs) permeates the vacuum, in Lorentz-violating models new degrees of freedom with tensorial structure coming from underlying fundamental theories — strings, for instance, see [6,7] — acquire nonvanishing VEV. For instance, a potential V of the form

$$V(T^\mu) = (T^\mu T_\mu - t^\mu t_\mu)^2$$

has zero as its lowest energy, but this vacuum configuration is characterized by a non-vanishing VEV of the field T^μ, namely $T^\mu_{\text{vacuum}} = \langle T^\mu \rangle = t^\mu$, where t^μ is a tensor-like constant — in the case, vector-like, but tensors with higher rank can also be considered.

The vector-like VEV acts as background field giving the vacuum preferred spacetime directions, ultimately breaking its isotropy. Coupling between the background and dynamical conventional Standard Model fields introduces Lorentz-violating behavior. Clearly, coordinate invariance, in the sense of symmetry under observer Lorentz transformations, is kept intact, but particle Lorentz invariance is no longer respected.

Spontaneous Lorentz symmetry breaking generates SME coefficients dynamically, thereby ensuring compatibility with the underlying spacetime structure. This is to be contrasted with explicit Lorentz violation, where SME coefficients are externally prescribed and it turns out, in the context of curved spacetimes, equations of motion are incompatible with Bianchi identities of General Relativity or its extension to Riemann-Cartan geometry.

1.4   Construction of the SME

Constructed as a Lorentz-violating extension of our current description of Nature based on conventional physics, the SME Lagrangian can be written as

$$\mathcal{L}_{\text{SME}} = \mathcal{L}_{\text{SM}} + \mathcal{L}_{\text{EH}} + \delta\mathcal{L}_{\text{LV}}, \tag{1.1}$$

where $\mathcal{L}_{\text{SM}}$ represents the Standard Model Lagrangian — describing conventional electromagnetic, weak and strong interactions — $\mathcal{L}_{\text{EH}}$ is the Einstein-Hilbert Lagrangian responsible for gravitational phenomena, and $\delta\mathcal{L}_{\text{LV}}$ introduces couplings between conventional fields and Lorentz-violating background fields. Since Lorentz symmetry is so far measured as an exact symmetry, Lorentz-violating corrections $\delta\mathcal{L}_{\text{LV}}$ are expected to be small in any frame moving nonrelativistically with respect to Earth — the so called *concordant frames*. Naturally, in the limit where all Lorentz-violating coefficients vanish, conventional Lorentz-symmetric physics is recovered.

Let us consider Lorentz-violating corrections comprised by the SME in flat spacetime, which we denote simply by $\delta\mathcal{L}_{\text{LV}}$ — discussion of the gravity sector [5] is more involved and is beyond our scope. By definition, the SME contains *all possible* hermitian Lorentz-violating structures constructed from contractions of known parti-

1. A very brief overview of the SME

cle fields — electromagnetic A^μ, fermionic ψ, gravitational $h^{\mu\nu}$, etc. — and Lorentz-violating coefficients such that coordinate scalars are formed. As an example, consider the field operators

$$\overline{\psi}(i\gamma_\mu\partial_\nu)\psi, \quad F^{\mu\nu}F^{\rho\sigma}, \quad \overline{\psi}(\partial_\mu\partial_\nu)\psi. \tag{1.2}$$

The first one, if contracted with the metric tensor $\eta^{\mu\nu}$ leads to a conventional kinetic term $\overline{\psi}(i\slashed{\partial})\psi$ of a massless fermion, but if contracted with a coefficient $c^{\mu\nu}$ it breaks Lorentz invariance. Similarly, the second term can be contracted with a four-indices coefficient $(k_F)_{\mu\nu\rho\sigma}$ to break Lorentz symmetry in the gauge sector. Both of them are operators of mass dimension four and lead to superficially renormalizable interactions. Nevertheless, the third operator, if contracted with a coefficient $m^{\mu\nu}$, introduces a nonrenormalizable coupling, a nonrenormalizable version of a fermion mass term. In this way, Lorentz-breaking extensions for the whole Standard Model can be constructed, containing both renormalizable and nonrenormalizable field operators. The full SME, by definition, contains all possible field operators constructed in similar fashion. Characterization of operators of arbitrary dimension have been done for the neutrino sector [23], electrodynamics [24], and free massive fermions [25].

The above approach allows construction of all possible coordinate scalar terms breaking Lorentz symmetry, but one could ask about construction of CPT violating terms. It turns out a rigorous result by Greenberg [1], often called the "anti-CPT theorem", demonstrates that any local, unitary, relativistic point particle field theory violating CPT also violates Lorentz symmetry. On the other hand, is important to emphasize the converse is not true, *i.e.*, Lorentz noninvariance does *not* imply CPT noninvariance. Therefore, only a subset of all Lorentz-violating terms in the SME also violates CPT symmetry.

SME coefficients are naturally divided into CPT even and CPT odd ones, in the sense of the behavior of their associated field operator under CPT[2]. For example, consider the Lorentz-breaking terms $b^\mu\overline{\psi}\gamma_5\gamma_\mu\psi$ and $H_{\mu\nu}\overline{\psi}\sigma^{\mu\nu}\psi$. In the first term, b^μ

---

[2]Typically, the number of Lorentz indices of a coefficient indicates the behavior of its associated field operator under CPT. Coefficients with even number of indices are associated with CPT even operators and coefficients with odd number of indices with CPT odd operators.

does not feel any of the transformations C, P, or T as it is an inaccessible background field, and the field operator $\overline{\psi}\gamma_5\gamma_\mu\psi$ is C even and PT odd, therefore CPT odd, thus mnemonically we say b^μ is a CPT odd coefficient. For the second term, $H_{\mu\nu}$ also does not feel any discrete transformation and $\overline{\psi}\sigma^{\mu\nu}\psi$ is a CPT even field operator, therefore we call $H_{\mu\nu}$ a CPT even coefficient. Behavior under discrete transformations gives a first information on whether or not a particular experiment is sensitive to effects of specific coefficients — for instance, experiments involving parity are insensitive to P even coefficients. Other information — behavior under rotations and boosts, for example — can be used to further improve knowledge on the sensitivity to different SME coefficients.

1.5   The SME as a framework

The SME is a *framework* for investigation of Lorentz symmetry violations. The approach for its construction reveals it is independent of fundamental models leading to Lorentz violation. In this sense, some fundamental models with mechanisms for breaking Lorentz invariance may be expected to constitute subsets of the SME in adequate limits — see, for example, models with noncommutative fields [26] and spacetime-varying couplings [27–29]. In a similar fashion, subsets of the SME may contain other Lorentz-violating theories — as studied in Ref. [24], for instance, for proposals of isotropic violations in the electromagnetic sector, or in Ref. [25], for the connection of the Robertson-Mansouri-Sexl formalism to the SME.

Subsets of the SME are often viewed as or used for construction of effective field theories and frequently further conditions are imposed on its structures to produce models with often desired features. For instance, the minimal Standard Model Extension (mSME) demands the Standard Model $SU(3) \times SU(2) \times U(1)$ gauge structure, translation invariance — effectively enforcing the SME coefficients are spacetime constants — and power-counting renormalizability — restricting the model to field operators of mass dimension less than or equal to four. Eventually, conventional quantization, microcausality and stability, etc., may be imposed, further constraining the

set of Lorentz-violating coefficients under consideration.

Theoretically, several aspects of the SME have been investigated. To cite a few, we mention stability and causality of the minimal QED fermionic sector was studied in [30], and for the electromagnetic sector in [31–34], and in [35] for $SO(3)$ Yang-Mills. Analysis of SME fermion dispersion relation have been done in [36,37], and for massive photons in [38]. The Källén-Lehmann representation has been investigated for particular Lorentz-violating models in [39]. One-loop renormalizability of the minimal QED was verified in flat spacetimes in [40] and in curved spacetimes in [41], and in [42] asymptotic states were also analysed for models with particular Lorentz-violating coefficients. One-loop renormalizability in flat spacetime was also performed for pure Yang-Mills and QCD [43], and the whole one-loop renormalization process for Lorentz-violating Yukawa field theories was accomplished in [44]. Renormalizability to all orders of the minimal QED and the determination of one-loop finite radiative corrections will be the topic of Chapters 2 and 3 of this thesis.

1.6   Experimental searches for Lorentz violation

An advantage of the SME is the possibility of constructing realistic models for Lorentz violation, in the sense that they can predict unique signals that can be looked for in very specific experiments. Currently, Lorentz symmetry has shown itself standing strong on solid grounds, and this observational fact allows for bounds on Lorentz-breaking coefficients of the SME. Often high precision experiments are used in the search for Lorentz violation, and for that reason stringent upper limits are placed on SME coefficients. A comprehensive list of current bounds can be found in Ref. [10], which contains references to all experiments associated to each bound. For a review on tests of Lorentz invariance in the SME framework and in other formalisms, see Ref. [45]. For the status of current searches for Lorentz violation, the reader is directed to Ref. [46]. Below we give a very brief overview of some bounds listed in Ref. [10].

Some sectors of the SME have been better bounded than others. For instance, the photon sector has been intensively investigated for a number of years now. Its mini-

1. A very brief overview of the SME

mal sector contains two Lorentz-violating contributions coming from coefficients $(k_{AF})_\mu$ and $(k_F)_{\mu\nu\rho\sigma}$. Experimental signals of the first include vacuum birefringence creating a change of the polarization plane of light as it travels in space — the two polarization modes are now distinct as Lorentz symmetry is broken. Observation of light coming from astrophysical sources — extremely far quasars, for instance — enforces strong bounds on $(k_{AF})_\mu$ of order 10^{-43} GeV as no Lorentz violation was found. The second coefficient results in a greater number of experimental signals and its components can be accessed by astrophysical observation, light resonators, collider experiments, among others, with bounds ranging from 10^{-9} to 10^{-38}. The nonminimal photon sector predicts signals analogous to the ones from the minimal sector, and also has a wide range of bounds, explicitly written in [10] for coefficients associated to operators with dimension up to nine.

The minimal electron sector has also been widely investigated. Typical tests are related to atomic spectroscopy as Lorentz symmetry violation may introduce shifts in energy levels or remove degeneracies analogously to the Zeeman effect due to an external magnetic field. Primarily devised as CPT tests, Lorentz-violating coefficients are also accessed in comparisons between particles and antiparticles, therefore spectroscopy of different atoms is also a venue for testing the electron sector. Synchrotron and inverse Compton radiation from ultrarelativistic electrons in astrophysical sources also provide access to Lorentz-violating coefficients as their presence may enforce existence of maximum attainable energies for subluminal electrons. Maybe unexpected at first sight, experiments with macroscopic samples of spin-polarized matter based on electrons — for instance, set up as a torsion pendulum experiment — actually offer the best constraints on coefficients with dimension of mass, with bounds from 10^{-28} GeV to 10^{-31} GeV. The same coefficients for the positron have much weaker bounds, of order 10^{-22} GeV, coming from Penning traps. Dimensionless coefficients, on the other hand, have competitive bounds typically of order 10^{-15} coming from astrophysical sources, resonators, atomic spectroscopy, among others. The nonminimal electron sector, on the other hand, has been much less explored experimentally. Current bounds come from astrophysical highly energetic electrons and constrain only a subset of isotropic

coefficients.

Intense investigation in the past few years has placed the neutrino sector among the ones with the greater number of bounds, only behind the photon sector, which is also stronger bounded. Other sectors — the proton, neutron, charged leptons, quark, electroweak, gluon, and gravity sectors — have varying number of bounds, and almost none in the nonminimal sector.

Of particular interest for this thesis is the muon sector, which so far has not been very explored experimentally. Currently, the minimal sector has most bounds coming from muon $(g-2)$ experiments, and two others from muonium spectroscopy and astrophysical sources, and the nonminimal sector has two bounds on isotropic coefficients also from astrophysical observation. Bounds coming from $(g-2)$ experiments on minimal coefficients are of order $10^{-23}\,\mathrm{GeV}$, and, in Chapter 4, we use data from these experiments to set up bounds on a wide range of nonminimal coefficients as well.

Chapter 2

Renormalizability of the minimal QED extension

Consistency under quantum corrections of different sectors of the SME has been regularly studied in the past years, for instance, investigation of the one-loop divergence structure of the Lorentz-violating quantum theory have been performed for the QED in Minkowski spacetime [40] as well as for curved spacetimes [41], and for pure Yang-Mills and QCD [43], the whole one-loop renormalization process was studied for Lorentz-violating Yukawa field theories in [44], several works investigated the radiative generation of a Chern-Simons-like term for the QED sector of the SME — to name a few, see Refs. [4,47–50] — and investigation of asymptotic states in the context of renormalization can be found in Ref. [42]. In this chapter we discuss our contribution [11,12] to the literature, and study the renormalizability of the minimal single-fermion QED extension. At one-loop order, a proof of multiplicative renormalizability was given in [40]. Here, renormalizability will be studied to all orders in perturbation theory in the algebraic approach [51], a regularization-independent method with focus on verifying the absence of gauge anomalies.

Despite being rendered as an effective model, analysis of renormalizability of the SME is important because it inevitably looks at its unitarity and, if we are to expect the high energy behavior of the underlying (yet unknown) fundamental model to be unitary, any non-unitarity appearing in the low energy effective regime would signal a limit of the domain of validity of the approximation. In this sense, the search for

2. Renormalizability of the minimal QED extension

anomalies and matters of renormalizability prove themselves worth investigating.

In our analysis, we encounter a Lorentz-violating generalization of the Adler-Bardeen-Bell-Jackiw (ABBJ) anomaly structure [52–54] for the three-photon vertex, and we also find that the Ward-Takashi identity (relating the vertex and fermion self-energy diagrams) and the transversality of the photon self-energy tensor (vacuum polarization) are generalized to include Lorentz-violating tensors such that conventional gauge conditions are not automatically enforced as in conventional QED, thus new anomaly structures besides the usual ABBJ are allowed in a Lorentz-violating QED. By explicit loop calculation of the three-photon vertex diagram, along with computation of other diagrams done elsewhere [40], we verify that all *candidate* anomalies vanish to one-loop order, but although the vanishing of the generalized ABBJ anomaly may remain under control to all orders thanks to the Adler-Bardeen non-renormalization theorem [55], the remaining *potential* anomalies can be dangerous at higher loop orders since no analogous theorem for the vanishing of their coefficients is known — although we present arguments that may prevent at least some of them to receive higher order corrections. On the other hand, we show that requiring the Lorentz-violating QED to be C or PT invariant automatically removes the potential anomalies to all loop orders.

This chapter is presented as follows. In Section 2.1, we introduce a QED extension allowing for Lorentz violation along with considerations for one-loop evaluations. Sec. 2.2 begins with a brief review of the Quantum Action Principle, which will be used to characterize general violations of gauge symmetry. In Sec. 2.3, we identify the diagrams related to each potential anomaly, and verify that all anomaly coefficients vanish to first order in loop expansion. Multiloop and higher order Lorentz-violation for the photon self-energy, and three-photon vertex are also briefly discussed.

2.1 Framework for a Lorentz-violating QED

2.1.1 The model

The action $\mathcal{S}$ of the minimal Lorentz- and CPT violating extension of QED for a single Dirac fermion is given by [4]

$$\mathcal{S} = \int d^4x \left[i\,\overline{\psi}(\gamma^\mu + \Gamma_1^\mu)D_\mu\,\psi - \overline{\psi}(m + M_1)\psi - \tfrac{1}{4}F^{\mu\nu}F_{\mu\nu} \right.$$
$$\left. - \tfrac{1}{4}(k_F)_{\mu\nu\rho\sigma}F^{\mu\nu}F^{\rho\sigma} + \tfrac{1}{2}\epsilon^{\mu\nu\rho\sigma}(k_{AF})_\mu A_\nu F_{\rho\sigma} \right], \qquad (2.1)$$

where the covariant derivative $D_\mu = \partial_\mu - ieA_\mu$ introduces the minimal coupling between fermions and electromagnetism, with the electromagnetic field strength tensor defined as $F^{\mu\nu} \equiv \partial^\mu A^\nu - \partial^\nu A^\mu$. Action (2.1) also includes Lorentz breaking terms whose coefficients have the form of *constant* background fields — see the last two terms in the photon sector[1] and the following definitions for the fermionic coefficients:

$$\Gamma_1^\mu \equiv c^{\lambda\mu}\gamma_\lambda + d^{\lambda\mu}\gamma_5\gamma_\lambda + e^\mu + if^\mu\gamma_5 + \tfrac{1}{2}\,g^{\kappa\lambda\mu}\sigma_{\kappa\lambda},$$

$$M_1 \equiv im_5\gamma_5 + a_\mu\gamma^\mu + b_\mu\gamma_5\gamma^\mu + \tfrac{1}{2}\,H_{\mu\nu}\sigma^{\mu\nu}, \qquad (2.2)$$

where terms with coefficients of even (odd) number of indexes respect (do not respect) CPT symmetry. As we are dealing with the *minimal* Lorentz-violating extension, introduction of new terms are based on requirements of hermiticity, classical U(1) symmetry, translation invariance and power-counting renormalizability.

Coefficients $(k_F)_{\mu\nu\rho\sigma}$ and those appearing in Γ_1^μ are dimensionless, while $(k_{AF})_\mu$ and the ones in M_1 have dimension of mass. The trace part of $c_{\mu\nu}$ and $d_{\mu\nu}$ is Lorentz invariant and only yields a redefinition of the fermion field, so we take it to be zero; $H_{\mu\nu}$ and the first two indices of $g_{\kappa\lambda\mu}$ are antisymmetric; $(k_F)_{\mu\nu\rho\sigma}$ have the symmetries of the Riemann tensor and, analogous to $c_{\mu\nu}$, can be taken as double traceless otherwise it leads to a mere redefinition of the photon field; at last, in the absence of chiral

---

[1] A linear operator A_μ coupled with a background field $(k_A)_\mu$ could also be present but would introduce linear instabilities in the potential and is therefore assumed to vanish at tree-level — radiative corrections to this term are not expected to be present, see Ref. [4].

2. Renormalizability of the minimal QED extension

anomalies, m_5 can be eliminated by a chiral rotation $\psi \to \exp\left(-\frac{i}{2}\gamma_5 \tan^{-1}\frac{m_5}{m}\right)\psi$.

Along with action (2.1), we may add

$$\mathcal{S}_{\text{GF+IR}} = \int d^4x \left[-\frac{1}{2\alpha}\left(\partial_\mu A^\mu\right)^2 + \frac{1}{2}\lambda^2 A_\mu A^\mu \right], \qquad (2.3)$$

i.e., a gauge-fixing term and an infrared (IR) regulator, introduced in order to avoid infrared singularities by means of a mass term for the photon field, respectively.

2.1.2 Classical Symmetries

Not only CPT symmetry is broken, but none of the discrete operations C, P, or T is a symmetry of the model — see Table 2.1, where the coefficients represent the associated field operators — and since Lorentz symmetry is also violated, invariance under U(1) gauge transformations is the only exact symmetry of the extended QED classical action (2.1). Variations under this transformation are functionally implemented by a local *vector* gauge operator $w_{\text{g}}(x)$, defined as

$$w_{\text{g}}(x) = -\partial^\mu \frac{\delta}{\delta A^\mu} + ie\left(\frac{\overleftarrow{\delta}}{\delta\psi}\psi - \overline{\psi}\frac{\overrightarrow{\delta}}{\delta\overline{\psi}}\right). \qquad (2.4)$$

This symmetry is verified for the action (2.1),

$$w_{\text{g}}(x)\mathcal{S} = 0, \qquad (2.5)$$

and the gauge-fixing and IR regulator (2.3) linearly breaks it,

$$w_{\text{g}}(x)\mathcal{S}_{\text{GF+IR}} = -\left(\frac{\square}{\alpha} + \lambda^2\right)\partial_\mu A^\mu(x), \qquad (2.6)$$

but due to this linearity, the right-hand side of this expression does not receive quantum corrections during the renormalization procedure, remaining a classical breaking.

When dealing with the issue of quantization of the model, one asks whether or not its symmetries survive after the process of quantization. If they do not, one says that there are anomalies. In the following, we study this issue for the U(1) vector gauge symmetry of the action (2.1) within the algebraic method of renormalization [51]. The

Table 2.1: Discrete-symmetry properties of the field operators associated with Lorentz-violating coefficients.

	C	P	T	CP	CT	PT	CPT
$c_{00}, (k_F)_{0j0k},$							
$c_{jk}, (k_F)_{jklm},$	$+$	$+$	$+$	$+$	$+$	$+$	$+$
$c_{0j}, c_{j0}, (k_F)_{0jkl}$	$+$	$-$	$-$	$-$	$-$	$+$	$+$
$b_j, g_{j0l}, g_{jk0}, (k_{AF})_j$	$+$	$+$	$-$	$+$	$-$	$-$	$-$
$b_0, g_{j00}, g_{jkl}, (k_{AF})_0$	$+$	$-$	$+$	$-$	$+$	$-$	$-$
a_0, e_0, f_j	$-$	$+$	$+$	$-$	$-$	$+$	$-$
a_j, e_j, f_0	$-$	$-$	$-$	$+$	$+$	$+$	$-$
H_{jk}, d_{0j}, d_{j0}	$-$	$+$	$-$	$-$	$+$	$-$	$+$
H_{0j}, d_{00}, d_{jk}	$-$	$-$	$+$	$+$	$-$	$-$	$+$

issue of anomalies, in the case of local gauge symmetries, is physically crucial because of its well known link to the unitarity of the corresponding quantum theory. As we will see, the Lorentz-violating QED (2.1) allows for anomaly structures not present in the conventional case, but we find the coefficient controlling these vanish to one-loop order in perturbation theory. The question whether or not these coefficients can receive higher order corrections remains open, but there are some indications at least some of them do not.

2.1.3   Setup for one-loop evaluations

On experimental grounds, precision experiments place very stringent upper bounds on coefficients for Lorentz violation of various sectors of the SME in any Earth-based reference frame or other inertial frame with low velocity relative to Earth [10]. To avoid spurious enlargement of these coefficients, we restrict our analysis to these frames, called *concordant frames*. Also, higher order Lorentz violation effects may be of the same order of magnitude as higher loop corrections and, for consistency of the approach, since we perform analyses to all orders in perturbation theory, we also consider contributions of arbitrarily high orders in these coefficients.

2. Renormalizability of the minimal QED extension

As those upper bounds place Lorentz violation several orders of magnitude below the fine structure constant $\alpha \approx 1/137$, and as we are interested in one-particle irreducible diagrams, where external legs are cut off, the Lorentz-violating pieces of (2.1) can be regarded as new interaction vertices, small perturbations to the conventional QED. Therefore, we have conventional QED Feynman rules and propagators along with new rules for Lorentz-violating vertices entering as propagator or vertex insertions. Propagator insertions for fermions of momentum p^μ read

$$\longrightarrow \times \longrightarrow \quad = \quad -iM_1, \tag{2.7}$$

$$\longrightarrow \bullet \longrightarrow \quad = \quad i\Gamma_1^\mu p_\mu, \tag{2.8}$$

and for photons of momentum k^μ

$$\mu \sim\!\!\bullet\!\!\sim \nu \quad = \quad -2ik^\kappa k^\lambda (k_F)_{\kappa\mu\lambda\nu}, \tag{2.9}$$

$$\mu \sim\!\!\times\!\!\sim \nu \quad = \quad 2(k_{AF})^\kappa \epsilon_{\kappa\mu\lambda\nu} k^\lambda, \tag{2.10}$$

and the extra interaction vertex is given by

$$\bullet\!\!\sim \quad = \quad -ie\Gamma_1^\mu. \tag{2.11}$$

Separation of (2.1) into a Lorentz invariant free action and a noninvariant interaction piece will also be important when discussing the applicability of the Quantum Action Principle in Sec. 2.2.2.

2.2 Searching for anomalies

In this section, we first review some basics of the Quantum Action Principle (QAP) [56–58], along with a general all orders recursive proof of gauge invariance and discuss the possible appearance of anomalies under the view of our approach. Then we consider the application of the QAP to the Lorentz-violating QED (2.1) and identify all anomaly candidates of our model. At the end of this section, before a deeper analysis

of the general case, we also consider the special C or PT invariant case based on (2.1), which shows the interesting feature of being anomaly-free to all orders.

2.2.1 Quantization

The algebraic renormalization approach is based on two fundamental steps: (i) application of the QAP, along with the Wess-Zumino consistency condition, in order to verify that the quantization of the model does not destroy any continuous classical symmetry, and (ii) the analysis of the stability of the action, guaranteeing that it is the most general power-counting renormalizable action obeying the symmetries of the model, ensuring that all counterterms will be properly reabsorbed by a redefinition of the parameters of the starting action. Verification of both proves the existence of a renormalized theory fulfilling symmetry identities — for instance, gauge identities (2.5) and (2.6) in our case — together with suitable renormalization conditions fixing the free parameters [51,59].

In order to define a perturbative expansion, we have to split the classical action (2.1) in a free and an interacting part. Since Lorentz breaking terms are supposed to be small on physical grounds, it appears reasonable to consider all of them, including the ones which are quadratic in the quantum fields, as interactions. We shall also limit the power in these external fields to a fixed finite number for the same physical reason. The practical consequence of the latter assumption is that it avoids occurrence of an infinite number of Feynman graphs having the same number of loops. We can therefore define as usual the expansion order as the number of loops, equivalent to the power in the Planck constant $\hbar$.

Another important consequence of the Lorentz invariance of the free action, hence of the free propagators, is that it is an essential assumption in the proofs of the Quantum Action Principle (QAP) available in the literature [56–58,60–63], which are given for Poincaré invariant theories. The presence of Lorentz breaking interaction vertices does not spoil these proofs, thus we can apply the QAP to the present case. Naturally, we have to suppose we are using some subtraction scheme of the UV singularities, for instance, such as the Bogoliubov-Parasiuk-Hepp-Zimmermann (BPHZ)

renormalization scheme, dimensional regularization, or Epstein-Glaser renormalization, for which the QAP has been proved [56–58,60–63].

2.2.2   Quantum Action Principle

In general lines, the QAP states that any variation of the vertex functional Γ — the generating functional of one-particle irreducible (1PI) graphs — due to a variation of the fields is equivalent to the insertion of a local field polynomial of dimension bounded by 4. For concreteness, to illustrate the meaning of this statement, consider the variation of a *classical* action $\mathcal{S}[\phi]$ under the field transformation $\phi \rightarrow \phi + \delta\phi$, where ϕ represents the transforming fields (for instance, the photon A^μ and the fermion ψ fields),

$$\delta_\phi \mathcal{S}[\phi] = \int d^4x \, \delta\phi \frac{\delta \mathcal{S}}{\delta \phi}. \tag{2.12}$$

Also, consider the expansion of Γ in powers of $\hbar$, $\Gamma = \sum \hbar^n \Gamma_n$, such that the classical action $\mathcal{S}[\phi]$ coincides with the zeroth-order vertex function $\Gamma_o[\phi]$, *i.e.*, $\mathcal{S}[\phi] \equiv \Gamma_o[\phi]$. The QAP provides a *quantum* extension of identity (2.12), *i.e.*,

$$\delta_\phi \Gamma[\phi] = \int d^4x \, \delta\phi \frac{\delta \Gamma}{\delta \phi} = \int d^4x \, \Delta \cdot \Gamma$$
$$= \int d^4x \, [\Delta(x) + \mathcal{O}(\hbar\Delta)]. \tag{2.13}$$

The second equality in the first line is due to the QAP, and represents possible violations of the symmetry implemented by δ_ϕ, comprised at zeroth order by $\Delta(x)$, a polynomial of the classical field ϕ. $\Delta \cdot \Gamma$ is the generating functional of 1PI graphs with an insertion Δ, such that it coincides with $\Delta(x)$ at zeroth order, as represented by the last equality of (2.13), which remains valid at any order, *i.e.*, $\hbar^n \Delta \cdot \Gamma = \hbar^n \Delta + \mathcal{O}(\hbar^{n+1}\Delta)$.

The QAP was first established using BPHZ renormalization scheme — see Refs. [51,59] and references therein — but may be viewed as a general result of perturbative renormalization theory, once it was verified in other schemes such as dimensional regularization [60] and, more recently, the Epstein-Glaser scheme [62]. A fundamental assumption of these proofs is the Lorentz invariance of the free action, and thus of the free propagators. The action (2.1) is not Lorentz invariant, but due to the experimen-

tally observed smallness of Lorentz-breaking coefficients it is reasonable to consider the noninvariant pieces of (2.1) as interaction vertices which do not spoil the proofs of the QAP as free particle propagation is then governed by Lorentz invariant propagators. With such considerations, the QAP is applicable even for Lorentz noninvariant actions such as (2.1).

2.2.3 Algebraic proof of gauge invariance to all orders and anomalies

For a consistent quantum theory of (2.1), gauge symmetry must be verified for the vertex functional Γ. If not, the model is called anomalous and its renormalizability may be seriously jeopardized. To study this latter possibility, in this section we first discuss a recursive general proof of gauge invariance and how the presence of anomalies may spoil it — for more details, see Sec. 3.4.1 of Ref. [51] and Sec. 5 of Ref. [59]. An important point is we are considering here only symmetry transformations that are *linear* in the transforming fields and will not be discussing nonlinear ones.

Suppose gauge invariance holds to order $\hbar^{n-1}$, *i.e.*, there exists an order $\hbar^{n-1}$ vertex functional $\Gamma_{(n-1)}$ such that

$$w_{\mathrm{g}}(x)\Gamma_{(n-1)} = \mathcal{O}(\hbar^n). \tag{2.14}$$

Applied to this case, the QAP states that

$$w_{\mathrm{g}}(x)\Gamma_{(n-1)} = \hbar^n \Delta_{\mathrm{g}}(x) \cdot \Gamma$$
$$= \hbar^n \Delta_{\mathrm{g}}(x) + \mathcal{O}(\hbar^{n+1}\Delta_{\mathrm{g}}), \tag{2.15}$$

where $\hbar^n \Delta_{\mathrm{g}}(x)$ is a local Lorentz covariant field polynomial with UV dimension (d_{UV}) equal or less than four, representing *potential*[2] violations of gauge symmetry of order

---

[2] "Potential" in the sense that the violation of the correspondent conservation law is parameterized by a factor called "the anomaly coefficient", and this coefficient may or may not vanish. The numerical value of these coefficients may be found, for instance, by means of explicit calculation of Feynman diagrams, thus even if a coefficient vanishes to one-loop order it can be nonvanishing due to higher loop corrections.

2. Renormalizability of the minimal QED extension

$\hbar^n$. Anomalies are *certainly absent* when $\Delta_{\mathrm{g}}(x)$ satisfies

$$\Delta_{\mathrm{g}}(x) = w_{\mathrm{g}}(x)\hat{\Delta}_{\mathrm{g}}, \qquad (2.16)$$

with $\hat{\Delta}_{\mathrm{g}}$ an integrated polynomial of the fields, and we call such $\Delta_{\mathrm{g}}(x)$ a "trivial solution." For such solution we can redefine a new order $\hbar^n$ vertex functional $\Gamma_{(n)} = \Gamma_{(n-1)} - \hbar^n \hat{\Delta}_{\mathrm{g}}$, where the second term is understood as comprising *noninvariant* counterterms. Note, we also have the freedom to add *invariant* counterterms Γ_{ct} ($w_{\mathrm{g}}\Gamma_{ct} \equiv 0$) to this redefinition, whose coefficients are to be fixed by renormalization conditions. The redefinition of the vertex functional can be understood as a *change of regularization* – for instance, from a gauge noninvariant regularization to an invariant one [64]. Gauge symmetry is then proven to hold to the next order, *i.e.*,

$$w_{\mathrm{g}}(x)\Gamma_{(n)} = \mathcal{O}(\hbar^{n+1}). \qquad (2.17)$$

Recursively, gauge invariance is shown to be true to all orders. Note that each noninvariant counterterm is cancelled in the next order of $\hbar$, leaving no physically measurable effect — to verify this, expand Γ in powers of $\hbar$ (such that it coincides with the classical action in the classical limit), operate with w_{g} and apply the QAP,

$$
\begin{aligned}
w_{\mathrm{g}}\Gamma &= w_{\mathrm{g}}\Gamma_o + \hbar w_{\mathrm{g}}\Gamma_1 + \hbar^2 w_{\mathrm{g}}\Gamma_2 + \cdots \\
&= (\hbar\hat{\Delta}_{\mathrm{g}} + \hbar^2\hat{\Delta}_{\mathrm{g}} + \cdots) + \hbar w_{\mathrm{g}}(\Gamma_{ct} - \hat{\Delta}_{\mathrm{g}}) + \hbar^2 w_{\mathrm{g}}(\Gamma_{ct} - \hat{\Delta}_{\mathrm{g}}) + \cdots \\
&= 0, \qquad (2.18)
\end{aligned}
$$

where we have explicitly included invariant counterterms Γ_{ct} as they are required for the removal of UV divergences.

The previous scenario is to be contrasted with the case in which $\Delta_{\mathrm{g}}(x)$ *cannot* be written as (2.16), and thus it represents, in a regularization-independent way, a *potential* anomaly because it cannot be reabsorbed by the vertex functional, and a algebraic evaluation of its anomaly coefficient may be necessary to see whether or not a *real* anomaly is present. Therefore, identifying *candidate* anomalies amounts to

listing all possible field polynomials that cannot be written in the form (2.16). In the following section we will see that some extra conditions may be imposed on $\Delta_{\mathrm{g}}(x)$ further restricting the form of candidate anomalies.

2.2.4   Conditions to be satisfied by $\Delta_{\mathrm{g}}(x)$

The field polynomials contained in $\Delta_{\mathrm{g}}(x)$ cannot be completely arbitrary. Power counting renormalizability requires mass dimension equal or less than four. Also, if the left-hand side of (2.15) has a definite symmetry under discrete transformations, $\Delta_{\mathrm{g}}(x)$ will also behave accordingly because discrete symmetries of the classical action are not affected by the quantization procedure and are extended to the whole vertex functional. Lastly, polynomials appearing in $\Delta_{\mathrm{g}}(x)$ must satisfy the so called Wess-Zumino consistency condition,

$$w_{\mathrm{g}}(x)\Delta_{\mathrm{g}}(y) - w_{\mathrm{g}}(y)\Delta_{\mathrm{g}}(x) = 0, \tag{2.19}$$

which is derived after applying to Γ the commutation rule satisfied by the local gauge operator, $[w_{\mathrm{g}}(x), w_{\mathrm{g}}(y)] = 0$, and using the QAP (2.15). Note the solution (2.16) trivially satisfies the Wess-Zumino condition (2.19).

2.2.5   Candidate anomalies in a Lorentz-violating QED

For what follows, we return to the Lorentz-violating extension of QED (2.1), to one-loop order, for which application of the QAP gives

$$w_{\mathrm{g}}(x)\,\Gamma = -\left(\frac{\Box}{\alpha} + \lambda^2\right)\partial_\mu A^\mu(x) + \hbar\Delta_{\mathrm{g}}(x) + \mathcal{O}(\hbar^2\Delta_{\mathrm{g}}), \tag{2.20}$$

which is to be understood as the quantum version of the sum of (2.5) and (2.6). Identification of all polynomials composing $\Delta_{\mathrm{g}}(x)$ reveals all potential anomalies in the model. This task is reduced to, first, listing all polynomials of the fields A^μ and ψ

2. Renormalizability of the minimal QED extension

composing $\Delta_g(x)$, with the restriction of $d_{UV} \leqslant 4$. Symbolically, these are of the form

$$A^4, \partial A^3, \partial^2 A^2, \partial^3 A, A^3, \partial A^2, \partial^2 A,$$
$$A^2, \partial A, A, \partial \overline{\psi} \, \psi, A \overline{\psi} \, \psi, \overline{\psi} \, \psi, \tag{2.21}$$

where we consider all possible contractions among indexes, possibly using γ matrices, Levi-Civita symbols $\epsilon_{\mu\nu\rho\sigma}$, background fields, and all possible ways of acting with derivatives ∂_μ. Because the classical action (2.1) has no definite symmetry under discrete transformations, $\Delta_g(x)$ may violate C, P, T, and any combination of these. The second step amounts to verifying which polynomials satisfy the Wess-Zumino condition. The final step is to check which of the remaining polynomials, or combinations among these, can be written in the form of a trivial solution (2.16).

Investigation reveals that polynomials involving derivatives can be cast as trivial solutions as long as there are no antisymmetric contractions with $\partial_\alpha A_\beta$; denoting the Levi-Civita symbol simply as ϵ, we find A^4, $\epsilon\partial A^3$, A^3, $\epsilon A \, \partial A$, A^2, A, and $A \overline{\psi} \, \psi$ also do not satisfy the Wess-Zumino condition (2.19) and are immediately excluded from the list (2.21). Therefore, $\Delta_g(x)$ is given by

$$\Delta_g(x) = \left\{ \overline{\psi} \, \psi, \epsilon\partial A \partial A, \epsilon\partial A \right\}. \tag{2.22}$$

If no extra conditions are imposed to remove these polynomials, they represent *potential* anomalies.

In conventional QED, discrete symmetries play a *crucial role*, ruling out all polynomials that are not of the form (2.16)[3]. The Lorentz-violating QED (2.1) has no definite discrete symmetries and as the field polynomials (2.22) cannot be written in the trivial form (2.16), they are candidates for anomalies. Therefore, writing (2.22)

---

[3]The gauge operator (2.4) is odd under C and odd under PT. For the conventional QED, this implies, by means of the QAP (2.20), that $\Delta_g(x)$ must also be *odd* under each of these operations. This removes all C or PT *even* terms from $\Delta_g(x)$. Since there is no C or PT odd polynomial to be included in $\Delta(x)$, the conventional QED is free of anomalies. More details on the algebraic method of renormalization for conventional QED can be found, for instance, on Section 5 of [59].

2. Renormalizability of the minimal QED extension

explicitly, the quantum gauge identity (2.20) reads

$$
w_{\mathrm{g}}(x)\,\Gamma = -\left(\frac{\Box}{\alpha} + \lambda^2\right)\partial_\mu A^\mu + \lambda^{(1)}\overline{\psi}\psi + i\lambda^{(2)}\overline{\psi}\gamma_5\psi + \lambda^{(3)}_\mu\overline{\psi}\gamma^\mu\psi
$$

$$
+ \lambda^{(4)}_\mu\overline{\psi}\gamma^\mu\gamma_5\psi + \lambda^{(5)}_{\mu\nu}\overline{\psi}\,\sigma^{\mu\nu}\psi + \lambda^{(6)}_{\mu\nu}F^{\mu\nu} + \lambda^{(7)}_{\mu\nu\rho\sigma}F^{\mu\nu}F^{\rho\sigma} + \mathcal{O}\left(\hbar^2\lambda\right). \quad (2.23)
$$

This expression states all possible ways gauge symmetry could be violated in the Lorentz-violation QED (2.1). The first term at the right-hand side of (2.23) is a linear breaking, coming from the gauge-fixing and photon mass term for the IR control in (2.1), it is zeroth order in $\hbar$ and receives no quantum corrections in the quantization process. The others represent candidate anomalies, with associated order $\hbar$ anomaly coefficients $\lambda^{(i)}$ as functions of parameters and Lorentz-violating coefficients appearing in (2.1). Although we have written the above expression to one-loop order, its structure remains exactly the same to all orders in perturbation theory, *i.e.*, multiloop corrections only (possibly) modify the value of the anomaly coefficients.

Each anomaly coefficient can be individually calculated, for instance, from (2.23) after convenient application of functional derivatives of fields and setting them to zero. In Sec. (2.3) we show that evaluation of coefficients $\lambda^{(1)}$ to $\lambda^{(5)}$ hinges on the computation of the vertex correction and fermion self-energy diagrams, the photon self-energy diagram for $\lambda^{(6)}$, and the three-photon vertex diagrams[4] for $\lambda^{(7)}$. We show that all potentially anomalous structures appearing come from gauge identities of conventional QED but generalized to consider possible violations due to new tensor structures coming from Lorentz noninvariance and the lack of discrete symmetries.

Before computing anomaly coefficients, we first consider an anomaly-free model that comes as a special case of the Lorentz-violating QED (2.1) when at least one discrete symmetry is respected. In Sec. (2.3) we return to the task of investigating all anomaly coefficients of (2.23) for the full model (2.1).

---

[4]Note that the Adler-Bardeen-Bell-Jackiw (ABBJ) anomaly structure is a special case of the seventh anomaly term, with $\lambda^{(7)}_{\mu\nu\rho\sigma}$ containing a contribution proportional to the Levi-Civita tensor $\epsilon_{\mu\nu\rho\sigma}$ — see Sec. 2.3.3.

2. Renormalizability of the minimal QED extension

Discrete symmetries C or PT

Now we turn our attention to the possibility of removing these potential anomalies by requiring the action (2.1) to satisfy C or PT symmetry, or both, but separately enforced. For definiteness, henceforth we choose PT symmetry — the other two cases go analogously. As can be checked in Table I, imposing this invariance requires the absence of the coefficients b^μ, $d^{\mu\nu}$, $g^{\alpha\beta\mu}$, $H^{\mu\nu}$, and $(k_{AF})^\mu$. The reason this model is anomaly-free is as follows. Because these background fields are not present, the action recovers PT invariance. Along with the fact the gauge operator (2.4) is PT odd, from the QAP (2.20) it follows $\Delta_{\mathrm{g}}(x)$ must also be PT odd. From the start, fields and coefficients in our PT invariant action only allow construction of PT invariant field polynomials as well, therefore there is no available PT odd polynomial to be constructed and included in $\Delta(x)$. The requirement of PT invariance for (2.1) removes all candidate anomalies (2.22) from $\Delta_{\mathrm{g}}(x)$, and therefore the PT invariant model is guaranteed to be anomaly-free — all coefficients at the right-hand side of (2.23) now vanish.

In passing we also remark that besides C and/or PT invariance no other discrete symmetry combining C, P or T could be imposed on the action (2.1) so that it would be free of any potential anomalies and still Lorentz-violating. Requirement of coordinate invariance while keeping particle Lorentz violation allows imposition of only C, PT, or CPT symmetries. Demanding only CPT symmetry turns out to be not enough to rule out all terms from (2.22), therefore only separate imposition of C or PT can ultimately remove such anomaly candidates.

As a side note, it is important to deal with care the requirement of discrete symmetries even if the gauge identity (2.23) turns out to be truly anomalous. When considering the full QED extension, with all fermion families, the possibility of anomaly cancellations may emerge — see Sec. V A of Ref. [4] — and this could avoid the necessity of requiring the vanishing of individual fermion contributions to the anomaly coefficients.

2. Renormalizability of the minimal QED extension

Stability

In the present context, once gauge invariance is proven to hold to all orders — e.g., thanks to one of the discrete symmetries already mentioned — "stability" means that radiative corrections can be absorbed by redefinition of parameters of the theory. For definiteness, we keep on with PT symmetry, as before. It is well-known that stability of the quantum perturbative theory is guaranteed if the classical theory, *i.e.*, classical action together with classical gauge identities, is itself stable under small perturbations of $d_{\mathrm{UV}} \leqslant 4$ [51]. We therefore perform such a perturbation, $\varepsilon\,\widetilde{S}$ ($\varepsilon \ll 1$) on the (PT invariant) action, $\mathcal{S} \to \mathcal{S} + \varepsilon\,\widetilde{\mathcal{S}}$, and by requiring this perturbed action to satisfy the classical gauge identity,

$$w_{\mathrm{g}}(x)(\mathcal{S} \,+\, \varepsilon\,\widetilde{\mathcal{S}}) = w_{\mathrm{g}}(x)\,\mathcal{S} \,+\, \varepsilon\, w_{\mathrm{g}}(x)\,\widetilde{\mathcal{S}} \equiv -\left(\frac{\Box}{\alpha} + \lambda^2\right)\partial_\mu A^\mu, \qquad (2.24)$$

we conclude that all possible corrections must be gauge invariant, $w_{\mathrm{g}}\,\widetilde{\mathcal{S}} \equiv 0$, and also PT even in order to guarantee the absence of anomalies. This selects all linearly independent PT invariant terms $\mathscr{P}_i$ that can be constructed with the fields and Lorentz-violating coefficients of the classical action (2.1),

$$\mathscr{P}_1 \;=\; i\overline{\psi}\,\gamma^\mu D_\mu\psi, \qquad \mathscr{P}_2 \;=\; i\overline{\psi}\,\mathbb{c}^{\mu\nu}\gamma_\nu D_\mu\psi, \qquad \mathscr{P}_3 \;=\; i\overline{\psi}\,\mathbb{e}^\mu D_\mu\psi,$$

$$\mathscr{P}_4 \;=\; i\overline{\psi}\,f^\mu\gamma_5\,D_\mu\psi, \qquad \mathscr{P}_5 \;=\; \overline{\psi}\,\psi, \qquad \mathscr{P}_6 \;=\; i\overline{\psi}\,\gamma_5\,\psi,$$

$$\mathscr{P}_7 \;=\; \overline{\psi}\,\mathbb{a}^\mu\gamma_\mu\,\psi, \qquad \mathscr{P}_8 \;=\; F^{\mu\nu}F_{\mu\nu}, \qquad \mathscr{P}_9 \;=\; (\mathbb{k}_F)_{\alpha\beta\kappa\lambda}F^{\alpha\beta}F^{\kappa\lambda},$$

where $\mathbb{a}^\mu$ and $\mathbb{e}^\mu$, and $\mathbb{c}^{\mu\nu}$ and $(\mathbb{k}_F)^{\mu\nu\rho\sigma}$ are combinations of coefficients a^μ and e^μ, and $c^{\mu\nu}$ and $(k_F)^{\mu\nu\rho\sigma}$, respectively, as expected because of shared properties under the discrete C and PT transformations of Table 2.1. To first order in Lorentz-violating coefficients, these combinations are fully determined by field redefinition arguments — see Sec. 3.1 — but to higher orders explicit evaluation of multiloop integrals may be required for their determination. Finally, the most general integrated local function $\widetilde{\mathcal{S}}$

2. Renormalizability of the minimal QED extension

which is gauge and PT invariant is therefore given by

$$\tilde{\mathcal{S}} = \int d^4x \sum_{i=1}^{9} a_i \mathscr{P}_i(x), \qquad (2.25)$$

where $a_1, \ldots, a_9$ represent renormalizations of the coefficients appearing in the gauge and PT invariant action. Note that these coefficients remain arbitrary. They are to be fixed by renormalization conditions at the classical zeroth order, and by induction, order by order in perturbation theory. If every coefficient a_i can be unambiguously fixed, this ends the proof of the renormalizability of this PT symmetric theory, and a similar proof holds for the C invariant theory as well as for the C and PT symmetric one.

For conventional QED case, this last task of fixing free parameters is accomplished straightforwardly, and at first it also seems to be the case for the Lorentz-violating model just discussed, but as will be seen in the next chapter, the presence of Lorentz violation introduces further issues — see the additional note below.

Additional note: A very interesting work [25], published about a year after publication of the results discussed above, presents the surprising result that field redefinitions of the form $\psi \rightarrow (1 + \hat{Z})\psi$, where $\hat{Z}$ has arbitrary dependence on momentum and γ matrices, reveal that some Lorentz-violating coefficients naively characterized with renormalizable dimension are actually naturally relocated to nonrenormalizable sectors — for instance, in Ref. [25] it is found that e_μ effectively behaves as a mass dimension -1 version of a^μ. Once power-counting renormalizability of the Lorentz-violating QED (2.1) is one of the fundamental hypotheses of the method we have employed to study its renormalizability, the before mentioned results on field redefinitions may have important consequences on our results for the C or PT invariant cases proved to be renormalizable in this section.

Explicit renormalization by means of evaluation of Feynman diagrams may be suitable to cope with all subtleties and determine what would change in our results. Incidentally, when Ref. [25] was published, we were working on the one-loop evaluation

of the fermion self-energy diagram and we actually find that all divergences related to this diagram can be eliminated by renormalization of parameters appearing in (2.1), but it seems renormalization conditions cannot be consistently fixed for the symmetric parts of $c^{\mu\nu}$ and $d^{\mu\nu}$ — namely, $c_S^{\mu\nu}$ and $d_S^{\mu\nu}$, respectively — and the mixed-symmetry irreducible representation of $g^{\kappa\lambda\mu}$ — call it $g_M^{\kappa\lambda\mu}$. Connecting with the results presented in this section, an extra requirement for renormalizability of lagrangian (2.1) would be imposing extra constraints on these coefficients. Setting them to zero at tree-level solves the problem to first order in Lorentz violation and loop expansion as they do not receive radiative corrections from other coefficients at this order. Nevertheless, the question whether or not this is true to higher orders has to be further investigated.

For our surprise, expectations that coefficients more naturally regarded as having nonrenormalizable dimension would lead to problems during renormalization were *not* realized, at least for renormalization of the fermion self-energy. Actually, some coefficients having natural *renormalizable* dimension — $c_S^{\mu\nu}$, $d_S^{\mu\nu}$, and $g_M^{\kappa\lambda\mu}$, as mentioned above — were problematic. Nevertheless, a common ground for these coefficients is that neither of them relate to other coefficients within the fermion sector by means of field redefinitions, and they are the only observable coefficients with renormalizable dimension to have this property. In this sense, field redefinitions seem to play an important role in these preliminary findings, to be discussed in Chapter 3.

2.3 Anomaly coefficients

In this section we use the quantum gauge relation (2.23) to identify potentially anomalous graphs — these are the vertex correction and fermion self-energy, photon self-energy, and the three-photon vertex diagrams — and derive generalizations of conventional QED gauge identities for the presence of Lorentz-violating interactions as described by (2.1). Evaluation of Feynman loop diagrams will give the value of the anomaly coefficients, which are found to vanish to one-loop order[5], meaning that

---

[5]As mentioned in the outline of this chapter, absence of anomalies associated to the vertex correction and fermion self-energy, and photon self-energy diagrams were already verified in Ref. [40]. These are also discussed here for completeness reasons — we mention all results we use here were explicitly checked, and some were also extended in Chapter 3.

the model is free of anomalies to this order. A brief discussion regarding multiloop corrections, as well as corrections coming from higher powers in Lorentz violation, is made for the photon self-energy and three-photon vertex diagrams, and we present an argument suggesting these give no contributions to gauge anomalies at any order.

2.3.1 Ward-Takahashi identity

Anomaly coefficients from $\lambda^{(1)}$ to $\lambda^{(5)}_{\mu\nu}$ are all related to the vertex correction $\Gamma_\mu(p, q)$ and fermion self-energy $\Sigma(p)$ diagrams. Acting on (2.23) with $\overrightarrow{\delta}/\delta\overline{\psi}$ and $\overleftarrow{\delta}/\delta\psi$, setting the fields to zero, and Fourier transforming the result leads to

$$-q^\mu \Gamma_\mu(p, q) - e\Sigma(p + q) + e\Sigma(p) = \lambda^{(1)} + i\lambda^{(2)}\gamma_5 + \lambda^{(3)}_\alpha \gamma^\alpha + \lambda^{(4)}_\alpha \gamma^\alpha \gamma_5 + \lambda^{(5)}_{\alpha\beta}\sigma^{\alpha\beta}.$$

$$(2.26)$$

In conventional QED, the right-hand side of this expression identically vanishes, resulting in the so called Ward-Takahashi identity. Our generalized expression exhibits all possible ways it could be broken for a Lorentz-violating model based in (2.1). Note that the form of this expression remains unchanged at higher orders in loop expansion — multiloop corrections appear only modifying the anomaly coefficients. Making use of the results for the divergent part of the one-loop fermion self-energy and vertex correction of Ref. [40] — their Eqs. (12) and (18), respectively — we verify that

$$- q^\mu \Gamma_\mu(p, q) = e\Sigma(p + q) - e\Sigma(p), \qquad (2.27)$$

i.e., the conventional Ward-Takahashi identity of QED still holds at one-loop order and, therefore,

$$\lambda^{(1)} = \lambda^{(2)} = \lambda^{(3)}_\alpha = \lambda^{(4)}_\alpha = \lambda^{(5)}_{\alpha\beta} = 0 \quad \text{to one-loop order}, \qquad (2.28)$$

which was to be expected in view of Eq. (20) of Ref. [40], which is the equivalent of this relation but in terms of renormalization factors. We should stress that we have found no compelling reason to expect these coefficients will not develop nonzero values when higher-loop diagrams are considered, therefore explicit multiloop evaluations of

the vertex and fermion self-energy diagrams may be desirable.

2.3.2 Transversality of the photon self-energy tensor

Coefficient $\lambda_{\mu\nu}^{(6)}$ is related to the photon self-energy tensor $\Pi_{\mu\nu}(k)$. To see this, apply $\delta/\delta A^\nu$ on (2.23), set the fields to zero, and Fourier transform it, to find

$$k^\mu \Pi_{\mu\nu}(k) = -2\lambda_{\mu\nu}^{(6)} k^\mu. \tag{2.29}$$

Transversality of $\Pi_{\mu\nu}$ was already verified in Ref. [40]. Thus, this anomaly coefficient also vanishes,

$$\lambda_{\mu\nu}^{(6)} = 0 \quad \text{to one-loop order.} \tag{2.30}$$

Appealing to the generalized Furry theorem [40] — stating that only overall C even insertions in fermion loops with even number of external photon legs give nonvanishing contributions — Lorentz-breaking may be expected to give no contribution to the C odd anomaly coefficient $\lambda_{\mu\nu}^{(6)}$ at higher orders in loop expansion or Lorentz-violating coefficients.

2.3.3 Three-photon vertex

Following the same procedure as before, but acting on (2.23) with two functional derivatives of the gauge field, we obtain the expression

$$(p+q)^\lambda \Gamma_{\lambda\mu\nu}(p,q) = -8i\lambda_{\kappa\mu\lambda\nu}^{(7)} p^\kappa q^\lambda, \tag{2.31}$$

with external momenta p and q as depicted in Fig. 2.1, relating $\lambda_{\kappa\mu\lambda\nu}^{(7)}$ to the one-loop three-photon vertex $\Gamma_{\lambda\mu\nu}(p,q)$. It represents *vector* current conservation if $\lambda_{\kappa\mu\lambda\nu}^{(7)} = 0$, otherwise an anomaly is present and gauge symmetry is broken. Instead of working on an expression for $\lambda_{\kappa\mu\lambda\nu}^{(7)}$, in what follows we evaluate the left-hand side of the above expression. Before, it is important to notice that in (2.23), due to the contraction with $F^{\kappa\lambda}F^{\mu\nu}$, only pieces of $\lambda_{\kappa\lambda\mu\nu}^{(7)}$ satisfying

$$\lambda_{\kappa\lambda\mu\nu}^{(7)} = -\lambda_{\lambda\kappa\mu\nu}^{(7)} = -\lambda_{\kappa\lambda\nu\mu}^{(7)} = \lambda_{\mu\nu\kappa\lambda}^{(7)} \tag{2.32}$$

2. Renormalizability of the minimal QED extension

Figure 2.1: One-loop three-photon vertex.

can contribute to the anomaly on the *right*-hand side of (2.31). Therefore, any piece without this index symmetries that may appear after evaluation of the *left*-hand side of (2.31) will not represent an anomaly. It represents noninvariant counterterms that can be reabsorbed by a redefinition of the vertex functional Γ at that loop order and are further cancelled, order by order in perturbation theory, leaving no physically measurable effect, as discussed in Sec. 2.2.3.

Bose symmetry must be taken into account and, as seen in Fig. 2.1, we consider both diagrams along with a convenient internal momenta routing. According to generalized Furry theorem [40], only C odd insertions give nonzero contribution to processes with odd number of external photon legs attached to a fermion loop. Therefore, the nonvanishing part of $\Gamma_{\lambda\mu\nu}(p,q)$ is given by the sum of all nine possible processes with one C odd propagator or vertex insertion as depicted in Fig. 2.2. Contraction of the integral representing $\Gamma_{\lambda\mu\nu}(p,q)$ with $(p+q)^\lambda$ leads to

$$(p+q)^\lambda \Gamma_{\lambda\mu\nu}(p,q) = (p+q)^\lambda \left(\Gamma^{(1)}_{\lambda\mu\nu} + \cdots + \Gamma^{(9)}_{\lambda\mu\nu} \right)$$

$$= e^3 \int \frac{d^4k}{(2\pi)^4} \mathrm{Tr}\left\{ \left[\Gamma_{1\lambda} p'^\lambda \frac{1}{\slashed{k}-\slashed{p}'-m}\gamma_\mu \frac{1}{\slashed{k}-\slashed{q}-m}\gamma_\nu \frac{1}{\slashed{k}-m} + (\mu;p\leftrightarrow\nu;q) \right] \right.$$

$$+ \left[\Gamma_{1\nu}\frac{1}{\slashed{k}-\slashed{p}'-m}\gamma_\mu \frac{1}{\slashed{k}-\slashed{q}-m} - \Gamma_{1\nu}\frac{1}{\slashed{k}-m}\gamma_\mu \frac{1}{\slashed{k}-\slashed{q}-m} + (\mu;p\leftrightarrow\nu;q) \right]$$

$$+ \left[\Gamma_{1\nu}\frac{1}{\slashed{k}-\slashed{p}-m}\gamma_\mu \frac{1}{\slashed{k}-\slashed{p}'-m} - \Gamma_{1\nu}\frac{1}{\slashed{k}-\slashed{p}-m}\gamma_\mu \frac{1}{\slashed{k}-m} + (\mu;p\leftrightarrow\nu;q) \right]$$

36

2. Renormalizability of the minimal QED extension
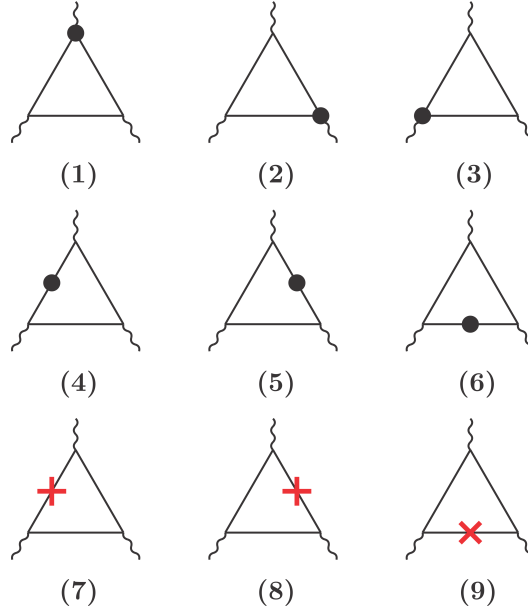
Figure 2.2: Lorentz-violating insertions in the one-loop three-photon vertex. Generalization of Furry theorem states that only C odd insertions can give nonvanishing contributions to this process.

$$
+ \Bigg[-\Gamma_{1\lambda}(k-p')^\lambda \frac{1}{\not{k}-\not{p}'-m} \gamma_\mu \frac{1}{\not{k}-\not{q}-m} \gamma_\nu \frac{1}{\not{k}-\not{p}'-m}
$$

$$
+ \Gamma_{1\lambda}(k-p')^\lambda \frac{1}{\not{k}-\not{p}'-m} \gamma_\nu \frac{1}{\not{k}-\not{p}-m} \gamma_\mu \frac{1}{\not{k}-m} + (\mu; p \leftrightarrow \nu; q) \Bigg]
$$

$$
+ \Bigg[-\Gamma_{1\lambda}k^\lambda \frac{1}{\not{k}-\not{p}'-m} \gamma_\mu \frac{1}{\not{k}-\not{q}-m} \gamma_\nu \frac{1}{\not{k}-m}
$$

$$
+ \Gamma_{1\lambda}k^\lambda \frac{1}{\not{k}-m} \gamma_\nu \frac{1}{\not{k}-\not{p}-m} \gamma_\mu \frac{1}{\not{k}-m} + (\mu; p \leftrightarrow \nu; q) \Bigg]
$$

$$
+ \Bigg[-\Gamma_{1\lambda}(k-q)^\lambda \frac{1}{\not{k}-\not{q}-m} \gamma_\nu \frac{1}{\not{k}-\not{p}'-m} \gamma_\mu \frac{1}{\not{k}-\not{q}-m}
$$

$$
+ \Gamma_{1\lambda}(k-p)^\lambda \frac{1}{\not{k}-\not{p}-m} \gamma_\mu \frac{1}{\not{k}-m} \gamma_\nu \frac{1}{\not{k}-\not{p}-m} + (\mu; p \leftrightarrow \nu; q) \Bigg] \Bigg\},
$$

$$
\tag{2.33}
$$

where the terms inside the first square brackets at the right-hand side are the contributions coming from $\Gamma^{(1)}_{\lambda\mu\nu}$, the ones inside the second are the contributions from $\Gamma^{(2)}_{\lambda\mu\nu}$, and so on until the last square brackets, which comprises the contributions from

2. Renormalizability of the minimal QED extension

$\Gamma^{(6)}_{\lambda\mu\nu}$. Diagrams (7), (8), and (9), involving propagator insertions of M_1, give vanishing contributions as will be explained below. First, we note the following in (2.33):

- A shift $k \to k - p$ in the second term from $\Gamma^{(2)}_{\lambda\mu\nu}$ cancels the first term from $\Gamma^{(3)}_{\lambda\mu\nu}$;

- A shift $k \to k - q$ in the second term from $\Gamma^{(3)}_{\lambda\mu\nu}$ cancels the first term from $\Gamma^{(2)}_{\lambda\mu\nu}$;

- A shift $k \to k - q$ in the second term from $\Gamma^{(5)}_{\lambda\mu\nu}$ cancels the first term from $\Gamma^{(6)}_{\lambda\mu\nu}$;

- A shift $k \to k - q$ in the second term from $\Gamma^{(6)}_{\lambda\mu\nu}$ cancels the first term from $\Gamma^{(4)}_{\lambda\mu\nu}$;

- Analogous results follows for the above with $\mu \leftrightarrow \nu$ and $p \leftrightarrow q$;

- All remaining non-mentioned terms add up to zero.

Care must be taken while doing these integration shifts since we are dealing with linearly[6] divergent integrals. In this case, shifts in the integration momenta generate finite nonvanishing surface terms[7],

$$(p+q)^\lambda \Gamma_{\lambda\mu\nu}(p,q)$$

$$= e^3 \int \frac{d^4k}{(2\pi)^4} \text{Tr}\left\{ p^\alpha \frac{\partial}{\partial k^\alpha}\left(\Gamma_{1\nu} \frac{1}{\slashed{k}-m}\gamma_\mu \frac{1}{\slashed{k}-\slashed{q}-m} \right) + q^\alpha \frac{\partial}{\partial k^\alpha}\left(\Gamma_{1\nu} \frac{1}{\slashed{k}-\slashed{p}-m}\gamma_\mu \frac{1}{\slashed{k}-m} \right) \right.$$

$$- q^\alpha \frac{\partial}{\partial k^\alpha}\left(\Gamma_{1\lambda} k^\lambda \frac{1}{\slashed{k}-m}\gamma_\nu \frac{1}{\slashed{k}-\slashed{p}-m}\gamma_\mu \frac{1}{\slashed{k}-m} \right.$$

$$\left. \left. - \Gamma_{1\lambda}(k-p)^\lambda \frac{1}{\slashed{k}-\slashed{p}-m}\gamma_\mu \frac{1}{\slashed{k}-m}\gamma_\nu \frac{1}{\slashed{k}-\slashed{p}-m} \right) + (\mu; p \leftrightarrow \nu; q) \right\}.$$

$$(2.34)$$

As stated before, propagator insertions of M_1 give vanishing contributions, and the reason is their associated integrals are logarithmically divergent, thus the resulting

---

[6]Each integral in (2.33) is quadratically divergent, but the sum, for each diagram, results in a linear divergent integral. To illustrate this point, consider, for instance, $\int d^4k \left[\frac{1}{k(k-a)} - \frac{1}{k^2} \right]$ which diverges linearly.

[7]To see this, consider the difference $\Delta(a) = \int_{-\infty}^{+\infty} d^4x[f(x+a) - f(x)] = \int_{-\infty}^{+\infty} d^4x[a^\mu \partial_\mu f(x) + a^\mu a^\nu \partial_\mu \partial_\nu f(x) + \cdots]$. If the integral of $f(x)$ converges, then $f(\pm\infty) = f'(\pm\infty) = \cdots = 0$ and $\Delta(a) = 0$. On the other hand, if the integral diverges linearly, then $f(\pm\infty) \neq 0$ and $f'(\pm\infty) = \cdots = 0$, and the shift generates a finite nonvanishing surface term, $\Delta(a) = \int_{-\infty}^{+\infty} d^4x\, a^\mu \partial_\mu f(x) = \oint_S d^3S_\mu a^\mu f(x)$.

2. Renormalizability of the minimal QED extension

surface integrals converge to zero, as seen when the surface is taken at infinity. More-over, only the $d^{\mu\nu}\gamma_5\gamma_\mu$ part of Γ_1^ν contributes because, as mentioned earlier, only C odd insertions give nonvanishing contributions and, of these, the contributions from the e_ν and f_ν parts of Γ_1^ν vanish because the trace of both an odd number of γ matrices or the product of γ_5 with an odd number of γ's vanish, remaining only $d^{\mu\nu}$.

Note that the surface integrals (2.34) are finite, thus there is no need to introduce UV regulators and the conventional approach to γ_5 holds. Therefore, to evaluate the integral (2.34), we use Gauss' theorem to change it into a surface integral, which is easy to solve considering an isotropic hypersurface at $k \to \infty$. Before, however, we need to evaluate traces involving the product of γ_5 with four and six γ's. For the former we use $\mathrm{Tr}(\gamma_5\gamma_\kappa\gamma_\lambda\gamma_\mu\gamma_\nu) = -4i\epsilon_{\kappa\lambda\mu\nu}$ and for the latter we make extensive use of identities $\slashed{a}\gamma_\mu\slashed{b} = 2\slashed{a}b_\mu - \slashed{a}\slashed{b}\gamma_\mu$ and $\slashed{a}\slashed{b} = 2a{\cdot}b - \slashed{b}\slashed{a}$ to reduce the trace to the first case. After evaluation of the traces and reorganizing, we find

$$
(p+q)^\lambda \Gamma_{\lambda\mu\nu}(p,q)
$$

$$
= 4ie^3 \int \frac{d^4k}{(2\pi)^4} \Bigg\{ d^\lambda_{\ \nu}\epsilon_{\lambda\mu\rho\sigma}(p^\sigma q^\alpha - p^\alpha q^\sigma)\frac{\partial}{\partial k^\alpha}\left[\frac{k^\rho}{(k^2-m^2)[(k-p)^2-m^2]}\right]
$$

$$
- 2d^\kappa_{\ \lambda}q^\alpha \frac{\partial}{\partial k^\alpha}\left[\frac{k^\zeta k^\lambda p^\sigma k^\tau(\eta_{\zeta\mu}\epsilon_{\kappa\nu\sigma\tau} - \eta_{\zeta\nu}\epsilon_{\kappa\mu\sigma\tau} + \eta_{\zeta\sigma}\epsilon_{\kappa\mu\nu\tau})}{(k^2-m^2)^2[(k-p)^2-m^2]}\right.
$$

$$
\left. + \frac{(k-p)^\zeta(k-p)^\lambda p^\sigma k^\tau(\eta_{\zeta\mu}\epsilon_{\kappa\nu\sigma\tau} - \eta_{\zeta\nu}\epsilon_{\kappa\mu\sigma\tau} - \eta_{\zeta\tau}\epsilon_{\kappa\mu\nu\sigma})}{(k^2-m^2)[(k-p)^2-m^2]^2}\right]
$$

$$
+ d^\kappa_{\ \lambda}\epsilon_{\kappa\mu\nu\rho}q^\alpha \frac{\partial}{\partial k^\alpha}\left[\frac{k^2 k^\lambda(k+p)^\rho}{(k^2-m^2)^2[(k-p)^2-m^2]} - \frac{(k^2-p^2)(k-p)^\lambda k^\rho}{(k^2-m^2)[(k-p)^2-m^2]^2}\right]
$$

$$
- m^2 d^\kappa_{\ \lambda}\epsilon_{\kappa\mu\nu\sigma}q^\alpha \frac{\partial}{\partial k^\alpha}\left[\frac{k^\lambda(k+p)^\sigma}{(k^2-m^2)^2[(k-p)^2-m^2]} + \frac{(k-p)^\lambda(k-2p)^\sigma}{(k^2-m^2)[(k-p)^2-m^2]^2}\right]
$$

$$
+ (\mu; p \leftrightarrow \nu; q)\Bigg\}. \tag{2.35}
$$

Making use of Gauss' theorem to transform the integrals (2.35) into surface integrals[8],

---

[8] For this purpose, we Wick rotate to Euclidean space, $k_o = ik_4$ and $d^4k = id^4k_E \equiv idk_1 dk_2 dk_3 dk_4$. Then $\int_V d^4k_E \frac{\partial}{\partial k^\alpha}(\ldots)^\alpha = \oint_S d^3 S_\alpha^E(\ldots)^\alpha = \oint_S d\Omega\, k^2 k_\alpha(\ldots)^\alpha$, where in the last integral the integration is along the solid angle of a 3-dimensional surface, where $\oint_S d\Omega = 2\pi^2$.

2. Renormalizability of the minimal QED extension

and evaluating it at an isotropic surface at $k \to \infty$, reveals that the difference inside the third square brackets vanishes at the boundary and the surface integral of the terms inside the fourth square brackets goes to zero as $k \to \infty$. Expression (2.35) simplifies and is given by

$$(p+q)^\lambda \Gamma_{\lambda\mu\nu}(p,q) = -4e^3 d^\lambda{}_\nu \epsilon_{\lambda\mu\rho\sigma}(p^\sigma q_\alpha - p_\alpha q^\sigma) \oint_{\mathcal{S}} \frac{d\Omega}{(2\pi)^4} \frac{k^\alpha k^\rho}{k^2}$$

$$+ 8e^3 d^\kappa{}_\lambda \left(2\eta_{\zeta\mu}\epsilon_{\kappa\nu\sigma\tau} - 2\eta_{\zeta\nu}\epsilon_{\kappa\mu\sigma\tau} + \eta_{\zeta\sigma}\epsilon_{\kappa\mu\nu\tau}\right.$$

$$\left. - \eta_{\zeta\tau}\epsilon_{\kappa\mu\nu\sigma}\right)p^\sigma q_\alpha \oint_{\mathcal{S}} \frac{d\Omega}{(2\pi)^4} \frac{k^\alpha k^\zeta k^\lambda k^\tau}{k^4} + (\mu; p \leftrightarrow \nu; q).$$

$$(2.36)$$

The surface integrals are evaluated at isotropic momenta $k_\mu \to \infty$, and we use

$$\frac{1}{2\pi^2} \oint_{\mathcal{S}} d\Omega \frac{k^\mu k^\nu}{k^2} = \frac{1}{4}\eta^{\mu\nu}, \tag{2.37}$$

$$\frac{1}{2\pi^2} \oint_{\mathcal{S}} d\Omega \frac{k^\kappa k^\lambda k^\mu k^\nu}{k^4} = \frac{1}{24}(\eta^{\kappa\lambda}\eta^{\mu\nu} + \eta^{\kappa\mu}\eta^{\lambda\nu} + \eta^{\kappa\nu}\eta^{\lambda\mu}), \tag{2.38}$$

which are derived by arguments of Lorentz covariance, to finally obtain

$$(p+q)^\lambda \Gamma_{\lambda\mu\nu}(p,q) = -\frac{e^3}{12\pi^2} \left(d^\lambda{}_\mu \epsilon_{\lambda\nu\rho\sigma} - d^\lambda{}_\nu \epsilon_{\lambda\mu\rho\sigma} - d^\lambda{}_\rho \epsilon_{\lambda\mu\nu\sigma} + d^\lambda{}_\sigma \epsilon_{\lambda\mu\nu\rho}\right) p^\rho q^\sigma$$

$$+ \frac{e^3}{12\pi^2} d^{\kappa\lambda} \left(\epsilon_{\kappa\lambda\nu\rho}\eta_{\mu\sigma} - \epsilon_{\kappa\lambda\nu\sigma}\eta_{\mu\rho} - \epsilon_{\kappa\lambda\mu\rho}\eta_{\nu\sigma} + \epsilon_{\kappa\lambda\mu\sigma}\eta_{\nu\rho}\right) p^\rho q^\sigma.$$

$$(2.39)$$

Expression (2.39) looks like as if there is a gauge anomaly, but fortunately this result is not the whole story. There is an internal momenta routing ambiguity, *i.e.*, we may relabel all internal momenta of the triangular diagram, Fig. 2.1, by adding a constant vector a, *i.e.*,

$$k \to k + a, \quad \text{where} \quad a = \alpha q + (\alpha - \beta)p, \tag{2.40}$$

with α and β arbitrary constants, and ask what would change in our results. If the

2. Renormalizability of the minimal QED extension

integral describing this process were perfectly finite, nothing would change, but it is actually linearly divergent and a relevant surface term emerges as a result of this routing ambiguity. Therefore, we should substitute result (2.39) for $\Gamma_{\lambda\mu\nu}(p, q)$ by another one $\Gamma_{\lambda\mu\nu}(p, q; a)$ which takes this ambiguity into account, *i.e.*, one valid for an arbitrary shift of internal momenta. A practical way of finding $\Gamma_{\lambda\mu\nu}(p, q; a)$ is to first compute the surface term $\Delta_{\lambda\mu\nu}(a)$,

$$\Delta_{\lambda\mu\nu}(a) = \Gamma_{\lambda\mu\nu}(p, q; a) - \Gamma_{\lambda\mu\nu}(p, q; 0), \tag{2.41}$$

where $\Gamma_{\lambda\mu\nu}(p, q; 0) \equiv \Gamma_{\lambda\mu\nu}(p, q)$ and use it to obtain

$$(p + q)^\lambda \Gamma_{\lambda\mu\nu}(p, q; a) = (p + q)^\lambda \left[\Gamma_{\lambda\mu\nu}(p, q; 0) + \Delta_{\lambda\mu\nu}(a)\right], \tag{2.42}$$

where the first term at the right-hand side is already known — it is Eq. (2.39) — and the second one is just the divergence of (2.41). In the end, we will have a result with explicit dependence on the routing ambiguity. Since our physical theory relies upon gauge invariance, we fix the ambiguity by requiring this symmetry to hold.

Computation of $(p + q)^\lambda \Delta_{\lambda\mu\nu}(a)$ follows very similarly the derivation of (2.39) such that its generalization to consider an arbitrary shift of internal momenta leads to

$$(p + q)^\lambda \Gamma_{\lambda\mu\nu}(p, q; a)$$

$$= -(1 + \beta)\frac{e^3}{12\pi^2} \left(d^\lambda{}_\mu \epsilon_{\lambda\nu\rho\sigma} - d^\lambda{}_\nu \epsilon_{\lambda\mu\rho\sigma} - d^\lambda{}_\rho \epsilon_{\lambda\mu\nu\sigma} + d^\lambda{}_\sigma \epsilon_{\lambda\mu\nu\rho}\right) p^\rho q^\sigma$$

$$+ (1 + \beta)\frac{e^3}{12\pi^2} d^{\kappa\lambda} \left(\epsilon_{\kappa\lambda\nu\rho}\eta_{\mu\sigma} - \epsilon_{\kappa\lambda\nu\sigma}\eta_{\mu\rho} - \epsilon_{\kappa\lambda\mu\rho}\eta_{\nu\sigma} + \epsilon_{\kappa\lambda\mu\sigma}\eta_{\nu\rho}\right) p^\rho q^\sigma$$

$$- \beta\frac{e^3}{6\pi^2} d^\lambda{}_\rho \epsilon_{\kappa\lambda\mu\nu}(p^\kappa p^\rho - q^\kappa q^\rho)$$

$$- \beta\frac{e^3}{12\pi^2} d^{\kappa\lambda} \left[\epsilon_{\kappa\lambda\mu\nu}(p^2 - q^2) + \epsilon_{\kappa\lambda\nu\rho}(p_\mu p^\rho - q_\mu q^\rho) - \epsilon_{\kappa\lambda\mu\rho}(p_\nu p^\rho - q_\nu q^\rho)\right], \tag{2.43}$$

where we note that terms proportional to β are contributions coming from $(p + q)^\lambda \Delta_{\lambda\mu\nu}(a)$ of (2.42). This is the left-hand side of the conservation law (2.31), but it is not very illuminating in this form, so we recast it in terms of the vertex functional

and fields,

$$
w_{\mathrm{g}}(x)\Gamma = -\,(1+\beta)\frac{e^3}{24\pi^2}i\left(d^\lambda{}_\mu\epsilon_{\lambda\nu\rho\sigma} + d^\lambda{}_\nu\epsilon_{\lambda\mu\rho\sigma} + d^\lambda{}_\rho\epsilon_{\lambda\mu\nu\sigma} + d^\lambda{}_\sigma\epsilon_{\lambda\mu\nu\rho}\right)\partial^\mu A^\nu\partial^\rho A^\sigma
$$

$$
+\,(1+\beta)\frac{e^3}{24\pi^2}id^{\kappa\lambda}\left(\epsilon_{\kappa\lambda\mu\nu}\eta_{\rho\sigma} + \epsilon_{\kappa\lambda\rho\sigma}\eta_{\mu\nu} - \epsilon_{\kappa\lambda\mu\sigma}\eta_{\nu\rho} + \epsilon_{\kappa\lambda\nu\rho}\eta_{\mu\sigma}\right)\partial^\mu A^\nu\partial^\rho A^\sigma
$$

$$
-\,\beta\frac{e^3}{6\pi^2}id^\lambda{}_\rho\epsilon_{\lambda\mu\nu\sigma}A^\mu\partial^\rho\partial^\sigma A^\nu
$$

$$
+\,\beta\frac{e^3}{12\pi^2}id^{\kappa\lambda}\epsilon_{\kappa\lambda\mu\nu}\left(A^\mu\Box A^\nu - A^\mu\partial^\nu\partial_\alpha A^\alpha - A_\alpha\partial^\alpha\,\partial^\mu A^\nu\right), \tag{2.44}
$$

which can be further rewritten as

$$
w_{\mathrm{g}}(x)\Bigg\{\Gamma - (1+\beta)\frac{e^3}{24\pi^2}i\int d^4y\left[(d^\lambda{}_\mu\epsilon_{\lambda\nu\rho\sigma} + d^\lambda{}_\nu\epsilon_{\lambda\mu\rho\sigma})A^\mu A^\nu\partial^\rho A^\sigma\right.
$$

$$
\left.\left.+\,d^{\kappa\lambda}\epsilon_{\kappa\lambda\mu\nu}(A^\mu A_\alpha\partial^\alpha A^\nu - A^\mu A_\alpha\partial^\nu A^\alpha - A^2\partial^\mu A^\nu)\right]\right\}
$$

$$
=\,(1+3\beta)\frac{e^3}{24\pi^2}i\left[(d^\lambda{}_\rho\epsilon_{\lambda\mu\nu\sigma} - d^\lambda{}_\mu\epsilon_{\lambda\nu\rho\sigma})A^\sigma\partial^\rho\partial^\mu A^\nu\right.
$$

$$
\left.+\,d^{\kappa\lambda}\epsilon_{\kappa\lambda\mu\nu}(A^\mu\Box A^\nu - A^\mu\partial^\nu\partial^\alpha A_\alpha - A_\alpha\partial^\alpha\partial^\mu A^\nu)\right]. \tag{2.45}
$$

The expression inside curly brackets in the left-hand side of (2.45) can be understood as a redefinition of the vertex functional but now comprising noninvariant counterterms — see Sec. 2.2.3. This expression is to be compared with Eq. (2.23), where potential anomalies coming from other diagrams were already found to vanish to one-loop order in Secs. 2.3.1 and 2.3.2. The objects with Lorentz indices and the numerical factors of $A\partial\partial A$ in the right-hand side of the above expression are identified as pieces composing $\lambda^{(7)}_{\kappa\lambda\mu\nu}$, and they must be zero in order to ensure *vector* gauge invariance at this order. This *physical* requirement fixes the parameter $\beta = -1/3$. Therefore, in the Lorentz-violating QED (2.1), the one-loop three-photon vertex does not contribute to a potential vector gauge anomaly, as expressed by

$$
\lambda^{(7)}_{\kappa\lambda\mu\nu} = 0 \qquad \text{(at one-loop order)}. \tag{2.46}
$$

2. Renormalizability of the minimal QED extension

Concerning this result, to first order in Lorentz violation, due to the contraction with the C and PT even operator $F^{\mu\nu}F^{\rho\sigma}$ in (2.23), it is expected that only C and PT even coefficients may give contribution to $\lambda^{(7)}_{\mu\alpha\kappa\beta}$. It turns out this anomaly coefficient vanishes to one-loop order and, according to the mentioned expectation, this was not to be a surprise as the only C and PT symmetric coefficients, $c_{\mu\nu}$ and $(k_{AF})_{\mu\nu\rho\sigma}$, do not contribute at all to $\Gamma_{\rho\mu\nu}(p,q)$ because of the generalized Furry theorem.

In a theory with chiral fermions, the ABBJ anomaly — a $\epsilon_{\kappa\lambda\mu\nu}$ contribution to $\lambda^{(7)}_{\kappa\lambda\mu\nu}$ — would be expected, and we actually found a Lorentz-violating generalization of its structure — the the right-hand side of (2.45) — because of the term $d^{\mu\nu}\overline{\psi}\gamma_{\mu}\gamma_5\partial_{\nu}\psi$ present in the action (2.1), with the isotropic (trace) part of $d^{\mu\nu}$ playing the role of a conventional chiral interaction. It turns out there is no contribution from $\epsilon_{\kappa\lambda\mu\nu}$ to $\lambda^{(7)}_{\kappa\lambda\mu\nu}$ and explicit evaluation actually reveals that the overall contribution of the trace part of $d^{\mu\nu}$ to $\Gamma_{\rho\mu\nu}(p,q)$ vanishes, even before contraction with $(p+q)^{\rho}$. Lorentz violation allows for a generalized structure as in the right-hand side of (2.45), but we found the coefficient for this anomaly structure vanishes to one-loop order, as it is to be expected on symmetry grounds as $d^{\mu\nu}$ is related to C odd field operators.

On dimensional grounds, $\lambda_{\mu\nu\rho\sigma}$ could receive contributions only from coefficients for Lorentz violation with mass dimension zero, therefore coefficients from M_1 are expected to give no contribution to the anomaly (2.31) at any order in Lorentz violation — as discussed after Eq. (2.34), contributions from M_1 insertions lead to vanishing surface integrals.

Regarding multiloop contributions along with higher powers in coefficients for Lorentz violation, the standard ABBJ anomaly vanishes to one-loop and do not receive further higher order corrections due to the nonrenormalization theorem of Adler and Bardeen [55]. We may also conjecture that $\lambda^{(7)}_{\kappa\lambda\mu\nu}$ will not receive corrections from higher powers in Lorentz violation. The reason is the C *symmetric* anomaly coefficient $\lambda^{(7)}_{\kappa\lambda\mu\nu}$ can receive only C *symmetric* corrections, but the generalized Furry theorem guarantees these corrections add up to zero for the three-point function $\Gamma_{\lambda\mu\nu}(p,q)$, protecting $\lambda^{(7)}_{\kappa\lambda\mu\nu}$ from receiving contributions from C even Lorentz-violating coefficients. In this line of reasoning, we expect the generalized form of the ABBJ anomaly — the right-hand side

43

of (2.45) — to vanish to all orders because $d^{\mu\nu}$ is C *antisymmetric.*

At last, we should point out that in Ref. [65] it was verified that addition of an isotropic Lorentz-violating coefficient ϵ, leading to a lagrangian for a Weyl spinor u coupled to gauge fields of the form $iu^{\dagger}\big[D_o - (1 - \frac{1}{2}\epsilon)\vec{\sigma} \cdot \vec{D}\big]u$, results in the very same anomaly of ABBJ, and for abelian gauge fields the anomaly vanishes, to all orders due to the Adler-Bardeen theorem, as in the standard Lorentz invariant case. Comparison with our case reveals this is analogous to considering (2.1) with only Lorentz-violating coefficient the isotropic part of $d_{\mu\nu}$, thus our results agree with [65]. The nonisotropic contribution from $d^{\mu\nu}$ leads to an anomaly similar to the ABBJ but with Lorentz-violating anomaly coefficients, as can be seen in (2.45), and we checked it vanishes to one-loop order. It would be interesting to study how the Adler-Bardeen theorem generalizes to this case, but this is beyond the scope of this work. As suggested before, there is a good indication the anomaly indeed vanishes to all orders.

2.4   Summary

In this chapter, we investigated renormalizability of the minimal Lorentz-violating QED extension. Making use of the algebraic method of renormalization, we have found that Lorentz symmetry violation typically introduces new possible anomalous structures — all of them forbidden in the conventional because of Lorentz invariance and the existence of discrete symmetries in the model. Those new structures were understood as extensions of conventional gauge identities to include Lorentz violation. The vanishing or not of each new structure is controlled by numerical factors which we have called anomaly coefficients. All diagrams contributing to anomaly coefficients were identified. Lorentz-violating corrections to the fermion self-energy and vertex correction can lead to violations of the Ward-Takahashi identity; corrections to the photon self-energy can spoil its transversality; and corrections to the three-photon triangular diagram can result in current nonconservation at its vertices.

We emphasize that our results by no means imply existence of gauge anomalies in the model, but indicate they are possible and therefore requires determination of

2. Renormalizability of the minimal QED extension

the numerical value of each anomaly coefficient by, for instance, explicit evaluation of Feynman diagrams. To first order in loop expansion, previous results in the literature found no anomalies related to the fermion self-energy, vertex correction, and photon self-energy diagrams. We investigated the remaining three-photon diagram and verified no gauge anomaly is present to this order. We have also suggested, using arguments related to discrete symmetries and a generalized version of Furry theorem, that anomaly coefficients related to the photon self-energy and the three-photon vertex vanish to all orders in perturbation theory. Further investigations aiming a formal proof of this conjecture would be interesting.

As a byproduct of the use of the algebraic method, we were able to identify submodels of the minimal QED extension which are completely free of gauge anomalies. We found that automatic vanishing of anomaly coefficients can be achieved by requiring discrete C or PT symmetry. It was surprising for us that discrete symmetries could play such decisive role in ruling out potential anomalies in a model. Once candidate anomalies were ruled out, renormalization of the model was immediately verified since the action describing this model is the most general one according its symmetries. Hence all loop divergences can be eliminated by a finite number of counterterms and redefinition of parameters appearing in the classical action. The question as to whether or not free parameters introduced by renormalization can be consistently fixed by suitably chosen renormalization conditions appears to be more subtle than expected, and preliminary results on this issue will be presented in the following chapter.

Chapter 3

Fermion self-energy of the minimal QED extension

Investigations on radiative corrections for the minimal Lorentz-violating QED extension have been performed regularly in the past years since the SME was devised. Loop calculations considering only the b^μ coefficient may have been the most investigated ones — for instance, dealing with radiatively induced Chern-Simons-like terms [4,47,48,66], radiative corrections giving mass to the photon [67], and corrections to the lamb shift and the electron anomalous magnetic moment [68]. Contributions from coefficients $c_{\mu\nu}$ and $(k_F)_{\mu\rho\nu}{}^\rho$ — as they are phenomelogically indistinguishable — were also studied, for instance, to the photon self-energy [4], to the vertex correction in order to extract bounds using the electron anomalous magnetic moment [69], to the fermion self-energy [42], and to the four-photon "box diagram" where it induces the Euler-Heisenberg lagrangian [70]. Investigations dealing with other coefficients includes, among others, one-loop renormalizability of the full minimal QED extension [40], analysis of vacuum photon splitting [71] and our analysis in the context of gauge anomalies [12], discussed in the previous chapter.

Different features related to radiative corrections have been studied, but few of them have dealt with the associated question of renormalization. Following the previous chapter, our main interest is the renormalization of the minimal Lorentz-violating QED extension. To one-loop order, it was shown in [40] that all *divergences* can be accommodated by renomalization of fields, parameters, and Lorentz-violating coefficients

3. Fermion self-energy of the minimal QED extension

appearing in the starting action. It is our intention to make a further step and treat radiatively induced Lorentz-violating *finite* corrections as well. As a starting point, we consider those from the fermion self-energy as it has a technically simpler structure compared to the photon self-energy or the vertex correction. Despite that, we will see Lorentz violation introduces unexpected new features. On one hand, renormalization introduces modifications of fermion kinematical properties as (finite) operators not present in the tree-level lagrangian are radiatively induced — we emphasize this is *not* the case for the conventional QED fermion self-energy — and interesting experimental signals may be further investigated. On the other hand, even though the theory can be rendered finite, we find some coefficients may not be consistently renormalized by conventional means as some arbitrariness introduced in the renormalization process apparently cannot be adequately fixed.

A very recent investigation [42] dealing with the $c_{\mu\nu}$ and $(k_F)_{\mu\rho\nu}{}^{\rho}$ coefficients has independently found results concordant with ours but using a different approach. They observed the same behavior with respect to the first point mentioned above, and our preliminary results indicates the radiative generation of structures not present in the tree-level lagrangian is a general feature for some other coefficients as well. For the second point we mentioned, our conclusions differ from those in the forementioned reference, where they find introduction of momentum-dependent wave-function renormalization factor adequately renormalizes contribution from $c_{\mu\nu}$ and $(k_F)_{\mu\rho\nu}{}^{\rho}$. Although, in the present work, we could follow this idea, we will see it appears it does not solves the problem for coefficients other than $c_{\mu\nu}$ and $(k_F)_{\mu\rho\nu}{}^{\rho}$.

The outline of this chapter is the following. In Sections 3.1 and 3.2, we reintroduce the framework we used in the previous chapter, but now with focus on its application to the evaluation of the fermion self-energy diagram. In Sec. 3.3, we evaluate the one-loop fermion self-energy, regularizating its divergences and renormalizing the final result by adjusting renormalization factors introduced by counterterms. In the end of this chapter we present our preliminary conclusions and perspectives.

3.1   Framework: Minimal QED extension revisited

The lagrangian $\mathcal{L}$ of the Lorentz- and CPT violating extension of the QED for a single Dirac fermion is based in the same action studied in Chapter 2, and is given by [4]

$$\mathcal{L} = i\,\overline{\psi}(\gamma^\mu + \Gamma_1^\mu)D_\mu\,\psi - \overline{\psi}(m + M_1)\psi$$

$$- \tfrac{1}{4}F^{\mu\nu}F_{\mu\nu} - \tfrac{1}{4}(k_F)_{\mu\nu\rho\sigma}F^{\mu\nu}F^{\rho\sigma} + \tfrac{1}{2}\epsilon^{\mu\nu\rho\sigma}(k_{AF})_\mu A_\nu F_{\rho\sigma}. \tag{3.1}$$

As previously discussed, besides the usual QED terms, lagrangian (3.1) is not invariant under particle Lorentz transformation once it contains constant background fields that break spacetime isotropy. In the photon sector, Lorentz violation is implemented by the last two terms of (3.1), and in the fermion sector it occurs because of the terms related to Γ_1^μ and M_1, defined as

$$\Gamma_1^\mu \;\; \equiv \;\; c^{\lambda\mu}\gamma_\lambda + d^{\lambda\mu}\gamma_5\gamma_\lambda + e^\mu + if^\mu\gamma_5 + \tfrac{1}{2}\,g^{\kappa\lambda\mu}\sigma_{\kappa\lambda},$$

$$M_1 \;\; \equiv \;\; im_5\gamma_5 + a_\mu\gamma^\mu + b_\mu\gamma_5\gamma^\mu + \tfrac{1}{2}\,H_{\mu\nu}\sigma^{\mu\nu}. \tag{3.2}$$

Terms with coefficients of even (odd) number of indexes respect (do not respect) CPT symmetry. Coefficients $(k_F)_{\mu\nu\rho\sigma}$ and those appearing in Γ_1^μ are dimensionless, while $(k_{AF})_\mu$ and the ones in M_1 have dimension of mass. The trace part of $c_{\mu\nu}$ and $d_{\mu\nu}$ is Lorentz invariant and amounts only to redefinitions of the fermion field, thus can be set as zero; $H_{\mu\nu}$ and the first two indices of $g_{\mu\nu\rho}$ are antisymmetric; $(k_F)_{\mu\nu\rho\sigma}$ have the symmetries of the Riemann tensor,

$$(k_F)_{\mu\nu\rho\sigma} = -(k_F)_{\nu\mu\rho\sigma} = -(k_F)_{\mu\nu\sigma\rho} = (k_F)_{\rho\sigma\mu\nu},$$

$$(k_F)_{\mu\nu\rho\sigma} + (k_F)_{\mu\sigma\nu\rho} + (k_F)_{\mu\rho\sigma\nu} = 0, \tag{3.3}$$

and can be taken as double traceless $(k_F)^{\mu\nu}{}_{\mu\nu} = 0$, otherwise it would lead to a mere redefinition of the photon field; at last, m_5 is Lorentz-invariant and can actually be reabsorbed by other coefficients after a chiral rotation $\psi \rightarrow \exp\left(-\tfrac{i}{2}\gamma_5 \tan^{-1}\tfrac{m_5}{m}\right)\psi$,

3. Fermion self-energy of the minimal QED extension

thus is it uninteresting to our analysis and will not be considered. Other effects of field redefinitions will be discussed below.

Additionally, lagrangian (3.1) will be considered together with an infrared (IR) regulator term, $\frac{1}{2}\lambda^2 A_\mu A^\mu$, by means of a photon mass λ, and also a gauge-fixing parameter α by means of $-\frac{1}{2\alpha}\left(\partial_\mu A^\mu\right)^2$. For simplicity, we work in the $\alpha = 1$ gauge.

A very interesting feature of lagrangian (3.1) is related to fermion field redefinitions [3,4,25,75–77,107] of the form $\psi \to [1 + Z(x, \partial)]\psi$, where $Z(x, \partial)$ is a 4×4 matrix linear in the coordinates and derivatives, with dependence on Lorentz-violating coefficients. These redefinitions reveal some coefficients are not observable at leading order in Lorentz violation, some are not observable to all orders, and also that only some specific coefficient combinations are observable. We restrict the following discussion for flat spacetime QED with a single Dirac fermion.

Coefficients a^μ, e^μ, the antisymmetric part $c_A^{\mu\nu}$ of $c^{\mu\nu}$ and the trace part of $g^{\kappa\lambda\mu}$, $g_T^{\kappa\lambda\mu} \equiv \frac{1}{3}(g^{\kappa\alpha}{}_\alpha\eta^{\lambda\mu} - g^{\lambda\alpha}{}_\alpha\eta^{\kappa\mu})$, can be removed at leading order [75], and f^μ can be removed to all orders in Lorentz violation [76]. Physically, we say these coefficients are *unobservable* at leading order (and to all orders in the case of f^μ).

Besides removing *unobservable* coefficients, those redefinitions also reveal the only *observable* coefficient combinations [75],

$$c_S^{\mu\nu} \equiv \tfrac{1}{2}(c_{\mu\nu} + c_{\nu\mu}),$$

$$d_S^{\mu\nu} \equiv \tfrac{1}{2}(d_{\mu\nu} + d_{\nu\mu}),$$

$$g_M^{\kappa\lambda\mu} \equiv \tfrac{1}{3}(g^{\kappa\lambda\mu} + g^{\kappa\mu\lambda} + \eta_{\alpha\beta}g^{\lambda\alpha\beta}\eta^{\kappa\mu}) - (\kappa \leftrightarrow \lambda),$$

$$b^\kappa - mg_A^\kappa,$$

$$H_{\kappa\lambda} - \tfrac{1}{2}m\epsilon_{\kappa\lambda\mu\nu}d_A^{\mu\nu}, \tag{3.4}$$

where the first and second line defines the symmetric part of $c^{\mu\nu}$ and $d^{\mu\nu}$, respectively; the third line defines the mixed-symmetry representation $g_M^{\kappa\lambda\mu}$ of $g^{\kappa\lambda\mu}$, and in the fourth line we have defined its axial representation, $g_A^\kappa = -\frac{1}{6}\epsilon^\kappa{}_{\lambda\mu\nu}g_A^{\lambda\mu\nu}$ where $g_A^{\kappa\lambda\mu} \equiv \frac{1}{6}g^{\nu\rho\sigma}\epsilon_{\nu\rho\sigma\alpha}\epsilon^{\alpha\kappa\lambda\mu}$; and in the last line we have defined the antisymmetric part $d_A^{\mu\nu}$ of $d^{\mu\nu}$. After field redefinitions of the form mentioned above, and in terms of coeffi-

3. Fermion self-energy of the minimal QED extension

cient combinations (3.4), lagrangian (3.1) can be rewritten in terms of only physically observable coefficient combinations,

$$
\begin{aligned}
\mathcal{L} \to \mathcal{L} = {}& \overline{\psi}\Big(i\slashed{\partial} - m\Big)\psi + \overline{\psi}\Big(c_S^{\mu\nu}\gamma_\mu + d_S^{\mu\nu}\gamma_5\gamma_\mu + \tfrac{1}{2}g_M^{\kappa\lambda\nu}\sigma_{\kappa\lambda}\Big)i\partial_\nu\psi \\
& - \tfrac{1}{4}\Big(\tfrac{1}{2}\epsilon_{\kappa\lambda\rho\sigma}d_A^{\rho\sigma} - \tfrac{1}{m}H_{\kappa\lambda}\Big)\overline{\psi}\Big(\epsilon^{\kappa\lambda\mu\nu}\gamma_5\gamma_\mu i\partial_\nu - m\sigma^{\kappa\lambda}\Big)\psi \\
& + \tfrac{1}{2}\Big(g_A^\mu - \tfrac{1}{m}b^\mu\Big)\overline{\psi}\Big(\tfrac{1}{2}\epsilon_{\kappa\lambda\mu\nu}\sigma^{\kappa\lambda}i\partial_\nu + m\gamma_5\gamma_\mu\Big) \\
& - \tfrac{1}{4}F^{\mu\nu}F_{\mu\nu} - \tfrac{1}{4}(k_F)_{\mu\nu\rho\sigma}F^{\mu\nu}F^{\rho\sigma} + \tfrac{1}{2}\epsilon^{\mu\nu\rho\sigma}(k_{AF})_\mu A_\nu F_{\rho\sigma}. \quad (3.5)
\end{aligned}
$$

Therefore, not all coefficients can be individually accessed in experiments, and some are intrinsically entangled with others — for instance, $d_A^{\mu\nu}$ and $H^{\mu\nu}$. In a purely practical point of view, coefficient combinations appearing in (3.5) can be redefined as new and fully observable coefficients. Additionally, it turns out that only the combination $2c_S^{\mu\nu} - (k_F)^{\mu\rho\nu}{}_\rho$ is observable [78], and also that $(k_{AF})^\mu$ may relate to b^μ and $g_A^{\kappa\lambda\mu}$.

We emphasize our starting point for evaluation of the fermion self-energy will *not* be the redefined lagrangian (3.5), instead we start from the original lagrangian (3.1) with all *fundamental* coefficients, as we call them. Therefore, as an extra consistency check of our calculations, our results for *observable* quantities must be in accordance with what should be expected from (3.5).

The lagrangian (3.5) for the observable coefficient combinations reveals important information related to its renormalization that was previously hidden. First of all, coefficients appearing in (3.1) are not independent at all, and are related to other coefficients by field redefinitions, therefore we can expect a mixing of the fundamental coefficients as they are renormalized.

No feature related to theoretical consistency or any measurable quantity can be affected by radiative corrections from unobservable coefficients. For instance, no contribution from f^μ to the fermion self-energy can raise new technical issues related to renormalization. Indeed, we will find none.

Because of field redefinitions, as a specific example, renormalization of contributions from $d^{\mu\nu}$ should exhibit two different behaviors — one for $d_S^{\mu\nu}$ and another for $d_A^{\mu\nu}$. In particular, only radiative corrections from $d_A^{\mu\nu}$ may mix with the ones from $H^{\mu\nu}$,

3. Fermion self-energy of the minimal QED extension

and divergences associated with one of them may eventually be cancelled by counterterms associated with the other, and vice-versa. The same is to be expected for other coefficients that mix under field redefinitions, and that is indeed what is found.

Finally, one issue is to be expected. As we will see, in order to fix free parameters introduced in the renormalization process, *two* renormalization conditions will be imposed in the fermion self-energy. As for the conventional case, these conditions are motivated by the appearance of *two* divergences, one proportional to $\not{p}$ and another to $m \times \mathbb{1}$, which demands *two* counterterms, each one carrying a free parameter to be fixed. In complete analogy to the conventional case, two renormalization conditions will be imposed on the complete fermion self-energy corrected by Lorentz-violating terms, which comprise individual contribution from all coefficients appearing in (3.1) and each of these contributions have to satisfy the same renormalization conditions. An issue introduced by Lorentz violation is that contribution from some coefficients demands only a single independent counterterm, effectively introducing only one free parameter, as can be readily guessed from the redefined lagrangian (3.5). For instance, because of the mixing between $d_A^{\mu\nu}$ and $H^{\mu\nu}$, two counterterms appear for each of these coefficients, proportional to $(p_\mu \gamma_5 \gamma_\nu - p_\nu \gamma_5 \gamma_\mu)$ and $\epsilon_{\mu\nu\rho\sigma}\sigma^{\rho\sigma}$, and each coefficient receives two free parameters, thus the two renormalization conditions can be fixed without any problem. On the other hand, $d_S^{\mu\nu}$ is a "single" coefficient, and its contribution receives only one counterterm proportional to $(p_\mu \gamma_5 \gamma_\nu + p_\nu \gamma_5 \gamma_\mu)$, leading to only one free parameter — the same happens to all other "single" fermionic coefficients in (3.5). Typically, we cannot fix two conditions with a single free parameter. In these cases, renormalization of those contributions fails to be consistent if we are to follow conventional procedures. On the other hand, contribution from f^μ, for instance, has a single free parameter but is not problematic because it turns out it satisfies both renormalization conditions trivially, *i.e.*, for any choice of its single free parameter — we will see this is a feature of all unobservable coefficients.

3.2   Set up for one-loop evaluations

Inclusion of Lorentz-violating interactions, as in lagrangian (3.1), leads to new Feynman rules, as previous discussed in Sec. 2.1.3. In that case, our focus was on one-particle irreducible (1PI) diagrams, where external legs are cut off, and because of the experimentally known smallness of upper bounds on the relevant Lorentz-violating terms of the lagrangian (3.1), those where taken as new interactions vertices, small perturbations on the conventional QED. This approach effectively introduces a set of new Feynman rules for Lorentz-violating insertions in propagator *internal* lines for a fermion of momentum p^μ,

$$\longrightarrow \textcolor{red}{\times} \longrightarrow \quad = \quad -iM_1, \tag{3.6}$$

$$\longrightarrow \bullet \longrightarrow \quad = \quad i\,\Gamma_1^\mu p_\mu, \tag{3.7}$$

and a photon of momentum k^μ,

$$\mu \wwave \bullet \wwave \nu \quad = \quad -2ik^\kappa k^\lambda (k_F)_{\kappa\mu\lambda\nu}, \tag{3.8}$$

$$\mu \wwave \textcolor{red}{\times} \wwave \nu \quad = \quad 2(k_{AF})^\kappa \epsilon_{\kappa\mu\lambda\nu} k^\lambda, \tag{3.9}$$

and in vertices,

$$\quad = \quad -ie\Gamma_1^\mu. \tag{3.10}$$

In this case, it would be less attractive to consider higher order Lorentz violation contributions to one-loop diagrams as they may be of the same order of magnitude as higher loop corrections, which we disregard in the present analysis.

The above approach is insufficient for all of our goals in this chapter. Evaluation of one-loop integrals from 1PI diagrams can be consistently performed with above considerations, but as we are looking for effects of finite radiative corrections, *external* legs are to be considered in order to determine full propagators, which must be constructed starting from tree-level propagators taking into account Lorentz violation to all orders

3. Fermion self-energy of the minimal QED extension

for a consistent use of the LSZ reduction formula [74].

As for the fermion self-energy, the external lines are fermionic only, thus the relevant complete tree-level propagator and corresponding Feynman rule are given by

$$\Longrightarrow = iS_F(p) = \frac{i}{\not{p} + \Gamma_1 \cdot p - m - M_1}. \tag{3.11}$$

Naturally, we could use this propagator for internal lines of loop diagrams as well, but as discussed before, for this case it is reasonable to consider Lorentz violation small enough to enter as insertions on the conventional QED fermion propagator,

$$\tag{3.12}$$

where $\longrightarrow = \frac{i}{\not{p}-m}$ is the conventional fermion propagator, and keep it only to first order in Lorentz-violation for *internal* lines of one-loop diagrams. Along with an analogous approach for the photon propagator, we recover the Feynman rules from (3.6) to (3.9).

As in conventional QED calculations, Feynman diagrams containing Lorentz-violating insertions may contain ultraviolet (UV) divergences, therefore an adequate regularization is required. We use dimensional regularization [72], as its techniques are not changed considering our approach to loop integrals with Lorentz-violating insertions. All integrals are still functions of internal momenta only, which behaves covariantly, and the role of Lorentz-violating coefficients is restricted to index contraction with results of these integrals.

Often divergent integrals come in conjunction to γ_5 matrices, whose properties are dimension dependent, raising potential complications during dimensional regularization where integrals are generalized to an arbitrary dimension d. Our approach for the generalization of γ_5 to d dimensions is to use 't Hooft-Veltman's definition of

γ_5 [73],

$$\{\gamma^\mu, \gamma_5\} = 0, \quad \mu = \{0, 1, 2, 3\},$$

$$[\gamma^\mu, \gamma_5] = 0, \quad \mu \geqslant 4. \tag{3.13}$$

By means of this definition, γ matrices can be conveniently split in two pieces, $\gamma^\mu = \overline{\gamma}^\mu + \widehat{\gamma}^\mu$, where

$$\overline{\gamma}^\mu = \begin{cases} \gamma^\mu, & \mu = \{0, 1, 2, 3\} \\ 0, & \mu \geqslant 4 \end{cases}, \quad \text{and} \quad \widehat{\gamma}^\mu = \begin{cases} 0, & \mu \leqslant 4 \\ \gamma^\mu, & \mu \geqslant 4 \end{cases}, \tag{3.14}$$

which amounts to a set of γ matrices for the first four dimensions and another orthogonal set for higher dimensions, respectively. These definitions introduce a technical breaking of Lorentz invariance in all dimensions except the first four. Nevertheless, no extra physical feature is introduced in our perturbative approach for Lorentz violation as the integrals to be regularized have conventional Lorentz properties.

3.3 One-loop fermion self-energy

The conventional QED fermion self-energy diagram is illustrated in Fig. 3.1. Lorentz violation modify it by means of replacing the conventional *external* leg ——▸—— by the complete Lorentz-violating tree-level propagator ══▸══, see (3.12), and also by propagator insertions in *internal* lines and vertex insertions, according to rules from (3.6) to (3.10). For the moment, we are interested only in *amputated* diagrams, those with external legs cut off. Therefore, the diagrams we have to compute are the amputated version of the conventional Lorentz-symmetric diagram of Fig. 3.1 and the Lorentz-violating diagrams of Fig. 3.2.

The Feynman rules are like the conventional QED ones along with extra interactions for internal line propagators and vertices, as dictated by rules from (3.6) to (3.10), as mentioned above. For instance, diagram (1) only differs from the conventional one

3. Fermion self-energy of the minimal QED extension
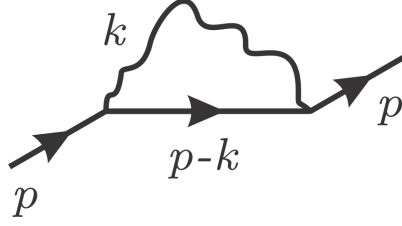
Figure 3.1: Conventional fermion self-energy diagram.

(1)   **(2)**   **(3)**

(4)   **(5)**   **(6)**
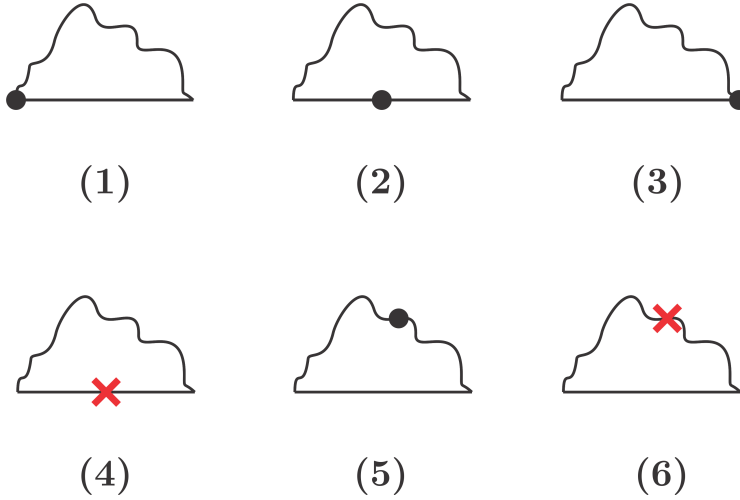
Figure 3.2: Lorentz-violating insertions in the one-loop fermion self-energy.

of Fig. 3.1 by modifying the vertex at the left side, from $-ie\gamma_\nu$ to $-ie\Gamma_{1\nu}$, such that

$$- i\Sigma^{(1)}(p) = \int \frac{d^4k}{(2\pi)^4} \frac{-i\eta^{\mu\nu}}{k^2 - \lambda^2}(-ie\gamma_\mu)\frac{i}{\not p - \not k - m}(-ie\Gamma_{1\nu}), \qquad (3.15)$$

and we note that the superficial degree of divergence of the integral remains the same as we have inserted a dimensionless Lorentz-violating coefficient. On the other hand, propagator insertions of mass dimension one coefficients make the integral more convergent. Diagram (6), for instance, has an insertion in the photon line,

$$- i\Sigma^{(6)}(p) = \int \frac{d^4k}{(2\pi)^4} \frac{-i\eta^{\mu\rho}}{k^2 - \lambda^2}\left[2(k_{AF})^\kappa \epsilon_{\kappa\rho\lambda\sigma}k^\lambda\right] \frac{-i\eta^{\sigma\nu}}{k^2 - \lambda^2}(-ie\gamma_\mu)\frac{i}{\not p - \not k - m}(-ie\gamma_\nu),$$
$$(3.16)$$

effectively introducing an extra momentum factor in the denominator.

As in conventional QED, it turns out the integrals associated with diagrams

from Figs. 3.1 and 3.2 contain divergences in the high momenta, ultraviolet region. As discussed in the previous section, to give meaningful results, our approach is based on the use of *dimensional regularization* to isolate the infinities as poles at $\varepsilon \to 0$ — where ε is a regulator introduced to render finite the integrals as long as $\varepsilon \neq 0$ — and later remove the divergences by means of a renormalization of parameters appearing in the lagrangian (3.1). In the next section, we go through the intermediate step of regularization of divergences.

3.3.1 Regularization

Evaluation of Feynman diagrams with Lorentz-violating insertions can be done with the same techniques used for conventional QED calculations. To illustrate this point and also to introduce some definitions, in the following we evaluate diagram (2) using dimensional regularization. This diagram is given by the integral

$$- i\Sigma^{(2)}(p) = \int \frac{d^4k}{(2\pi)^4} \frac{-i\eta^{\mu\nu}}{k^2 - \lambda^2} (-ie\gamma_\mu) \frac{i}{\not{p} - \not{k} - m} i\Gamma_1^\rho(p-k)_\rho \frac{i}{\not{p} - \not{k} - m}(-ie\gamma_\nu), \quad (3.17)$$

and its generalization to d dimensions reads

$$-i\Sigma_{reg}^{(2)}(p) = \int \frac{d^dk}{(2\pi)^d} \frac{-i\eta^{\mu\nu}}{k^2 - \lambda^2} (-ie\mu^{2-\frac{d}{2}}\gamma_\mu) \frac{i}{\not{p} - \not{k} - m} i\Gamma_1^\rho(p-k)_\rho \frac{i}{\not{p} - \not{k} - m}(-ie\mu^{2-\frac{d}{2}}\gamma_\nu)$$

$$= (e\mu^{2-\frac{d}{2}})^2 \int \frac{d^dk}{(2\pi)^d} \frac{1}{k^2 - \lambda^2} \frac{1}{[(p-k)^2 - m^2]^2} \gamma^\mu(\not{p} - \not{k} + m)\Gamma_1^\rho(p-k)_\rho(\not{p} - \not{k} + m)\gamma_\mu,$$

$$(3.18)$$

where the mass parameter μ was introduced to give the correct dimension to the electric charge e in d dimensions, and effectively introduces an arbitrary mass scale. Feynman parameters can be introduced as usual to combine the denominators,

$$\frac{1}{k^2 - \lambda^2} \frac{1}{[(p-k)^2 - m^2]^2} = 2 \int_0^1 dx \int_0^1 dy \delta(x+y-1) \frac{y}{(\ell^2 - \Delta)^3}, \quad (3.19)$$

where we have already performed a shift in the integration variable k, $k \to \ell \equiv k - yp$, and defined $\Delta \equiv -\overline{x}(p^2x - m^2) + \lambda^2 x$ where $\overline{x} \equiv 1 - x$. The shift in k also changes the

3. Fermion self-energy of the minimal QED extension

product of matrices in the second equality of (3.18),

$$\gamma^\mu(\not{p} - \not{k} + m)\Gamma_1^\rho(p-k)_\rho(\not{p} - \not{k} + m)\gamma_\mu$$
$$\longrightarrow \gamma^\mu\gamma^\alpha\Gamma_1^\lambda\gamma^\beta\gamma_\mu\Big[(1-y)^3 p_\alpha p_\beta p_\lambda + (1-y)\ell_\rho\ell_\sigma\Big(p_\alpha\delta^\rho{}_\lambda\delta^\sigma{}_\beta + p_\lambda\delta^\rho{}_\alpha\delta^\sigma{}_\beta + p_\beta\delta^\rho{}_\alpha\delta^\sigma{}_\lambda\Big)\Big]$$
$$+ m\gamma^\mu\{\gamma^\rho, \Gamma_1^\sigma\}\gamma_\mu\Big[(1-y)^2 p_\rho p_\sigma + \ell_\rho\ell_\sigma\Big] + m^2(1-y)p_\nu\gamma_\mu\Gamma_1^\nu\gamma_\mu, \qquad (3.20)$$

where linear terms in ℓ_μ were not written foreseeing the integration in $d^d\ell$ is spherically symmetric thus only even powers of ℓ contribute. Integral (3.18) now reads

$$-i\Sigma_{reg}^{(2)}(p) = 2(e\mu^{2-\frac{d}{2}})^2 \int_0^1 dx\overline{x} \int \frac{d^d\ell}{(2\pi)^d}\left[\frac{1}{(\ell^2-\Delta)^3} \times \text{Eq.}(3.20)\right]_{y=\overline{x}}. \qquad (3.21)$$

The integration in ℓ has the general form $\int d^d\ell(\ell_\mu\ell_\sigma\cdots)/(\ell^2-\Delta)^n$ and the solutions are well-known — for instance, see Appendix A of [79]. Defining $\varepsilon = 2 - \frac{d}{2}$ and the fine-structure constant $\alpha = \frac{e^2}{4\pi}$, the result is

$$\Sigma_{reg}^{(2)}(p) = -\frac{\alpha}{4\pi}\int_0^1 dx\overline{x}\,\Gamma(\varepsilon)\left(\frac{4\pi\mu^2}{\Delta}\right)^\varepsilon\Big[x\gamma^\mu\gamma^\alpha\Gamma_1^\lambda\gamma^\beta\gamma_\mu\Big(p_\alpha\eta_{\beta\lambda} + p_\lambda\eta_{\alpha\beta} + p_\beta\eta_{\alpha\lambda}\Big)$$
$$+ m\gamma^\mu\{\gamma_\nu, \Gamma_1^\nu\}\gamma_\mu\Big]$$
$$+ \frac{\alpha}{4\pi}\int_0^1 dx\,\frac{\overline{x}}{\Delta}\Big[x^3 p_\nu\gamma^\mu\not{p}\Gamma_1^\nu\not{p}\gamma_\mu + mx^2 p_\nu\gamma^\mu\{\not{p}, \Gamma_1^\nu\}\gamma_\mu + m^2 x p_\nu\gamma^\mu\Gamma_1^\nu\gamma_\mu\Big]. \qquad (3.22)$$

The gamma function $\Gamma(\varepsilon)$ is singular as $\varepsilon \to 0$, $\Gamma(\varepsilon) = \frac{1}{\varepsilon} - \gamma_E + \mathcal{O}(\varepsilon)$, where $\gamma_E = 0.577216\ldots$ is the Euler-Mascheroni constant. Along with $a^\varepsilon = 1 + \varepsilon\ln a + \mathcal{O}(\varepsilon)$, we have

$$\Gamma(\varepsilon)\left(\frac{4\pi\mu^2}{\Delta}\right)^\varepsilon = \frac{1}{\varepsilon} - \gamma_E + \ln\left(\frac{4\pi\mu^2}{\Delta}\right) + \mathcal{O}(\varepsilon). \qquad (3.23)$$

In Eq. (3.22), the second integral is perfectly finite in the UV region ($\varepsilon \to 0$), but the first one may contain divergences as bad as $\frac{1}{\varepsilon}$. Evaluation of all other diagrams in Fig. 3.2 are done in completely analogous way.

At this point in the evaluation of self-energy diagrams, we can go no further without considering individual Lorentz-violating coefficients contained in M_1 and Γ_1^μ, along with $(k_{AF})^\mu$ and $(k_F)^{\mu\nu\rho\sigma}$. Each coefficient comes with a different γ matrix structure, formed by any of the 16 linearly independent matrices of the basis

3. Fermion self-energy of the minimal QED extension

$\{\mathbb{1}, \gamma_5, \gamma_\mu, \gamma_5\gamma_\mu, \sigma_{\mu\nu} = \frac{i}{2}[\gamma_\mu, \gamma_\nu]\}$, as in definitions (3.2). As an intermediate step, before proceeding to the removal of the divergences $\frac{1}{\varepsilon}$ and renormalization of parameters, simplification of products of γ matrices — as the ones in (3.22) — to the fundamental basis is needed because they can generate factors of ε in the numerators as we are working in $d = 2(2-\varepsilon)$ dimensions. This task presents no technical difficulty, but it is lengthy and tedious due the extensive use of relations between γ matrices, making the use of computer programs a valuable tool for this end. For the results to be presented, we used the package $FeynCalc$ [80] for the software $Mathematica$ to perform algebraic manipulations with γ matrices. Because of limitations of the mentioned package, manipulations involving γ_5 in divergent integrals had to be done by hand using the 't Hooft-Veltman approach based in (3.13).

The complete contribution of first-order Lorentz violation to the one-loop fermion self-energy is the sum of all diagrams of Fig. 3.2. For practical reasons, we write $\Sigma_x(p)$ to represent the total contribution of each individual Lorentz-violating coefficient x. As an example, Σ_a is given by only the a_μ contribution to $\Sigma^{(4)}$, and Σ_c is obtained by the sum $\Sigma^{(1)} + \Sigma^{(2)} + \Sigma^{(3)}$ with only $c_{\mu\nu}$ insertions.

Finally, in the Lorentz-violating QED (3.1), the conventional regularized one-loop fermion self-energy,

$$\Sigma_{\text{QED}} = \frac{\alpha}{2\pi}\left\{ \not{p}\left[-\frac{1}{2}\left(\frac{1}{\varepsilon} - \gamma_E - 1\right) - \int_0^1 dx\, x \ln\left(\frac{4\pi\mu^2}{\Delta}\right)\right]\right.$$
$$\left. + m\left[2\left(\frac{1}{\varepsilon} - \gamma_E - \frac{1}{2}\right) + 2\int_0^1 dx \ln\left(\frac{4\pi\mu^2}{\Delta}\right)\right]\right\}, \qquad (3.24)$$

is corrected, to first order in Lorentz violation, by the sum of the following:

$$\Sigma_a(p) = \frac{\alpha}{2\pi}\left\{ \not{a}\left[\frac{1}{2}\left(\frac{1}{\varepsilon} - \gamma_E - 2\right) + \int_0^1 dx\, \overline{x} \ln\left(\frac{4\pi\mu^2}{\Delta}\right) - \int_0^1 dx\, \frac{\overline{x}}{\Delta}\left(x^2 p^2 - m^2\right)\right]\right.$$
$$\left. + 2a\cdot p \int_0^1 dx\, \frac{\overline{x}x}{\Delta}\left(\not{p}x - 2m\right)\right\}, \qquad (3.25)$$

3. Fermion self-energy of the minimal QED extension

$$\Sigma_b(p) = \frac{\alpha}{2\pi}\left\{\gamma_5\slashed{p}\left[\frac{1}{2}\left(\frac{1}{\varepsilon}-\gamma_E+2\right)+\int_0^1 dx\,\overline{x}\ln\left(\frac{4\pi\mu^2}{\Delta}\right)-\int_0^1 dx\,\frac{\overline{x}}{\Delta}\left(x^2p^2+m^2\right)\right]\right.$$

$$\left. + 2b\cdot p\gamma_5\slashed{p}\int_0^1 dx\,\frac{\overline{x}x^2}{\Delta}\right\}, \tag{3.26}$$

$$\Sigma_c(p) = \frac{\alpha}{2\pi}\left\{p^\nu\gamma^\mu\left[\left[\frac{1}{6\varepsilon}(4c_{\nu\mu}+c_{\mu\nu})-\frac{1}{6}c_{\nu\mu}\left[4\gamma_E+1-6\int_0^1 dx\,x(2-x)\ln\left(\frac{4\pi\mu^2}{\Delta}\right)\right]\right.\right.\right.$$

$$\left.\left.-\frac{1}{6}c_{\mu\nu}\left(\gamma_E-3+6\int_0^1 dx\,x(1-2x)\ln\left(\frac{4\pi\mu^2}{\Delta}\right)\right)+c_{\mu\nu}\int_0^1 dx\,\frac{\overline{x}x}{\Delta}\left(x^2p^2-m^2\right)\right]\right]$$

$$\left.-2c_{\mu\nu}p^\mu p^\nu\int_0^1\frac{\overline{x}x^2}{\Delta}\left(\slashed{p}x-2m\right)\right\}, \tag{3.27}$$

$$\Sigma_d(p) = \frac{\alpha}{2\pi}\left\{\frac{1}{6}p^\nu\gamma_5\gamma^\mu\left[\left[\frac{1}{\varepsilon}(4d_{\nu\mu}+d_{\mu\nu})-d_{\nu\mu}\left[4\gamma_E-1-6\int_0^1 dx\,x(2-x)\ln\left(\frac{4\pi\mu^2}{\Delta}\right)\right]\right.\right.\right.$$

$$\left.\left.-d_{\mu\nu}\left[\gamma_E+1+6\int_0^1 dx\,x(1-2x)\ln\left(\frac{4\pi\mu^2}{\Delta}\right)\right]+6\,d_{\mu\nu}\int_0^1 dx\,\frac{\overline{x}x}{\Delta}\left(x^2p^2+m^2\right)\right]\right]$$

$$\left.-2d_{\mu\nu}p^\mu p^\nu\gamma_5\slashed{p}\int_0^1\frac{\overline{x}x^3}{\Delta}+\frac{1}{4}md_{\mu\nu}\epsilon^{\mu\nu\rho\sigma}\sigma_{\rho\sigma}\left[\frac{2}{\varepsilon}-2\gamma_E+1+2\int_0^1 dx\ln\left(\frac{4\pi\mu^2}{\Delta}\right)\right]\right\}, \tag{3.28}$$

$$\Sigma_e(p) = \frac{\alpha}{2\pi}\left\{e\cdot p\left[-\frac{1}{2}\left(\frac{1}{\varepsilon}-\gamma_E-\frac{5}{3}\right)-\int_0^1 dx(6-7x)\ln\left(\frac{4\pi\mu^2}{\Delta}\right)\right.\right.$$

$$\left.+2\int_0^1 dx\,\frac{\overline{x}x}{\Delta}\left(p^2x^2-m\slashed{p}x+m^2\right)\right]$$

$$\left.+m\slashed{e}\left[\frac{1}{2}\left(\frac{3}{\varepsilon}-3\gamma_E-1\right)+\int_0^1 dx(2-x)\ln\left(\frac{4\pi\mu^2}{\Delta}\right)\right]\right\}, \tag{3.29}$$

$$\Sigma_f(p) = \frac{\alpha}{2\pi}if\cdot p\gamma_5\left[-\frac{1}{2}\left(\frac{1}{\varepsilon}-\gamma_E+\frac{5}{3}\right)-\int_0^1 dx\,x(5-6x)\ln\left(\frac{4\pi\mu^2}{\Delta}\right)\right.$$

$$\left.+2\int_0^1 dx\,\frac{\overline{x}x}{\Delta}\left(p^2x^2-m^2\right)\right], \tag{3.30}$$

3. Fermion self-energy of the minimal QED extension

$$\Sigma_g(p) = \frac{\alpha}{2\pi}\left\{ -\frac{1}{4}p^\mu\sigma^{\kappa\lambda}\left[-g_{\kappa\lambda\mu}\left(\frac{1}{\varepsilon}-\gamma_E+\frac{1}{3}\right)-(g_{\kappa\mu\lambda}-g_{\lambda\mu\kappa})\left(\frac{1}{\varepsilon}-\gamma_E-\frac{1}{3}\right)\right.\right.$$

$$\left.+\frac{1}{2}(g_{\kappa\nu}{}^\nu\eta_{\mu\lambda}-g_{\lambda\nu}{}^\nu\eta_{\mu\kappa})\left(\frac{1}{\varepsilon}-\gamma_E+\frac{1}{3}\right)\right]$$

$$-\frac{1}{2}p^\mu\sigma^{\kappa\lambda}\left[-g_{\kappa\lambda\mu}-(g_{\kappa\mu\lambda}-g_{\lambda\mu\kappa})+\frac{1}{2}(g_{\kappa\nu}{}^\nu\eta_{\mu\lambda}-g_{\lambda\nu}{}^\nu\eta_{\mu\kappa})\right]\int_0^1 dx\,x\ln\left(\frac{4\pi\mu^2}{\Delta}\right)$$

$$+\frac{1}{2}mg_{\kappa\lambda\mu}\epsilon^{\kappa\lambda\mu\nu}\gamma_5\gamma_\nu\left[\frac{1}{2}\left(\frac{1}{\varepsilon}-\gamma_E-1\right)+\int_0^1 dx\,x\ln\left(\frac{4\pi\mu^2}{\Delta}\right)\right]$$

$$\left.-mg_{\kappa\lambda\mu}\epsilon^{\kappa\lambda\nu\rho}p^\mu p_\rho\gamma_5\gamma_\nu\int_0^1 dx\,\frac{\overline{x}x^2}{\Delta}\right\}, \tag{3.31}$$

$$\Sigma_H(p) = \frac{\alpha}{2\pi}mH_{\kappa\lambda}\epsilon^{\kappa\lambda\mu\nu}p_\nu\gamma_5\gamma_\mu\int_0^1 dx\,\frac{\overline{x}x}{\Delta}, \tag{3.32}$$

$$\Sigma_{k_{AF}}(p) = \frac{\alpha}{2\pi}\left\{\gamma_5\slashed{k}_{AF}\left[-\frac{3}{2}\left(\frac{1}{\varepsilon}-\gamma\right)+3\int_0^1 dx\,x\ln\left(\frac{4\pi\mu^2}{\Delta}\right)-2p^2\int_0^1 dx\,\frac{\overline{x}x^2}{\Delta}\right]\right.$$

$$\left.+2k_{AF}\cdot p\gamma_5\slashed{p}\int_0^1 dx\,\frac{\overline{x}x^2}{\Delta}+m(k_{AF})_\mu\epsilon^{\mu\nu\rho\sigma}p_\nu\sigma_{\rho\sigma}\int_0^1 dx\,\frac{\overline{x}x}{\Delta}\right\}, \tag{3.33}$$

$$\Sigma_{k_F}(p) = -\frac{\alpha}{3\pi}(k_F)_{\mu\rho\nu}{}^\rho p^\mu\gamma^\nu\left[\frac{1}{\varepsilon}-\gamma_E+\frac{3}{2}\int_0^1 dx\,x(2-x)\ln\left(\frac{4\pi\mu^2}{\Delta}\right)\right]$$

$$-\frac{\alpha}{2\pi}(k_F)_{\mu\rho\nu}{}^\rho p^\mu p^\nu\int_0^1 dx\,\frac{\overline{x}^2x}{\Delta}(\slashed{p}x-m). \tag{3.34}$$

It is worth mentioning that our results for the *divergent* corrections — the ones proportional to $\frac{1}{\varepsilon}$ — are in agreement with the ones found in Ref. [40]. Our original contribution comes from the finite corrections, requiring a more involved analysis of the self-energy corrections, which we perform in the next section. Removal of the divergences are essential to produce a meaningful theory, and fixing the arbitrariness introduced during regularization is equally important. Although in the conventional case both are fully taken care by means of renormalization of the fields and parameters in the original lagrangian without modifying the dynamics of free fermions, we will see that introduction of Lorentz violation will lead to new features — the modification of the effective kinematics of fermions — and some issues — the apparent impossibility of consistently renormalizing the contribution from some coefficients.

3.3.2 Renormalization

The intent of the *regularization* procedure just performed is to isolate the divergences associated with the processes illustrated in Figs. 3.1 and 3.2, and the next step is the *renormalization* of parameters appearing in the Lorentz-violating QED lagrangian (3.1), which will suffice to render the model UV finite.

For the renormalization and removal of the divergences $\frac{1}{\varepsilon}$, we first write the *full* fermion propagator, which is obtained after summing the infinite series of radiative correction to all loop orders and to arbitrarily (but finite) high order in Lorentz violation,

$$
\begin{aligned}
&\equiv iS_{\mathrm{F}}(p) + iS_{\mathrm{F}}(p)[-i\Sigma_{\mathrm{reg}}(p)]iS_{\mathrm{F}}(p) + \ldots \\
&= \frac{i}{\not{p} - m + \Gamma_1 \cdot p - M_1 - \Sigma_{\mathrm{reg}}(p)},
\end{aligned}
\tag{3.35}
$$

where $\Sigma_{\mathrm{reg}}(p)$ is the *regularized* fermion self-energy, defined as the sum of the regularized conventional QED self-energy and its Lorentz-violating corrections, calculated to all orders in loop expansion and Lorentz violation, and given by

$$
\Sigma_{\mathrm{reg}} = \Sigma_{\mathrm{QED}} + \Sigma_{\mathrm{LV}},
\tag{3.36}
$$

where, to one-loop order, the conventional QED contribution is given by (3.24) and the Lorentz-violating contribution by

$$
\Sigma_{\mathrm{LV}} = \Sigma_a + \Sigma_b + \Sigma_c + \Sigma_d + \Sigma_e + \Sigma_f + \Sigma_g + \Sigma_H + \Sigma_{k_{AF}} + \Sigma_{k_F},
\tag{3.37}
$$

with individual one-loop contributions given by Eqs. (3.25) to (3.34). The full fermion propagator (3.35) is the quantum-corrected extension of the full tree-level fermion propagator (3.11) and, as we have mentioned before, it is exact to all orders in Lorentz-violating coefficients, as required for consistency with the LSZ reduction formula.

3. Fermion self-energy of the minimal QED extension

Counterterms

Removal of divergences will be done as prescribed by the *counterterm* renormalization procedure, which amounts to add a counterterm lagrangian $\mathcal{L}_{ct}$ to the original one $\mathcal{L}$,

$$\mathcal{L} \longrightarrow \mathcal{L} + \mathcal{L}_{ct}, \tag{3.38}$$

where $\mathcal{L}_{ct}$ is *at least* of order α, and is judiciously chosen to cancel all UV divergences at this order (and higher orders in α in multiloop analysis). Here, we follow the *on mass-shell renormalization scheme* (for short, on shell renormalization), which amounts to specify the divergent *and* finite parts of counterterms, such that divergences in the original theory based in (3.1) are cancelled by counterterms and no dependence in an arbitrary energy scale μ remains after renormalization — it is effectively set at the fermion mass. Other schemes could be used — for instance, the *minimal subtraction* deals with removal of divergences only, without changing finite contributions, effectively keeping the arbitrary energy μ unspecified — but as the on shell scheme for QED has a more evident connection with experiments it seems more suitable for our future purposes of searching for Lorentz-violating signals due to radiative corrections.

The structure of the relevant counterterms for the fermion self-energy calculation can be inferred from the original lagrangian (3.1),

$$\mathcal{L}_{ct} \supset (Z_\psi - 1)\,\overline{\psi} i \slashed{\partial} \psi - (Z_m - 1)\, m \overline{\psi} \psi + \mathcal{L}_{ct(\mathrm{LV})}, \tag{3.39}$$

where the Z factors are (potentially divergent) renormalization factors to be chosen so as to cancel eventual divergences and fix the finite pieces of ⟹⬤⟹ once an energy scale μ — often called *subtraction point* — and suitable *renormalization conditions* are chosen (to be discussed soon), and $\mathcal{L}_{ct(\mathrm{LV})}$ are the counterterms for the Lorentz-violating corrections, to be discussed in the next section.

It is worth a brief note on another equivalent renormalization scheme called *multiplicative* renormalization, which amounts to a reinterpretation of fields and parameters of the original lagrangian as *bare* (divergent) quantities, in the sense they are not observable and must be renormalized to their measured (finite) values. Bare quan-

3. Fermion self-energy of the minimal QED extension

tities are conveniently chosen to absorb the divergences. For instance, the conventional free fermion piece of the lagrangian written in terms of the bare fermion field and its bare mass reads $\overline{\psi}_B \left(i \slashed{\partial} - m_B \right) \psi_B$, where $\psi_B = Z_\psi^{1/2} \psi$ and $m_B = Z_m m$, with ψ and m the finite fermion field and mass, respectively, and a convenient choice of ψ_B and m_B is expected to remove associated divergences. For what is relevant to our analysis, the correspondence from the counterterm renormalization we use to the multiplicative one can be written as $Z_\psi \to Z_\psi$, $Z_m \to Z_\psi^{-1} Z_m$, and $Z_x \to Z_\psi^{-1} Z_x$, where Z_x renormalizes a Lorentz-violating coefficient denoted by x.

At this point we emphasize that, with the exception of Z factors, within the *counterterm* renormalization all parameters in the lagrangian $\mathcal{L}$ and $\mathcal{L}_{\text{ct}}$ are already *finite*, and Z factors coming along with the counterterms — as in Eq. (3.39) — are responsible for removal of divergences and renormalization of the fermion self-energy — and all other processes in a broader analysis.

The renormalization factors Z are of order α or greater, therefore its tree-level contribution gives order α corrections to the full fermion propagator, and it reads

$$
(-i \, \text{━➤━}⬭\text{➤━})^{-1} = \slashed{p} - m + \Gamma_1 \cdot p - M_1
$$
$$
- \left[\Sigma_{\text{QED}} + \Sigma_{\text{LV}} - (Z_\psi - 1)\slashed{p} + (Z_m - 1)m + \cdots \right]
$$
$$
\equiv \slashed{p} - m + \Gamma_1 \cdot p - M_1 - \Sigma_{\text{R}}(p), \tag{3.40}
$$

where the ellipsis comprises Lorentz-violating counterterms and will be made explicit soon, and $\Sigma_{\text{R}}(p)$ is the *finite renormalized* fermion self-energy. Explicit determination of $\Sigma_{\text{R}}(p)$ to one-loop will be done soon.

From previous experience with the conventional QED case, one would expect the Lorentz-violating Σ_{R} to result in mere renormalization of parameters of the tree-level lagrangian — namely, fermion wave-function ψ and mass m, and Lorentz-violating coefficients inside Γ_1^μ and M_1 — nevertheless we will see a *new feature* is introduced by Lorentz violation, namely, the radiative generation by Σ_{R} of new structures *not present* in the tree-level lagrangian (3.1) which effectively changes the free fermion dynamics as it changes its kinematical structure away from the tree-level one.

3. Fermion self-energy of the minimal QED extension

Lorentz-violating counterterms

A look at the lagrangian (3.1) reveals

$$\mathcal{L}_{ct(\text{LV})} \supset \overline{\psi}\left\{\left[(Z_c)^{\mu\nu}{}_{\rho\sigma}c^{\rho\sigma} - c^{\mu\nu}\right]\gamma_\mu + \left[(Z_d)^{\mu\nu}{}_{\rho\sigma}d^{\rho\sigma} - d^{\mu\nu}\right]\gamma_5\gamma_\mu + \left[(Z_e)^\nu{}_\rho e^\rho - e^\nu\right]\right.$$

$$\left. + i\left[(Z_f)^\nu{}_\rho f^\rho - f^\nu\right]\gamma_5 + \frac{1}{2}\left[(Z_g)^{\lambda\mu\nu}{}_{\rho\sigma\tau}g^{\rho\sigma\tau} - g^{\lambda\mu\nu}\right]\sigma_{\lambda\mu}\right\}i\partial_\nu\psi$$

$$- \overline{\psi}\left\{\left[(Z_a)_\mu{}^\nu a_\nu - a_\mu\right]\gamma^\mu + \left[(Z_b)_\mu{}^\nu b_\nu - b_\mu\right]\gamma_5\gamma^\mu\right.$$

$$\left. + \frac{1}{2}\left[(Z_H)^{\mu\nu}{}_{\rho\sigma}H^{\rho\sigma} - H^{\mu\nu}\right]\sigma_{\mu\nu}\right\}\psi \tag{3.41}$$

are the relevant counterterms for the Lorentz-violating part of the self-energy, and the Z factors with indices are Lorentz-violating generalizations of renormalization factors, as introduced in [40]. It will be shown that these counterterms are enough to render the fermion self-energy finite. It is important to note there is no explicit counterterm for $(k_F)^{\mu\nu\rho\sigma}$ or $(k_{AF})^\mu$ as they do not contribute to the tree-level fermion propagator. Nevertheless, a glance at Eqs. (3.27) and (3.34) reveals $c_{\mu\nu}$ and $(k_F)_{\mu\nu\rho\sigma}$ share the same combined structure of momentum and γ matrix, therefore the factor $(Z_c)^{\mu\nu}{}_{\rho\sigma}$ can be adjusted to cancel $(k_F)^{\mu\nu\rho\sigma}$'s divergences as well. The same reasoning applies to b^μ, $g_A^{\mu\nu\rho}$, and $(k_{AF})^\mu$. This also happens to coefficients *within* the same sector: contributions from a_μ and e_μ share the same structure, and analogously the same is true for $H^{\mu\nu}$ and $d_A^{\mu\nu}$. This discussion will be made explicit soon, but this already suggests that Lorentz-violating coefficients *mix* under quantum corrections, and this effect is not limited to the removal of divergences, instead it is a real feature of the renormalization process for the Lorentz-violating QED (3.1). As already mentioned in the end of Sec. 3.1, this feature is intrinsically related to redefinitions of the fermion field ψ.

Determination of the renormalization factors Z are made easier and clearer if we first write them as if each Lorentz-violating contribution $\Sigma_x(p)$ had its own un-mixed factors, and later group together the ones with the same structure. An illus-

3. Fermion self-energy of the minimal QED extension

tration of this point is as follows. The only specific counterterm for the coefficient e_μ is $i\overline{\psi}\Big[(Z_e)^\mu{}_\nu e^\nu - e^\mu\Big]\partial_\mu\psi$ and it will cancel the divergent factor $\frac{1}{\varepsilon}$ that appears together with a p^μ structure in $\Sigma_e(p)$ of Eq. (3.29) and will renormalize the associated finite factors as well. However, $\Sigma_e(p)$ also has a divergent factor associated with a γ^μ structure. It turns out that a_μ has a counterterm $\overline{\psi}\Big[(Z_a)_\mu{}^\nu a_\nu - a_\mu\Big]\gamma^\mu\psi$ which can be adjusted so as to renormalize factors associated with γ^μ in $\Sigma_a(p)$ and *also* in $\Sigma_e(p)$. In this sense, focusing at the structures of $\Sigma_e(p)$, we can conveniently write $(Z_e)^\mu{}_\nu e^\nu p_\mu = (\mathcal{Z}_{e\cdot p})^\mu{}_\nu e^\nu p_\mu$ and $(Z_a)^\mu{}_\nu a^\nu \gamma_\mu \supset (\mathcal{Z}_{\not{e}})^\mu{}_\nu e^\nu \gamma_\mu$. For practical purposes, the renormalized contribution of e^μ to the self-energy will be written as $\Sigma_e^{\mathrm{R}}(p) = \Sigma_e(p) - \Big[(\mathcal{Z}_{e\cdot p})^\mu{}_\nu e^\nu - e^\mu\Big]p_\mu + \Big[(\mathcal{Z}_{\not{e}})^\mu{}_\nu e^\nu - e^\mu\Big]\gamma_\mu$. Once we determine the factors $\mathcal{Z}$, construction of the factors Z is immediate.

Renormalization conditions

Dimensional regularization of the divergent integrals associated with diagrams in Figs. 3.1 and 3.2 isolates divergences as poles in ε and also introduces an arbitrary energy scale μ. These features are naturally introduced in the regularization process, and are fixed by means of renormalization. In particular, introduction of renormalizing factors Z can be made so as to cancel divergences and remove the arbitrariness of μ. Nevertheless, the Z factors naturally introduce finite unspecified parameters due to the freedom on how to remove the divergences. These arbitrary finite contributions have to be fixed, and this is done imposing *renormalization conditions* at a then specified energy scale μ.

In the conventional case, as each counterterm brings up one free parameter, we need as many conditions are there are counterterms. There, the Lorentz-invariant fermion self-energy receives two counterterms, and therefore two conditions are required — we discuss them below. In the Lorentz-noninvariant case, the self-energy receives extra counterterms — one for each Lorentz-violating coefficient if we consider renormalization factors Z or, equivalently, at most two counterterms if we consider $\mathcal{Z}$ factors as discussed before. Only two conditions on the self-energy are still required as each Lorentz-violating correction from different coefficients has to independently

3. Fermion self-energy of the minimal QED extension

satisfy them — more details will be given soon.

Often it is suitable to choose conditions related to the way physical quantities are experimentally measured. For a moment, consider the conventional QED case, where asymptotic states (free particles) are measured, motivating the use of so called *on shell* conditions. Defining the *physical* mass m_P as the *pole* of the full propagator $\frac{i}{\not{p}-m-\Sigma_R(\not{p})}$ sets the condition $\Sigma_R(\not{p})|_{\not{p}=m} = m_P - m$. Demanding the on shell full propagator to have its residue coinciding with the one for the free propagator, the condition $[\partial \Sigma_R(\not{p})/\partial\not{p}]_{\not{p}=m} = 0$ is introduced. These conditions define the pole mass as the physical mass and are independent of the subtraction scheme for the counterterms. Particularly, in the *on shell subtraction* m is chosen to coincide with the physical mass, $m = m_P$, such that the first condition takes the special form $\Sigma_R(\not{p})|_{\not{p}=m_P} = 0$, and the second remains unchanged, but they are now enforced on shell, at values of the momentum p satisfying the Dirac equation, *i.e.*, at $\overline{u}(p)\not{p}u(p) = \overline{u}(p)m_Pu(p)$. This is equivalent to set the subtraction point at $p^2 = m_P^2$, *i.e.*, setting the energy scale at the fermion physical mass, $\mu^2 = m_P^2$.

For the Lorentz-violating full propagator $\frac{i}{\not{p}-m+\Gamma_1\cdot p-M_1-\Sigma_R(p)}$ the situation is analogous, but to exactly parallel the above discussion we would need to find the zero of the function $P(p) = \not{p} - m + \Gamma_1 \cdot p - M_1$, which we define as coinciding with the physical mass. Nevertheless, due to the complexity of $P(p)$ — the explicit dispersion relation is known in the literature [30,36,37] — instead of finding the pole we take a more pragmatic approach and simply impose renormalization conditions on $\Sigma_R(p)$ such that the pole of the full propagator coincides with the zero of $P(p)$. This leads to conditions completely analogous to the conventional case with the sole difference the on shell relation has changed because of Lorentz violation — now it is given by $\overline{u}(p)(\not{p} + \Gamma_1 \cdot p)u(p) = \overline{u}(p)(m + M_1)u(p)$. Therefore, with this choice, the renormalization conditions the Lorentz-violating fermion self-energy has to satisfy are given by

$$\Sigma_R(p)\Big|_{\not{p}+\Gamma_1\cdot p=m+M_1} = 0, \qquad \text{and} \qquad \frac{\partial}{\partial\not{p}}\Sigma_R(p)\Big|_{\not{p}+\Gamma_1\cdot p=m+M_1} = 0, \qquad (3.42)$$

which guarantee the pole of the full propagator coincides with the physical mass, also

3. Fermion self-energy of the minimal QED extension

keeping its residue at i.

As we have seen, the regularized fermion self-energy can be split into conventional and Lorentz-violating pieces, $\Sigma_{\mathrm{reg}} = \Sigma_{\mathrm{QED}} + \Sigma_{\mathrm{LV}}$, as in (3.36). The renormalized conventional QED piece has to satisfy the analogous of conditions (3.42) but for $\Sigma_{\mathrm{QED}}^{\mathrm{R}}$. On the other hand, it turns out the conditions for the renormalized Lorentz-violating contribution $\Sigma_{\mathrm{LV}}^{\mathrm{R}}$ can be approximately taken at the conventional on shell point $\overline{u}(p)\slashed{p}u(p) = \overline{u}(p)mu(p)$, such that

$$\Sigma_{\mathrm{LV}}^{\mathrm{R}}(p)\Big|_{\slashed{p}=m} = 0, \qquad \text{and} \qquad \frac{\partial}{\partial\slashed{p}}\Sigma_{\mathrm{LV}}^{\mathrm{R}}(p)\Big|_{\slashed{p}=m} = 0, \tag{3.43}$$

with errors appearing only at second order in Lorentz violation, which are disregarded in our analysis. Additionally, considering each individual Lorentz-violating coefficient as responsible for an independent contribution to the self-energy as discussed at the end of the previous section, each of these contributions has to separately satisfy the above conditions (3.43). For instance, contributions from a^{μ} and e^{μ} mix under renormalization, but for all practical purposes, with the approach using $\mathcal{Z}$ factors, we can consider Σ_a and Σ_e as being renormalized independently of each other, therefore Σ_a^{R} and Σ_e^{R} must *each* satisfy conditions (3.43). Furthermore, to strengthen this point, we point out the renormalization conditions we have chosen are enforced on shell, and it turns out fermionic coefficients unrelated by field redefinitions do have to independently satisfy these conditions. For instance, a^{μ} and b^{μ} are completely unrelated to each other, and the on shell fermion self-energy contribution from the first is associated with p_{μ} and γ_{μ} structures while contribution from the second is associated with $\gamma_5\gamma_{\mu}$ and $\epsilon_{\mu\nu\rho\sigma}p^{\nu}\sigma^{\rho\sigma}$, therefore it is clear that the contribution of each coefficient to the fermion self-energy must independently satisfy the above renormalization conditions.

Concluding the above discussion, to first order in Lorentz violation, renormalization conditions for $\Sigma_{\mathrm{R}}(p)$ can be written as

(i) $\Sigma_{\mathrm{R}}(p)\Big|_{\slashed{p}+\Gamma_1\cdot p = m+M_1} = \Sigma_{\mathrm{QED}}^{\mathrm{R}}(p)\Big|_{\slashed{p}+\Gamma_1\cdot p = m+M_1} + \Sigma_{\mathrm{LV}}^{\mathrm{R}}(p)\Big|_{\slashed{p}=m} = 0,$

(ii) $\dfrac{\partial}{\partial\slashed{p}}\Sigma_{\mathrm{R}}(p)\Big|_{\slashed{p}+\Gamma_1\cdot p = m+M_1} = \dfrac{\partial}{\partial\slashed{p}}\Sigma_{\mathrm{QED}}^{\mathrm{R}}(p)\Big|_{\slashed{p}+\Gamma_1\cdot p = m+M_1} + \dfrac{\partial}{\partial\slashed{p}}\Sigma_{\mathrm{LV}}^{\mathrm{R}}(p)\Big|_{\slashed{p}=m} = 0,$ (3.44)

3. Fermion self-energy of the minimal QED extension

where each of these terms individually vanishes. Nevertheless, it turns out to be not practical to evaluate the conditions on $\Sigma_{\mathrm{QED}}^{\mathrm{R}}$ at the Lorentz violating on shell point $\overline{u}(p)(\slashed{p} + \Gamma_1 \cdot p)u(p) = \overline{u}(p)(m + M_1)u(p)$, where it is rather intractable. Conversely, we can choose to satisfy the conditions for $\Sigma_{\mathrm{QED}}^{\mathrm{R}}$ at the *conventional* point $\overline{u}(p)\slashed{p}u(p) = \overline{u}(p)mu(p)$, introducing an error of first order in Lorentz violation, but taking it into account by modifying the conditions satisfied by the Lorentz violating contributions $\Sigma_{\mathrm{LV}}^{\mathrm{R}}$.

An example to explicitly illustrate this point is in place. The regularized conventional QED contribution Σ_{QED}, as given by (3.24), will be renormalized in the next section. Counterterms in (3.39) associated with Z_ψ and Z_m remove the divergences of Σ_{QED} and introduce two free parameters κ_ψ and κ_m, such that the renormalized expression reads

$$\Sigma_{\mathrm{QED}}^{\mathrm{R}} = \frac{\alpha}{2\pi}\left\{ -\int_0^1 dx(\slashed{p}x - 2m)\ln\left(\frac{\Delta_{\mathrm{os}}}{\Delta}\right) - (\slashed{p}\,\kappa_\psi + m\,\kappa_m) \right\}. \tag{3.45}$$

Renormalization conditions (3.42) are used to fix the two parameters. Clearly, when evaluated at the Lorentz-violating on shell point, contributions from Lorentz violation will be introduced by $\overline{u}(p)\slashed{p}u(p) = \overline{u}(p)(-\Gamma_1 \cdot p + m + M_1)u(p)$. This introduces further technical complications when trying to fix κ_ψ and κ_m. On the other hand, this task is straightforward to accomplish working with the *conventional* on shell point $\overline{u}(p)\slashed{p}u(p) = \overline{u}(p)mu(p)$, such that

$$\Sigma_{\mathrm{QED}}^{\mathrm{R}}(p)\Big|_{\slashed{p}=m} = 0, \qquad \text{and} \qquad \frac{\partial}{\partial\slashed{p}}\Sigma_{\mathrm{QED}}^{\mathrm{R}}(p)\Big|_{\slashed{p}=m} = 0. \tag{3.46}$$

After using these conditions to fix κ_ψ and κ_m — which will be identical to the conventional ones — it can be easily shown that the renormalization conditions at the *Lorentz-violating* on shell point for the conventional QED contribution in (3.44) *do not* vanish, instead

$$\Sigma_{\mathrm{QED}}^{\mathrm{R}}(p)\Big|_{\slashed{p}+\Gamma_1\cdot p=m+M_1} = -\frac{\alpha}{\pi}\left(\Gamma_1 \cdot p - M_1\right)\Big|_{\slashed{p}=m}\int_0^1 dx\frac{\overline{x}x(x-2)}{(\Delta_{\mathrm{os}}/m^2)}, \tag{3.47}$$

3. Fermion self-energy of the minimal QED extension

$$\frac{\partial}{\partial \not{p}} \Sigma_{\text{QED}}^{\text{R}}(p) \Big|_{\not{p}+\Gamma_1 \cdot p = m + M_1} = -\frac{2\alpha}{\pi} \left(\Gamma_1 \cdot \frac{p}{m} - \frac{M_1}{m} \right) \Big|_{\not{p}=m} \int_0^1 dx \frac{\overline{x}^2 x}{(\Delta_{\text{os}}/m^2)}, \qquad (3.48)$$

where use of the convention on shell point at the right-hand side introduces errors of second order in Lorentz violation, which can be ignored in our approximation. Therefore, for the fermion self-energy $\Sigma_{\text{R}}(p)$ to still satisfy the on shell conditions (3.44), with the conventional QED part $\Sigma_{\text{QED}}^{\text{R}}(p)$ satisfying (3.46), we have to modify the conditions for the Lorentz-violating part $\Sigma_{\text{LV}}^{\text{R}}(p)$, which instead of (3.43) now will be given by

(i) $\Sigma_{\text{LV}}^{\text{R}}(p) \Big|_{\not{p}=m} = +\frac{\alpha}{\pi} \left(\Gamma_1 \cdot p - M_1 \right) \Big|_{\not{p}=m} \int_0^1 dx \frac{\overline{x} x (x-2)}{(\Delta_{\text{os}}/m^2)},$

(ii) $\frac{\partial}{\partial \not{p}} \Sigma_{\text{LV}}^{\text{R}}(p) \Big|_{\not{p}=m} = +\frac{2\alpha}{\pi} \left(\Gamma_1 \cdot \frac{p}{m} - \frac{M_1}{m} \right) \Big|_{\not{p}=m} \int_0^1 dx \frac{\overline{x}^2 x}{(\Delta_{\text{os}}/m^2)}. \qquad (3.49)$

Because of (3.37), the left-hand side of conditions (3.49) is naturally split into contributions from each Lorentz-violating coefficient, and the right-hand side splits accordingly. As a consequence, for instance, the conditions for the a^μ contribution are

(i) $\Sigma_a^{\text{R}}(p) \Big|_{\not{p}=m} = -\frac{\alpha}{\pi} a_\mu \gamma^\mu \int_0^1 dx \frac{\overline{x} x (x-2)}{(\Delta_{\text{os}}/m^2)},$

(ii) $\frac{\partial}{\partial \not{p}} \Sigma_a^{\text{R}}(p) \Big|_{\not{p}=m} = -\frac{2\alpha}{\pi} \frac{a_\mu}{m} \gamma^\mu \int_0^1 dx \frac{\overline{x}^2 x}{(\Delta_{\text{os}}/m^2)}. \qquad (3.50)$

Contribution from the other *fermionic* coefficients satisfy analogous conditions, and we point out the right-hand side of conditions for $(k_{AF})^\mu$ and $(k_F)^{\mu\nu\rho\sigma}$ actually vanish, for instance,

(i) $\Sigma_{k_{AF}}^{\text{R}}(p) \Big|_{\not{p}=m} = 0,$

(ii) $\frac{\partial}{\partial \not{p}} \Sigma_{k_{AF}}^{\text{R}}(p) \Big|_{\not{p}=m} = 0. \qquad (3.51)$

Therefore, summarizing this section, renormalization of the fermion self-energy will proceed as subjected to renormalization conditions (3.46) on the convention QED contribution and (3.49) on the Lorentz-violating one. Because of these conditions, from now on, by "on shell" we really mean the *conventional* on shell point $\overline{u}(p)\not{p}u(p) = \overline{u}(p)mu(p)$.

69

3. Fermion self-energy of the minimal QED extension

Subtraction and Renormalization

In the following, we perform the subtraction of divergences along with renormalization of the one-loop fermion self-energy. As an illustration, for the conventional QED contribution we explicitly show counterterms depending on free parameters and how these are fixed by renormalization conditions. The procedure for Lorentz-violating contributions are completely analogous, and do not introduce any procedural issue. Nevertheless, we will find out renormalization of contributions from $c_S^{\mu\nu}$, $d_S^{\mu\nu}$, $g_M^{\kappa\lambda\mu}$, and $(k_F)_{\mu\rho\nu}{}^\rho$ fails to consistently fix the arbitrary parameters, thus it appears renormalization of such contributions cannot be consistently accomplished by conventional means.

Renormalization of the conventional QED contribution

The regularized conventional QED contribution to the fermion self-energy (3.24) is renormalized according to

$$\Sigma_{\text{QED}}^{\text{R}} = \Sigma_{\text{QED}} - (Z_\psi - 1)\not{p} + (Z_m - 1)m, \tag{3.52}$$

as can be inferred by counterterms shown in (3.39) and lagrangian (3.1). The counterterms are chosen to cancel the $\frac{1}{\varepsilon}$ divergences, but the freedom to choose the counterterms also introduce free parameters κ renormalizing the finite contributions,

$$Z_\psi = 1 + \frac{\alpha}{2\pi}\left\{-\frac{1}{2}\left(\frac{1}{\varepsilon} - \gamma_E - 1\right) - \int_0^1 dx\, x \ln\left(\frac{4\pi\mu^2}{\Delta_{\text{os}}}\right) + \kappa_\psi\right\},$$

$$Z_m = 1 - \frac{\alpha}{2\pi}\left\{2\left(\frac{1}{\varepsilon} - \gamma_E - \frac{1}{2}\right) + 2\int_0^1 dx \ln\left(\frac{4\pi\mu^2}{\Delta_{\text{os}}}\right) + \kappa_m\right\}, \tag{3.53}$$

where $\Delta_{\text{os}}(x) \equiv \Delta(x)|_{p^2=m^2} = m^2\overline{x}^2 + \lambda^2 x$. Such Z factors lead to a renormalized (UV finite) expression,

$$\Sigma_{\text{QED}}^{\text{R}} = \frac{\alpha}{2\pi}\left\{-\int_0^1 dx\,(\not{p}x - 2m)\ln\left(\frac{\Delta_{\text{os}}}{\Delta}\right) - (\not{p}\,\kappa_\psi + m\,\kappa_m)\right\}, \tag{3.54}$$

3. Fermion self-energy of the minimal QED extension

and we see the dependence on the arbitrary parameter μ disappears, as we had effectively set the energy scale at the fermion mass $p^2 = m^2$. Two free parameters κ_ψ and κ_m have been introduced, but they are fixed as we require $\Sigma^{\mathrm{R}}_{\mathrm{QED}}(p)$ to satisfy renormalization conditions (3.46). This is readily done without any difficulty — for instance, we make use of $\partial\Delta/\partial\slashed{p} = -2\overline{x}x\slashed{p}$ and $\partial\ln\Delta/\partial\slashed{p} = -2\overline{x}x\slashed{p}/\Delta$ — and the free parameters can be determined,

$$\kappa_\psi = -\kappa_m = -2\int_0^1 dx \frac{\overline{x}x(x-2)}{(\Delta_{\mathrm{os}}/m^2)}. \tag{3.55}$$

Thus, the resulting renormalized contribution from the conventional QED to the fermion self-energy reads

$$\Sigma^{\mathrm{R}}_{\mathrm{QED}} = \frac{\alpha}{2\pi}\left\{ -\int_0^1 dx(\slashed{p}x - 2m)\ln\left(\frac{\Delta_{\mathrm{os}}}{\Delta}\right) + 2(\slashed{p}-m)\int_0^1 dx \frac{\overline{x}x(x-2)}{(\Delta_{\mathrm{os}}/m^2)} \right\}. \tag{3.56}$$

This expression satisfy both conditions (3.46), is UV finite, and has no dependence on the mass parameter μ, as desired. As expected, it exhibits the low momenta, infrared divergences of the conventional Lorentz symmetric QED, which are further cancelled in scattering cross sections when soft-photon emission by the external legs are taken into account [81].

An important point to be emphasized is the interplay between $\slashed{p}$ and m. On mass shell they are related to each other by $\overline{u}(p)\slashed{p}u(p) = \overline{u}(p)mu(p)$, making possible for the free parameters κ_ψ and κ_m to relate to each other so $\Sigma^{\mathrm{R}}_{\mathrm{QED}}$ satisfies both renormalization conditions of (3.46). This sort of on shell interplay is fundamental in fixing the free parameters, and we see it extends to more complicated structures[1] accompanying Lorentz-violating contributions to the fermion self-energy — see Table 3.1. Nevertheless, we see there are fermionic coefficients associated with only one structure.

---

[1]The most basic relation is $\overline{u}(p)\slashed{p}u(p) = \overline{u}(p)mu(p)$, and it is nothing more than the (free) conventional Dirac equation for external leg spinors $u(p)$. We call this relation, and any other derived using it, an *on shell relation*, and they have the form $\overline{u}(p)(\dots)u(p) = \overline{u}(p)(\dots)u(p)$, where usually the left-hand side contains more factors of momentum than the right-hand side, in analogy to (and because of) the previous relation between $\slashed{p}$ and m. Along with use of the Dirac equation, a suitable starting point to deduce more complicated relations makes use of the trivial identity $p^\mu = \frac{1}{2}\{\slashed{p}, \gamma^\mu\}$. For instance, the Gordon identity $\overline{u}(p)p^\mu u(p) = \overline{u}(p)m\gamma^\mu u(p)$ and also $\overline{u}(p)(p^\mu\gamma_5)u(p) = 0$ are immediately derived with the mentioned "trick".

3. Fermion self-energy of the minimal QED extension

Unless the "single" structure vanishes on shell — thus trivially satisfying conditions (3.49) — renormalization of the contribution to the fermion self-energy from those "single" coefficients cannot be consistently done by conventional means. From Table 3.1, we expect contributions from $c_A^{\mu\nu}$, f^μ, and $g_T^{\kappa\lambda\mu}$ to satisfy renormalization conditions (3.49) trivially — which could be expected as these coefficients are unobservable to first order. We also expect issues for the renormalization of contributions from $c_S^{\mu\nu}$, $d_S^{\mu\nu}$, and $g_M^{\kappa\lambda\mu}$. Renormalization of the contribution from the remaining coefficients is expected to be accomplished without issues.

Table 3.1: On shell expressions for functions $M(p,\gamma)$ involving powers of p^μ and γ matrices. For functions $M(p,\gamma)$ appearing in the Lorentz-violating QED lagrangian, its associated coefficients are indicated.

Coefficients	$M(p,\gamma)$	$\overline{u}(p)[M(p,\gamma)]u(p)$
—	$\not{p}$	m
a^μ, e^μ	p_μ	$m\gamma_\mu$
b^μ, $g_{\kappa\lambda\nu}\epsilon^{\kappa\lambda\mu\nu}$	$\epsilon_{\mu\rho\sigma\tau}p^\rho\sigma^{\sigma\tau}$	$2m\gamma_5\gamma_\mu$
$c_S^{\mu\nu}$	$p_\mu\gamma_\nu + p_\nu\gamma_\mu$	—
$c_A^{\mu\nu}$	$p_\mu\gamma_\nu - p_\nu\gamma_\mu$	0
—	$p_\mu p_\nu$	$\frac{1}{2}m(p_\mu\gamma_\nu + p_\nu\gamma_\mu)$
$d_S^{\mu\nu}$	$p_\mu\gamma_5\gamma_\nu + p_\nu\gamma_5\gamma_\mu$	—
$d_A^{\mu\nu}$, $\epsilon^{\kappa\lambda\mu\nu}H_{\kappa\lambda}$	$p_\mu\gamma_5\gamma_\nu - p_\nu\gamma_5\gamma_\mu$	$-\frac{1}{2}m\epsilon_{\mu\nu\rho\sigma}\sigma^{\rho\sigma}$
—	$p_\mu p_\nu\gamma_5$	0
f^μ	$p_\mu\gamma_5$	0
$g_A^{\kappa\lambda\mu}$, $b_\nu\epsilon^{\kappa\lambda\mu\nu}$	$p_\mu\sigma_{\kappa\lambda} + p_\lambda\sigma_{\mu\kappa} + p_\kappa\sigma_{\lambda\mu}$	$m\epsilon_{\kappa\lambda\mu\rho}\gamma_5\gamma^\rho$
$g_T^{\kappa\lambda\mu}$	$p_\lambda\sigma_{\kappa\lambda}$	0
$g_M^{\kappa\lambda\mu}$	$p_\mu\sigma_{\kappa\lambda}$	—
—	$\epsilon_{\kappa\lambda\nu\rho}p_\mu p^\rho\gamma_5\gamma^\nu$	$-mp_\mu\sigma_{\kappa\lambda}$
$H^{\mu\nu}$, $d_{\kappa\lambda}^A\epsilon^{\kappa\lambda\mu\nu}$	$\epsilon_{\mu\nu\rho\sigma}p^\rho\gamma_5\gamma^\sigma$	$m\sigma_{\mu\nu}$

3. Fermion self-energy of the minimal QED extension

Renormalized contribution from a^μ

For the renormalization of Lorentz-violating contributions, it is enough to consider the on shell point at $p^2 = m^2$ as the error introduced is of second order in the Lorentz-violating coefficients at least — see discussion before Eq. (3.43). Similarly, we can use the conventional Dirac equation $\not{p}u(p) = mu(p)$ to simplify on shell expression. We will make use of the Gordon identity $\overline{u}(p)p^\mu u(p) = \overline{u}(p)m\gamma^\mu u(p)$ for renormalization of the a^μ contribution to the fermion self-energy, as it involves the structures p^μ and γ^μ. This renormalized contribution reads

$$\Sigma_a^{\mathrm{R}} = \Sigma_a - \left[(\mathcal{Z}_{a\cdot p})^\mu{}_\nu a^\nu - a^\mu \right] \frac{p_\mu}{m} + \left[(\mathcal{Z}_{\not{a}})^\mu{}_\nu a^\nu - a^\mu \right] \gamma_\mu, \tag{3.57}$$

where the expression for Σ_a is given by (3.25), and determination of the $\mathcal{Z}$ factors proceeds analogously to the conventional case, except that we need to know how to perform derivatives like $\partial p^\mu / \partial \not{p}$, which are seldom seen in the conventional case. By the chain rule we can write derivatives with respect to $\not{p}$ as $\partial / \partial \not{p} = 2\not{p}\partial / \partial p^2$, where we have used $\partial p^2 / \partial \not{p} = 2\not{p}$. The last piece of information we need is given by $\partial p^\mu / \partial p^2 = p^\mu / 2p^2$, which can be derived by arguments of Lorentz covariance. Thus we finally have the desired derivative, $\partial p^\mu / \partial \not{p} = p^\mu \not{p} / p^2$.

After using the Gordon identity to relate p^μ and γ^μ and fix the free parameters with the renormalization condition (3.49), the $\mathcal{Z}$ factors can be determined,

$$(\mathcal{Z}_{a\cdot p})^\mu{}_\nu a^\nu = a^\mu + \frac{\alpha}{2\pi} a^\mu \left\{ -2 \int_0^1 dx \frac{\overline{x}x(2x-1)}{(\Delta_{\mathrm{os}}/m^2)} + 2 \int_0^1 dx \frac{\overline{x}^2 x(\overline{x}^2 - 2x)}{(\Delta_{\mathrm{os}}/m^2)^2} \right\}, \tag{3.58}$$

$$(\mathcal{Z}_{\not{a}})^\mu{}_\nu a^\nu = a^\mu - \frac{\alpha}{2\pi} a^\mu \left\{ \frac{1}{2} \left(\frac{1}{\varepsilon} - \gamma_E - 2 \right) + \int_0^1 dx \overline{x} \ln \left(\frac{4\pi\mu^2}{\Delta_{\mathrm{os}}} \right) \right.$$

$$\left. + \int_0^1 dx \frac{\overline{x}(7x^2 - 10x + 1)}{(\Delta_{\mathrm{os}}/m^2)} - 2 \int_0^1 dx \frac{\overline{x}^2 x(\overline{x}^2 - 2x)}{(\Delta_{\mathrm{os}}/m^2)^2} \right\}, \tag{3.59}$$

3. Fermion self-energy of the minimal QED extension

and the a^μ renormalized contribution to the self-energy then reads

$$\Sigma_a^{\mathrm{R}} = \frac{\alpha}{2\pi}\left\{\slashed{a}\left[\int_0^1 dx\,\overline{x}\ln\left(\frac{\Delta_{\mathrm{os}}}{\Delta}\right) - \int_0^1 dx\frac{\overline{x}}{(\Delta/m^2)}\left(\frac{p^2}{m^2}x^2 - 1\right) - \int_0^1 dx\frac{\overline{x}(7x^2 - 10x + 1)}{(\Delta_{\mathrm{os}}/m^2)}\right.\right.$$

$$\left. + 2\int_0^1 dx\frac{\overline{x}^2 x(\overline{x}^2 - 2x)}{(\Delta_{\mathrm{os}}/m^2)^2}\right]$$

$$\left. + 2a\cdot\frac{p}{m}\left[\int_0^1 dx\frac{\overline{x}x}{(\Delta/m^2)}\left(\frac{\slashed{p}}{m}x - 2\right) + \int_0^1 dx\frac{\overline{x}x(2x - 1)}{(\Delta_{\mathrm{os}}/m^2)} - \int_0^1 dx\frac{\overline{x}^2 x(\overline{x}^2 - 2x)}{(\Delta_{\mathrm{os}}/m^2)^2}\right]\right\}.$$

$$(3.60)$$

Although the coefficient a^μ is unobservable at leading order in flat spacetime — it can be removed from lagrangian (3.1) by a field redefinition $\psi \to e^{-ia\cdot x}\psi$ — the above expression already reveals some curious feature due to Lorentz violation. The term proportional to $a \cdot \frac{p}{m}\frac{\slashed{p}}{m}$ in the last line is a radiative correction modifying the tree-level propagator by a finite structure not present in the original lagrangian, effectively changing its kinematics. Further more, it resembles an a-like coefficient — we could identify $a^{(5)}_{\mu\alpha\beta} \leftrightarrow \frac{1}{m^2}a_\alpha\eta_{\beta\mu}$ — associated with a dimension 5 operator $\overline{\psi}\gamma^\mu\partial^\alpha\partial^\beta\psi$. In the conventional QED, this situation — radiative generation of finite terms of nonrenormalizable dimension — only occurs for the vertex correction where it is responsible for corrections to the fermion gyromagnetic factor, but never for the fermion self-energy. Although no leading order effect from a^μ is observable, this *new* feature may be expected for other coefficients as well. Indeed, we will see this is a typical feature of the Lorentz-violating QED (3.1).

Renormalized contribution from b^μ

Renormalization of b^μ contributions is more interesting because it involves the structures $\epsilon_{\mu\nu\rho\sigma}p^\nu\sigma^{\rho\sigma}$ and $\gamma_5\gamma_\mu$,

$$\Sigma_b^{\mathrm{R}} = \Sigma_b - \left[(\mathcal{Z}_{bp\sigma})_\mu{}^\nu b_\nu - b_\mu\right]\epsilon^{\mu\nu\rho\sigma}\frac{p_\nu}{m}\sigma_{\rho\sigma} + \left[(\mathcal{Z}_{\gamma_5\slashed{b}})^\mu{}_\nu b^\nu - b^\mu\right]\gamma_5\gamma_\mu, \qquad (3.61)$$

although a glance at $\Sigma_b(p)$, Eq. (3.26), reveals it contains no piece proportional to $\epsilon_{\mu\nu\rho\sigma}p^\nu\sigma^{\rho\sigma}$. Latter we will see that this counterterm actually comes from $g_A^{\mu\nu\rho}$ coun-

3. Fermion self-energy of the minimal QED extension

terterms, $(Z_{g_A})^{\kappa\lambda\mu}{}_{\nu\rho\sigma}g_A^{\nu\rho\sigma} \supset (\mathcal{Z}_{bp\sigma})_\alpha{}^\beta b_\beta \epsilon^{\alpha\kappa\lambda\mu}$, as we would expect if we take field redefinitions in consideration, as in lagrangian (3.5). Even before knowing that, the on shell relation $\overline{u}(p)(\epsilon^{\mu\nu\rho\sigma}p_\nu\sigma_{\rho\sigma})u(p) = \overline{u}(p)(2m\gamma_5\gamma^\mu)u(p)$ already suggests such a counterterm for Σ_b is to be expected. Therefore, in (3.61) this counterterm renormalizes a factor of (zero) $\times\, \epsilon_{\mu\nu\rho\sigma}b^\mu p^\nu \sigma^{\rho\sigma}$ in $\Sigma_b(p)$.

The $\mathcal{Z}$ factors are given by

$$(\mathcal{Z}_{bp\sigma})^\mu{}_\nu b^\nu = b^\mu + \frac{\alpha}{2\pi}b^\mu \left\{ -\int_0^1 dx\frac{\overline{x}x(4x-3)}{(\Delta_{\rm os}/m^2)} - \int_0^1 dx\frac{\overline{x}^2 x(x^2+1)}{(\Delta_{\rm os}/m^2)^2} \right\}, \tag{3.62}$$

$$(\mathcal{Z}_{\gamma_5\not{p}})^\mu{}_\nu b^\nu = b^\mu - \frac{\alpha}{2\pi}b^\mu \left\{ \frac{1}{2}\left(\frac{1}{\varepsilon} - \gamma_E + 2\right) + \int_0^1 dx\overline{x}\ln\left(\frac{4\pi\mu^2}{\Delta_{\rm os}}\right) \right.$$

$$\left. + \int_0^1 dx\frac{\overline{x}(9x^2 - 10x - 1)}{(\Delta_{\rm os}/m^2)} + 2\int_0^1 dx\frac{\overline{x}^2 x(x^2+1)}{(\Delta_{\rm os}/m^2)^2} \right\}. \tag{3.63}$$

Therefore, the renormalized b^μ correction to the self-energy reads

$$\Sigma_b^{\rm R} = \frac{\alpha}{2\pi}\left\{ \gamma_5\not{b}\left[\int_0^1 dx\overline{x}\ln\left(\frac{\Delta_{\rm os}}{\Delta}\right) - \int_0^1 dx\frac{\overline{x}}{(\Delta/m^2)}\left(\frac{p^2}{m^2}x^2 + 1\right) - \int_0^1 dx\frac{\overline{x}(9x^2 - 10x - 1)}{(\Delta_{\rm os}/m^2)} \right.\right.$$

$$\left. - 2\int_0^1 dx\frac{\overline{x}^2 x(x^2+1)}{(\Delta_{\rm os}/m^2)^2} \right] + 2b\cdot\frac{p}{m}\gamma_5\frac{\not{p}}{m}\int_0^1 dx\frac{\overline{x}x^2}{(\Delta/m^2)}$$

$$\left. + b_\mu\epsilon^{\mu\nu\rho\sigma}\frac{p_\nu}{m}\sigma_{\rho\sigma}\left[\int_0^1 dx\frac{\overline{x}x(4x-3)}{(\Delta_{\rm os}/m^2)} + \int_0^1 dx\frac{\overline{x}^2 x(x^2+1)}{(\Delta_{\rm os}/m^2)^2} \right] \right\}. \tag{3.64}$$

Similar to the a^μ case, but now leading to *observable* effects, Lorentz violation radiatively induces a new structure $b\cdot\frac{p}{m}\gamma_5\frac{\not{p}}{m}$ to the fermion propagator, different from any other present at tree-level. Its coefficient effectively acts as a b-like coefficient $b_{\mu\alpha\beta}^{(5)} \leftrightarrow \frac{1}{m^2}b_\alpha\eta_{\beta\mu}$ associated to a dimension 5 operator $\overline{\psi}\gamma_5\gamma^\mu\partial^\alpha\partial^\beta\psi$. Only combinations between b^μ and $g_A^{\kappa\lambda\mu}$ are observable — therefore we expect a similar term radiatively induced by $\Sigma_{g_A}^{\rm R}$ — but we can already see that modifications of the fermion kinematics is a feature of observable Lorentz-violating coefficients as well.

3. Fermion self-energy of the minimal QED extension

Renormalized contribution from $c^{\mu\nu}$

Renormalization of $c^{\mu\nu}$ seems to be problematic because it involves only one structure, $p_\nu\gamma_\mu$. This lone term induces only one counterterm, and therefore only *one* free parameter to be adjusted in the need of satisfying *two* renormalization conditions. As will be seen soon, if the whole contribution of a coefficient vanishes on shell for any value of the free parameter, the renormalization conditions are satisfied trivially. If that does not happen, and there is only one free parameter, it cannot be fixed in a consistent way by conventional means.

To isolate the problem, we decompose $c^{\mu\nu}$ in symmetric $c_S^{\mu\nu}$ and antisymmetric $c_A^{\mu\nu}$ pieces. From Eq. (3.27), the contribution from $c_A^{\mu\nu}$ to the fermion self-energy reads

$$\Sigma_{c_A}(p) = \frac{\alpha}{2\pi}\left\{\frac{1}{12}(p_\mu\gamma_\nu - p_\nu\gamma_\mu)c_A^{\mu\nu}\left[\frac{3}{\varepsilon} - 3\gamma_E - 4 + 18\int_0^1 dx\,\overline{x}x\ln\left(\frac{4\pi\mu^2}{\Delta}\right)\right.\right.$$
$$\left.\left. - 6\int_0^1 dx\frac{\overline{x}x}{(\Delta/m^2)}\left(\frac{p^2}{m^2}x^2 - 1\right)\right]\right\}, \qquad (3.65)$$

and is renormalized by a single counterterm,

$$\Sigma_{c_A}^{\mathrm{R}} = \Sigma_{c_A} - \frac{1}{2}\left[(\mathcal{Z}_{c_A p\gamma})^{\mu\nu}{}_{\rho\sigma}c_A^{\rho\sigma} - c_A^{\mu\nu}\right](p_\mu\gamma_\nu - p_\nu\gamma_\mu), \qquad (3.66)$$

where

$$(\mathcal{Z}_{c_A p\gamma})^{\mu\nu}{}_{\rho\sigma}c_A^{\rho\sigma} = c_A^{\mu\nu} + \frac{\alpha}{2\pi}c_A^{\mu\nu}\left\{\frac{1}{6}\left[\frac{3}{\varepsilon} - 3\gamma_E - 4 + 18\int_0^1 dx\,\overline{x}x\ln\left(\frac{4\pi\mu^2}{\Delta_{\mathrm{os}}}\right)\right] + \kappa_{c_A}\right\}, \qquad (3.67)$$

resulting in the renormalized expression

$$\Sigma_{c_A}^R(p) = \frac{\alpha}{2\pi}\left\{\frac{1}{2}(p_\mu\gamma_\nu - p_\nu\gamma_\mu)c_A^{\mu\nu}\left[3\int_0^1 dx\,\overline{x}x\ln\left(\frac{\Delta_{\mathrm{os}}}{\Delta}\right) - \kappa_{c_A}\right.\right.$$
$$\left.\left. - \int_0^1 dx\frac{\overline{x}x}{(\Delta/m^2)}\left(\frac{p^2}{m^2}x^2 - 1\right)\right]\right\}. \qquad (3.68)$$

In this particular case, having a single free parameter is not a problem because this

76

3. Fermion self-energy of the minimal QED extension

expression vanishes on shell since $\bar{u}(p)(p_\mu\gamma_\nu - p_\nu\gamma_\mu)u(p) = 0$, and automatically satisfies *both* renormalization conditions, thus we can actually set $\kappa_{c_A} = 0$. This should not come as a surprise once we already knew, by arguments of field redefinitions, that the coefficient $c_A^{\mu\nu}$ is unobservable at leading order — see the end of Sec. 3.1. Also, no new structure is radiatively induced.

The situation drastically changes for the symmetric part $c_S^{\mu\nu}$. From (3.27), its regularized contribution to the self-energy reads

$$
\Sigma_{c_S}(p) = \frac{\alpha}{2\pi}\left\{ \frac{1}{12}(p_\mu\gamma_\nu + p_\nu\gamma_\mu)c_S^{\mu\mu}\left[\frac{5}{\varepsilon} - 5\gamma_E + 2 + 18\int_0^1 dx\, x(1+x)\ln\left(\frac{4\pi\mu^2}{\Delta}\right)\right.\right.
$$
$$
\left.\left. + 6\int_0^1 dx\, \frac{\overline{x}x}{(\Delta/m^2)}\left(\frac{p^2}{m^2}x^2 - 1\right) - 2c_S^{\mu\nu}p_\mu\frac{p_\nu}{m}\int_0^1 dx\, \frac{\overline{x}x^2}{(\Delta/m^2)}\left(\frac{\not{p}}{m}x - 2\right)\right\},
$$

(3.69)

and it is renormalized similarly as its antisymmetric counterpart, but with a symmetric counterterm

$$
\Sigma_{c_S}^{\mathrm{R}} = \Sigma_{c_S} - \frac{1}{2}\Big[(\mathcal{Z}_{c_S p\gamma})^{\mu\nu}{}_{\rho\sigma}c_S^{\rho\sigma} - c_S^{\mu\nu}\Big](p_\mu\gamma_\nu + p_\nu\gamma_\mu),
$$

(3.70)

where

$$
(\mathcal{Z}_{c_S p\gamma})^{\mu\nu}{}_{\rho\sigma}c_S^{\rho\sigma} = c_S^{\mu\nu} + \frac{\alpha}{2\pi}c_S^{\mu\nu}\left\{\frac{1}{6}\left[\frac{5}{\varepsilon} - 5\gamma_E + 2 + 18\int_0^1 dx\, x(1+x)\ln\left(\frac{4\pi\mu^2}{\Delta_{\mathrm{os}}}\right)\right] + \kappa_{c_S}\right\},
$$

(3.71)

such that

$$
\Sigma_{c_S}^{R}(p) = \frac{\alpha}{2\pi}\left\{\frac{1}{2}(p_\mu\gamma_\nu + p_\nu\gamma_\mu)c_S^{\mu\nu}\left[3\int_0^1 dx\, x(1+x)\ln\left(\frac{\Delta_{\mathrm{os}}}{\Delta}\right) - \kappa_{c_S}\right.\right.
$$
$$
\left.\left. + \int_0^1 dx\, \frac{\overline{x}x}{(\Delta/m^2)}\left(\frac{p^2}{m^2}x^2 - 1\right)\right] - 2c_S^{\mu\nu}p_\mu\frac{p_\nu}{m}\int_0^1 dx\, \frac{\overline{x}x^2}{(\Delta/m^2)}\left(\frac{\not{p}}{m}x - 2\right)\right\}.
$$

(3.72)

Contrary to the previous case, this expression does *not* automatically satisfy the renormalization conditions — the on shell relation leads to a trivial relation,

3. Fermion self-energy of the minimal QED extension

$\overline{u}(p)(p_\mu \gamma_\nu)u(p) = \overline{u}(p)(p_\nu \gamma_\mu)u(p)$. Therefore, with κ_{c_S} as the only free parameter, the two renormalization conditions of (3.49) *cannot* be consistently satisfied.

This Lorentz-violating correction to the fermion self-energy also radiatively induces two new structures not present in the tree-level propagator. The first is proportional to $c_S^{\mu\nu} p^\mu \frac{p^\nu}{m} \frac{\not{p}}{m}$, and resembles a c-like coefficient $c_S^{(6)\mu\nu\rho\sigma} \leftrightarrow \frac{1}{m^2} \eta^{\mu\nu} c_S^{\rho\sigma}$ associated to a dimension 6 operator $i\overline{\psi}(\gamma_\nu \partial_\mu + \gamma_\mu \partial_\nu)\partial_\rho \partial_\sigma \psi$. The second structure comes from the term proportional to $c_S^{\mu\nu} p^\mu \frac{p^\nu}{m}$, and it effectively behaves as a mass-like coefficient $m^{(5)\mu\nu} \leftrightarrow \frac{1}{m} c_S^{\mu\nu}$ associated to a dimension 5 operator $\overline{\psi}\partial_\mu \partial_\nu \psi$.

Incidentally, we point out the interesting on shell relation $\overline{u}(p)(p_\mu p_\nu \frac{\not{p}}{m})u(p) = \overline{u}(p)(p_\mu p_\nu)u(p) = \overline{u}(p)[\frac{1}{2}m(p_\mu \gamma_\nu + p_\nu \gamma_\mu)]u(p)$, but the term associated to $p_\mu p_\nu$ in (3.69) does *not* receive counterterms as it is not in the original lagrangian (3.1), therefore by conventional procedures we *cannot* add a free parameter by means of a counterterm with this structure.

To enforce renormalization, a departure from conventional procedure may suggest adding such nonrenormalizable term, $\overline{u}(p)(p_\mu p_\nu)u(p)$, to the tree-level lagrangian (3.1). It would be, from the start, of order α, thus it would not spoil renormalizability to one-loop order as it enters effectively as a counterterm. No decrease in the predictive power of the model to this order would be expected once no extra renormalization condition is required to fix the free parameter this term introduces. Nevertheless, this may not be an adequate approach. In the following, we show renormalization of the fermion self-energy contribution from $d_S^{\mu\nu}$ presents issues similar to the ones we have just encountered, but there we will see there is no naturally appearing on shell relation, similar to the one mentioned above, which could help enforcing renormalization even if introducing order α nonrenormalizable terms in the tree-level lagrangian.

A somewhat similar departure from the conventional approach could be the introduction of renormalization factors with momentum dependence, as done in Ref. [42]. In this case, the adequate modification would be in the wave-function renormalization factor Z_ψ, introducing a term $c_S^{\mu\nu} p_\mu p_\nu$ inside it, with a free paramenter $\kappa_{c_{Spp}}$ as its coefficient. Such a modification would require the sum $\Sigma_{\text{QED}}^{\text{R}} + \Sigma_{c_S}^{\text{R}}$ to satisfy renormalization conditions (3.46) and (3.49) simultaneously. As there would be, now, two

3. Fermion self-energy of the minimal QED extension

free parameters, κ_{c_S} and κ_{c_Spp}, associated to $c_S^{\mu\nu}$, these could be consistently fixed so as to satisfy all renormalization conditions. Nevertheless, once more, in the next section we will see this apparently does not work for the also problematic contributions from $d_S^{\mu\nu}$. It is our opinion such procedure is not the proper solution to the more general problem.

Renormalized contribution from $d^{\mu\nu}$

Renormalization of $d^{\mu\nu}$ presents issues similar to the previous case for the $c^{\mu\nu}$ coefficient. At first, from (3.28), it seems to involve two structures, $p_\mu\gamma_5\gamma_\nu$ and $\epsilon^{\mu\nu\rho\sigma}\sigma_{\rho\sigma}$, nevertheless the only relation between them is $\overline{u}(p)(p_\mu\gamma_5\gamma_\nu - p_\nu\gamma_5\gamma_\mu)u(p) = \overline{u}(p)(-\frac{1}{2}m\epsilon_{\mu\nu\rho\sigma}\sigma^{\rho\sigma})u(p)$, which is associated only with the antisymmetric part of $d^{\mu\nu}$. For the symmetric part of $p_\mu\gamma_5\gamma_\nu$, we only get trivial on shell equalities. As a consequence, the contribution to the fermion self-energy from $d_A^{\mu\nu}$ can be consistently renormalized, but the one from $d_S^{\mu\nu}$ seems to fall into the same issues encountered for $c_S^{\mu\nu}$, as we see next.

Inspection of (3.28) reveals the correction to the fermion self-energy from the antisymmetric coefficient $d_A^{\mu\nu}$ reads

$$\Sigma_{d_A}(p) = \frac{\alpha}{2\pi}\left\{\frac{1}{12}(p_\mu\gamma_5\gamma_\nu - p_\nu\gamma_5\gamma_\mu)d_A^{\mu\nu}\left[\frac{3}{\varepsilon} - 3\gamma_E + 2 + 18\int_0^1 dx\overline{x}x\ln\left(\frac{4\pi\mu^2}{\Delta}\right)\right.\right.$$
$$\left. -6\int_0^1 dx\frac{\overline{x}x}{(\Delta/m^2)}\left(\frac{p^2}{m^2}x^2 + 1\right)\right]$$
$$\left. +\frac{1}{4}md_A^{\mu\nu}\epsilon_{\mu\nu\rho\sigma}\sigma^{\rho\sigma}\left[\frac{2}{\varepsilon} - 2\gamma_E + 1 + 2\int_0^1 dx\ln\left(\frac{4\pi\mu^2}{\Delta}\right)\right]\right\}, \quad (3.73)$$

and renormalization of this contribution proceeds as usual,

$$\Sigma_{d_A}^{\mathrm{R}} = \Sigma_{d_A} - \frac{1}{2}\left[(\mathcal{Z}_{d_Ap\gamma_5\gamma})^{\mu\nu}{}_{\rho\sigma}d_A^{\rho\sigma} - d_A^{\mu\nu}\right](p_\mu\gamma_5\gamma_\nu - p_\nu\gamma_5\gamma_\mu)$$
$$+ \frac{1}{2}\left[(\mathcal{Z}_{d_A\sigma})^{\mu\nu}{}_{\rho\sigma}d_A^{\rho\sigma} - d_A^{\mu\nu}\right]m\epsilon_{\mu\nu\rho\sigma}\sigma^{\rho\sigma}, \quad (3.74)$$

3. Fermion self-energy of the minimal QED extension

where the renormalization factors are given by

$$(\mathcal{Z}_{d_A p\gamma_5\gamma})^{\mu\nu}{}_{\rho\sigma}d_A^{\rho\sigma} = d_A^{\mu\nu} + \frac{\alpha}{2\pi}d_A^{\mu\nu}\left\{\frac{1}{6}\left[\frac{3}{\varepsilon} - 3\gamma_E + 2 + 18\int_0^1 dx\,\overline{x}x\ln\left(\frac{4\pi\mu^2}{\Delta_{\text{os}}}\right)\right]\right.$$

$$\left. - \int_0^1 dx\frac{\overline{x}x(9\overline{x}^2 + 8x)}{(\Delta_{\text{os}}/m^2)} - 2\int_0^1 dx\frac{\overline{x}^2 x^2(x^2 + 1)}{(\Delta_{\text{os}}/m^2)^2}\right\},$$

$$(\mathcal{Z}_{d_A\sigma})^{\mu\nu}{}_{\rho\sigma}d_A^{\rho\sigma} = d_A^{\mu\nu} - \frac{\alpha}{2\pi}d_A^{\mu\nu}\left\{\frac{1}{2}\left[\frac{2}{\varepsilon} - 2\gamma_E + 1 + 2\int_0^1 dx\ln\left(\frac{4\pi\mu^2}{\Delta_{\text{os}}}\right)\right]\right.$$

$$\left. - 2\int_0^1 dx\frac{\overline{x}x(2\overline{x}^2 + x + 1)}{(\Delta_{\text{os}}/m^2)} - \int_0^1 dx\frac{\overline{x}^2 x^2(x^2 + 1)}{(\Delta_{\text{os}}/m^2)^2}\right\}, \tag{3.75}$$

such that the renormalized contribution from $d_A^{\mu\nu}$ is

$$\Sigma_{d_A}^R(p) = \frac{\alpha}{2\pi}\left\{\frac{1}{2}(p_\mu\gamma_5\gamma_\nu - p_\nu\gamma_5\gamma_\mu)d_A^{\mu\nu}\left[3\int_0^1 dx\,\overline{x}x\ln\left(\frac{\Delta_{\text{os}}}{\Delta}\right) - \int_0^1 dx\frac{\overline{x}x}{(\Delta/m^2)}\left(\frac{p^2}{m^2}x^2 + 1\right)\right.\right.$$

$$\left. + \int_0^1 dx\frac{\overline{x}x(9\overline{x}^2 + 8x)}{(\Delta_{\text{os}}/m^2)} + 2\int_0^1 dx\frac{\overline{x}^2 x^2(x^2 + 1)}{(\Delta_{\text{os}}/m^2)^2}\right]$$

$$+ \frac{1}{2}md_A^{\mu\nu}\epsilon_{\mu\nu\rho\sigma}\sigma^{\rho\sigma}\left[\int_0^1 dx\ln\left(\frac{\Delta_{\text{os}}}{\Delta}\right) + 2\int_0^1 dx\frac{\overline{x}x(2\overline{x}^2 + x + 1)}{(\Delta_{\text{os}}/m^2)}\right.$$

$$\left.\left. + \int_0^1 dx\frac{\overline{x}^2 x^2(x^2 + 1)}{(\Delta_{\text{os}}/m^2)^2}\right]\right\}. \tag{3.76}$$

It can be readily checked that this expression satisfy both renormalization conditions of (3.49). Interestingly, for contributions of this coefficient to the fermion self-energy, no new structure is radiatively induced — by arguments of field redefinition, the same is to be expected for contributions from $H^{\mu\nu}$.

As for the symmetric coefficient $d_S^{\mu\nu}$, inspection of (3.28) once more reveals

$$\Sigma_{d_S}(p) = \frac{\alpha}{2\pi}\left\{\frac{1}{12}(p_\mu\gamma_5\gamma_\nu + p_\nu\gamma_5\gamma_\mu)d_S^{\mu\nu}\left[\frac{5}{\varepsilon} - 5\gamma_E + 6\int_0^1 dx\,x(1 + x)\ln\left(\frac{4\pi\mu^2}{\Delta}\right)\right.\right.$$

$$\left.\left. + 6\int_0^1 dx\frac{\overline{x}x}{(\Delta/m^2)}\left(\frac{p^2}{m^2}x^2 + 1\right)\right] - 2d_S^{\mu\nu}p^\mu\frac{p^\nu}{m}\gamma_5\frac{\not{p}}{m}\int_0^1\frac{\overline{x}x^3}{(\Delta/m^2)}\right\}. \tag{3.77}$$

3. Fermion self-energy of the minimal QED extension

Renormalization of this contribution involves only one counterterm,

$$\Sigma_{d_S}^{\mathrm{R}} = \Sigma_{d_S} - \frac{1}{2}\Big[(\mathcal{Z}_{d_S p\gamma_5\gamma})^{\mu\nu}{}_{\rho\sigma}d_S^{\rho\sigma} - d_S^{\mu\nu}\Big](p_\mu\gamma_5\gamma_\nu + p_\nu\gamma_5\gamma_\mu), \qquad (3.78)$$

where

$$(\mathcal{Z}_{d_S p\gamma_5\gamma})^{\mu\nu}{}_{\rho\sigma}d_S^{\rho\sigma} = d_S^{\mu\nu} + \frac{\alpha}{2\pi}d_S^{\mu\nu}\left\{\frac{1}{6}\left[\frac{5}{\varepsilon} - 5\gamma_E + 6\int_0^1 dx\, x(1+x)\ln\left(\frac{4\pi\mu^2}{\Delta_{\mathrm{os}}}\right)\right] + \kappa_{d_S}\right\}$$
$$(3.79)$$

which is enough to render $\Sigma_{d_S}(p)$ finite,

$$\Sigma_{d_S}(p) = \frac{\alpha}{2\pi}\left\{\frac{1}{2}(p_\mu\gamma_5\gamma_\nu + p_\nu\gamma_5\gamma_\mu)d_S^{\mu\nu}\left[\int_0^1 dx\, x(1+x)\ln\left(\frac{\Delta_{\mathrm{os}}}{\Delta}\right) - \kappa_{d_S}\right.\right.$$
$$\left.\left. + \int_0^1 dx\,\frac{\overline{x}x}{(\Delta/m^2)}\left(\frac{p^2}{m^2}x^2 + 1\right)\right] - 2d_S^{\mu\nu}p^\mu\frac{p^\nu}{m}\gamma_5\frac{\not{p}}{m}\int_0^1 dx\,\frac{\overline{x}x^3}{(\Delta/m^2)}\right\}.$$
$$(3.80)$$

but because κ_{d_S} is the only one free parameter, it is not enough to consistently satisfy both renormalization conditions of (3.49).

The radiatively generated new structure comes from the term proportional to $d_S^{\mu\nu}p^\mu\frac{p^\nu}{m}\gamma_5\frac{\not{p}}{m}$, which can be seen as a d-like coefficient $d_S^{(6)\mu\nu\rho\sigma} \leftrightarrow \frac{1}{m^2}\eta^{\mu\nu}d_S^{\rho\sigma}$ associated to a dimension 6 operator $i\overline{\psi}(\gamma_5\gamma_\nu\partial_\mu + \gamma_5\gamma_\mu\partial_\nu)\partial_\rho\partial_\sigma\psi$.

Differently from the $c_S^{\mu\nu}$ case, the induced new finite contribution in (3.80) does not give any contribution on shell because $\overline{u}(p)(p^\mu p^\nu\gamma_5\not{p})u(p) = 0$. Therefore, even a departure from conventional renormalization procedure, as suggested by the $c_S^{\mu\nu}$ case, by adding this nonrenormalizable structure to the tree-level lagrangian to act as a counterterm — effectively introducing a desired extra free parameter — *would not* fix the problem because the renormalization conditions (3.49) are based on on shell relations and, as mentioned, this nonrenormalizable structure vanishes on shell, being unable to introduce a suitable extra free parameter. Similarly, introduction of renormalization factors with momentum-dependence may not solve the problem for the same reason.

3. Fermion self-energy of the minimal QED extension

Renormalized contribution from e^μ

Renormalization of e^μ involves two structures, p^μ and γ^μ,

$$\Sigma_e^{\mathrm{R}} = \Sigma_e - \left[(\mathcal{Z}_{e \cdot p})^\mu{}_\nu e^\nu - e^\mu \right] p_\mu + \left[(\mathcal{Z}_{\not{e}})^\mu{}_\nu e^\nu - e^\mu \right] m \gamma_\mu, \tag{3.81}$$

as motivated by $\overline{u}(p) p^\mu u(p) = \overline{u}(p) m \gamma^\mu u(p)$, where the renormalization factors are given by

$$(\mathcal{Z}_{e \cdot p})^\mu{}_\nu e^\nu = e^\mu + \frac{\alpha}{2\pi} e^\mu \left\{ -\frac{1}{2} \left(\frac{1}{\varepsilon} - \gamma_E - \frac{5}{3} \right) + \int_0^1 dx (7x - 6) \ln \left(\frac{4\pi \mu^2}{\Delta_{\mathrm{os}}} \right) \right.$$
$$\left. + 2 \int_0^1 dx \frac{\overline{x} x (3x^2 + 6x - 5)}{(\Delta_{\mathrm{os}}/m^2)} - 4 \int_0^1 dx \frac{\overline{x}^2 x^2 (\overline{x} x - 1)}{(\Delta_{\mathrm{os}}/m^2)^2} \right\}, \tag{3.82}$$

$$(\mathcal{Z}_{\not{e}})^\mu{}_\nu e^\nu = e^\mu - \frac{\alpha}{2\pi} e^\mu \left\{ \frac{1}{2} \left(\frac{3}{\varepsilon} - 3\gamma_E - 1 \right) + \int_0^1 dx (2 - x) \ln \left(\frac{4\pi \mu^2}{\Delta_{\mathrm{os}}} \right) \right.$$
$$\left. - 4 \int_0^1 dx \frac{\overline{x} x (x^2 - 4\overline{x})}{(\Delta_{\mathrm{os}}/m^2)} + 4 \int_0^1 dx \frac{\overline{x}^2 x^2 (\overline{x} x - 1)}{(\Delta_{\mathrm{os}}/m^2)^2} \right\}, \tag{3.83}$$

resulting in the e^μ renormalized correction to the fermion self-energy,

$$\Sigma_e^{\mathrm{R}} = \frac{\alpha}{2\pi} \left\{ e \cdot p \left[\int_0^1 dx (7x - 6) \ln \left(\frac{\Delta_{\mathrm{os}}}{\Delta} \right) + 2 \int_0^1 dx \frac{\overline{x} x}{(\Delta/m^2)} \left(\frac{p^2}{m^2} x^2 - \frac{\not{p}}{m} x + 1 \right) \right. \right.$$
$$\left. - 2 \int_0^1 dx \frac{\overline{x} x (3x^2 + 6x - 5)}{(\Delta_{\mathrm{os}}/m^2)} + 4 \int_0^1 dx \frac{\overline{x}^2 x^2 (\overline{x} x - 1)}{(\Delta_{\mathrm{os}}/m^2)^2} \right]$$
$$+ m \not{e} \left[\int_0^1 dx (2 - x) \ln \left(\frac{\Delta_{\mathrm{os}}}{\Delta} \right) + 4 \int_0^1 dx \frac{\overline{x} x (x^2 - 4\overline{x})}{(\Delta_{\mathrm{os}}/m^2)} \right.$$
$$\left. \left. - 4 \int_0^1 dx \frac{\overline{x}^2 x^2 (\overline{x} x - 1)}{(\Delta_{\mathrm{os}}/m^2)^2} \right] \right\}. \tag{3.84}$$

The new radiatively induced term reads from the first line, $e \cdot p \frac{\not{p}}{m}$, and actually resembles an a-like coefficient $a_{\mu\nu\rho}^{(5)} \leftrightarrow \frac{1}{m} e_\mu \eta_{\nu\rho}$ associated to the dimension 5 operator $\overline{\psi} \gamma^\rho \partial^\mu \partial^\nu \psi$. This sort of mixing, even for radiatively induced structures, can be traced back to the

3. Fermion self-energy of the minimal QED extension

arguments of field redefinition discussed in Sec. 3.1.

Renormalized contribution from f^μ

Renormalization of f^μ, similarly to the $c_A^{\mu\nu}$ case, involves only a single structure, namely $p_\mu\gamma_5$, such that

$$\Sigma_f^{\mathrm{R}} = \Sigma_f - i\left[(\mathcal{Z}_{f\cdot p\gamma_5})^\mu{}_\nu f^\nu - f^\mu\right]p_\mu\gamma_5. \tag{3.85}$$

This could be foreseen noticing the on shell relation $\overline{u}(p)(p_\mu\gamma_5)u(p) = 0$, and because Σ_f^{R} involves only this structure both renormalization conditions of (3.49) are automatically satisfied. Therefore, we have room for only a single counterterm which we choose so as to ensure the finiteness of Σ_f^{R} and absence of the mass scale μ. The counterterm then reads

$$(\mathcal{Z}_{f\cdot p\gamma_5})^\mu{}_\nu f^\nu = f^\mu + \frac{\alpha}{2\pi}f^\mu\left\{ -\frac{1}{2}\left(\frac{1}{\varepsilon} - \gamma_E + \frac{5}{3}\right) - \int_0^1 dx\, x(5 - 6x)\ln\left(\frac{4\pi\mu^2}{\Delta_{\mathrm{os}}}\right) + \kappa_f\right\}, \tag{3.86}$$

such that, for the f^μ correction to the renormalized fermion self-energy, we obtain

$$\Sigma_f^{\mathrm{R}}(p) = \frac{\alpha}{2\pi}if\cdot p\gamma_5\left\{ -\int_0^1 dx\, x(5 - 6x)\ln\left(\frac{\Delta_{\mathrm{os}}}{\Delta}\right) + 2\int\frac{\overline{x}x}{(\Delta/m^2)}\left(\frac{p^2}{m^2}x - 1\right) - \kappa_f\right\}, \tag{3.87}$$

where the free parameter κ_f can be set, for instance, to zero for simplicity. The absence of on shell contributions from f^μ is expected by arguments of field redefinition, where it is known the f^μ coefficient can be eliminated from lagrangian (3.1) by a choice of spinor basis such that its effects are unobservable to all orders [76]. As expected, f^μ leads no new structure by means of radiative corrections to the fermion self-energy.

Renormalized contribution from $g^{\kappa\lambda\mu}$

Renormalization of the $g^{\kappa\lambda\mu}$ contribution to the fermion self-energy suffers from the same issues found for $c^{\mu\nu}$ and $d^{\mu\nu}$, i.e., not all contributions from its irreducible

3. Fermion self-energy of the minimal QED extension

representations can be adequately renormalized. This coefficient can be decomposed into axial $g_A^{\kappa\lambda\mu}$, trace $g_T^{\kappa\lambda\mu}$, and mixed-symmetry $g_M^{\kappa\lambda\mu}$ representations, explicitly given by [77]

$$g_A^{\kappa\lambda\mu} = \tfrac{1}{6} g^{\nu\rho\sigma} \epsilon_{\nu\rho\sigma\alpha} \epsilon^{\alpha\kappa\lambda\mu} = \tfrac{1}{3}(g^{\kappa\lambda\mu} + g^{\mu\kappa\lambda} + g^{\lambda\mu\kappa}), \tag{3.88}$$

$$g_T^{\kappa\lambda\mu} = \tfrac{1}{3} \eta_{\alpha\beta}(g^{\kappa\alpha\beta}\eta^{\lambda\mu} - g^{\lambda\alpha\beta}\eta^{\kappa\mu}), \tag{3.89}$$

$$g_M^{\kappa\lambda\mu} = \tfrac{1}{3}(g^{\kappa\lambda\mu} + g^{\kappa\mu\lambda} + \eta_{\alpha\beta}g^{\lambda\alpha\beta}\eta^{\kappa\mu}) - (\kappa \leftrightarrow \lambda). \tag{3.90}$$

Inspection of the regularized $g^{\kappa\lambda\mu}$ contribution (3.31) to the fermion self-energy suggests two counterterms proportional to $p^\mu\sigma^{\kappa\lambda}$ and $\epsilon^{\kappa\lambda\mu\nu}\gamma_5\gamma_\nu$. The on shell relation between these structures is $\bar{u}(p)(p^\mu\sigma^{\kappa\lambda} + p^\lambda\sigma^{\mu\kappa} + p^\kappa\sigma^{\lambda\mu})u(p) = \bar{u}(p)(m\epsilon^{\kappa\lambda\mu\nu}\gamma_5\gamma_\nu)u(p)$. This relation suggests these counterterms renormalize contributions from the totally antisymmetric axial piece $g_A^{\kappa\lambda\mu}$. This is in agreement with expectations motivated by a glance at the lagrangian (3.5) obtained after field redefinitions.

Renormalization of the antisymmetric piece is expected to proceed without problems. Indeed, using the total antisymmetry of $g_A^{\kappa\lambda\mu}$, from (3.31) its regularized contribution reads

$$
\begin{aligned}
i\Sigma_{g_A}(p) = \frac{\alpha}{2\pi} \Bigg\{ & -\frac{1}{12}(p_\mu\sigma_{\kappa\lambda} + p_\lambda\sigma_{\mu\kappa} + p_\kappa\sigma_{\lambda\mu})g_A^{\kappa\lambda\mu}\left[\left(\frac{1}{\varepsilon} - \gamma_E - 1\right) + 2\int_0^1 dx\, x \ln\left(\frac{4\pi\mu^2}{\Delta}\right)\right] \\
& + \frac{1}{2}m g_A^{\kappa\lambda\mu}\epsilon_{\kappa\lambda\mu\nu}\gamma_5\gamma^\nu \left[\frac{1}{2}\left(\frac{1}{\varepsilon} - \gamma_E - 1\right) + \int_0^1 dx\, x \ln\left(\frac{4\pi\mu^2}{\Delta}\right)\right] \\
& - m g_A^{\kappa\lambda\mu}\epsilon_{\kappa\lambda\nu\rho}\frac{p_\mu}{m}\frac{p^\rho}{m}\gamma_5\gamma^\nu \int_0^1 dx\, \frac{\bar{x}x^2}{(\Delta/m^2)} \Bigg\},
\end{aligned}
\tag{3.91}
$$

which is renormalized according to

$$
\begin{aligned}
\Sigma_{g_A}^{\mathrm{R}} = \Sigma_{g_A} & -\frac{1}{3}\Big[(\mathcal{Z}_{g_A p\sigma})^{\kappa\lambda\mu}{}_{\nu\rho\sigma}g_A^{\nu\rho\sigma} - g_A^{\kappa\lambda\mu}\Big](p_\mu\sigma_{\kappa\lambda} + p_\lambda\sigma_{\mu\kappa} + p_\kappa\sigma_{\lambda\mu}) \\
& + \frac{1}{2}\Big[(\mathcal{Z}_{g_A \gamma_5\gamma})^{\kappa\lambda\mu}{}_{\nu\rho\sigma}g^{\nu\rho\sigma} - g^{\kappa\lambda\mu}\Big]m\epsilon_{\kappa\lambda\mu\nu}\gamma_5\gamma^\nu,
\end{aligned}
\tag{3.92}
$$

3. Fermion self-energy of the minimal QED extension

with counterterms given by

$$(\mathcal{Z}_{g_A p \sigma})^{\kappa\lambda\mu}{}_{\nu\rho\sigma} g_A^{\nu\rho\sigma} = g_A^{\kappa\lambda\mu} + \frac{\alpha}{2\pi} g_A^{\kappa\lambda\mu} \left\{ -\frac{1}{4}\left(\frac{1}{\varepsilon} - \gamma_E - 1\right) - \frac{1}{2}\int_0^1 dx\, x \ln\left(\frac{4\pi\mu^2}{\Delta_{\text{os}}}\right) \right.$$
$$\left. +2\int_0^1 dx\, \frac{\overline{x}x(11x-6)}{(\Delta_{\text{os}}/m^2)} + 8\int_0^1 dx\, \frac{\overline{x}^2 x^3}{(\Delta_{\text{os}}/m^2)^2} \right\},$$

(3.93)

$$(\mathcal{Z}_{g_A \gamma_5 \gamma})^{\kappa\lambda\mu}{}_{\nu\rho\sigma} g_A^{\nu\rho\sigma} = g_A^{\kappa\lambda\nu} - \frac{\alpha}{2\pi} g_A^{\kappa\lambda\mu} \left\{ \frac{1}{2}\left(\frac{1}{\varepsilon} - \gamma_E - 1\right) + \int_0^1 dx\, x \ln\left(\frac{4\pi\mu^2}{\Delta_{\text{os}}}\right) \right.$$
$$\left. +16\int_0^1 dx\, \frac{\overline{x}^2 x}{(\Delta_{\text{os}}/m^2)} - \frac{16}{3}\int_0^1 dx\, \frac{\overline{x}^2 x^3}{(\Delta_{\text{os}}/m^2)^2} \right\}.$$

(3.94)

Finally, the renormalized contribution of the axial piece $g_A^{\kappa\lambda\mu}$ to the self-energy reads

$$\Sigma_{g_A}^R(p) = \frac{\alpha}{2\pi} \left\{ \frac{1}{3}(p_\mu \sigma_{\kappa\lambda} + p_\lambda \sigma_{\mu\kappa} + p_\kappa \sigma_{\lambda\mu}) g_A^{\kappa\lambda\mu} \left[-\frac{1}{2}\int_0^1 dx\, x \ln\left(\frac{\Delta_{\text{os}}}{\Delta}\right) \right. \right.$$
$$\left. -2\int_0^1 dx\, \frac{\overline{x}x(11x-6)}{(\Delta_{\text{os}}/m^2)} - 8\int_0^1 dx\, \frac{\overline{x}^2 x^3}{(\Delta_{\text{os}}/m^2)^2} \right]$$
$$+ \frac{1}{2} m g_A^{\kappa\lambda\mu} \epsilon_{\kappa\lambda\mu\nu} \gamma_5 \gamma^\nu \left[\int_0^1 dx\, x \ln\left(\frac{\Delta_{\text{os}}}{\Delta}\right) \right.$$
$$\left. -16\int_0^1 dx\, \frac{\overline{x}^2 x}{(\Delta_{\text{os}}/m^2)} + \frac{16}{3}\int_0^1 dx\, \frac{\overline{x}^2 x^3}{(\Delta_{\text{os}}/m^2)^2} \right]$$
$$\left. - m g_A^{\kappa\lambda\mu} \epsilon_{\kappa\lambda\nu\rho} \frac{p_\mu}{m}\frac{p^\rho}{m} \gamma_5 \gamma^\nu \int_0^1 dx\, \frac{\overline{x}x^2}{(\Delta/m^2)} \right\}.$$

(3.95)

Using also the identity $\overline{u}(p)(g_A^{\kappa\lambda\mu}\epsilon_{\kappa\lambda\nu\rho}p_\mu p^\rho \gamma_5 \gamma^\nu)u(p) = \overline{u}(p)(-\frac{4}{3}m^2 g_A^{\kappa\lambda\mu}\epsilon_{\kappa\lambda\mu\nu}\gamma_5\gamma^\nu)u(p)$, the above renormalized expression is found to satisfy both renormalization conditions of (3.49).

Arguments of field redefinition entangle b^μ and $g_A^{\kappa\lambda\mu}$ into a single observable coefficient combination. In this sense, the new structure radiatively induced by Σ_b^R should also be induced by $\Sigma_{g_A}^R$. Indeed, the last line of (3.95) reveals an induced term of the form $m g_A^{\kappa\lambda\mu}\epsilon_{\kappa\lambda\nu\rho}\frac{p_\mu}{m}\frac{p^\rho}{m}\gamma_5\gamma^\nu$, in agreement to the structure induced by Σ_b^R.

3. Fermion self-energy of the minimal QED extension

Effectively, this term behaves as a b-like coefficient $b^{(5)\mu\alpha\beta} \leftrightarrow \frac{1}{m} g_A^{\kappa\lambda\alpha} \epsilon_{\kappa\lambda}{}^{\beta\mu}$ associated to a dimension 5 operator $\overline{\psi}\gamma_5 \gamma_\mu \partial_\alpha \partial_\beta \psi$.

As for the trace part $g_T^{\kappa\lambda\mu}$, the regularized contribution reads

$$\Sigma_{g_T}(p) = \frac{\alpha}{2\pi} \left\{ \frac{1}{3} p^\lambda \sigma_{\kappa\lambda} g_{T}^{\kappa\mu}{}_\mu \left[\frac{1}{4} \left(\frac{1}{\varepsilon} - \gamma_E - 1 \right) - \frac{1}{2} \int_0^1 dx\, x \ln \left(\frac{4\pi\mu^2}{\Delta} \right) \right] \right\}, \qquad (3.96)$$

and is renormalized receiving only one counterterm,

$$\Sigma_{g_T}^{\mathrm{R}} = \Sigma_{g_T} - \frac{1}{3} \left[(\mathcal{Z}_{g_T p\sigma})^{\kappa\lambda\mu}{}_{\nu\rho\sigma} g_T^{\nu\rho\sigma} - g_T^{\kappa\lambda\mu} \right] \eta_{\lambda\mu} p^\tau \sigma_{\kappa\tau}, \qquad (3.97)$$

where

$$(\mathcal{Z}_{g_T p\sigma})^{\kappa\lambda\mu}{}_{\nu\rho\sigma} g_T^{\nu\rho\sigma} = g_T^{\kappa\lambda\mu} + \frac{\alpha}{2\pi} g_T^{\kappa\lambda\mu} \left\{ \frac{1}{4} \left(\frac{1}{\varepsilon} - \gamma_E - 1 \right) - \frac{1}{2} \int_0^1 dx\, x \ln \left(\frac{4\pi\mu^2}{\Delta_{\mathrm{os}}} \right) + \kappa_{g_T} \right\}. \qquad (3.98)$$

The final expression for the $g_T^{\kappa\lambda\mu}$ contribution to the fermion energy reads

$$\Sigma_{g_T}^{\mathrm{R}}(p) = \frac{\alpha}{2\pi} \left\{ -\frac{1}{3} p^\lambda \sigma_{\kappa\lambda} g_T^{\kappa\mu}{}_\mu \left[\frac{1}{2} \int_0^1 dx\, x \ln \left(\frac{\Delta_{\mathrm{os}}}{\Delta} \right) - \kappa_{g_T} \right] \right\}. \qquad (3.99)$$

Similarly to other unobservable coefficients, having only one free parameter is not a problem here because this expression vanishes on shell, $\overline{u}(p)(p^\lambda \sigma_{\kappa\lambda})u(p) = 0$, automatically satisfying both renormalization conditions of (3.49), thus we can simply set $\kappa_{g_T} = 0$. Once more, this result does not come as a surprise because, as discussed in Sec. 3.1, the $g_T^{\kappa\lambda\mu}$ is unobservable at leading order. Also, no new structure is radiatively induced.

On the other hand, contribution from the mixed-symmetry $g_M^{\kappa\lambda\mu}$ part of $g^{\kappa\lambda\mu}$ cannot be consistently renormalized because it involves only one counterterm related to $p_\mu \sigma_{\kappa\lambda}$,

$$\Sigma_{g_M}^{R}(p) = \Sigma_{g_M}(p) - \left[(\mathcal{Z}_{g_M p\sigma})^{\kappa\lambda\mu}{}_{\nu\rho\sigma} g_M^{\nu\rho\sigma} - g_M^{\kappa\lambda\mu} \right] p_\mu \sigma_{\kappa\lambda}, \qquad (3.100)$$

3. Fermion self-energy of the minimal QED extension

as we can see from the regularized expression (3.31) by setting $g^{\kappa\lambda\mu} \to g_M^{\kappa\lambda\mu}$,

$$\Sigma_{g_M}(p) = \frac{\alpha}{2\pi} \left\{ \frac{1}{2} p_\mu \sigma_{\kappa\lambda} g_M^{\kappa\lambda\mu} \left[\frac{1}{\varepsilon} - \gamma_E + 2 \int_0^1 dx\, x \ln\left(\frac{4\pi\mu^2}{\Delta} \right) \right] \right.$$
$$\left. - m g_M^{\kappa\lambda\mu} \epsilon_{\kappa\lambda\nu\rho} \frac{p_\mu}{m} \frac{p^\rho}{m} \gamma_5 \gamma^\nu \int_0^1 dx\, \frac{\overline{x} x^2}{(\Delta/m^2)} \right\}, \tag{3.101}$$

and writing the $\mathcal{Z}$ factor of (3.100 as,

$$(\mathcal{Z}_{g_M p\sigma})^{\kappa\lambda\mu}{}_{\nu\rho\sigma} g_M^{\nu\rho\sigma} = g_M^{\kappa\lambda\mu} - \frac{\alpha}{2\pi} g_M^{\kappa\lambda\mu} \left\{ \frac{1}{2} \left[\frac{1}{\varepsilon} - \gamma_E + 2 \int_0^1 dx\, x \ln\left(\frac{4\pi\mu^2}{\Delta_{\text{os}}} \right) \right] + \kappa_{g_M} \right\}, \tag{3.102}$$

such that renormalization of this contribution introduces only one free parameter κ_{g_M},

$$\Sigma_{g_M}^R(p) = \frac{\alpha}{2\pi} \left\{ \frac{1}{2} p_\mu \sigma_{\kappa\lambda} g_M^{\kappa\lambda\mu} \left[2 \int_0^1 dx\, x \ln\left(\frac{\Delta_{\text{os}}}{\Delta} \right) - \kappa_{g_M} \right] \right.$$
$$\left. - m g_M^{\kappa\lambda\mu} \epsilon_{\kappa\lambda\nu\rho} \frac{p_\mu}{m} \frac{p^\rho}{m} \gamma_5 \gamma^\nu \int_0^1 dx\, \frac{\overline{x} x^2}{(\Delta/m^2)} \right\}, \tag{3.103}$$

such that renormalization conditions (3.49) cannot be simultaneously satisfied.

Similarly to $c_S^{\mu\nu}$, but differently from the $d_S^{\mu\nu}$ case, the new structure radiatively induced by $\Sigma_{g_M}^{\text{R}}$ — as inferred from the last line of (3.103) — satisfy an interesting identity, $\overline{u}(p)(\epsilon_{\kappa\lambda\nu\rho} p_\mu p^\nu \gamma_5 \gamma^\rho) u(p) = \overline{u}(p)(m p_\mu \sigma_{\kappa\lambda}) u(p)$, but again this term does not receive a counterterm as it is not in the original lagrangian (3.1).

Renormalized contribution from $H^{\mu\nu}$

Renormalization of $H^{\mu\nu}$ involves two structures, $p_\mu \gamma_5 \gamma_\nu$ and $\sigma_{\mu\nu}$,

$$\Sigma_H^{\text{R}} = \Sigma_H - \left[(\mathcal{Z}_{Hp\gamma_5\gamma})^{\mu\nu}{}_{\rho\sigma} H^{\rho\sigma} - H^{\mu\nu} \right] \epsilon_{\mu\nu\rho\sigma} \frac{p^\rho}{m} \gamma_5 \gamma^\sigma + \frac{1}{2} \left[(\mathcal{Z}_{H\sigma})^{\mu\nu}{}_{\rho\sigma} H^{\rho\sigma} - H^{\mu\nu} \right] \sigma_{\mu\nu}, \tag{3.104}$$

where the second counterterm renormalizes (zero) $\times\, H^{\mu\nu} \sigma_{\mu\nu}$, and is motivated by $\overline{u}(p)(\epsilon_{\mu\nu\rho\sigma} p^\nu \gamma_5 \gamma^\mu) u(p) = \overline{u}(p)(m \sigma_{\rho\sigma}) u(p)$, similarly to previous cases. The renormal-

ization factors read

$$(\mathcal{Z}_{Hp\gamma_5\gamma})^{\mu\nu}{}_{\rho\sigma}H^{\rho\sigma} = H^{\mu\nu} + \frac{\alpha}{2\pi}H^{\mu\nu}\left\{\int_0^1 dx\,\frac{\overline{x}x(4\overline{x}+1)}{(\Delta_{\mathrm{os}}/m^2)} + 2\int_0^1 dx\,\frac{\overline{x}^2x^2}{(\Delta_{\mathrm{os}}/m^2)^2}\right\}, \quad (3.105)$$

$$(\mathcal{Z}_{H\sigma})^{\mu\nu}{}_{\rho\sigma}H^{\rho\sigma} = H^{\mu\nu} - \frac{\alpha}{2\pi}H^{\mu\nu}\left\{4\int_0^1 dx\,\frac{\overline{x}x(3x-4)}{(\Delta_{\mathrm{os}}/m^2)} - 4\int_0^1 dx\,\frac{\overline{x}^2x^2}{(\Delta_{\mathrm{os}}/m^2)^2}\right\},$$
$$(3.106)$$

leading to the renormalized contribution of $H^{\mu\nu}$ to the self-energy,

$$\Sigma_H^{\mathrm{R}} = \frac{\alpha}{2\pi}\left\{H_{\mu\nu}\epsilon^{\mu\nu\rho\sigma}\frac{p_\rho}{m}\gamma_5\gamma_\sigma\left[\int_0^1 dx\,\frac{\overline{x}x}{(\Delta/m^2)} - \int_0^1 dx\,\frac{\overline{x}x(4\overline{x}+1)}{(\Delta_{\mathrm{os}}/m^2)} - 2\int_0^1 dx\,\frac{\overline{x}^2x^2}{(\Delta_{\mathrm{os}}/m^2)^2}\right]\right.$$
$$\left. - 2H_{\mu\nu}\sigma^{\mu\nu}\left[\int_0^1 dx\,\frac{\overline{x}x(3x-4)}{(\Delta_{\mathrm{os}}/m^2)} - \int_0^1 dx\,\frac{\overline{x}^2x^2}{(\Delta_{\mathrm{os}}/m^2)^2}\right]\right\}. \quad (3.107)$$

Field redefinitions entangle $d_A^{\mu\nu}$ and $H^{\mu\nu}$ into a single observable coefficient combination. Renormalization of Σ_{d_A} revealed no radiatively induced new structure, and the same happened for Σ_H, as expected.

Renormalized contribution from $(k_{AF})^\mu$

As the $(k_{AF})_\mu$ coefficient has no tree-level contribution to the fermion propagator and its contribution to the fermion self-energy receives counterterms only indirectly, from counterterms of the b_μ and $g_A^{\kappa\lambda\mu}$ contributions to the self-energy, thus its renormalized contribution has the form

$$\Sigma_{k_{AF}}^{\mathrm{R}} = \Sigma_{k_{AF}} - \left[(\mathcal{Z}_{k_{AF}p\sigma})_\mu{}^\nu(k_{AF})_\nu - (k_{AF})_\mu\right]\epsilon^{\mu\nu\rho\sigma}\frac{p_\nu}{m}\sigma_{\rho\sigma}$$
$$+ \left[(\mathcal{Z}_{\gamma_5\slashed{k}_{AF}})^\mu{}_\nu(k_{AF})^\nu - (k_{AF})^\mu\right]\gamma_5\gamma_\mu, \quad (3.108)$$

which is completely analogous to the b_μ case. Therefore, renormalization of $\Sigma_{k_{AF}}$ comes from one counterterm from the $g_A^{\kappa\lambda\mu}$ part of the counterterm lagrangian (3.41) and another from the b_μ part, respectively, and these structures are related by $\overline{u}(p)(\epsilon^{\mu\nu\rho\sigma}p_\nu\sigma_{\rho\sigma})u(p) = \overline{u}(p)(2m\gamma_5\gamma^\mu)u(p)$.

3. Fermion self-energy of the minimal QED extension

Renormalization conditions (3.49) lead to $\mathcal{Z}$ factors as given by

$$(\mathcal{Z}_{k_{AF}p\sigma})^\mu{}_\nu (k_{AF})^\nu = (k_{AF})^\mu + \frac{\alpha}{2\pi}(k_{AF})^\mu \left\{ \int_0^1 dx \frac{\overline{x}x(1+x)}{(\Delta_{\rm os}/m^2)} + 2\int_0^1 dx \frac{\overline{x}^3 x^2}{(\Delta_{\rm os}/m^2)^2} \right\},$$

(3.109)

$$(\mathcal{Z}_{\gamma_5 k_{AF}})^\mu{}_\nu (k_{AF})^\nu = (k_{AF})^\mu - \frac{\alpha}{2\pi}(k_{AF})^\mu \left\{ -\frac{3}{2}\left(\frac{1}{\varepsilon} - \gamma \right) + 3\int_0^1 dx\, x \ln\left(\frac{4\pi\mu^2}{\Delta_{\rm os}} \right) \right.$$
$$\left. - 4\int_0^1 dx \frac{\overline{x}x^2}{(\Delta_{\rm os}/m^2)} - 4\int_0^1 dx \frac{\overline{x}^3 x^2}{(\Delta_{\rm os}/m^2)^2} \right\},$$

(3.110)

such that the renormalized $(k_{AF})_\mu$ correction to the self-energy reads

$$\Sigma_{k_{AF}}^R(p) = \frac{\alpha}{2\pi} \left\{ \gamma_5 \slashed{k}_{AF} \left[3\int_0^1 dx\, x \ln\left(\frac{\Delta_{\rm os}}{\Delta} \right) - 2\frac{p^2}{m^2}\int_0^1 dx \frac{\overline{x}x^2}{(\Delta/m^2)} + 4\int_0^1 dx \frac{\overline{x}x^2}{(\Delta_{\rm os}/m^2)} \right.\right.$$
$$\left. + 4\int_0^1 dx \frac{\overline{x}^3 x^2}{(\Delta_{\rm os}/m^2)^2} \right] + 2k_{AF} \cdot \frac{p}{m}\gamma_5 \frac{\slashed{p}}{m}\int_0^1 dx \frac{\overline{x}x^2}{(\Delta/m^2)}$$
$$+ (k_{AF})_\mu \epsilon^{\mu\nu\rho\sigma} \frac{p_\nu}{m}\sigma^{\rho\sigma} \left[\int_0^1 dx \frac{\overline{x}x}{(\Delta/m^2)} - \int_0^1 dx \frac{\overline{x}x(1+x)}{(\Delta_{\rm os}/m^2)} \right.$$
$$\left.\left. - 2\int_0^1 dx \frac{\overline{x}^3 x^2}{(\Delta_{\rm os}/m^2)^2} \right] \right\}.$$

(3.111)

It is important to emphasize that the renormalization factors (3.109) will be later reinterpreted as renormalizing the b_μ and $g_A^{\kappa\lambda\mu}$ coefficients, effectively mixing them with $(k_{AF})_\mu$ to one-loop order. Renormalization of the $(k_{AF})_\mu$ coefficient is determined by means of renormalization of the photon self-energy, which we do not deal with in this work.

The radiatively induced term with new structure is $k_{AF} \cdot \frac{p}{m}\gamma_5 \frac{\slashed{p}}{m}$, which can be seen as b-like coefficient $b_{\mu\alpha\beta}^{(5)} \leftrightarrow \frac{1}{m^2}(k_{AF})_\alpha \eta_{\beta\mu}$ associated with a dimension 5 operator $\overline{\psi}\gamma_5\gamma^\mu \partial^\alpha \partial^\beta \psi$.

3. Fermion self-energy of the minimal QED extension

Renormalized contribution from $(k_F)^{\mu\nu\rho\sigma}$

Contributions from $(k_F)^{\mu\nu\rho\sigma}$ to the fermion self-energy are all related to the symmetric coefficient $(k_F)^{\mu\lambda\nu}{}_\lambda = (k_F)^{\nu\lambda\mu}{}_\lambda$, and inspection of (3.34) reveals it receives counterterms originating from the symmetric $c_S^{\mu\nu}$ part of the lagrangian, and thus suffers from the same problems found for Σ_{c_S} in (3.72). It receives only one counterterm,

$$\Sigma_{k_F}^{\mathrm{R}} = \Sigma_{k_F} - \frac{1}{2}\Big[(\mathcal{Z}_{k_F p\gamma})^{\mu\nu}{}_{\rho\sigma}(k_F)^{\rho\lambda\sigma}{}_\lambda - (k_F)^{\mu\lambda\nu}{}_\lambda\Big](p_\mu\gamma_\nu + p_\nu\gamma_\mu), \qquad (3.112)$$

where

$$(\mathcal{Z}_{k_F p\gamma})^{\mu\nu}{}_{\rho\sigma}(k_F)^{\rho\lambda\sigma}{}_\lambda$$
$$= (k_F)^{\mu\lambda\nu}{}_\lambda - \frac{\alpha}{3\pi}(k_F)^{\mu\lambda\nu}{}_\lambda\left\{\frac{1}{\varepsilon} - \gamma_E + \frac{3}{2}\int_0^1 dx\, x(2-x)\ln\left(\frac{4\pi\mu^2}{\Delta_{\mathrm{os}}}\right) + \kappa_{k_F}\right\}. \quad (3.113)$$

The renormalized contribution reads

$$\Sigma_{k_F}^{\mathrm{R}}(p) = -\frac{\alpha}{2\pi}\left\{\frac{1}{2}(p^\mu\gamma^\nu + p^\nu\gamma^\mu)(k_F)_{\mu\rho\nu}{}^\rho\left[\frac{3}{2}\int_0^1 dx\, x(2-x)\ln\left(\frac{\Delta_{\mathrm{os}}}{\Delta}\right) - \frac{2}{3}\kappa_{k_F}\right]\right.$$
$$\left. + (k_F)_{\mu\rho\nu}{}^\rho p^\mu \frac{p^\nu}{m}\int_0^1 dx\,\frac{\overline{x}^2 x}{(\Delta/m^2)}\left(\frac{\slashed{p}}{m}x - 1\right)\right\}, \qquad (3.114)$$

and the problem of having only one free parameter to fix two renormalization conditions persists. This was to be expected, as coefficients $c_S^{\mu\nu}$ and $(k_F)^{\mu\lambda\nu}{}_\lambda$ are phenomenologically indistinguishable.

Paralleling the $c_S^{\mu\nu}$ case, two new structures are radiatively induced by $\Sigma_{k_F}^{\mathrm{R}}$. One proportional to $(k_F)_{\mu\lambda\nu}{}^\lambda p^\mu \frac{p^\nu}{m}\frac{\slashed{p}}{m}$, and resembles a c-like coefficient $c_S^{(6)\mu\nu\rho\sigma} \leftrightarrow \frac{1}{m^2}\eta^{\mu\nu}(k_F)^{\rho\lambda\sigma}{}_\lambda$ associated to a dimension 6 operator $i\overline{\psi}(\gamma_\mu\partial_\nu + \gamma_\nu\partial_\mu)\partial_\rho\partial_\sigma\psi$. The other comes from the term proportional to $(k_F)^{\mu\lambda\nu}{}_\lambda p^\mu \frac{p^\nu}{m}$, and it effectively behaves as a mass-like coefficient $m^{(5)\mu\nu} \leftrightarrow \frac{1}{m}(k_F)^{\mu\lambda\nu}{}_\lambda$ associated to a dimension 5 operator $\overline{\psi}\partial_\mu\partial_\nu\psi$.

3.3.3 Renormalization factors

Finally, we are in position to organize our results and write down the counterterms with corresponding renormalization factors Z for the Lorentz-violating corrections

3. Fermion self-energy of the minimal QED extension

to the fermion self-energy.

The one-loop renormalized fermion self-energy $\Sigma_{\mathrm{R}}(p)$ is finally given by

$$
\begin{aligned}
\Sigma_{\mathrm{R}} = & \Sigma_{\mathrm{QED}}^{\mathrm{R}} + (\Sigma_a^{\mathrm{R}} + \Sigma_e^{\mathrm{R}}) + (\Sigma_b^{\mathrm{R}} + \Sigma_{g_A}^{\mathrm{R}} + \Sigma_{k_{AF}}^{\mathrm{R}}) + (\Sigma_{d_A}^{\mathrm{R}} + \Sigma_H^{\mathrm{R}}) \\
& + \Sigma_{c_A}^{\mathrm{R}} + \Sigma_f^{\mathrm{R}} + \Sigma_{g_T}^{\mathrm{R}} + (\Sigma_{c_S}^{\mathrm{R}} + \Sigma_{k_F}^{\mathrm{R}}) + \Sigma_{d_S}^{\mathrm{R}} + \Sigma_{g_M}^{\mathrm{R}},
\end{aligned} \tag{3.115}
$$

where each individual contribution was calculated in the previous section, and we have grouped them in a suggestive way to be explained soon. Each of these contributions contain $\mathcal{Z}$ factors that carries out renormalization — we have also found all of them in the previous section. The counterterm lagrangians (3.39) and (3.41) contains renormalization factors Z instead of $\mathcal{Z}$, but from our approach explained after Eq. (3.41), we know (in a symbolic sense) that $Z \supset \mathcal{Z}$. In what follows, it is our intention to write the explicit renormalization factors Z that appear in the counterterm lagrangians (3.39) and (3.41). These truly reveals the mixing of Lorentz-violating coefficients under quantum corrections, giving a new look to results previously presented. We emphasize that all quantities to be presented next were determined in previous sections, except for the Z factors.

The way individual contributions to the fermion self-energy are grouped together in (3.115) reflects how they mix under quantum corrections, as expected by field redefinition arguments and discussed in what follows. Ungrouped contributions do not mix at all. Furthermore, renormalization of the last four contributions in the second line, from coefficients $c_S^{\mu\nu}$, $(k_F)^{\mu\rho\nu}{}_\rho$, $d_S^{\mu\nu}$, and $g_M^{\kappa\lambda\mu}$, respectively, failed to be consistent as they do not satisfy renormalization conditions (3.49).

The conventional QED contribution $\Sigma_{\mathrm{QED}}^{\mathrm{R}}$ is given by (3.56), and we have seen it comes solely from $\Sigma_{\mathrm{QED}}^{\mathrm{R}} = \Sigma_{\mathrm{QED}} - (Z_\psi - 1)\not{p} + (Z_m - 1)m$, where

$$
Z_\psi = 1 - \frac{\alpha}{2\pi} \left\{ \frac{1}{2} \left(\frac{1}{\varepsilon} - \gamma_E - 1 \right) + \int_0^1 dx\, x \ln \left(\frac{4\pi\mu^2}{\Delta_{\mathrm{os}}} \right) + 2 \int_0^1 dx\, \frac{\overline{x} x(x-2)}{(\Delta_{\mathrm{os}}/m^2)} \right\},
$$

$$
Z_m = 1 - \frac{\alpha}{2\pi} \left\{ 2 \left(\frac{1}{\varepsilon} - \gamma_E - \frac{1}{2} \right) + 2 \int_0^1 dx \ln \left(\frac{4\pi\mu^2}{\Delta_{\mathrm{os}}} \right) + 2 \int_0^1 dx\, \frac{\overline{x} x(x-2)}{(\Delta_{\mathrm{os}}/m^2)} \right\}, \tag{3.116}
$$

3. Fermion self-energy of the minimal QED extension

matching with the conventional result — see, for instance [82].

Coefficients a^μ and e^μ are known to be entangled by field redefinitions. Accordingly, renormalization of their contributions to the fermion self-energy is consistently carried on only if both coefficients mix under quantum corrections. In this sense, renormalization have to be perform in the combination

$$\Sigma_a^{\mathrm{R}} + \Sigma_e^{\mathrm{R}} = \Sigma_a + \Sigma_e + \left[(Z_a)^\mu_{\ \nu}a^\nu - a^\mu\right]\gamma_\mu - \left[(Z_e)^\mu_{\ \nu}e^\nu - e^\mu\right]p_\mu, \qquad (3.117)$$

where we have already determined Σ_a^{R} (3.60) and Σ_e^{R} (3.84), and the renormalization factors are given by

$$(Z_a)^\mu_{\ \nu}a^\nu = a^\mu - \frac{\alpha}{2\pi}a^\mu \left\{ \frac{1}{2}\left(\frac{1}{\varepsilon} - \gamma_E - 2\right) + \int_0^1 dx\,\overline{x}\ln\left(\frac{4\pi\mu^2}{\Delta_{\mathrm{os}}}\right) \right.$$

$$\left. + \int_0^1 dx\frac{\overline{x}(7x^2 - 10x + 1)}{(\Delta_{\mathrm{os}}/m^2)} - 2\int_0^1 dx\frac{\overline{x}^2 x(\overline{x}^2 - 2x)}{(\Delta_{\mathrm{os}}/m^2)^2} \right\}$$

$$- \frac{\alpha}{2\pi}me^\mu \left\{ \frac{1}{2}\left(\frac{3}{\varepsilon} - 3\gamma_E - 1\right) + \int_0^1 dx(2 - x)\ln\left(\frac{4\pi\mu^2}{\Delta_{\mathrm{os}}}\right) \right.$$

$$\left. - 4\int_0^1 dx\frac{\overline{x}x(x^2 - 4\overline{x})}{(\Delta_{\mathrm{os}}/m^2)} + 4\int_0^1 dx\frac{\overline{x}^2 x^2(\overline{x}x - 1)}{(\Delta_{\mathrm{os}}/m^2)^2} \right\}, \quad (3.118)$$

$$(Z_e)^\mu_{\ \nu}e^\nu = e^\mu + \frac{\alpha}{2\pi}e^\mu \left\{ -\frac{1}{2}\left(\frac{1}{\varepsilon} - \gamma_E - \frac{5}{3}\right) + \int_0^1 dx(7x - 6)\ln\left(\frac{4\pi\mu^2}{\Delta_{\mathrm{os}}}\right) \right.$$

$$\left. + 2\int_0^1 dx\frac{\overline{x}x(3x^2 + 6x - 5)}{(\Delta_{\mathrm{os}}/m^2)} - 4\int_0^1 dx\frac{\overline{x}^2 x^2(\overline{x}x - 1)}{(\Delta_{\mathrm{os}}/m^2)^2} \right\}$$

$$+ \frac{\alpha}{2\pi}\frac{a^\mu}{m} \left\{ -2\int_0^1 dx\frac{\overline{x}x(2x - 1)}{(\Delta_{\mathrm{os}}/m^2)} + 2\int_0^1 dx\frac{\overline{x}^2 x(\overline{x}^2 - 2x)}{(\Delta_{\mathrm{os}}/m^2)^2} \right\}. \qquad (3.119)$$

This shows the intrinsic mixing of coefficients a^μ and e^μ suggested by field redefinitions and here realized by quantum corrections.

3. Fermion self-energy of the minimal QED extension

Similarly, contributions from b^μ, $g_A^{\kappa\lambda\mu}$, and $(k_{AF})^\mu$ are considered together,

$$\Sigma_b^{\text{R}} + \Sigma_{g_A}^{\text{R}} + \Sigma_{k_{AF}}^{\text{R}} = \Sigma_b + \Sigma_{g_A} + \Sigma_{k_{AF}} + \left[(Z_b)^\mu{}_\nu b^\nu - b^\mu \right] \gamma_5 \gamma_\mu$$

$$- \frac{1}{3} \left[(Z_{g_A})^{\kappa\lambda\mu}{}_{\nu\rho\sigma} g_A^{\nu\rho\sigma} - g_A^{\kappa\lambda\mu} \right] (p_\mu \sigma_{\kappa\lambda} + p_\lambda \sigma_{\mu\kappa} + p_\kappa \sigma_{\lambda\mu}), \quad (3.120)$$

with Σ_b^{R} (3.64), $\Sigma_{g_A}^{\text{R}}$ (3.95), and $\Sigma_{k_{AF}}^{\text{R}}$ (3.111) previously determined, and

$$(Z_b)^\mu{}_\nu b^\nu = b^\mu - \frac{\alpha}{2\pi} b^\mu \left\{ \frac{1}{2} \left(\frac{1}{\varepsilon} - \gamma_E + 2 \right) + \int_0^1 dx\, \overline{x} \ln \left(\frac{4\pi\mu^2}{\Delta_{\text{os}}} \right) \right.$$

$$\left. + \int_0^1 dx \frac{\overline{x}(9x^2 - 10x - 1)}{(\Delta_{\text{os}}/m^2)} + 2 \int_0^1 dx \frac{\overline{x}^2 x(x^2 + 1)}{(\Delta_{\text{os}}/m^2)^2} \right\}$$

$$+ \frac{\alpha}{2\pi} \frac{1}{2} m \epsilon^{\mu\nu\rho\sigma} (g_A)_{\nu\rho\sigma} \left\{ \frac{1}{2} \left(\frac{1}{\varepsilon} - \gamma_E - 1 \right) + \int_0^1 dx\, x \ln \left(\frac{4\pi\mu^2}{\Delta_{\text{os}}} \right) \right.$$

$$\left. + 16 \int_0^1 dx \frac{\overline{x}^2 x}{(\Delta_{\text{os}}/m^2)} - \frac{16}{3} \int_0^1 dx \frac{\overline{x}^2 x^3}{(\Delta_{\text{os}}/m^2)^2} \right\}$$

$$- \frac{\alpha}{2\pi} (k_{AF})^\mu \left\{ -\frac{3}{2} \left(\frac{1}{\varepsilon} - \gamma \right) + 3 \int_0^1 dx\, x \ln \left(\frac{4\pi\mu^2}{\Delta_{\text{os}}} \right) \right.$$

$$\left. - 4 \int_0^1 dx \frac{\overline{x} x^2}{(\Delta_{\text{os}}/m^2)} - 4 \int_0^1 dx \frac{\overline{x}^3 x^2}{(\Delta_{\text{os}}/m^2)^2} \right\}, \quad (3.121)$$

$$(Z_{g_A})^{\kappa\lambda\mu}{}_{\nu\rho\sigma} g_A^{\nu\rho\sigma} = g_A^{\kappa\lambda\mu} + \frac{\alpha}{2\pi} g_A^{\kappa\lambda\mu} \left\{ -\frac{1}{4} \left(\frac{1}{\varepsilon} - \gamma_E - 1 \right) - \frac{1}{2} \int_0^1 dx\, x \ln \left(\frac{4\pi\mu^2}{\Delta_{\text{os}}} \right) \right.$$

$$\left. + 2 \int_0^1 dx \frac{\overline{x} x(11x - 6)}{(\Delta_{\text{os}}/m^2)} + 8 \int_0^1 dx \frac{\overline{x}^2 x^3}{(\Delta_{\text{os}}/m^2)^2} \right\}$$

$$- \frac{\alpha}{2\pi} b_\alpha \epsilon^{\alpha\kappa\lambda\mu} \left\{ \int_0^1 dx \frac{\overline{x} x(4x - 3)}{(\Delta_{\text{os}}/m^2)} + \int_0^1 dx \frac{\overline{x}^2 x(x^2 + 1)}{(\Delta_{\text{os}}/m^2)^2} \right\}$$

$$+ \frac{\alpha}{2\pi} (k_{AF})_\alpha \epsilon^{\alpha\kappa\lambda\mu} \left\{ \int_0^1 dx \frac{\overline{x} x(1 + x)}{(\Delta_{\text{os}}/m^2)} + 2 \int_0^1 dx \frac{\overline{x}^3 x^2}{(\Delta_{\text{os}}/m^2)^2} \right\}.$$

$$(3.122)$$

It is now clear that all renormalization of the $(k_{AF})^\mu$ contribution to the fermion self-energy comes out due to mixing of this coefficient with b^μ and $g_A^{\kappa\lambda\mu}$.

3. Fermion self-energy of the minimal QED extension

As we have seen, the $c^{\mu\nu}$ coefficient splits into antisymmetric $c_A^{\mu\nu}$ and symmetric $c_S^{\mu\nu}$ representations. The renormalized contribution $\Sigma_{c_A}^{\mathrm{R}}$ from the antisymmetric part is given by (3.68), coming solely from $\Sigma_{c_A}^{\mathrm{R}} = \Sigma_{c_A} - \frac{1}{2}\left[(Z_{c_A})^{\mu\nu}{}_{\rho\sigma}c_A^{\rho\sigma} - c_A^{\mu\nu}\right](p_\mu\gamma_\nu - p_\nu\gamma_\mu)$, where

$$(Z_{c_A})^{\mu\nu}{}_{\rho\sigma}c_A^{\rho\sigma} = c_A^{\mu\nu} + \frac{\alpha}{2\pi}c_A^{\mu\nu}\left\{\frac{1}{6}\left[\frac{3}{\varepsilon} - 3\gamma_E - 4 + 18\int_0^1 dx\,\overline{x}x\ln\left(\frac{4\pi\mu^2}{\Delta_{\mathrm{os}}}\right)\right] + \kappa_{c_A}\right\}. \tag{3.123}$$

As we have discussed before, contribution from $c_A^{\mu\nu}$ to the one-loop fermion self-energy automatically satisfy both renormalization conditions of (3.49) without the need to fix a specific value for the free parameter κ_{c_A} contained in $(Z_{c_A})^{\mu\nu}{}_{\rho\sigma}$, thus we can set $\kappa_{c_A} = 0$ for simplicity. The arbitrariness for κ_{c_A} is not a problem as $c_A^{\mu\nu}$ has no observable effect to this order.

The symmetric part $c_S^{\mu\nu}$ and the coefficient $(k_F)^{\mu\rho\nu}{}_\rho$ are phenomenologically indistinguishable, thus they should be taken together for renormalization of their contributions,

$$\Sigma_{c_S}^{\mathrm{R}} + \Sigma_{k_F}^{\mathrm{R}} = \Sigma_{c_S} + \Sigma_{k_F} - \frac{1}{2}\left[(Z_{c_S})^{\mu\nu}{}_{\rho\sigma}c_S^{\rho\sigma} - c_S^{\mu\nu}\right](p_\mu\gamma_\nu + p_\nu\gamma_\mu). \tag{3.124}$$

But this renormalized contribution *cannot* be fully determined as the parameters κ_{c_S} and κ_{k_F} introduced by the counterterm,

$$(Z_{c_S})^{\mu\nu}{}_{\rho\sigma}c_S^{\rho\sigma} = c_S^{\mu\nu} + \frac{\alpha}{2\pi}c_S^{\mu\nu}\left\{\frac{1}{6}\left[\frac{5}{\varepsilon} - 5\gamma_E + 2 + 18\int_0^1 dx\,x(1+x)\ln\left(\frac{4\pi\mu^2}{\Delta_{\mathrm{os}}}\right)\right] + \kappa_{c_S}\right\}$$

$$- \frac{\alpha}{3\pi}(k_F)^{\mu\rho\nu}{}_\rho\left\{\frac{1}{\varepsilon} - \gamma_E + \frac{3}{2}\int_0^1 dx\,x(2-x)\ln\left(\frac{4\pi\mu^2}{\Delta_{\mathrm{os}}}\right) + \kappa_{k_F}\right\}, \tag{3.125}$$

cannot be consistently fixed so as to satisfy both renormalization conditions of (3.49), as discussed in previous section when considering renormalization of contributions from each individual Lorentz-violating coefficient. Although there are two free parameters they are entangled as they appear together with the same structure $(p_\mu\gamma_\nu + p_\nu\gamma_\mu)$.

3. Fermion self-energy of the minimal QED extension

The $d^{\mu\nu}$ coefficient is also split into antisymmetric $d_A^{\mu\nu}$ and symmetric $d_S^{\mu\nu}$ parts. Arguments of field redefinition tell us $d_A^{\mu\nu}$ and $H^{\mu\nu}$ are entangled to each other, thus only their combined contribution to the fermion self-energy can be properly renormalized,

$$\Sigma_{d_A}^{\mathrm{R}} + \Sigma_H^{\mathrm{R}} = \Sigma_{d_A} + \Sigma_H - \frac{1}{2} \left[(Z_{d_A})^{\mu\nu}{}_{\rho\sigma} d_A^{\rho\sigma} - d_A^{\mu\nu} \right] (p_\mu \gamma_5 \gamma_\nu - p_\nu \gamma_5 \gamma_\mu)$$
$$+ \frac{1}{2} \left[(Z_H)^{\mu\nu}{}_{\rho\sigma} H^{\rho\sigma} - H^{\mu\nu} \right] \sigma_{\mu\nu}, \qquad (3.126)$$

where $\Sigma_{d_A}^{\mathrm{R}}$ and Σ_H^{R} are given by (3.76) and (3.107), respectively, and the renormalization factors by

$$(Z_{d_A})^{\mu\nu}{}_{\rho\sigma} d_A^{\rho\sigma} = d_A^{\mu\nu} + \frac{\alpha}{2\pi} d_A^{\mu\nu} \left\{ \frac{1}{6} \left[\frac{3}{\varepsilon} - 3\gamma_E + 2 + 18 \int_0^1 dx \, \overline{x} x \ln \left(\frac{4\pi\mu^2}{\Delta_{\mathrm{os}}} \right) \right] \right.$$
$$\left. - \int_0^1 dx \frac{\overline{x} x (9\overline{x}^2 + 8x)}{(\Delta_{\mathrm{os}}/m^2)} - 2 \int_0^1 dx \frac{\overline{x}^2 x^2 (x^2 + 1)}{(\Delta_{\mathrm{os}}/m^2)^2} \right\}$$
$$+ \frac{\alpha}{2\pi} \epsilon^{\mu\nu\rho\sigma} \frac{H_{\rho\sigma}}{m} \left\{ \int_0^1 dx \frac{\overline{x} x (4\overline{x} + 1)}{(\Delta_{\mathrm{os}}/m^2)} + 2 \int_0^1 dx \frac{\overline{x}^2 x^2}{(\Delta_{\mathrm{os}}/m^2)^2} \right\}, \qquad (3.127)$$

$$(Z_H)^{\mu\nu}{}_{\rho\sigma} H^{\rho\sigma} = H^{\mu\nu} - \frac{\alpha}{2\pi} H^{\mu\nu} \left\{ 4 \int_0^1 dx \frac{\overline{x} x (3x - 4)}{(\Delta_{\mathrm{os}}/m^2)} - 4 \int_0^1 dx \frac{\overline{x}^2 x^2}{(\Delta_{\mathrm{os}}/m^2)^2} \right\}$$
$$- \frac{\alpha}{2\pi} m \epsilon^{\mu\nu\rho\sigma} d_A^{\rho\sigma} \left\{ \frac{1}{2} \left[\frac{2}{\varepsilon} - 2\gamma_E + 1 + 2 \int_0^1 dx \ln \left(\frac{4\pi\mu^2}{\Delta_{\mathrm{os}}} \right) \right] \right.$$
$$\left. - 2 \int_0^1 dx \frac{\overline{x} x (2\overline{x}^2 + x + 1)}{(\Delta_{\mathrm{os}}/m^2)} - \int_0^1 dx \frac{\overline{x}^2 x^2 (x^2 + 1)}{(\Delta_{\mathrm{os}}/m^2)^2} \right\}. \qquad (3.128)$$

As expected, only the antisymmetric part of $d^{\mu\nu}$ mixes with the (also antisymmetric) $H^{\mu\nu}$ coefficient.

We have seen the $d_S^{\mu\nu}$ symmetric contribution $\Sigma_{d_S}^{\mathrm{R}}$ (3.80) is not related to any other, and is given by $\Sigma_{d_S}^{\mathrm{R}} = \Sigma_{d_S} - \frac{1}{2} \left[(Z_{d_S})^{\mu\nu}{}_{\rho\sigma} d_S^{\rho\sigma} - d_S^{\mu\nu} \right] (p_\mu \gamma_5 \gamma_\nu + p_\nu \gamma_5 \gamma_\mu)$, where

$$(Z_{d_S})^{\mu\nu}{}_{\rho\sigma} d_S^{\rho\sigma} = d_S^{\mu\nu} + \frac{\alpha}{2\pi} d_S^{\mu\nu} \left\{ \frac{1}{6} \left[\frac{5}{\varepsilon} - 5\gamma_E + 6 \int_0^1 dx \, x(1 + x) \ln \left(\frac{4\pi\mu^2}{\Delta_{\mathrm{os}}} \right) \right] + \kappa_{d_S} \right\}, \qquad (3.129)$$

and it is *not* determined as its free parameter κ_{d_S} cannot be consistently adjusted to satisfy both renormalization conditions of (3.49).

The f^μ renormalized contribution Σ_f^R to the fermion self-energy is given by (3.84). It does not mix with other coefficients, and comes from $\Sigma_f^R = \Sigma_f - i\left[(Z_f)^\mu{}_\nu f^\nu - f^\mu\right] p_\mu \gamma_5$, where

$$(Z_f)^\mu{}_\nu f^\nu = f^\mu + \frac{\alpha}{2\pi} f^\mu \left\{ -\frac{1}{2}\left(\frac{1}{\varepsilon} - \gamma_E + \frac{5}{3}\right) - \int_0^1 dx\, x(5 - 6x) \ln\left(\frac{4\pi\mu^2}{\Delta_{\mathrm{os}}}\right) + \kappa_f \right\}.$$
(3.130)

As it happened to $c_A^{\mu\nu}$, the f^μ contribution to the fermion self-energy automatically satisfies both renormalization conditions of (3.49) without the need to fix a value for κ_f, thus we can set it to zero. Again, this is not an issue as effects genuinely from f^μ are unobservable to all orders.

As for the trace part contribution $\Sigma_{g_T}^R$ from $g_T^{\kappa\lambda\mu}$, given by (3.99), it comes solely from $\Sigma_{g_T}^R = \Sigma_{g_T} - \frac{1}{3}\left[(Z_{g_T})^{\kappa\lambda\mu}{}_{\nu\rho\sigma} g_T^{\nu\rho\sigma} - g_T^{\kappa\lambda\mu}\right] \eta_{\lambda\mu} p^\tau \sigma_{\kappa\tau}$, where

$$(Z_{g_T})^{\kappa\lambda\mu}{}_{\nu\rho\sigma} g_T^{\nu\rho\sigma} = g_T^{\kappa\lambda\mu} + \frac{\alpha}{2\pi} g_T^{\kappa\lambda\mu} \left\{ \frac{1}{4}\left(\frac{1}{\varepsilon} - \gamma_E - 1\right) - \frac{1}{2}\int_0^1 dx\, x \ln\left(\frac{4\pi\mu^2}{\Delta_{\mathrm{os}}}\right) + \kappa_{g_T} \right\}.$$
(3.131)

Once more, $\Sigma_{g_T}^R$ satisfies renormalization conditions (3.49) for all values of the free parameter κ_{g_T}, thus we can set $\kappa_{g_T} = 0$ for simplicity. As in similar situations discussed before, $g_T^{\mu\nu\lambda}$ leads to no observable effects to first order.

Finally, the renormalized fermion self-energy correction $\Sigma_{g_M}^R$ due to the mixed-symmetry representation of $g^{\mu\nu\lambda}$, as given by (3.103), also comes from a single counterterm, $\Sigma_{g_M}^R(p) = \Sigma_{g_M}(p) - \left[(Z_{g_M})^{\kappa\lambda\mu}{}_{\nu\rho\sigma} g_M^{\nu\rho\sigma} - g_M^{\kappa\lambda\mu}\right] p_\mu \sigma_{\kappa\lambda}$, where

$$(Z_{g_M})^{\kappa\lambda\mu}{}_{\nu\rho\sigma} g_M^{\nu\rho\sigma} = g_M^{\kappa\lambda\mu} - \frac{\alpha}{2\pi} g_M^{\kappa\lambda\mu} \left\{ \frac{1}{2}\left[\frac{1}{\varepsilon} - \gamma_E + 2\int_0^1 dx\, x \ln\left(\frac{4\pi\mu^2}{\Delta_{\mathrm{os}}}\right)\right] + \kappa_{g_M} \right\},$$
(3.132)

but it cannot be fully determined as the free parameter κ_{g_M} cannot be consistently

fixed so as to satisfy renormalization conditions (3.49).

As a last note, in Ref. [40] the authors employed *multiplicative* renormalization to determine the *divergences* of the Z factors. As we have used *counterterm* renormalization, the correspondence between our approach and the one of the mentioned reference is accomplished by $Z_\psi \to Z_\psi$, $Z_m \to Z_\psi^{-1} Z_m$, and $Z_x \to Z_\psi^{-1} Z_x$, where Z_x renormalize a Lorentz-violating contribution due to a coefficient denoted by x. Under this correspondence we find our results agree with those of Ref. [40] for the divergences of each Z factor — although mostly straightforward, we point out some care should be taken as some coefficients were not decomposed in irreducible representations in the aforementioned reference.

3.4 Summary and Perspectives

In this chapter we initiated investigation of one-loop radiative corrections to the single-fermion minimal QED sector of the SME. Evaluation of the fermion self-energy revealed all new divergences introduced due to Lorentz violation can be removed by means of renormalization of the Lorentz-violating coefficients. For the finite radiative corrections, a set of on shell renormalization corrections were chosen to fix free parameters introduced by renormalization, but some issues were found. All parameters could be adequately fixed with the sole exception of those associated to contributions from coefficients $c_S^{\mu\nu}$, $d_S^{\mu\nu}$, $g_M^{\kappa\lambda\mu}$, and $(k_F)^{\mu\rho\nu}{}_\rho$. A common ground to these coefficients is, in the tree-level lagrangian, they are associated with single structures only, therefore renormalization of their contributions to the fermion self-energy introduces only one free parameter. Within our *chosen* set of renormalization conditions — the so called on shell conditions, for their interpretation makes direct contact with experiments — each contribution to the fermion self-energy has to satisfy two conditions, therefore we cannot consistently fix the single free parameter associated with each of the mentioned coefficients.

Although so far we have not discussed other possible sets of renormalization conditions, we mention we have tried others — often conditions without a link to re-

3. Fermion self-energy of the minimal QED extension

alistic experimental set ups, leading to so called intermediate renormalizations. The conclusion remains as troublesome as before, but for different reasons: it seems to be possible to find sets of renormalization conditions unambiguously fixing all free parameters, but those typically lead to mixing between contributions from CPT odd and CPT even coefficients — for instance, the fixed value of the free parameters coming from counterterms of e^μ would also have contributions coming from $c_S^{\mu\nu}$ corrections to the fermion self-energy. Behavior of individual coefficients under discrete transformations forbids such mixing of CPT odd and CPT even contributions. Another related issue comes from unobservable coefficients contributing to the fixed value of parameters associated to observable coefficients — for instance, the free parameter κ_{c_S} associated to $c_S^{\mu\nu}$ receives contributions from the unobservable coefficient $c_A^{\mu\nu}$. Therefore, even though we have found different sets of renormalization conditions unambiguously fixing all free parameters, their fixed value seem to be inconsistent with expected behavior under discrete transformations or observable contents of the model.

In Ref. [42], the authors considered a model with $c_S^{\mu\nu}$ as the only fermionic coefficient and also $(k_F)^{\mu\rho\nu}{}_\rho$ in the photon sector, and — although using a different approach from ours — consistent renormalization of the model forced the introduction of a wave-function renormalization factor with momentum-dependence. It is worth mentioning such modification would also fix the problem for contributions from this coefficient in our approach, but it seems similar modifications would not solve the problem for contributions coming from $d_S^{\mu\nu}$ and $g_M^{\kappa\lambda\mu}$. It is our aim to further investigate this question to discover whether or not contributions from these coefficients can be consistently renormalized and, if so, to see if this is achieved by conventional means or if an unconventional solution — such as having renormalization factors with momentum-dependence — is ultimately required.

For coefficients whose contributions to the fermion self-energy were consistently renormalized, an interesting new effect was found. Typically, Lorentz violation seems to fundamentally modify the fermion kinetic term by means of finite radiative corrections. In the conventional QED, radiative corrections to the fermion self-energy amount only to renormalization of the fermion field and mass, and a shift of the propagator's pole,

3. Fermion self-energy of the minimal QED extension

from the bare to the renormalized mass. Here, Lorentz violation effectively changes the free fermion dynamics by introducing field operators of dimension five or six to the effective lagrangian. For instance, the b_μ contribution to the classical action is $b_\mu \overline{\psi} \gamma_5 \gamma^\mu \psi$, and — besides renormalizing b_μ — radiative corrections changes it by adding an extra order α contribution of the form $b^{(5)}_{\mu\alpha\beta} \overline{\psi} \gamma_5 \gamma^\mu \partial^\alpha \partial^\beta \psi$, where $b^{(5)}_{\mu\alpha\beta} \equiv \frac{1}{m^2} b_\alpha \eta_{\beta\mu}$. This definition is motivated by Ref. [25], where a general formalism were developed to deal with free fermions with Lorentz-violating field operators of arbitrary dimension. In the next chapter, we use such formalism to place bounds on nonminimal Lorentz-violating coefficients of the muon sector in the context of muon $(g-2)$ experiments. For instance, considering the identification just mentioned, bounds on the nonminimal $b^{(5)}_{\mu\alpha\beta}$ coefficient can be directly translated into bounds on the minimal b_μ coefficient in the context of radiative corrections to the Lorentz-violating minimal QED extension.

Unexpectedly, this phenomenon reveals Lorentz-violating radiative corrections can be experimentally as relevant as tree-level contributions because, depending on the induced operator, these radiative contributions naturally come with factors of $\frac{\alpha}{m}$ or $\frac{\alpha}{m^2}$, where $\alpha \approx \frac{1}{137}$ characterizes the natural loop suppression and the enhancing factors of $\frac{1}{m}$ or $\frac{1}{m^2}$ are because of the extra momenta factor of the radiatively induced operator, therefore processes with typical energy of order $\frac{m}{\alpha}$ are expected to receive relevant contributions due to radiative corrections. For instance, considering induced operators naturally suppressed by $\frac{\alpha}{m}$, radiative effects of the same order of magnitude as tree-level ones may be achieved in experiments with energies of about $70\,\mathrm{MeV}$ for electrons — which are common in experiments testing Lorentz symmetry — and effects in muon experiments with expected suppression of a factor of 10 relative to tree-level contributions can be accessed with energies of about $1.4\,\mathrm{GeV}$ — which is the case for muon $(g-2)$ experiments, the subject of the next chapter. Similarly, for induced operators naturally suppressed by $\frac{\alpha}{m^2}$, radiative effects of the same order of magnitude as tree-level contributions may be achieved using electrons of about $6\,\mathrm{MeV}$ and muons of $1.2\,\mathrm{GeV}$.

The above discussion is mostly qualitative as a quantitative description requires explicit determination of the effective fermion equation of motion, which constitutes

3. Fermion self-energy of the minimal QED extension

one of our next goals. Comprising a systematic investigation, finite radiative corrections coming from the vertex correction and photon self-energy diagrams are also envisaged for the future. We expect new finite radiative corrections due to Lorentz violation modifying the conventional interaction vertex in such a way as to accommodate the modifications described above in the fermion kinetic term to keep intact gauge invariance of the action by means of the Ward-Takahashi identity.

Chapter 4

Testing Lorentz symmetry with muon $(g-2)$ experiments

Experiments measuring the muon anomalous magnetic moment are very suitable in the search of physics beyond the Standard Model, due to muon's $g-2$ intrinsic high sensitivity to corrections coming from higher energy scales, and particularly CPT and Lorentz violation because of the high precision attainable in such experiments. In the past decade, measurements with precision of about 0.5 ppm were achieved at the Brookhaven National Laboratory (BNL) [83], and upcoming Fermilab Muon $(g-2)$ [84] and Japan's J-PARC [85] experiments expect roughly a fivefold improvement over this mark. Currently, Standard Model evaluations are about 3.3 σ below the experimental results [86,87], giving enough room for expectations on new physics playing a role there.

Effects of CPT and Lorentz violation on the muon $g-2$ have been studied in the past [2,88,89] using the framework of the *minimal* Standard Model Extension [3,4] for muons. The full extension also enjoys nonrenormalizable interactions that may be relevant as we probe higher energy scales. Investigation of such nonminimal contributions in the neutrino [23] and photon [24] sectors have already been made, and a general framework for massive fermions was recently developed in [25]. In this chapter, we extend the analysis done in [88] to consider also Lorentz-violating couplings from operators of *arbitrary* dimension in the context of muon $(g-2)$ experiments. In the following, we give a brief overview of such experiments in Sections 4.1 and 4.2, and in Sec. 4.3 we employ the SME framework to investigate Lorentz-violating signals in

this context.

4.1   Why muons?

Why use muons for testing fundamental physics? To answer this question, we consider the anomalous contribution $a \equiv g/2 - 1$ to the gyromagnetic factor g of a charged lepton. This contribution comes entirely from quantum fluctuations of the vacuum, *i.e.*, loop corrections to tree-level processes. It turns out that quantum corrections δa to a due to higher energies or heavier states scale proportional to the squared lepton mass m_{lepton},

$$\frac{\delta a_{\text{lepton}}}{a_{\text{lepton}}} \propto \frac{m_{\text{lepton}}^2}{M^2}, \qquad (M \gg m_{\text{lepton}}), \tag{4.1}$$

where M may be a heavier Standard Model particle, or a heavy state beyond SM, or an energy scale or UV cutoff where the SM no longer holds. In this sense, muons are much more sensitive to physics coming from higher energy scales, whether conventional or not, than electrons because $m_\mu^2 = (0.1057\,\text{GeV})^2 \sim 4 \times 10^4\, m_e^2$. Therefore, the advantages of using muons in high precision experiments can be twofold: for testing conventional physics coming from sectors other than QED that may give relevant contributions to the muon anomaly factor a_μ, and also for looking for signals of non-standard physics from higher energy scales. For an experiment aiming to measure $g - 2$, we highlight some features due to the use of muons (or, analogously, antimuons as well):

- High sensitivity to distinct Standard Model sectors (weak and strong, besides QED itself) and potentially new physics beyond SM.

- High precision measurements can be achieved. This is made possible because of parity-violating weak decays that make it easy to produce polarized muons through pion decay, $\pi^- \to \mu^- + \overline{\nu}_\mu$, and which also make it easy to understand the final muon polarization state right before it decays into lighter leptons, $\mu^- \to \nu_\mu + e^- + \overline{\nu}_e$.

- There is a "magic" value for the relativistic γ factor that matches the anomaly factor. Theoretically, the advantage of working at such γ is that equations of motion are greatly simplified, and experimentally it is that the muon lifetime is increased by a factor of roughly 30, which is enough to collect them in a storage ring and have time enough to make precise measurements by performing enough cycles along the ring.

A question may arise as "why not use taus, which are 17 times heavier than muons?" Because taus are heavier and more unstable than muons, they have much shorter lifetime, leading to fewer cycles in a storage ring, significantly decreasing the precision of the measurements. Indeed, so far the tau sector remains vastly unexplored mostly due to difficulties in determining its properties with higher precision — see, for instance [90,91].

4.2 Basics of the BNL Muon $(g-2)$ experiment

In this section we give a very basic overview of the physics of the BNL $(g-2)$ experiment — for a detailed introduction, see Refs. [92–94], and see Ref. [95] for the final report of the BNL experiment. It tested physics for both muons μ^- and antimuons μ^+, but for simplicity from now on we will refer to muons only. The experiment is primarily designed as a means of testing conventional physics with higher precision. Nevertheless, as will be discussed in Sec. 4.3, the experiment can also be used in the search of signals coming from unconventional physics.

4.2.1 The anomalous magnetic moment

At tree-level, the gyromagnetic factor g is predicted by the Dirac equation to be $g = 2$ for all charged leptons. Radiative corrections due to vacuum fluctuation corrects this value to $g = 2(1 + a)$, where a is called the anomalous magnetic moment. The one-loop correction is $a_{\text{one-loop}} = \alpha/2\pi \approx 1/137 \sim 10^{-3}$ [96] and it is also the same for all charged leptons, but higher order effects are not universal and lead to different corrections due to mass hierarchy and the way different charged leptons feel effects of

4. Testing Lorentz symmetry with muon $(g-2)$ experiments

weak and strong interactions. For instance, contributions from QED and electroweak interactions to the muon anomalous magnetic moment a_μ are currently well-understood at the level required by the experimental precision, and most theoretical uncertainties comes from hadronic ones (hadronic vacuum polarization and hadronic scattering of light-by-light). Current results put the SM theoretical prediction for a_μ off by 3.3 σ with respect to the experimental value [86], which could be due to some missing conventional physics effect or some yet unknown new physics.

An indirect measurement of a_μ could be made through a direct measurement of g, which could be performed by placing muons in a magnetic field $\boldsymbol{B}$ and measuring the ratio $\boldsymbol{\omega}_L/\boldsymbol{\omega}_c$ of the Larmor spin-precession frequency $\boldsymbol{\omega}_L = -\frac{g}{2}\frac{e}{m}\boldsymbol{B}$ to the cyclotron frequency $\boldsymbol{\omega}_c = -\frac{1}{\gamma}\frac{e}{m}\boldsymbol{B}$. This could be accomplished by means of *Penning traps*. However, because $a_\mu \sim 10^{-3}$, measuring a_μ with a precision of 10^{-6} requires measuring g to one part per billion. This is a very feasible approach for stable particles, like electrons — for instance, see Sec. 6.7 of Ref. [93], and, in the context of Lorentz-violation, see Ref. [97] — but currently such a precision cannot be obtained for unstable particles like muons.

An alternative approach was put into work at CERN's Muon $(g-2)$ experiment in the late 70's [98], and then about twenty years later at BNL, and will be used again in the upcoming Fermilab $(g-2)$ experiment and also in J-PARC's one (although with a different experimental setup). It sets muons in a constant uniform magnetic field $\boldsymbol{B}$, perpendicular to the muon's plane of motion. The orbital motion is characterized by the cyclotron (orbital) frequency $\boldsymbol{\omega}_c = -\frac{1}{\gamma}\frac{e}{m}\boldsymbol{B}$ and the spin-precession frequency[1] $\boldsymbol{\omega}_s = -\left(\frac{g}{2} - 1 + \frac{1}{\gamma}\right)\frac{e}{m}\boldsymbol{B}$. The approach for muon $g-2$ measurements is to define the anomaly frequency $\boldsymbol{\omega}_a$,

$$\boldsymbol{\omega}_a \equiv \boldsymbol{\omega}_s - \boldsymbol{\omega}_c = -a_\mu \frac{e}{m}\boldsymbol{B}, \tag{4.2}$$

which describes the rate of precession of the orbit plane parallel component of the spin around the muon momentum $\boldsymbol{p}$. Because $a_\mu \neq 0$, there is a Larmor precession of

---

[1]The spin-precession frequency $\boldsymbol{\omega}_s$ is most clearly understood when written as $\boldsymbol{\omega}_s = \boldsymbol{\omega}_L + \boldsymbol{\omega}_T$, where $\boldsymbol{\omega}_L = -\frac{g}{2}\frac{e}{m}\boldsymbol{B}$ is the Larmor precession of the spin, and $\boldsymbol{\omega}_T = \left(1 - \frac{1}{\gamma}\right)\frac{e}{m}\boldsymbol{B}$ is the Thomas precession which comes as a relativistic correction due to orbital motion.

the direction of the muon spin with respect to the momentum — see Fig. 4.1 for a qualitative illustration of the effect. This approach allows for a direct measurement of a_μ, which gives an improvement in sensitivity of about 10^3 from the start. The strategy to determine a_μ is to make two separate measurements, one of $\boldsymbol{\omega}_a$ by looking for muon decay particles along the cyclotron orbit, and another measurement by using proton nuclear magnetic resonance (NMR) techniques to measure $\boldsymbol{B}$. Some more details are given in the next sections. In our search for Lorentz-violating effects, ω_a will play the central role, as we will discuss in Sec. 4.3.
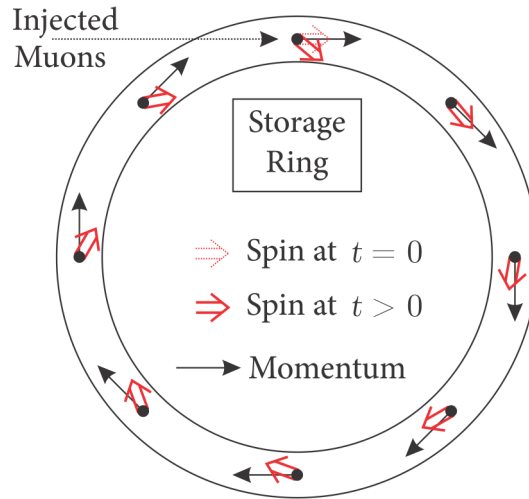
Figure 4.1: Muon spin-precession due to the anomalous magnetic moment.

4.2.2 Experimental method of the BNL experiment

The aim of this section is to give a brief and overly simplified overview of some aspects of the BNL $(g-2)$ experiment that will be relevant for our search for Lorentz-violating signals. We refer the reader to Chap. 6 of [93], Sec. II of [95], or Ref. [99] for all technical details of the BNL experiment.

Instead of a single muon, a bunch of muons is used to form a beam. The beam needs to be as narrow as possible and an electric quadrupole field $\boldsymbol{E}$ normal to the muon orbit plane is used for focusing. This is a major issue because the electric field

4. Testing Lorentz symmetry with muon $(g-2)$ experiments

interacts directly with the muon spin, changing expression (4.2)for $\boldsymbol{\omega}_a$ to

$$\boldsymbol{\omega}_a = -a\frac{e}{m}\boldsymbol{B} + \left(a - \frac{1}{\gamma^2 - 1}\right)\frac{e}{m}\boldsymbol{v} \times \boldsymbol{E}. \tag{4.3}$$

Following CERN's experimental set up closely, to avoid the daunting issue of precise tuning a quadrupole field, BNL's set up made use of the fortuitous cancellation of the term inside curly brackets in the second term above when $\gamma = \sqrt{1/a + 1} \approx 29.3$. Setting the muon beam energy $E_0 = \gamma m$ at $3.096\,\mathrm{GeV}$ corresponds to the "magic" γ of 29.3, reducing expression (4.3) to the same form as (4.2). Setting the energy of the beam to this precise value is not a major experimental problem. Therefore, at this energy, the electric field is used only for focusing of the beam, and the anomaly frequency is influenced only by the magnetic field, and this is central to the precision achieved by the experiment. For a brief discussion of other experimental issues, see Ref. [100].

The basic idea of the experimental set up performed at the BNL, see Fig. 4.2, was to collide proton beams with a hadronic target, producing energetic pions. In a decay channel, because of a parity-violating weak decay, pions produce polarized muons which are guided by a beam inflector and then captured by a uniform constant magnetic field of $1.5\,\mathrm{T}$ in a storage ring of diameter $14.2\,\mathrm{m}$. Kicker modules at the beginning of the ring give an initial short current pulse to stabilize the beam orbit. The spin direction of polarized muons is aligned with the momentum direction when they enter the storage ring at $t = 0$. Relativistic muons traveling at the "magic" momentum $|\boldsymbol{p}| \simeq 3.094\,\mathrm{GeV}$ have long enough lifetime — $\tau_{\text{in-flight}} = 64.4\,\mu\mathrm{s}$, compared to $\tau_{\text{rest}} = 2.2\,\mu\mathrm{s}$ when at rest — allowing sufficiently many spin oscillations ($\omega_s^{-1} = 4.37\,\mu\mathrm{s}$) while completing many orbits ($\omega_c^{-1} = 149\,\mathrm{ns}$) before decaying into electrons. Muons then undergo parity-violating weak decay into electrons, and a correlation exists between the muon polarization state right before the decay and the direction of the emitted electron, which is known once the electron hits any of the detectors (calorimeters) spread along the storage ring, see Fig. 4.3. When a decay electron is detected at some moment after injection, we have information about the final polarization state of a muon of the beam, and eventually all muons decay. Each injection of pions was

followed by a measurement period typically of $700\,\mu\text{s}$, with the whole process being periodically repeated for half an hour, and several "runs" being performed during each day.
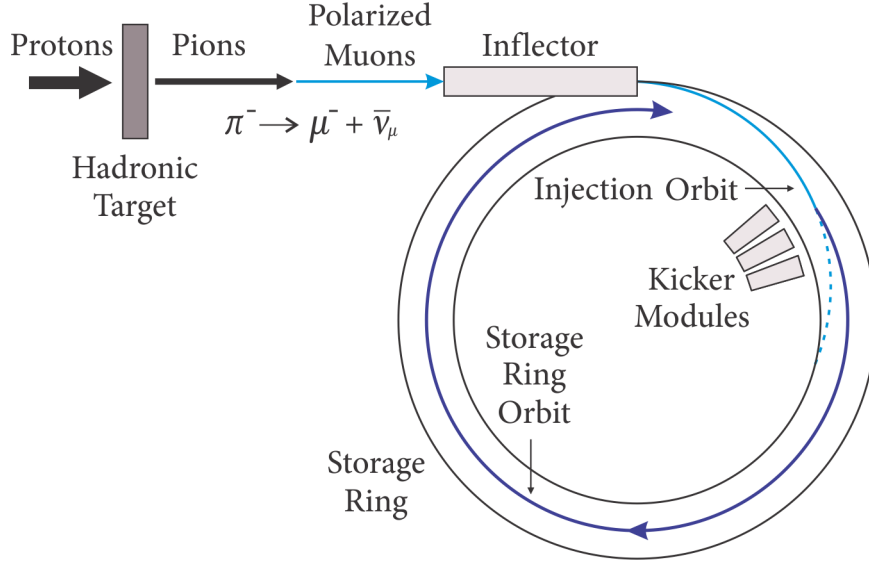
Figure 4.2: Simple schematic of the Muon $(g-2)$ experiment at BNL.
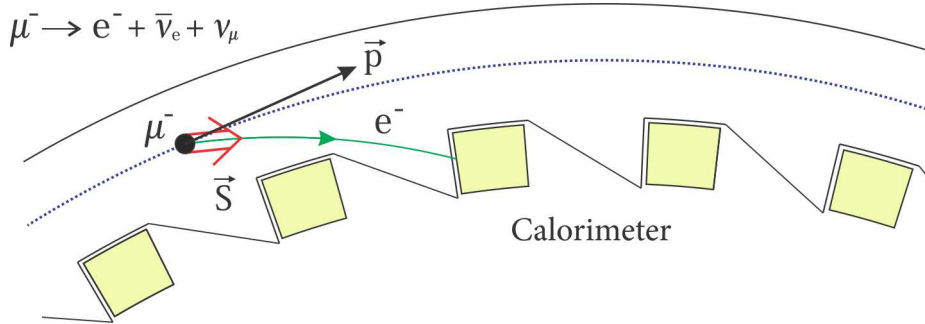
Figure 4.3: Muon parity-violating weak decay and detection of electrons by calorimeters spread along the storage ring.

4.2.3   Measurement of ω_a

Conventional QED calculation for the tree-level weak decay of muons into electrons predicts the number $N(t)$ of decay electrons with energy greater than E emitted

4. Testing Lorentz symmetry with muon $(g-2)$ experiments

at a time t after muons are injected into the storage ring,

$$N(t) = N_o(E)e^{-t/\gamma\tau_{\text{rest}}} \left[1 + A(E)\cos\left(\omega_a t + \phi(E)\right)\right], \qquad (4.4)$$

where $N_o(E)$ is a normalization factor, $\gamma\tau_{\text{rest}} = 64.4\,\mu\text{s}$ is the dilated muon lifetime, $A(E)$ is the asymmetry factor for electrons of energy greater than E, and $\phi(E)$ is the average muon spin angle as a function of E at $t = 0$. This expression is to be compared with the fit of the electron arrival-time spectrum $N(t) \times t$ for electrons detected by calorimeters after injection of muons in the storage ring. This gives the value of ω_a, which controls the modulation of the exponential decay law of the decaying muons. A typical plot of the electron time-arrival spectrum is shown in Fig. 4.4.
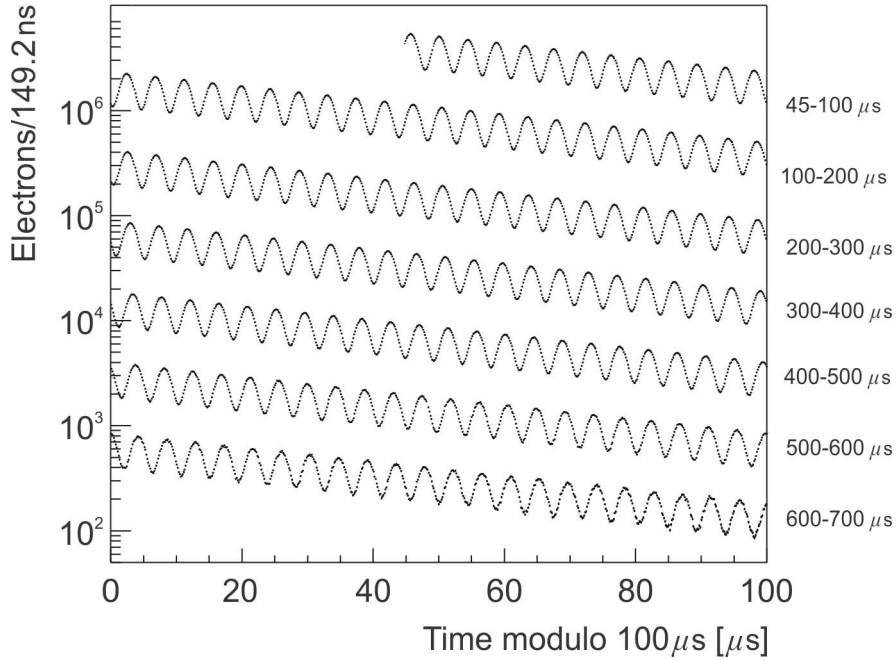
Figure 4.4: Typical plot of the decay electrons detected after a full run.

4.2.4   Measurement of B

High precision measurements of ω_a and a_μ are strongly related to the ability of manufacturing a constant homogeneous magnetic field and being able to determine its value with great accuracy. As mentioned before, it is possible to measure the mag-

netic field by measuring ω_c, but this is not a reasonable approach for high precision muon experiments. Instead, measurements of the *free* proton Larmor spin-precession frequency $\overline{\omega}_p = (g_P/2)(e/m_P)\langle B \rangle$ with NMR are used to determined $\langle B \rangle$, the average magnetic field over muon trajectories during each run. Along with NMR probes distributed around the ring, this was done with a trolley carrying NMR probes, periodically moved throughout the entire muon storage region. See Sec. II G of [95] for more details.

4.2.5 Determination of a_μ

To improve the precision of the experiment, measured frequencies are written relative to $\overline{\omega}_p$ such that, from Eq. (4.2), the muon $g-2$ anomaly is written as

$$a_\mu = \frac{\omega_a}{\omega_L - \omega_a} = \frac{\omega_a/\overline{\omega}_p}{\omega_L/\overline{\omega}_p - \omega_a/\overline{\omega}_p} = \frac{\mathcal{R}}{\lambda - \mathcal{R}}, \tag{4.5}$$

where $\mathcal{R} \equiv \omega_a/\overline{\omega}_p$ is measured in the $(g-2)$ experiment, and a high precision value of the muon-to-proton magnetic moment ratio $\lambda \equiv \omega_L/\overline{\omega}_p = \mu_\mu/\mu_p$ is available in the literature from previous muonium hyperfine level structure measurements [101].

Assuming CPT invariance to average between a_{μ^+} and a_{μ^-}, the measured value obtained at the BNL $(g-2)$ experiment gives the anomalous magnetic moment [95]

$$a_\mu(\text{Expt}) = 11659208.0(6.3) \times 10^{-10}(0.54\,\text{ppm}), \tag{4.6}$$

which the Muon $(g-2)$ Collaboration compared with the theoretical Standard Model predictions

$$a_\mu(\text{SM}) = 11659185.7(8.0) \times 10^{-10}(0.69\,\text{ppm}), \tag{4.7}$$

$$a_\mu(\text{SM}) = 11659182.0(7.3) \times 10^{-10}(0.62\,\text{ppm}), \tag{4.8}$$

from Refs. [102,103] respectively, resulting in the difference

$$\delta a_\mu(\text{Expt} - \text{SM}) = [(22.4 \pm 10) \,\text{to}\, (26.1 \pm 9.4)] \times 10^{-10} \tag{4.9}$$

4. Testing Lorentz symmetry with muon $(g-2)$ experiments

with a significance of 2.2–2.7 standard deviation. In 2008 the last digit of (4.6) has changed from 0 to 9 [104,105] as the published proton-to-muon magnetic moment ratio $\lambda = \mu_\mu/\mu_p$ has also changed [106], and along with recent improvements on the theoretical prediction of a_μ [86], the discrepancy $\delta a_\mu(\text{Expt} - \text{SM})$ was further extended to a significance of 3.3 standard deviation. As mentioned in the beginning of this chapter, this gives enough room to expect some new physics playing a role in the muon sector. In the following section, we look for experimental signals that could arise in a Lorentz-violating QED for muons, antimuons and photons, and in particular we use the BNL data for ω_a to impose constraints on Lorentz-violating coefficients and also estimate bounds that could be obtained in the upcoming Fermilab $(g-2)$ and J-PARC experiments.

A brief note on the Fermilab and J-PARC $(g-2)$ experiments

The Fermilab $(g-2)$ experiment will be done following the same experimental set up as the one at the BNL, with improved control to systematic errors [84]. Although the J-PARC experiment will be fundamentally different, the key measurable quantities will be the same [85]. At the J-PARC, instead of the "magic" energy, highly polarized muon beams will be produced at $320\,\text{MeV}$, corresponding to a value of γ roughly ten times smaller than the one used at the BNL. Instead of choosing the "magic" γ to cancel the electric field contribution to the anomaly frequency (4.2), by using ultra-cold muons with almost no transverse dispersion, no focusing electric field will be used at all, therefore the anomaly factor a_μ can be derived in the same way as in the BNL experiment. A uniform constant $3\,\text{T}$ magnetic field will be used for muon storage in a orbit with $66\,\text{cm}$ in diameter, much smaller than the storage ring to be used at Fermilab and better to control the magnetic field with precision. Determination of a_μ will again follow the measurement of ω_a by counting of decay positrons at detectors together with precise knowledge of the magnetic field. Both experiments are primarily intended to run with antimuons only, but as happened with the BNL experiment, future upgrades may allow the use of muons as well.

4.3 Search for Lorentz violation in muon $(g-2)$ experiments

Search for CPT and Lorentz violation coming from minimal SME coefficients in the context of muon $(g-2)$ experiments have been performed in the past [2,88,89]. Viewed as an effective theory, the SME framework also allows for nonrenormalizable interactions which may be relevant as higher energy scales are probed. A general framework for dealing with free fermions with Lorentz-violating field operators of arbitrary dimension was developed in [25], and now we use it to extend the analysis of muon $(g-2)$ experiments beyond operators associated to minimal coefficients.

As discussed in previous sections, determination of $g-2$ at the BNL experiment required the intermediate step of measuring the angular anomaly frequency ω_a, which is the difference between the spin-precession frequency ω_s and the cyclotron frequency ω_c. In different runs, relativistic polarized μ^- or μ^+ beams were injected into cyclotron orbits in a constant $1.45\,\mathrm{T}$ magnetic field, and adjusted to the "magic" momentum $|\boldsymbol{p}| = 3.094\,\mathrm{GeV}$ and $\gamma = 29.3$ at which the dependence of ω_a on the focusing electric field is eliminated. Fitting the decay spectrum of $\mu^{\pm}$ to specified time functions, allows the anomaly frequency ω_a to be inferred. The Fermilab experiment will be performed in the same fashion as the BNL one, but J-PARC's will be significantly different. The latter will be based on the use of ultra-cold highly polarized muon beams at $320\,\mathrm{MeV}$ $(\gamma = 3.03)$, with almost no transverse dispersion, that can be stored in a $3\,\mathrm{T}$ magnetic field during their lifetime without requiring a focusing electric field. In our context, apart from different setups, the key quantities to be measured in both experiments remain the same.

Departing from conventional Standard Model predictions, CPT and Lorentz violation allows, for instance, different behavior between μ^- and μ^+, and also sidereal and annual variations of $\omega_a^{\mu^{\pm}}$, as we discuss in what follows.

4.3.1   The Lorentz-violating model for muons

We consider the QED limit of the nonminimal SME for muons, antimuons and photons,

$$\mathcal{L} = \tfrac{1}{2}\overline{\psi}\left(i\gamma^{\nu}\overleftrightarrow{D}_{\nu} - m_{\mu} + \widehat{\mathcal{Q}}\right)\psi + \text{h.c.,} \tag{4.10}$$

where m_{μ} is the mass of the muon, $iD_{\nu} \equiv i\partial_{\nu} - qA_{\nu}$ with charge $q = -|e|$, and $\widehat{\mathcal{Q}}$ represents couplings to Lorentz-violating coefficients, to be defined soon. Couplings between those and electromagnetism are highly suppressed given typical values for the magnetic field in $(g-2)$ experiments, and were ignored. In this approximation, for contributions from Lorentz violation, we can make use of the framework developed in [25], for free fermions with Lorentz-violating operators of arbitrary dimension. In this section, we give a brief overview of key results derived in the before-mentioned reference which will make our starting point to study Lorentz-violating signals in muon $(g-2)$ experiments. To avoid confusion with the notation, from now on, we reserve the letter μ to refer to the muon only, and never as a tensorial index.

In momentum space, the explicit form of $\widehat{\mathcal{Q}}$ in terms of *fundamental* SME coefficients can be written as

$$\widehat{\mathcal{Q}} = \left(\hat{c}^{\rho\sigma}\gamma_{\rho} + \hat{d}^{\rho\sigma}\gamma_{5}\gamma_{\rho} + \hat{e}^{\sigma} + i\hat{f}^{\sigma}\gamma_{5} + \frac{1}{2}\hat{g}^{\nu\rho\sigma}\sigma_{\nu\rho}\right)p_{\sigma}$$

$$- \left(\hat{m} + i\hat{m}_{5}\gamma_{5} + \hat{a}^{\nu}\gamma_{\nu} + \hat{b}^{\nu}\gamma_{5}\gamma_{\nu} + \frac{1}{2}H^{\nu\sigma}\sigma_{\nu\sigma}\right), \tag{4.11}$$

where the "hat" notation means $\hat{\mathcal{C}}^{\kappa\lambda...} = \sum_{d}\mathcal{C}^{(d)\kappa\lambda...\alpha_{1}\alpha_{2}...\alpha_{d-3}}p_{\alpha_{1}}p_{\alpha_{2}}\cdots p_{\alpha_{d-3}}$, with $\hat{\mathcal{C}}^{\kappa\lambda...}$ representing any of the Lorentz-violating terms in (4.11), where $d\,(\text{odd}) \geqslant 5$ for $\hat{m}$, and $\hat{m}_{5}$, and $d\,(\text{even}) \geqslant 4$ for $\hat{c}^{\rho\sigma}$, $\hat{d}^{\rho\sigma}$, $\hat{e}^{\sigma}$, $\hat{f}^{\sigma}$, and $\hat{g}^{\nu\rho\sigma}$, and $d\,(\text{odd}) \geqslant 3$ for $\hat{a}^{\nu}$, $\hat{b}^{\nu}$, and $H^{\nu\sigma}$. Indices $\kappa\lambda\ldots$ in the coefficients $\mathcal{C}^{(d)\kappa\lambda...\alpha_{1}\alpha_{2}...\alpha_{d-3}}$ control the spin nature of the operator and the $d-3$ symmetric indices $\alpha_{1}\alpha_{2}\ldots\alpha_{d-3}$ control the momentum dependence. Note that imposing $d \leqslant 4$ recovers the minimal Lorentz-violating QED for muons.

Well-known field redefinitions for the minimal SME reveal some coefficients are completely unobservable to first order in Lorentz violation and some other appear

4. Testing Lorentz symmetry with muon $(g-2)$ experiments

only as specific coefficient combinations [3,4,75–77,107]. In Ref. [25] these results are extended to the nonminimal coefficients. For instance, by means of the transformation $\psi \to (1 + \hat{Z})\psi$, with $\hat{Z}$ a suitably chosen momentum-dependent operator containing γ matrices and Lorentz-violating coefficients, to first order in the coefficients, lagrangian (4.10) is shown to be equivalent to

$$\mathcal{L} = \tfrac{1}{2}\overline{\psi} \left(i\gamma^\nu \overleftrightarrow{D}_\nu - m_\mu + \hat{\mathcal{Q}}' \right) \psi + \text{h.c.}, \tag{4.12}$$

where $\hat{\mathcal{Q}}'$ is written in terms of *effective* coefficients,

$$\hat{\mathcal{Q}}' = \left(\hat{c}_{\text{eff}}^\lambda - \hat{a}_{\text{eff}}^\lambda \right) \gamma_\lambda + \tfrac{1}{2} \left(\tilde{\hat{g}}_{\text{eff}}^{\kappa\lambda} - \tilde{\hat{H}}_{\text{eff}}^{\kappa\lambda} \right) \sigma_{\kappa\lambda}, \tag{4.13}$$

with dual coefficients defined by $\tilde{\mathcal{C}}^{\mu\nu} = \tfrac{1}{2}\epsilon^{\mu\nu\rho\sigma}\mathcal{C}_{\rho\sigma}$, and where the "hat" notation follows previous definitions but with $d\,(\text{even}) \geqslant 4$ for c_{eff}^λ and $\tilde{g}_{\text{eff}}^{\kappa\lambda}$, and $d\,(\text{odd}) \geqslant 3$ for a_{eff}^λ and $\tilde{H}_{\text{eff}}^{\kappa\lambda}$. The explicit relations between fundamental SME coefficients and effective ones are

$$\hat{a}_{\text{eff}}^\kappa = \left(\hat{a}^\kappa - \tfrac{1}{m_\mu}p^\kappa \hat{e}^\lambda p_\lambda \right),$$

$$\hat{c}_{\text{eff}}^\kappa = \left(\hat{c}^{\kappa\lambda}p_\lambda - \tfrac{1}{m_\mu}p^\kappa \hat{m} \right),$$

$$\tilde{\hat{g}}_{\text{eff}}^{\kappa\lambda} = \left(\tfrac{1}{2}\epsilon^{\kappa\lambda\rho\sigma}\hat{g}_{\rho\sigma\nu}p^\nu - \tfrac{1}{m_\mu}p^{[\kappa}\hat{b}^{\lambda]} \right),$$

$$\hat{H}_{\text{eff}}^{\kappa\lambda} = \left(\tfrac{1}{2}\epsilon^{\kappa\lambda\rho\sigma}\hat{H}_{\rho\sigma} - \tfrac{1}{m_\mu}p^{[\kappa}\hat{d}^{\lambda]\nu}p_\nu \right). \tag{4.14}$$

We point out that coefficients $\hat{m}_5$ and $\hat{f}^\nu$ are completely unobservable to first order in Lorentz-violation in flat spacetime.

A perturbative hamiltonian, to leading order in Lorentz-violation, can be derived by means of a generalized Foldy-Wouthuysen transformation [25] that decouples positive and negative energy states, with diagonal blocks giving 2×2 relativistic hamiltonians for particles and antiparticles. The relativistic Lorentz-violating correction δh reads

$$\delta h = h_a + h_c + \boldsymbol{h}_g \cdot \boldsymbol{\sigma} + \boldsymbol{h}_H \cdot \boldsymbol{\sigma}. \tag{4.15}$$

4. Testing Lorentz symmetry with muon $(g-2)$ experiments

Aiming use of this expression for the setup of muon $(g-2)$ experiments, we will write the explicit form of the Lorentz-violating correction δh in spherical coordinates, introducing spherical polar angles θ and ϕ by means the unit 3-momentum vector $\hat{\boldsymbol{p}} = (\sin\theta\cos\phi, \sin\theta\sin\phi, \cos\theta)$ and defining the helicity basis as $\hat{\boldsymbol{\epsilon}}_r = \hat{\boldsymbol{\epsilon}}^r = \hat{\boldsymbol{p}}$ and $\hat{\boldsymbol{\epsilon}}_\pm = \hat{\boldsymbol{\epsilon}}^\mp = (\hat{\boldsymbol{\theta}} \pm i\hat{\boldsymbol{\phi}})/\sqrt{2}$. In this basis, rotation scalars are expanded in terms of spherical harmonics ${}_0Y_{jm}(\hat{\boldsymbol{p}})$ and rotation tensors are expanded in terms of spin-weighted spherical harmonics[2] ${}_sY_{jm}(\hat{\boldsymbol{p}})$. The rotation scalar part (4.15) then reads

$$h_a = \sum_{dnjm} E_0^{d-3-n}|\boldsymbol{p}|^n {}_0Y_{jm}(\hat{\boldsymbol{p}})a_{njm}^{(d)},$$

$$h_c = -\sum_{dnjm} E_0^{d-3-n}|\boldsymbol{p}|^n {}_0Y_{jm}(\hat{\boldsymbol{p}})c_{njm}^{(d)}, \tag{4.16}$$

and using the helicity basis decomposition with the Pauli matrices written as

$$\sigma_r = \sigma^r = \begin{pmatrix} \cos\theta & \sin\theta e^{-i\phi} \\ \sin\theta e^{i\phi} & -\cos\theta \end{pmatrix},$$

$$\sigma_\pm = \sigma^\mp = \frac{1}{\sqrt{2}} \begin{pmatrix} -\sin\theta & (\cos\theta \pm 1)e^{-i\phi} \\ (\cos\theta \mp 1)e^{i\phi} & \sin\theta \end{pmatrix}, \tag{4.17}$$

the rotation tensor part reads

$$(h_g)_r = -m_\mu \sum_{dnjm} E_0^{d-4-n}|\boldsymbol{p}|^n {}_0Y_{jm}(\hat{\boldsymbol{p}})(n+1)g_{njm}^{(d)(0B)},$$

$$(h_g)_\pm = \sum_{dnjm} E_0^{d-3-n}|\boldsymbol{p}|^n {}_{\pm 1}Y_{jm}(\hat{\boldsymbol{p}}) \times \left[\pm\sqrt{\frac{j(j+1)}{2}}g_{njm}^{(d)(0B)} \pm g_{njm}^{(d)(1B)} + ig_{njm}^{(d)(1E)} \right],$$

$$(h_H)_r = m_\mu \sum_{dnjm} E_0^{d-4-n}|\boldsymbol{p}|^n {}_0Y_{jm}(\hat{\boldsymbol{p}})(n+1)H_{njm}^{(d)(0B)},$$

---

[2]Spin-weighted spherical harmonics can be seen as a generalization of spherical harmonics for objects transforming as tensors under rotations. For a concise introduction to this subject, see, for instance, Appendix A of [108].

4. Testing Lorentz symmetry with muon $(g-2)$ experiments

$$(h_H)_\pm = -\sum_{dnjm} E_0^{d-3-n}|\boldsymbol{p}|^n {}_{\pm 1}Y_{jm}(\hat{\boldsymbol{p}}) \times \left[\pm\sqrt{\frac{j(j+1)}{2}}H_{njm}^{(d)(0B)} \pm H_{njm}^{(d)(1B)} + iH_{njm}^{(d)(1E)}\right],$$

(4.18)

with $E_0 = \gamma\, m_\mu$ and where the Cartesian coefficients $\mathcal{C}_{\text{eff}}^{(d)\kappa\lambda...\alpha_1\alpha_2...\alpha_{d-3}}$ were decomposed in spherical ones $\mathcal{C}_{njm}^{(d)}$ — see Sec. V C of Ref. [25] for the explicit relation between the Cartesian coefficients and the spherical ones. All information contained in the *cartesian* indices of $\mathcal{C}_{\text{eff}}^{(d)\kappa\lambda...\alpha_1\alpha_2...\alpha_{d-3}}$ are now encoded in the *spherical* indices of $\mathcal{C}_{njm}^{(d)}$. The CPT behavior and index ranges of the coefficients are listed in Table 4.1. Superscripts "E" and "B" represents the behavior of the operators under parity in analogy to the electric and magnetic fields.

Table 4.1: Spherical coefficients appearing in the Lorentz-violating hamiltonian.

Coefficient	CPT	d	n	j
$a_{njm}^{(d)}$	Odd	Odd, $\geqslant 3$	$0,1,\ldots,d-2$	$n,n-2,\cdots \geqslant 0$
$c_{njm}^{(d)}$	Even	Even, $\geqslant 4$	$0,1,\ldots,d-2$	$n,n-2,\cdots \geqslant 0$
$g_{njm}^{(d)(0B)}$	Odd	Even, $\geqslant 4$	$0,1,\ldots,d-3$	$n+1,n-1,\cdots \geqslant 0$
$g_{njm}^{(d)(1B)}$	Odd	Even, $\geqslant 4$	$2,3,\ldots,d-2$	$n-1,n-3,\cdots \geqslant 1$
$g_{njm}^{(d)(1E)}$	Odd	Even, $\geqslant 4$	$1,2,\ldots,d-2$	$n,n-2,\cdots \geqslant 1$
$H_{njm}^{(d)(0B)}$	Even	Odd, $\geqslant 3$	$0,1,\ldots,d-3$	$n+1,n-1,\cdots \geqslant 0$
$H_{njm}^{(d)(1B)}$	Even	Odd, $\geqslant 5$	$2,3,\ldots,d-2$	$n-1,n-3,\cdots \geqslant 1$
$H_{njm}^{(d)(1E)}$	Even	Odd, $\geqslant 3$	$1,2,\ldots,d-2$	$n,n-2,\cdots \geqslant 1$

4.3.2 Application to muon $(g-2)$ experiments

Fundamental quantities for muon $(g-2)$ experiments are the anomaly frequency ω_a, the free proton Larmor frequency and the muon-to-proton magnetic ratio. In our experimental context, the anomaly frequency is the cleanest quantity for the study of

4. Testing Lorentz symmetry with muon $(g-2)$ experiments

Lorentz violation in the muon sector, and in the following we predict Lorentz-violating signals affecting this observable.

Laboratory frame

Starting from the Lorentz-violating correction δh (4.15), we see that only coefficients $\tilde{\tilde{g}}_{\text{eff}}^{\kappa\lambda}$ and $\hat{\tilde{H}}_{\text{eff}}^{\kappa\lambda}$ induce couplings between Lorentz violation and the muon spin $\boldsymbol{S} = \frac{1}{2}\boldsymbol{\sigma}$ in the hamiltonian. This coupling leads to birefringence, which can be understood as an intrinsic Larmor-like precession of $\boldsymbol{S}$ around preferred spacetime directions as the particle travels. Since deviations from the conventional cyclotron frequency can be neglected, the Lorentz-violating contribution $\delta\boldsymbol{\omega}_a$ to the anomaly frequency $\boldsymbol{\omega}_a$ (4.2) can be taken as entirely due to the birefringent effect, which is calculated as a Larmor-like spin-precession frequency,

$$\frac{d\langle\boldsymbol{S}\rangle}{dt}\bigg|_{\text{LV}} = \langle i[\delta h, \boldsymbol{S}]\rangle \approx \delta\boldsymbol{\omega}_a \times \langle\boldsymbol{S}\rangle, \quad \text{where} \quad \delta\boldsymbol{\omega}_a = 2(\boldsymbol{h}_g + \boldsymbol{h}_H), \qquad (4.19)$$

where $\boldsymbol{h}_g$ and $\boldsymbol{h}_H$ are given by (4.18). In the above equation, we have explicitly separated the contribution from Lorentz violation as $d\langle\boldsymbol{S}\rangle/dt$ also contains the conventional spin-precession frequency $\boldsymbol{\omega}_s$, which added to the cyclotron frequency $\boldsymbol{\omega}_c$ gives the conventional anomaly frequency $\boldsymbol{\omega}_a$, as discussed before Eq. (4.2).

At the BNL Muon $(g-2)$ experiment, the detectors are in the $\hat{x}$-$\hat{y}$ plane, thus only the $\hat{z}$-component of $\boldsymbol{\omega}_a$ is measured, and for the Lorentz-violating contribution this means

$$\delta\omega_a \equiv (\delta\boldsymbol{\omega}_a)_z = 2\,(h_g + h_H)_r \cos\theta - \sqrt{2}\left[(h_g + h_H)_+ + (h_g + h_H)_-\right]\sin\theta. \qquad (4.20)$$

Because the muon beam is also confined in this plane, the above expression is evaluated at $\theta = \pi/2$, and as for what concerns data collection, only averages of the anomaly frequency over full cycles are meaningful, $\delta\omega_a \longrightarrow \frac{1}{2\pi}\int_0^{2\pi} d\phi\, \delta\omega_a$, where the identification $\phi = 2\pi\, t_{\text{run}}/T_{\text{run}}$ can be made with T_{run} the characteristic time as measured by t_{run} that each muon takes to complete a full run before decaying. After averaging, only azimuthally symmetric couplings ($m = 0$) between Lorentz violation and momentum

4. Testing Lorentz symmetry with muon $(g-2)$ experiments

factors contribute to $\delta\omega_a$. Moreover, because only spin-weighted spherical harmonics of the form $_{\pm 1}Y_{j,m=0}(\theta = \frac{\pi}{2})$ contribute to $\delta\omega_a$, only *odd* values of j (and therefore only *even* values of n, see Table 4.1) give nonvanishing contributions. After these considerations, the Lorentz-violating correction $\delta\omega_a$ to the anomaly frequency of a muon μ^- or an antimuon μ^+ in the *laboratory* frame reads

$$\delta\omega_{a(\text{lab})}^{\pm} = 2 \sum_{dnj} E_0^{d-3} \sqrt{j(j+1)}\, _{+1}Y_{j0}\left(\theta = \frac{\pi}{2}\right)\left[\check{H}_{nj0}^{(d)} \pm \check{g}_{nj0}^{(d)}\right], \qquad (4.21)$$

where we have introduced the definitions

$$\check{H}_{njm}^{(d)} \equiv \left(1 - \frac{1}{\gamma^2}\right)^{\frac{n}{2}}\left[H_{njm}^{(d)(0B)} + \sqrt{\frac{2}{j(j+1)}}\left(1 - \frac{1}{\gamma^2}\right)H_{(n+2)jm}^{(d)(1B)}\right], \qquad (4.22)$$

$$\check{g}_{njm}^{(d)} \equiv \left(1 - \frac{1}{\gamma^2}\right)^{\frac{n}{2}}\left[g_{njm}^{(d)(0B)} + \sqrt{\frac{2}{j(j+1)}}\left(1 - \frac{1}{\gamma^2}\right)g_{(n+2)jm}^{(d)(1B)}\right], \qquad (4.23)$$

which are the measurable coefficient combinations for the $(g-2)$ experiment (see next sections). The index ranges of $\check{H}_{njm}^{(d)}$ and $\check{g}_{njm}^{(d)}$ are listed in Table 4.2. It is important to note that indices of individual coefficients inside the above definitions still have independent constraints as shown in Table 4.2. For instance, for $d = 3$, we have $\check{H}_{njm}^{(3)} = \left(1 - \frac{1}{\gamma^2}\right)^{\frac{n}{2}} H_{njm}^{(3)(0B)}$ because $H_{njm}^{(d)(1B)}$ exists only for $d(\text{odd}) \geqslant 5$; similarly, $\check{H}_{2jm}^{(5)} = \left(1 - \frac{1}{\gamma^2}\right)^{\frac{n}{2}} H_{2jm}^{(5)(0B)}$ because $H_{4jm}^{(5)(1B)}$ vanishes as $n = 2$ is the highest value possible for $H_{njm}^{(5)(1B)}$.

As a consistency check, we obtain the minimal SME limit of (4.21) in terms of *fundamental* coefficients,

$$\delta\omega_{a(\text{lab})}^{\pm(\text{mSME})} = 2\check{b}_3^{(3)\pm}$$

$$\equiv 2\left[\pm\frac{1}{\gamma}\left(b_3^{(3)} + m_\mu g_{120}^{(4)}\right) \pm \frac{3}{2}\gamma\left(1 - \frac{1}{\gamma^2}\right)m_\mu g_{120}^{(4)(\text{M})} + m_\mu d_{30}^{(4)} + H_{12}^{(3)}\right], \quad (4.24)$$

where $g_{\kappa\lambda\nu}^{(4)(\text{M})} = \frac{1}{3}\left[\left(g_{\kappa\lambda\nu}^{(4)} + g_{\kappa\nu\lambda}^{(4)} + \eta^{\alpha\beta}g_{\lambda\alpha\beta}^{(4)}\eta_{\kappa\nu}\right) - (\kappa \leftrightarrow \lambda)\right]$ is the mixed-symmetry irreducible representation of $g_{\kappa\lambda\nu}^{(4)}$. This result matches with $\delta\omega_a^{\pm}$ found in Ref. [88], but we have extra contributions coming from the coefficient $g_{\kappa\lambda\nu}^{(4)}$ in the definition of $\check{b}_3^{(3)\pm}$, which was not considered in the analysis done in the mentioned reference.

The origin of the γ factors of the coefficient combination in (4.24) can be un-

4. Testing Lorentz symmetry with muon $(g-2)$ experiments

Table 4.2: Ranges for indices appearing in key quantities.

Quantity	Coefficient	d	n	j
$\delta\omega_a^\pm$	$\check{H}_{njm}^{(d)}$	Odd, $\geqslant 3$	$0, 2, \ldots, d-3$	$1, 3, \ldots, n+1$
	$\check{g}_{njm}^{(d)(0B)}$	Even, $\geqslant 4$	$0, 2, \ldots, d-4$	$1, 3, \ldots, n+1$
$\check{H}_{njm}^{(d)}$	$H_{njm}^{(d)(0B)}$	Odd, $\geqslant 3$	$0, 2, \ldots, d-3$	$1, 3, \ldots, n+1$
	$H_{njm}^{(d)(1B)}$	Odd, $\geqslant 5$	$2, 4, \ldots, d-3$	$1, 3, \ldots, n-1$
$\check{g}_{njm}^{(d)}$	$g_{njm}^{(d)(0B)}$	Even, $\geqslant 4$	$0, 2, \ldots, d-4$	$1, 3, \ldots, n+1$
	$g_{njm}^{(d)(1B)}$	Even, $\geqslant 4$	$2, 4, \ldots, d-2$	$1, 3, \ldots, n-1$
$\mathcal{K}_{\tilde{m}}^\pm$	$\check{\mathcal{K}}_{nj\tilde{m}}^{(d)\pm}$	Odd, $\geqslant \tilde{m}+2$	Even, from $j-1$ to $d-3$	Odd, from $\tilde{m}$ to $d-2$

derstood as follows. Consider, first, the $\gamma \to 1$ nonrelativistic limit, where the above coefficient combination reduces to $\tilde{b}_3^{(3)} \equiv b_3^{(3)} + m_\mu g_{120}^{(4)} + m_\mu d_{30}^{(4)} + H_{12}^{(3)}$, where $\tilde{b}_3^{(3)}$ is the observable combination between $b_\nu^{(3)}$ and $g_{\kappa\lambda\nu}^{(4)}$, and $d_{\kappa\lambda}^{(4)}$ and $H_{\kappa\lambda}^{(3)}$ for the nonrelativistic limit of this kind of experiment, in agreement with field redefinition arguments — see discussion at the end of Sec. 3.1. Indeed, several nonrelativistic experiments set bounds specifically on $\tilde{b}_3^{(3)}$ [10], and we see our combination agrees with what should be expected in this limit, and now we argument the relativistic generalization of $\tilde{b}_3^{(3)}$ is consistent with $\check{b}_3^{(3)}$, Eq. (4.24). From Eq. (4.19), we note the muon spin precession is measured in the muon rest frame, but using laboratory time t, therefore use of the muon proper time τ introduces a time dilatation factor of $1/\gamma$ multiplying $\tilde{b}_3^{(3)}$ (because it is proportional to $\delta\omega_a$). Also, we want the result in the laboratory frame instead of the muon rest frame, thus we perform a boost in the $\hat{x}$-$\hat{y}$ plane, where the muon orbit is confined. The boost does not affect $b_3^{(3)}$, therefore it ends up accompanied only by $1/\gamma$. On the other hand, $\frac{1}{\gamma}g_{120}^{(4)} \xrightarrow{\text{boost}} \frac{1}{\gamma}g_{120}^{(4)} + \frac{3}{2}\gamma\left(1 - \frac{1}{\gamma^2}\right)g_{120}^{(4)(M)}$. At last, both $d_{30}^{(4)}$ and $H_{12}^{(3)}$ acquire a γ under the boost, which is then cancelled by the time dilatation $1/\gamma$ factor. In conclusion, moving from the muon rest frame to the laboratory frame

4. Testing Lorentz symmetry with muon $(g-2)$ experiments

changes the observable coefficient combination $\tilde{b}_3^{(3)}$ into $\check{b}_3^{(3)}$, in accordance to what we have explicitly found in (4.24) from a relativistic treatment from the start.

Sun-centered frame

The Lorentz-violating correction $\delta\omega_{a(\text{lab})}^{\pm}$ (4.21) to the anomaly frequency already shows different behaviors for particles and antiparticles, and it could be used to place bounds on CPT and Lorentz violation in the laboratory frame. However, for comparison among different experiments, it is useful to write it in a more suitable frame. Moreover, due to Earth's rotation and orbital motion around the Sun, coupling between Lorentz violation and the muon $(g-2)$ experiment changes over time, and this time-depence is hidden for our expressions written in the noninertial Earth-based laboratory frame. For the moment, we neglect the Earth's orbital motion as in the next two sections we look for effects separated by time intervals of the order of days or weeks, such that a nonrotating frame centered at the Earth can be well-approximated as an inertial one. An extra translation centers this frame at the Sun, defining the standard nonrotating Sun-centered frame, as discussed in Appendix A.

We choose to work with coefficients $\mathcal{K}_{njm}^{(d)}$ defined in the standard nonrotating Sun-centered frame. A coefficient $\mathcal{C}_{njm}^{(d)}$ in a *laboratory* frame with x axis pointing south and y axis pointing east is related to the *Sun-centered* frame coefficient $\mathcal{K}_{njm}^{(d)}$ by [108]

$$\mathcal{C}_{njm}^{(d)} = \sum_{m'} e^{im'\Omega t} d_{mm'}^{(j)}(-\chi)\mathcal{K}_{njm'}^{(d)}, \tag{4.25}$$

where $\Omega = 2\pi/(23\,\text{h}\,56\,\text{min})$ is the sidereal rotation frequency of Earth as measured by the sidereal time t, the "little" Wigner matrix $d_{mm'}^{(j)}$ is given in Eq. (A.4) and χ is the colatitude of the experiment in the northern hemisphere. Finally, in the *nonrotating Sun-centered* frame, the Lorentz-violating contribution to the anomaly frequency reads

$$\delta\omega_a^{\pm} = 2\sum_{dnj} E_0^{d-3} \sum_{m'} e^{im'\Omega t} G_{jm'}(\chi)\Big[\check{H}_{njm'}^{(d)} \pm \check{g}_{njm'}^{(d)}\Big], \tag{4.26}$$

where $G_{jm'}(\chi) \equiv \sqrt{j(j+1)}_{+1}Y_{j0}\left(\theta = \frac{\pi}{2}\right) d_{0m'}^{(j)}(-\chi)$ is a purely geometrical factor — see Table 4.3 for some useful values — and the index ranges of the coefficients are

the same as in (4.21). The above expression for $\delta\omega_a$ extends the analogous result of [88] to encompass Lorentz-violating operators of arbitrary dimensions. It predicts for nonminimal coefficients the same effects as those for the minimal SME, for instance, the difference of the anomaly frequency between particles and antiparticles, $\Delta\omega_a = \delta\omega_a^+ - \delta\omega_a^-$, and also sidereal and annual variations of $\delta\omega_a^\pm$. It is important to emphasize these signals are absent in conventional QED predictions, representing a precise way of testing Lorentz and CPT invariance.

We note from (4.26) that sensitivity to higher dimensional coefficients typically increases with powers of the energy. As detailed below, this behavior places Fermilab and J-PARC experiments in very distinct positions as each of them may enjoy very different sensitivity to some coefficient combinations. Both may typically achieve similar sensitivities to minimal spherical coefficients, but J-PARC's smaller γ due to the use of ultra-cold muons results in improved sensitivity of order 10 to Cartesian coefficients tied to factors of $1/\gamma$. On the other hand, Fermilab's use of high energetic muons may lead to comparatively stronger bounds on the nonminimal coefficients. Moreover, combined use of results from both experiments can be used to place bounds on different coefficient combinations, usually inaccessible in single experiments. Having both experiments running in completely different experimental setup opens a great venue for deep investigations of Lorentz violation in the muon sector.

4.3.3 Muon/Antimuon comparison

Comparison between μ^- and μ^+ anomaly frequency can be used to access time-independent $(m' = 0)$ Lorentz-violating signals in the measurement of the anomaly frequency $\delta\omega_a^\pm$ (4.26) and, for instance, *disentangle* contributions from CPT even and CPT odd coefficients as well. If CPT symmetry is broken — implying Lorentz symmetry is broken as well — differences between particles and antiparticles are to be expected. Actual measurements of $g-2$ are made in different runs for μ^+ and μ^-, therefore we consider the time-averaged difference $\langle\Delta\omega_a\rangle = \langle\delta\omega_a^+\rangle - \langle\delta\omega_a^-\rangle$ over many

4. Testing Lorentz symmetry with muon $(g - 2)$ experiments

Table 4.3: Some useful values of $G_{jm}(\chi)$ for the BNL, Fermilab, and J-PARC experiments.

j	m	CERN (43.7°)	BNL (49.1°)	Fermilab (48.2°)	J-PARC (53.5°)
1	0	0.353	0.320	0.326	0.291
	± 1	∓ 0.239	∓ 0.261	∓ 0.258	∓ 0.278
3	0	0.156	0.314	0.291	0.410
	± 1	± 0.540	± 0.419	± 0.441	± 0.300
	± 2	-0.529	-0.573	-0.568	-0.589
	± 3	± 0.206	± 0.270	± 0.259	± 0.325
5	0	-0.694	-0.493	-0.536	-0.245
	± 1	± 0.241	± 0.518	± 0.481	± 0.639
	± 2	0.623	0.340	0.392	0.0750
	± 3	∓ 0.792	∓ 0.801	∓ 0.806	∓ 0.736
	± 4	0.453	0.588	0.566	0.684
	± 5	∓ 0.137	∓ 0.215	∓ 0.200	∓ 0.292
7	0	-0.170	-0.634	-0.576	-0.773

sidereal days, leading to

$$\langle \Delta \omega_a \rangle = 4 \sum_{d\,n\,j} E_0^{d-3} G_{j0}(\chi) \breve{g}_{nj0}^{(d)}. \tag{4.27}$$

Comparison using data collected at the same geographical location has access to CPT odd coefficients only, but as we will see soon, comparison between data from different locations allows access to CPT even coefficients as well.

The Muon $(g - 2)$ Collaboration found no differences between μ^+ and μ^- anomaly frequency within the achieved experimental precision [83], leading to $\langle \Delta \omega_a \rangle = (-9.2 \pm 9.4) \times 10^{-25}\,\text{GeV}$. They (separately) used μ^+ and μ^- beams with $E_0 = 3.096\,\text{GeV}$ in the BNL experiment, and using their bound on $\langle \Delta \omega_a \rangle$ along with expression (4.27), we set new constraints on Lorentz- and CPT-violating coefficients $\breve{g}_{njm}^{(d)}$ of arbitrary dimension. Bounds on coefficient combinations of $d = 4$, 6, 8, 10 are listed

4. Testing Lorentz symmetry with muon $(g-2)$ experiments

Table 4.4: Constraints on combinations of CPT odd coefficients from comparison between μ^+ and μ^- anomaly frequency using data from BNL Muon $(g-2)$ experiment. Units are GeV^{4-d}.

d	Combination	Upper bound
4	$\check{g}_{010}^{(4)}$	$(-2.3 \pm 2.4) \times 10^{-25}$
6	$\displaystyle\sum_{n=0,2} \check{g}_{n10}^{(6)} + 0.98\,\check{g}_{230}^{(6)}$	$(-2.4 \pm 2.5) \times 10^{-26}$
8	$\displaystyle\sum_{n=0,2,4} \check{g}_{n10}^{(8)} + 0.98 \sum_{n=2,4} \check{g}_{n30}^{(8)} - 1.5\,\check{g}_{450}^{(8)}$	$(-2.5 \pm 2.6) \times 10^{-27}$
10	$\displaystyle\sum_{n=0,2,4,6} \check{g}_{n10}^{(10)} + 0.98 \sum_{n=2,4,6} \check{g}_{n30}^{(10)} - 1.5 \sum_{n=4,6} \check{g}_{n50}^{(10)} - 2.0\,\check{g}_{670}^{(10)}$	$(-2.6 \pm 2.7) \times 10^{-28}$

in Table 4.4, and bounds for individual coefficients are listed in Table 4.5.

In terms of fundamental SME coefficients, the minimal coefficient $\check{g}_{010}^{(4)}$ can be written as

$$\check{g}_{010}^{(4)} = \frac{2}{E_0}\sqrt{\frac{\pi}{3}}\left[\frac{1}{\gamma}\left(b_Z^{(3)} + m_\mu g_{XYT}^{(4)}\right) + \frac{3}{2}\gamma\left(1 - \frac{1}{\gamma^2}\right)m_\mu g_{XYT}^{(4)(\mathrm{M})}\right], \qquad (4.28)$$

where the notation $\mathcal{K}_{\nu\ldots}$ with $\nu = \{T, X, Y, Z\}$ is a reminder that these are quantities defined in the Sun-centered frame. The bound on the spherical *effective* coefficient $\check{g}_{010}^{(4)}$ — see first line of Table 4.4 — is naturally translated into a bound on a combination of *fundamental* coefficients, and individual bounds on such coefficients can be readily inferred. For the BNL experiment, $E_0 = 3.096\,\mathrm{GeV}$ and $\gamma = 29.3$, and using the bound $\check{g}_{010}^{(4)} = (-2.3 \pm 2.4) \times 10^{-25}$, we find $b_Z^{(3)} = (-1.0 \pm 1.1) \times 10^{-23}\,\mathrm{GeV}$, in agreement with Ref. [2]. We can also provide new bounds on $g_{XYT}^{(4)}$. Its axial contribution $g_{XYT}^{(4)(\mathrm{A})}$ only appears in the combination $b_Z^{(3)} + m_\mu g_{XYT}^{(4)(\mathrm{A})}$, thus it is bounded accordingly to the bound on $b_Z^{(3)}$. The trace part $g_{XYT}^{(4)(\mathrm{T})}$ contribution vanishes. Finally, the mixed-symmetry part contribution is bounded as $g_{XYT}^{(4)(\mathrm{M})} = (-7.3 \pm 8.0) \times 10^{-26}$. The coefficient combination is constrained as $(b_Z^{(3)} + m_\mu g_{XYT}^{(4)(\mathrm{A})}) + 1.3 \times 10^3\,m_\mu g_{XYT}^{(4)(\mathrm{M})} = (-1.0 \pm 1.1) \times 10^{-23}\,\mathrm{GeV}$.

As we can see from (4.27), comparison between μ^+ and μ^- anomaly frequency within a single experiment has access to CPT odd coefficients only. On the other hand,

4. Testing Lorentz symmetry with muon $(g-2)$ experiments

Table 4.5: Bounds on spherical CPT odd coefficients from the antimuon/muon anomaly-frequency difference in the BNL Muon $(g-2)$ experiment. Given in units of GeV^{4-d}.

d	Coefficient	Constraint
4	$\check{g}_{010}^{(4)}$	$(-2.3 \pm 2.4) \times 10^{-25}$
6	$\check{g}_{010}^{(6)}, \check{g}_{210}^{(6)}$	$(-2.4 \pm 2.5) \times 10^{-26}$
	$\check{g}_{230}^{(6)}$	$(-2.5 \pm 2.5) \times 10^{-26}$
8	$\check{g}_{010}^{(8)}, \check{g}_{210}^{(8)}, \check{g}_{410}^{(8)}$	$(-2.5 \pm 2.6) \times 10^{-27}$
	$\check{g}_{230}^{(8)}, \check{g}_{430}^{(8)}$	$(-2.6 \pm 2.6) \times 10^{-27}$
	$\check{g}_{450}^{(8)}$	$(1.6 \pm 1.7) \times 10^{-27}$
10	$\check{g}_{010}^{(10)}, \check{g}_{210}^{(10)}, \check{g}_{410}^{(10)}, \check{g}_{610}^{(10)}$	$(-2.6 \pm 2.7) \times 10^{-28}$
	$\check{g}_{230}^{(10)}, \check{g}_{430}^{(10)}, \check{g}_{630}^{(10)}$	$(-2.7 \pm 2.7) \times 10^{-28}$
	$\check{g}_{450}^{(10)}, \check{g}_{650}^{(10)}$	$(1.7 \pm 1.7) \times 10^{-28}$
	$\check{g}_{670}^{(10)}$	$(1.3 \pm 1.4) \times 10^{-28}$

comparison among experiments in *different* locations can be used for constraining CPT even coefficients as well,

$$\langle \Delta\mathcal{R}(1,2) \rangle = 2 \sum_{dnj} E_0^{d-3} \left\{ \left[\frac{G_{j0}(\chi_1)}{\overline{\omega}_{p_1}} + \frac{G_{j0}(\chi_2)}{\overline{\omega}_{p_2}} \right] \check{g}_{nj0}^{(d)} + \left[\frac{G_{j0}(\chi_1)}{\overline{\omega}_{p_1}} - \frac{G_{j0}(\chi_2)}{\overline{\omega}_{p_2}} \right] \check{H}_{nj0}^{(d)} \right\},$$

(4.29)

where $\langle \Delta\mathcal{R}(1,2) \rangle \equiv \delta\mathcal{R}^+(\chi_1) - \delta\mathcal{R}^-(\chi_2)$, with $\langle \delta\mathcal{R}^\pm(\chi_i) \rangle \equiv \langle \delta\omega_a^\pm(\chi_i) \rangle / \overline{\omega}_{p_i}^\pm$, and $\overline{\omega}_{p_i}^\pm$ accounts for the magnetic field used at the experiment located at χ_i running with $\mu^\pm$ — see Sec. 4.2.4. Therefore, differences between ω_a for μ^+ and μ^- are not caused only by CPT violation, but by pure Lorentz violation as well.

Data available from muon $(g-2)$ experiments at CERN [98] and BNL [83] can be used to impose new constraints on CPT even spherical coefficients. The strongest bounds come from $\Delta\mathcal{R}(\text{CERN}, \text{BNL}) = (-3.5 \pm 3.6) \times 10^{-8}$, where we have used $\mathcal{R}^+(\chi_{\text{CERN}}) = 3.707173(36) \times 10^{-3}$, $\mathcal{R}^-(\chi_{\text{BNL}}) = 3.7072083(26) \times 10^{-3}$, $\omega_{p(\text{CERN})}^+/(2\pi) \simeq$

Table 4.6: Constraints on combinations of CPT even coefficients from comparison between μ^+ and μ^- anomaly frequency using data from CERN's and BNL's muon $(g-2)$ experiments. Units are GeV^{4-d}.

d	Combination	Upper bound
3	$\check{H}^{(3)}_{010}$	$(-1.6 \pm 1.7) \times 10^{-22}$
5	$\displaystyle\sum_{n=0,2} \check{H}^{(5)}_{n10} - 5.8\,\check{H}^{(5)}_{230}$	$(-1.7 \pm 1.7) \times 10^{-23}$
7	$\displaystyle\sum_{n=0,2,4} \check{H}^{(7)}_{n10} - 5.8 \sum_{n=2,4} \check{H}^{(7)}_{n30} - 6.9\,\check{H}^{(7)}_{450}$	$(-1.7 \pm 1.8) \times 10^{-24}$
9	$\displaystyle\sum_{n=0,2,4,6} \check{H}^{(9)}_{n10} - 5.8 \sum_{n=2,4,6} \check{H}^{(9)}_{n30} - 6.9 \sum_{n=4,6} \check{H}^{(9)}_{n50} + 17\,\check{H}^{(9)}_{670}$	$(-1.8 \pm 1.9) \times 10^{-25}$

$6.278302(5) \times 10^7$ Hz, and $\omega^-_{p(\mathrm{BNL})}/(2\pi) \simeq 6.1791400(11) \times 10^7$ Hz. These bounds are given in Table 4.6 for coefficient combinations and in Table 4.7 for individual coefficients. Bounds on CPT odd coefficients from comparison of different experiments are typically weaker than bounds coming from a single experiment — as in Table 4.5 — and, therefore, were omited.

Upcoming Fermilab and J-PARC experiments are primarily intended to measure $g-2$ for μ^+ only, but if later upgrades allow the use of μ^- as well, both experiments could improve current bounds on CPT odd coefficients from muon/antimuon comparison, as in (4.27), roughly by a factor of 5 because of improved precision alone. For some coefficients — for instance, see (4.28) — J-PARC could also achieve another extra improvement by a factor of 10 because $\gamma_{\text{J-PARC}} \sim \gamma_{\text{Fermilab}}/10$. Also, data from both experiments could be used together to specify new bounds on CPT even coefficients appearing in (4.29).

4.3.4 Sidereal variations of the anomaly frequency

Sidereal variations of the anomaly frequency, *i.e.*, daily oscillations of its measured value as the Earth spins, are to be expected if Lorentz symmetry is broken. Lorentz-violating background fields are taken as constant in our approach, meaning

4. Testing Lorentz symmetry with muon $(g-2)$ experiments

Table 4.7: Bounds on spherical CPT even coefficients from the antimuon/muon anomaly-frequency difference between the CERN and BNL experiments, given in units of GeV^{4-d}.

d	Coefficient	Constraint
3	$\check{H}_{010}^{(3)}$	$(-1.6 \pm 1.7) \times 10^{-22}$
5	$\check{H}_{010}^{(5)}, \check{H}_{210}^{(5)}$	$(-1.7 \pm 1.7) \times 10^{-23}$
	$\check{H}_{230}^{(5)}$	$(2.9 \pm 3.0) \times 10^{-24}$
7	$\check{H}_{010}^{(7)}, \check{H}_{210}^{(7)}, \check{H}_{410}^{(7)}$	$(-1.7 \pm 1.8) \times 10^{-24}$
	$\check{H}_{230}^{(7)}, \check{H}_{430}^{(7)}$	$(3.0 \pm 3.1) \times 10^{-25}$
	$\check{H}_{450}^{(7)}$	$(2.6 \pm 2.6) \times 10^{-25}$
9	$\check{H}_{010}^{(9)}, \check{H}_{210}^{(9)}, \check{H}_{410}^{(9)}, \check{H}_{610}^{(9)}$	$(-1.8 \pm 1.9) \times 10^{-25}$
	$\check{H}_{230}^{(9)}, \check{H}_{430}^{(9)}, \check{H}_{630}^{(9)}$	$(3.2 \pm 3.3) \times 10^{-26}$
	$\check{H}_{450}^{(9)}, \check{H}_{650}^{(9)}$	$(2.7 \pm 2.7) \times 10^{-26}$
	$\check{H}_{670}^{(9)}$	$(-1.1 \pm 1.1) \times 10^{-26}$

they have a fixed direction in spacetime. Nevertheless, as the Earth rotates, the perceived direction of the background field changes over the sidereal day, as illustrated in Fig. 4.5. Any physical quantity depending on Lorentz-violating coefficients will accordingly exhibit variations of its absolute value on the course of a day. In our case, this quantity is the anomaly frequency ω_a, which receives a contribution $\delta\omega_a$ due to Lorentz violation. Expressing $\delta\omega_a$ in the nonrotating Sun-centered frame reveals the time-dependence of the Lorentz-violating correction, as we can infer from the time-dependent $(m' \neq 0)$ part of (4.26), which can be rewritten as

$$\delta\omega_{a(\mathrm{SV})}^{\pm} = \sum_{\tilde{m}} A_{\tilde{m}\Omega}^{\pm} \cos(\tilde{m}\Omega t + \phi_{\tilde{m}}), \tag{4.30}$$

where $\tilde{m} = 1, 2, \ldots$ and $\phi_{\tilde{m}}$ an associated phase, revealing an interference pattern coming from oscillations with different integer multiples $\tilde{m}$ of Earth's rotational frequency

4. Testing Lorentz symmetry with muon $(g-2)$ experiments

Ω, each oscillation with amplitude

$$A_{\tilde{m}\Omega}^{\pm} = \sqrt{\mathrm{Re}\left(\mathcal{K}_{\tilde{m}}^{\pm}\right)^2 + \mathrm{Im}\left(\mathcal{K}_{\tilde{m}}^{\pm}\right)^2}, \quad \text{where} \quad \mathcal{K}_{\tilde{m}}^{\pm} \equiv 4\sum_{d\,n\,j} E_0^{d-3} G_{j\tilde{m}}(\chi)\check{\mathcal{K}}_{nj\tilde{m}}^{(d)\pm}, \quad (4.31)$$

and the Lorentz-violating factor $\check{\mathcal{K}}_{nj\tilde{m}}^{(d)\pm}$ as defined by the observable coefficient combination for this sort of signal given by

$$\check{\mathcal{K}}_{nj\tilde{m}}^{(d)\pm} \equiv \check{H}_{nj\tilde{m}}^{(d)} \pm E_0\, \check{g}_{nj\tilde{m}}^{(d+1)}, \quad (4.32)$$

with the summation ranges listed in Table 4.2. Note the above expressions are valid for arbitrarily high values of d, and the maximum value of $\tilde{m}$ for a model with a specific d is determined by the restriction $d\,(\mathrm{odd}) \geqslant \tilde{m} + 2$ of the summation in d of Eq. (4.31). For instance, in this context, signals with $\tilde{m} = 2, 3$ come from spherical coefficients with $d \geqslant 5$, and signals with $\tilde{m} = 4, 5$ come from $d \geqslant 7$. Typically, minimal coefficients contribute to signals repeating within no more than one sidereal frequency but when studying signals with *annual* variation in the next section, we will see minimal coefficients can also generate subleading-order signals within two sidereal variations suppressed by a factor of order 10^6 due to Earth's rotational speed.

Once more, for a consistency check, considering only contributions from the minimal SME, in terms of fundamental coefficients, signals within one sidereal frequency have amplitude given by

$$A_{1\Omega}^{\pm(\mathrm{mSME})} = 2\,|\sin\chi|\sqrt{\left(\check{b}_X^{(3)\pm}\right)^2 + \left(\check{b}_Y^{(3)\pm}\right)^2}, \quad (4.33)$$

which follows from (4.31) using

$$\mathrm{Re}\left(\check{\mathcal{K}}_{011}^{(3)\pm}\right) = \mathrm{Re}\left(\check{H}_{011}^{(3)} \pm E_0\,\check{g}_{011}^{(4)}\right) = -\sqrt{\frac{2\pi}{3}}\check{b}_X^{(3)\pm},$$

$$\mathrm{Im}\left(\check{\mathcal{K}}_{011}^{(3)\pm}\right) = \mathrm{Im}\left(\check{H}_{011}^{(3)} \pm E_0\,\check{g}_{011}^{(4)}\right) = -\sqrt{\frac{2\pi}{3}}\check{b}_Y^{(3)\pm}, \quad (4.34)$$

Nonrotating Sun-centered frame

| 6:00 a.m. | 9:30 a.m. | 1:00 p.m. |

Earth-based laboratory frame

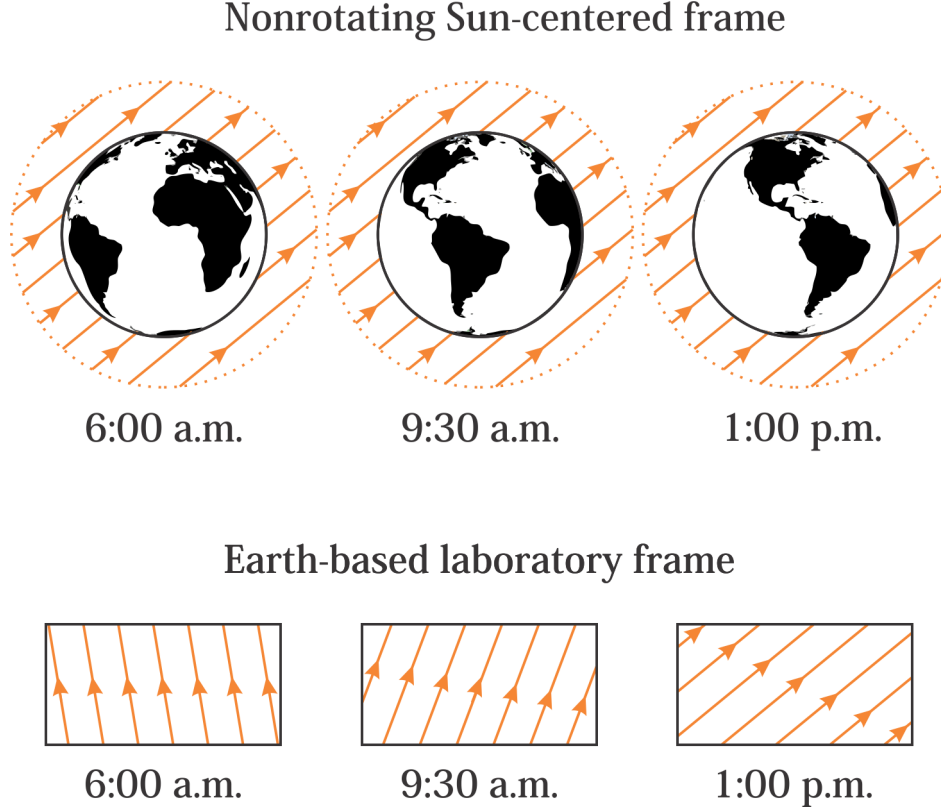| 6:00 a.m. | 9:30 a.m. | 1:00 p.m. |

Figure 4.5: Approximate constancy of the background field with respect to Earth's position in space in the course of a day (top) and apparent sidereal variation of the background vector as seen by an observer at a rotating Earth-based frame (bottom).

where the definition

$$\breve{b}_J^{(3)\pm} \equiv \pm \frac{1}{\gamma}\left(b_J^{(3)} + \frac{1}{2}m\epsilon_{JKL}g_{KLT}^{(4)}\right) + \frac{1}{2}\epsilon_{JKL}H_{KL}^{(3)} + m_\mu d_{JT}^{(4)} \pm \frac{3}{4}\gamma\left(1 - \frac{1}{\gamma^2}\right)m_\mu\epsilon_{JKL}\,g_{KLT}^{(4)(\mathrm{M})},$$

$$(4.35)$$

follows from the one introduced in Eq. (4.24), now in terms of Sun-frame quantities, as indicated by the uppercase indices. These expressions agree with the results of Ref. [2], but again we have extra contributions from the $g_{\kappa\lambda\nu}^{(4)}$ coefficient which was not considered in the aforementioned reference. Note that inclusion of nonminimal coefficients alters the amplitude (4.33) by adding such coefficients inside each of the squared factors, as dictated by (4.31).

The Muon $(g-2)$ Collaboration searched for sidereal variations considering time stamps on frequency measurements at BNL and studied the data collected under the

4. Testing Lorentz symmetry with muon $(g-2)$ experiments

hypothesis of a signal within one sidereal frequency [2]. For instance, the data set from 1999 for μ^+ was acquired from 806 runs, each with duration of about 30 minutes, spread along 25 days [89]. A run i was associated with a time t_i assigned by the center of the time interval which encompassed the run i — for example, if the run started at 8:45AM and ended at 9:15AM, then $t_i = 9.0$. Data from each run i were individually processed and fitted to give $\omega_a(t_i)$, along with a measured $\overline{\omega}_p(t_i)$, leading to $\mathcal{R}(t_i) \equiv \omega_a(t_i)/\overline{\omega}_p$. Data $\mathcal{R}(t_i) \times t_i$ from 1999 and 2000 for μ^+, and from 2001 for μ^- were then fitted under the hypothesis of signals within one sidereal variation, *i.e.*,

$$\mathcal{R}(t_i) = k + \frac{A_{1\Omega}}{\overline{\omega}_p} \cos\left(\Omega t_i + \phi\right), \tag{4.36}$$

where the constant $k \equiv \frac{\lambda a_\mu}{1+a_\mu}$ is chosen in order to recover (4.5) if $A_{1\Omega} = 0$. No statistically significant sidereal variation was observed, resulting in the bounds $A_{1\Omega}^+ \leqslant 2.12 \times 10^{-24}\,\text{GeV}$ and $A_{1\Omega}^- \leqslant 3.93 \times 10^{-24}\,\text{GeV}$ at the 95% confidence level. In our framework, this is translated into bounds on Lorentz-violating coefficients by means of (4.31), which constrains not only minimal coefficients, but a combination involving also nonminimal ones from operators of arbitrarily high dimension — see Table 4.8 for bounds on the combination $\check{\mathcal{K}}_{nj1}^{(d)\pm}$ and Table 4.9 for bounds on the modulus of real or imaginary parts of individual spherical coefficients of dimension up to eight. Reanalysis of the BNL data could be used to impose new constraints on sidereal variations with higher frequencies $(\tilde{m} > 1)$ due to nonminimal coefficients.

Assuming precisions of 140 ppb (Fermilab) and 100 ppb (J-PARC) for the measurement of $\delta\omega_a$ in upcoming $(g-2)$ experiments, we estimate new constraints from sidereal variations, listed in Table 4.10, and sensitivities for individual coefficients in Table 4.11. The energy dependence of the amplitude (4.31) implies that the coefficient combination (4.32) has an upper bound roughly of order $A_{\tilde{m}\Omega}^\pm/4E_0^{d_{min}-3}$, where $d_{min} = \tilde{m} + 2$ is the lowest (odd) dimension appearing in the combination, therefore Fermilab and J-PARC experiments typically have about the same sensitivity to minimal spherical coefficients $(d = 3)$, but the latter's sensitivity to nonminimal ones $(d > 3)$ is gradually suppressed roughly by a factor of $(E_0^{\text{Fermilab}}/E_0^{\text{J-PARC}})^{d-3} \sim 10^{d-3}$

Table 4.8: Constraints on combinations $\check{\mathcal{K}}_{nj1}^{(d)\pm} \equiv \check{H}_{nj1}^{(d)} \pm E_0 \, \check{g}_{nj1}^{(d+1)}$, where $E_0 = 3.096\,\text{GeV}$, from the BNL data for one-sidereal variations of ω_a. Given in units of GeV^{4-d}.

d	Combination (C)	Constraint on $\sqrt{\text{Re}(C)^2 + \text{Im}(C)^2}$	
		for μ^+	for μ^-
3	$\check{\mathcal{K}}_{011}^{(3)\pm}$	2.03×10^{-24}	3.76×10^{-24}
5	$\sum_{n=0,2} \check{\mathcal{K}}_{n11}^{(5)\pm} - 1.60\,\check{\mathcal{K}}_{231}^{(5)\pm}$	2.12×10^{-25}	3.93×10^{-25}
7	$\sum_{n=0,2,4} \check{\mathcal{K}}_{n11}^{(7)\pm} - 1.60 \sum_{n=2,4} \check{\mathcal{K}}_{n31}^{(7)\pm} - 1.99\,\check{\mathcal{K}}_{451}^{(7)\pm}$	2.21×10^{-26}	4.09×10^{-26}

in comparison to Fermilab's. On the other hand, once more, J-PARC's smaller value of γ may lead to an extra improvement of a factor of 10 on sensitivity to fundamental coefficients tied to $1/\gamma$ factors.

It is important to mention that Lorentz violating signals within up to two sidereal variations are not signatures coming solely from *nonminimal* coefficients as it can also be induced from *minimal* ones by *annual* variations, as discussed in the next section.

4.3.5   Annual variations of the anomaly frequency

In the course of days or a few weeks, the Earth's motion around the Sun can be neglected, and a rotating Earth-based laboratory frame and a nonrotating Sun-centered frame are related by a simple rotation once contributions proportional to Earth's rotational speed $\beta_L \sim 10^{-6}$ are disregarded as they are highly suppressed. This is the case for the search for *sidereal* variations of the anomaly frequency, as performed in the previous section. On the other hand, in the search for month- or year-long spanning effects — the case for *annual* variations — the Earth's orbital motion is to be taken into account, introducing extra contributions proportional to its orbital speed $\beta_\oplus \sim 10^{-4}$ encoding these effects since an extra *boost* is involved when relating laboratory and Sun-centered reference frames. In Appendix A we derive the transformation to the Sun-centered frame, considering all contributions up to first

4. Testing Lorentz symmetry with muon $(g-2)$ experiments

Table 4.9: Constraints on the modulus of real or imaginary parts of spherical coefficients from searches for one-sidereal variations of ω_a obtained from the BNL experiment data. Given in unit of GeV^{4-d}.

d	Coefficient	Constraint for μ^+	Constraint for μ^-
3	$\check{H}_{011}^{(3)}$	2.03×10^{-24}	3.76×10^{-24}
4	$\check{g}_{011}^{(4)}$	6.56×10^{-25}	1.21×10^{-24}
5	$\check{H}_{011}^{(5)}, \check{H}_{211}^{(5)}$	2.12×10^{-25}	3.93×10^{-25}
	$\check{H}_{231}^{(5)}$	1.32×10^{-25}	2.45×10^{-25}
6	$\check{g}_{011}^{(6)}, \check{g}_{211}^{(6)}$	6.84×10^{-26}	1.27×10^{-25}
	$\check{g}_{231}^{(6)}$	4.26×10^{-26}	7.90×10^{-26}
7	$\check{H}_{011}^{(7)}, \check{H}_{211}^{(7)}, \check{H}_{411}^{(7)}$	2.21×10^{-26}	4.09×10^{-26}
	$\check{H}_{231}^{(7)}, \check{H}_{431}^{(7)}$	1.38×10^{-26}	2.55×10^{-26}
	$\check{H}_{451}^{(7)}$	1.11×10^{-26}	2.06×10^{-26}
8	$\check{g}_{011}^{(8)}, \check{g}_{211}^{(8)}, \check{g}_{411}^{(8)}$	7.13×10^{-27}	1.32×10^{-26}
	$\check{g}_{231}^{(8)}, \check{g}_{431}^{(8)}$	4.45×10^{-27}	8.24×10^{-27}
	$\check{g}_{451}^{(8)}$	3.59×10^{-27}	6.66×10^{-27}

order in the speeds $\beta_\oplus$ and β_L (the last one included for completeness reasons).

In what follows, we restrict ourselves to *Cartesian minimal* coefficients. The reason for this restriction is twofold: (i) a spherical description of the coefficients is suitable for analysis of rotational properties, but is intractable when boosts are considered, and (ii) nonminimal coefficients are neatly described in the formalism based in spherical coordinates, as done before, but in Cartesian coordinates the large number of indices makes the analysis much more cumbersome. Therefore, only minimal coefficients in Cartesian coordinates will be studied in this section. To simplify the notation, from now on indices indicating the dimension of coefficients will be suppressed and the mass will be denoted by m instead of m_μ. In what follows, we present the analysis for μ^+ first, and then for μ^-.

4. Testing Lorentz symmetry with muon $(g-2)$ experiments

Table 4.10: Estimated bounds on combinations $\check{\mathcal{K}}^{(d)\pm}_{nj\tilde{m}} \equiv \check{H}^{(d)}_{nj\tilde{m}} \pm E_0 \check{g}^{(d+1)}_{nj\tilde{m}}$, where $E_0 = 3.096\,\text{GeV}$ (Fermilab) or $E_0 = 0.320\,\text{GeV}$ (J-PARC), from sidereal variations of ω_a. Given in units of GeV^{4-d}.

d	$\tilde{m}$	Combination (C)	Bound on $\sqrt{\text{Re}(C)^2 + \text{Im}(C)^2}$	
			Fermilab	J-PARC
3	1	$\check{\mathcal{K}}^{(3)\pm}_{011}$	1.3×10^{-25}	8.5×10^{-26}
5	1	$\sum\limits_{n=0,2} \check{\mathcal{K}}^{(5)\pm}_{n11} + \frac{G_{31}(\chi)}{G_{11}(\chi)} \check{\mathcal{K}}^{(5)\pm}_{231}$	1.3×10^{-26}	8.3×10^{-25}
	2	$\check{\mathcal{K}}^{(5)\pm}_{232}$	6.1×10^{-27}	3.9×10^{-25}
	3	$\check{\mathcal{K}}^{(5)\pm}_{233}$	1.3×10^{-26}	7.1×10^{-25}
7	1	$\sum\limits_{n=0,2,4} \check{\mathcal{K}}^{(7)\pm}_{n11} + \frac{G_{31}(\chi)}{G_{11}(\chi)} \sum\limits_{n=2,4} \check{\mathcal{K}}^{(7)\pm}_{n31} + \frac{G_{51}(\chi)}{G_{11}(\chi)} \check{\mathcal{K}}^{(7)\pm}_{451}$	1.4×10^{-27}	8.1×10^{-24}
	2	$\sum\limits_{n=2,4} \check{\mathcal{K}}^{(7)\pm}_{n32} + \frac{G_{52}(\chi)}{G_{32}(\chi)} \check{\mathcal{K}}^{(7)\pm}_{452}$	6.4×10^{-28}	3.8×10^{-24}
	3	$\sum\limits_{n=2,4} \check{\mathcal{K}}^{(7)\pm}_{n33} + \frac{G_{53}(\chi)}{G_{33}(\chi)} \check{\mathcal{K}}^{(7)\pm}_{453}$	1.4×10^{-27}	6.9×10^{-24}
	4	$\check{\mathcal{K}}^{(7)\pm}_{454}$	6.47×10^{-28}	3.3×10^{-24}
	5	$\check{\mathcal{K}}^{(7)\pm}_{455}$	1.8×10^{-27}	7.7×10^{-24}

Antimuons

We have seen in Sec. 4.3.2 the Lorentz-violating correction to the anomaly frequency for μ^+ due to *minimal* coefficients in the *laboratory* frame is given by (4.24),

$$\delta\omega_a^+ = 2\check{b}_3^*, \qquad (4.37)$$

where we had defined the "haček" coefficient

$$\check{b}_3^* \equiv \frac{1}{\gamma}\left(b_3 + mg_{120}\right) + \frac{3}{2}\gamma\left(1 - \frac{1}{\gamma^2}\right)mg_{120}^M + md_{30} + H_{12}, \qquad (4.38)$$

which is the measurable *laboratory* combination of minimal fundamental coefficients to which the experiment is sensitive. Note we have changed our notation, and instead of a superscript "+" for the antimuon, we are using "*" to match the conventions of

4. Testing Lorentz symmetry with muon $(g-2)$ experiments

Table 4.11: Estimated sensitivities to real or imaginary parts of individual coefficients $\check{H}_{nj\tilde{m}}^{(d)}$ and $\check{g}_{nj\tilde{m}}^{(d)}$ from sidereal variations of ω_a, given in units of GeV^{4-d}.

Coefficient	Fermilab	J-PARC	Coefficient	Fermilab	J-PARC
$\check{H}_{011}^{(3)}$	1.3×10^{-25}	8.5×10^{-26}	$\check{g}_{011}^{(4)}$	4.2×10^{-26}	2.7×10^{-25}
$\check{H}_{011}^{(5)}, \check{H}_{211}^{(5)}$	1.3×10^{-26}	8.3×10^{-25}	$\check{g}_{011}^{(6)}, \check{g}_{211}^{(6)}$	4.3×10^{-27}	2.6×10^{-24}
$\check{H}_{231}^{(5)}$	7.9×10^{-27}	7.7×10^{-25}	$\check{g}_{231}^{(6)}$	2.5×10^{-27}	2.4×10^{-24}
$\check{H}_{232}^{(5)}$	6.1×10^{-27}	3.9×10^{-25}	$\check{g}_{232}^{(6)}$	2.0×10^{-27}	1.2×10^{-24}
$\check{H}_{233}^{(5)}$	1.3×10^{-26}	7.1×10^{-25}	$\check{g}_{233}^{(6)}$	4.3×10^{-27}	2.2×10^{-24}
$\check{H}_{011}^{(7)}, \check{H}_{211}^{(7)}, \check{H}_{411}^{(7)}$	1.4×10^{-27}	8.1×10^{-24}	$\check{g}_{011}^{(8)}, \check{g}_{211}^{(8)}, \check{g}_{411}^{(8)}$	4.5×10^{-28}	2.5×10^{-23}
$\check{H}_{231}^{(7)}, \check{H}_{431}^{(7)}$	8.2×10^{-28}	7.5×10^{-24}	$\check{g}_{231}^{(8)}, \check{g}_{431}^{(8)}$	2.7×10^{-28}	2.3×10^{-23}
$\check{H}_{451}^{(7)}$	7.4×10^{-28}	3.5×10^{-24}	$\check{g}_{451}^{(8)}$	2.4×10^{-28}	1.1×10^{-23}
$\check{H}_{232}^{(7)}, \check{H}_{432}^{(7)}$	6.3×10^{-28}	3.8×10^{-24}	$\check{g}_{232}^{(8)}, \check{g}_{432}^{(8)}$	2.0×10^{-28}	1.2×10^{-23}
$\check{H}_{452}^{(7)}$	9.2×10^{-28}	3.0×10^{-23}	$\check{g}_{452}^{(8)}$	3.0×10^{-28}	9.4×10^{-23}
$\check{H}_{233}^{(7)}, \check{H}_{433}^{(7)}$	1.4×10^{-27}	6.9×10^{-24}	$\check{g}_{233}^{(8)}, \check{g}_{433}^{(8)}$	4.5×10^{-28}	2.2×10^{-23}
$\check{H}_{453}^{(7)}$	4.5×10^{-28}	3.1×10^{-24}	$\check{g}_{453}^{(8)}$	1.4×10^{-28}	9.6×10^{-24}
$\check{H}_{454}^{(7)}$	6.4×10^{-28}	3.3×10^{-24}	$\check{g}_{454}^{(8)}$	2.1×10^{-28}	1.0×10^{-23}
$\check{H}_{455}^{(7)}$	1.8×10^{-27}	7.7×10^{-24}	$\check{g}_{455}^{(8)}$	5.8×10^{-28}	2.4×10^{-23}

Ref. [10] for minimal coefficients. As we have seen before, one of the interesting features of signals with sidereal variations is that it allows to measure *different components* of $\check{b}_\mu^*$ besides the axial one, namely, $\check{b}_X^*$ and $\check{b}_Y^*$. For the case of annual variations, due to the boost involved in the transformation to the Sun-frame, we get access to *different coefficient combinations* besides $\check{b}_\mu^*$. To know $\delta\omega_a$ in the Sun-centered frame all we need is the expression for $\check{b}_3^*$ in this reference frame. Explicitly, in the *Sun-frame*, $\check{b}_3^*$ is given by

$$\check{b}_3^* = \cos\chi\,\check{b}_Z^* + \beta_L \sin\chi \left(\frac{2\gamma}{(\gamma+1)^2}\check{d}_{XY} - \frac{11\gamma^2-6\gamma-1}{2(\gamma+1)(2\gamma-1)}\check{g}_{ZX} - \frac{1-3\gamma}{2-4\gamma}\check{g}_{ZY} - \frac{2\gamma}{\gamma+1}\check{H}_{ZT} \right)$$

$$+ \beta_\oplus \cos\chi \cos\Omega_\oplus T \left[\cos\eta \left(-\frac{7\gamma^2-2\gamma-1}{(\gamma+1)(2\gamma-1)}\check{g}_{XY} - \frac{2\gamma}{\gamma+1}\check{H}_{XT} \right) \right.$$

$$\left. + \sin\eta \left(-\frac{7\gamma^4+2\gamma^2-1}{2\gamma(3\gamma^2-1)}\check{b}_T + \frac{7\gamma^4-4\gamma^2+1}{2\gamma(3\gamma^2-1)}\check{g}_T - \frac{2\gamma(\gamma^2+1)}{3\gamma^2-1}\check{d}_+ + \frac{2\gamma^3}{3\gamma^2-1}\check{d}_Q \right) \right]$$

4. Testing Lorentz symmetry with muon $(g-2)$ experiments

$$+ \beta_\oplus \cos\chi \sin\Omega_\oplus T \left[\left(\tfrac{4\gamma}{(\gamma+1)^2} \check{d}_{ZX} - \tfrac{4\gamma(\gamma-1)}{(\gamma+1)(2\gamma-1)} \check{g}_{YZ} - \tfrac{1-3\gamma}{1-2\gamma} \check{g}_{YX} - \tfrac{2\gamma}{\gamma+1} \check{H}_{YT} \right) \right]$$

$$+ \cos\Omega t \Big\{ \sin\chi \check{b}_X^* + \beta_L \cos\chi \left(\tfrac{7\gamma^2-2\gamma-1}{(\gamma+1)(2\gamma-1)} \check{g}_{XY} + \tfrac{2\gamma}{\gamma+1} \check{H}_{XT} \right)$$

$$- \beta_\oplus \sin\chi \cos\Omega_\oplus T \Big[\cos\eta \left(\tfrac{4\gamma}{(\gamma+1)^2} \check{d}_{XY} - \tfrac{4\gamma(\gamma-1)}{(\gamma+1)(2\gamma-1)} \check{g}_{ZX} - \tfrac{1-3\gamma}{1-2\gamma} \check{g}_{ZY} - \tfrac{2\gamma}{\gamma+1} \check{H}_{ZT} \right)$$

$$+ \sin\eta \left(\tfrac{7\gamma^2-2\gamma-1}{(\gamma+1)(2\gamma-1)} \check{g}_{YZ} + \tfrac{2\gamma}{\gamma+1} \check{H}_{YT} \right) \Big]$$

$$+ \beta_\oplus \sin\chi \sin\Omega_\oplus T \left(-\tfrac{(6\gamma^2-7)(\gamma+2)\gamma^3 - 2\gamma(5\gamma-1)+3}{2\gamma(\gamma+1)^2(3\gamma^2-1)} \check{b}_T + \tfrac{2\gamma}{(\gamma+1)^2} \check{d}_- + \tfrac{4}{(\gamma+1)^2} \check{g}_c \right.$$

$$\left. + \tfrac{(6\gamma^2-1)(\gamma+2)\gamma^3 - 2\gamma(3\gamma+1)+1}{2\gamma(\gamma+1)^2(3\gamma^2-1)} \check{g}_T + \tfrac{4\gamma}{3\gamma^2-1} \check{d}_+ - \tfrac{\gamma}{3\gamma^2-1} \check{d}_Q \right) \Big\}$$

$$+ \sin\Omega t \Big\{ \sin\chi \check{b}_Y^* - \beta_L \cos\chi \left(\tfrac{4\gamma}{(\gamma+1)^2} \check{d}_{ZX} - \tfrac{4\gamma(\gamma-1)}{(\gamma+1)(2\gamma-1)} \check{g}_{YZ} - \tfrac{1-3\gamma}{1-2\gamma} \check{g}_{YX} - \tfrac{2\gamma}{\gamma+1} \check{H}_{YT} \right)$$

$$+ \beta_\oplus \sin\chi \cos\Omega_\oplus T \Big[\cos\eta \left(-\tfrac{3\gamma^4(\gamma+2)+4(\gamma^3-1)+\gamma(14\gamma+1)}{2(\gamma+1)^2(3\gamma^2-1)} \check{b}_T + \tfrac{2\gamma}{(\gamma+1)^2} \check{d}_- + \tfrac{4}{(\gamma+1)^2} \check{g}_c \right.$$

$$\left. + \tfrac{3\gamma^5(\gamma+2)-2(\gamma^4-1)+\gamma^2(2\gamma-3)}{2\gamma(\gamma+1)^2(3\gamma^2-1)} \check{g}_T - \tfrac{4}{3\gamma^2-1} \check{d}_+ + \tfrac{\gamma}{3\gamma^2-1} \check{d}_Q \right)$$

$$+ \sin\eta \left(-\tfrac{4\gamma}{(\gamma+1)^2} \check{d}_{YZ} + \tfrac{4\gamma(\gamma-1)}{(\gamma+1)(2\gamma-1)} \check{g}_{XY} + \tfrac{1-3\gamma}{1-2\gamma} \check{g}_{XZ} + \tfrac{2\gamma}{\gamma+1} \check{H}_{XT} \right) \Big]$$

$$+ \beta_\oplus \sin\chi \sin\Omega_\oplus T \Big[\left(\tfrac{7\gamma^2-2\gamma-1}{(\gamma+1)(2\gamma-1)} \check{g}_{ZX} + \tfrac{2\gamma}{\gamma+1} \check{H}_{ZT} \right) \Big] \Big\}$$

$$+ \cos 2\Omega t \Big[\beta_L \sin\chi \left(\tfrac{2\gamma}{(\gamma+1)^2} \check{d}_{XY} + \tfrac{1-3\gamma}{2-4\gamma} (\check{g}_{ZX} - \check{g}_{ZY}) \right) \Big]$$

$$+ \sin 2\Omega t \Big[\beta_L \sin\chi \left(\tfrac{3\gamma^3(\gamma+2)+2\gamma-3}{4\gamma(\gamma+1)^2} \check{b}_T - \tfrac{2\gamma}{(\gamma+1)^2} \check{d}_- - \tfrac{4}{(\gamma+1)^2} \check{g}_c - \tfrac{3\gamma^3(\gamma+2)+2\gamma-3}{4\gamma(\gamma+1)^2} \check{g}_T \right) \Big],$$

$$\tag{4.39}$$

where Ω is Earth's rotational frequency and χ is the colatitude of the experiment in the northern hemisphere, as defined before, and $\Omega_\oplus = 2\pi/(365.26\,\text{days})$ and $\eta = 23.5°$ are the Earth's orbital frequency and orbital tilt with respect to the equator, respectively, and we have introduced haček coefficients by the definitions

$$\check{b}_J = \tfrac{1}{\gamma}(b_J + \tfrac{1}{2}m\epsilon_{JKL}g_{KLT}) - \tfrac{1}{2}\epsilon_{JKL}H_{KL} - md_{JT} + \tfrac{3}{4}\gamma\left(1 - \tfrac{1}{\gamma^2}\right) m\epsilon_{JKL} g_{KLT}^{(\text{M})},$$

$$\check{b}_J^* = \tfrac{1}{\gamma}(b_J + \tfrac{1}{2}m\epsilon_{JKL}g_{KLT}) + \tfrac{1}{2}\epsilon_{JKL}H_{KL} + md_{JT} + \tfrac{3}{4}\gamma\left(1 - \tfrac{1}{\gamma^2}\right) m\epsilon_{JKL} g_{KLT}^{(\text{M})},$$

$$\check{b}_T = b_T + mg_{XYZ},$$

$$\check{g}_T = (b_T + mg_{XYZ}) - 3mg_{XYZ}^{(\text{M})},$$

$$\check{H}_{XT} = \tfrac{1}{2}\left(1 + \tfrac{1}{\gamma}\right)(H_{XT} + md_{ZY}) - \tfrac{1}{2}\left(2\gamma + 1 - \tfrac{1}{\gamma}\right) m \left(g_{XTT}^{(\text{M})} + g_{XYY}^{(\text{M})}\right),$$

4. Testing Lorentz symmetry with muon $(g-2)$ experiments

$$\check{H}_{YT} = \tfrac{1}{2}\left(1 + \tfrac{1}{\gamma}\right)(H_{YT} + md_{XZ}) - \tfrac{1}{2}\left(2\gamma + 1 - \tfrac{1}{\gamma}\right)m\left(g^{(M)}_{YTT} + g^{(M)}_{YZZ}\right),$$

$$\check{H}_{ZT} = \tfrac{1}{2}\left(1 + \tfrac{1}{\gamma}\right)(H_{ZT} + md_{YX}) - \tfrac{1}{2}\left(2\gamma + 1 - \tfrac{1}{\gamma}\right)m\left(g^{(M)}_{ZTT} + g^{(M)}_{ZXX}\right),$$

$$\check{d}_{+} = \tfrac{1}{2}\gamma\left(3 - \tfrac{1}{\gamma^2}\right)m(d_{XX} + d_{YY}) + \gamma\left(1 - \tfrac{1}{\gamma^2}\right)md_{ZZ},$$

$$\check{d}_{-} = \tfrac{1}{4}\left(\gamma + 2 + \tfrac{1}{\gamma}\right)m(d_{XX} - d_{YY}),$$

$$\check{d}_{Q} = \tfrac{1}{2}\gamma\left(3 - \tfrac{1}{\gamma^2}\right)m\left(d_{XX} + d_{YY}\right) + \gamma\left(1 - \tfrac{3}{\gamma^2}\right)md_{ZZ} + 3mg^{(M)}_{XYZ},$$

$$\check{d}_{J} = m\left(d_{TJ} + \tfrac{1}{2}d_{JT}\right) - \tfrac{1}{4}\varepsilon_{JKL}H_{KL},$$

$$\check{d}_{YZ} = \tfrac{1}{4}\left(\gamma + 2 + \tfrac{1}{\gamma}\right)m\left(d_{YZ} + d_{ZY} - g^{(M)}_{XYY} + g^{(M)}_{XZZ}\right),$$

$$\check{d}_{ZX} = \tfrac{1}{4}\left(\gamma + 2 + \tfrac{1}{\gamma}\right)m\left(d_{ZX} + d_{XZ} - g^{(M)}_{YZZ} + g^{(M)}_{YXX}\right),$$

$$\check{d}_{XY} = \tfrac{1}{4}\left(\gamma + 2 + \tfrac{1}{\gamma}\right)m\left(d_{XY} + d_{YX} - g^{(M)}_{ZXX} + g^{(M)}_{ZYY}\right),$$

$$\check{g}_{c} = \tfrac{1}{4}\left(\gamma + 2 + \tfrac{1}{\gamma}\right)m\left(g^{(M)}_{XYZ} - g^{(M)}_{ZXY}\right) - \tfrac{3}{8}\left(\gamma - 2 + \tfrac{1}{\gamma}\right)mg^{(M)}_{XYZ},$$

$$\check{g}_{-} = \tfrac{1}{4}\left(\gamma + 2 + \tfrac{1}{\gamma}\right)m\left(g^{(M)}_{XTX} - g^{(M)}_{YTY}\right),$$

$$\check{g}_{Q} = m\left(g^{(M)}_{XTX} + g^{(M)}_{YTY} - 2g^{(M)}_{ZTZ}\right),$$

$$\check{g}_{TJ} = \tfrac{1}{4}\left(\gamma + 2 + \tfrac{1}{\gamma}\right)m|\varepsilon_{JKL}|g^{(M)}_{KTL},$$

$$\check{g}_{DJ} = -\tfrac{1}{\gamma}\left(b_{J} + \tfrac{1}{2}m\varepsilon_{JKL}g_{KLT}\right) + \tfrac{3}{2}\gamma m\varepsilon_{JKL}g^{(M)}_{KLT},$$

$$\check{g}_{JK} = \tfrac{1}{2}\left(2\gamma + 1 - \tfrac{1}{\gamma}\right)m\left(g^{(M)}_{JTT} + g^{(M)}_{JKK}\right), \quad \text{(no } K \text{ sum, } J \neq K\text{).} \tag{4.40}$$

Definition of haček coefficients is motivated by the corresponding nonrelativistic "tilde" coefficients of [10], which constitute the set of observable coefficients in nonrelativistic experiments. Our approach to obtain these coefficients follows the same reasoning used to obtain $\check{b}_3$ from $\tilde{b}_3$, in Sec. 4.3.2, i.e., by multiplying a tilde coefficient by the time dilatation factor $1/\gamma$ and boosting it from the muon rest frame to the laboratory frame. This reveals the haček definitions are the natural ones [3] when discussing boost effects as each of them represents an independent observable coefficient combination. An additional point is the above notation is defined to be the same for μ^+ and μ^-,

---

[3]Although this reasoning to define the haček coefficients seems natural, the unappealing dependence on Lorentz γ factors both in the boosted expression for $\check{b}_3^*$ and in the mentioned haček coefficients may redeem these definitions unattractive to handle. As an alternative, in Ref. [13] we have introduced "cleaner" definitions for these coefficients based on simpler, although potentially artificial, modifications of the tilde coefficients.

with *no* sign change. This is again motivated by the fact the tilde definitions behave the same way.

The constant terms in the first line of (4.39) are inaccessible in single $(g-2)$ experiments, but can be bounded when considering comparison between μ^+ and μ^- anomaly frequency or comparison between experiments in different geographical locations, as discussed in Sec. 4.3.3. The pieces proportional to β_L may be neglected once they are suppressed by a factor of 10^6.

Terms proportional to $\cos\Omega t$ and $\sin\Omega t$ from the fifth to the fourteenth line bring up one-sidereal variations. The contributions of zeroth order in velocities were previously studied in Sec. 4.3.4, and are the dominant one-sidereal contributions. The four coefficient combinations proportional to $\beta_\oplus$,

(i) $\cos\eta \left(\frac{4\gamma}{(\gamma+1)^2}\check{d}_{XY} - \frac{4\gamma(\gamma-1)}{(\gamma+1)(2\gamma-1)}\check{g}_{ZX} - \frac{1-3\gamma}{1-2\gamma}\check{g}_{ZY} - \frac{2\gamma}{\gamma+1}\check{H}_{ZT} \right)$

$$+ \sin\eta \left(\frac{7\gamma^2-2\gamma-1}{(\gamma+1)(2\gamma-1)}\check{g}_{YZ} + \frac{2\gamma}{\gamma+1}\check{H}_{YT} \right),$$

(ii) $\frac{(6\gamma^2-7)(\gamma+2)\gamma^3-2\gamma(5\gamma-1)+3}{2\gamma(\gamma+1)^2(3\gamma^2-1)}\check{b}_T - \frac{2\gamma}{(\gamma+1)^2}\check{d}_- - \frac{4}{(\gamma+1)^2}\check{g}_c$

$$- \frac{(6\gamma^2-1)(\gamma+2)\gamma^3-2\gamma(3\gamma+1)+1}{2\gamma(\gamma+1)^2(3\gamma^2-1)}\check{g}_T - \frac{4\gamma}{3\gamma^2-1}\check{d}_+ + \frac{\gamma}{3\gamma^2-1}\check{d}_Q,$$

(iii) $\cos\eta \left(-\frac{3\gamma^4(\gamma+2)+4(\gamma^3-1)+\gamma(14\gamma+1)}{2(\gamma+1)^2(3\gamma^2-1)}\check{b}_T + \frac{2\gamma}{(\gamma+1)^2}\check{d}_- + \frac{4}{(\gamma+1)^2}\check{g}_c \right.$

$$\left. + \frac{3\gamma^5(\gamma+2)-2(\gamma^4-1)+\gamma^2(2\gamma-3)}{2\gamma(\gamma+1)^2(3\gamma^2-1)}\check{g}_T - \frac{4}{3\gamma^2-1}\check{d}_+ + \frac{\gamma}{3\gamma^2-1}\check{d}_Q \right)$$

$$+ \sin\eta \left(-\frac{4\gamma}{(\gamma+1)^2}\check{d}_{YZ} + \frac{4\gamma(\gamma-1)}{(\gamma+1)(2\gamma-1)}\check{g}_{XY} + \frac{1-3\gamma}{1-2\gamma}\check{g}_{XZ} + \frac{2\gamma}{\gamma+1}\check{H}_{XT} \right),$$

(iv) $\frac{7\gamma^2-2\gamma-1}{(\gamma+1)(2\gamma-1)}\check{g}_{ZX} + \frac{2\gamma}{\gamma+1}\check{H}_{ZT},$ $\qquad\qquad\qquad$ (4.41)

are signals varying with Earth's sidereal frequency but slowly modulated by its annual frequency. The remaining ones proportional to β_L may be neglected as before as their signals are suppressed by a factor of at least 100 with respect to the others and suppressed by 10^6 compared to the leading signal.

The last two lines show that even *minimal* coefficients can induce twice-sidereal signals, which was a feature that naturally appeared when considering *nonminimal* coefficients in Sec. 4.3.4. However, in the present context, these signals coming from

4. Testing Lorentz symmetry with muon $(g-2)$ experiments

minimal coefficients are suppressed by factors of at least 10^6 relative to the other signals.

Finally, the second, third, and fourth lines,

$$
\begin{aligned}
\check{b}_3^* \supset{}& \beta_\oplus \cos\chi \cos\Omega_\oplus T \Big[\cos\eta \left(-\tfrac{7\gamma^2-2\gamma-1}{(\gamma+1)(2\gamma-1)}\check{g}_{XY} - \tfrac{2\gamma}{\gamma+1}\check{H}_{XT} \right) \\
&+ \sin\eta \left(-\tfrac{7\gamma^4+2\gamma^2-1}{2\gamma(3\gamma^2-1)}\check{b}_T + \tfrac{7\gamma^4-4\gamma^2+1}{2\gamma(3\gamma^2-1)}\check{g}_T - \tfrac{2\gamma(\gamma^2+1)}{3\gamma^2-1}\check{d}_+ + \tfrac{2\gamma^3}{3\gamma^2-1}\check{d}_Q \right) \Big] \\
&+ \beta_\oplus \cos\chi \sin\Omega_\oplus T \Big[\left(\tfrac{4\gamma}{(\gamma+1)^2}\check{d}_{ZX} - \tfrac{4\gamma(\gamma-1)}{(\gamma+1)(2\gamma-1)}\check{g}_{YZ} - \tfrac{1-3\gamma}{1-2\gamma}\check{g}_{YX} - \tfrac{2\gamma}{\gamma+1}\check{H}_{YT} \right) \Big],
\end{aligned}
\tag{4.42}
$$

represent signals with pure *annual* variation. Sensitivity to these coefficients is naturally suppressed by Earth's orbital speed $\beta_\oplus \sim 10^{-4}$, but this is the leading order signal with annual variation to be searched for. Similarly to our estimates for sidereal varying signals, we can estimate bounds on coefficient combinations by measuring $\delta\omega_a$ within annual time range. In the context of minimal coefficients, $\delta\omega_a^+ = 2\check{b}_3^*$ in the laboratory frame, therefore assuming precision of $140\,\mathrm{ppb}$ for the measurement of ω_a at the Fermilab experiment ($\gamma = 29.3$ and $\chi = 48.2°$) and using the result above for the Sun-frame coefficient, we predict an attainable bound of

$$
\begin{aligned}
&\sqrt{\left(3.1\check{g}_{XY} + 1.8\check{H}_{XT} + 14\check{b}_T - 14\check{g}_T + 7.8\check{d}_+ - 7.8\check{d}_Q\right)^2 \cdots} \\
&\quad \overline{\cdots + \left(0.13\check{d}_{ZX} - 1.9\check{g}_{YZ} - 1.5\check{g}_{YX} - 1.9\check{H}_{YT}\right)^2} \lesssim 1.0 \times 10^{-21}\,\mathrm{GeV},
\end{aligned}
\tag{4.43}
$$

and assuming precision of $100\,\mathrm{ppb}$ for J-PARC ($\gamma = 3.03$ and $\chi = 53.5°$) we predict the bound

$$
\begin{aligned}
&\sqrt{\left(2.6\,\check{g}_{XY} + 1.4\,\check{H}_{XT} + 1.5\,\check{b}_T - 1.4\,\check{g}_T + 9.2\times10^{-1}\,\check{d}_+ - 8.3\times10^{-1}\,\check{d}_Q\right)^2 \cdots} \\
&\quad \overline{\cdots + \left(7.5\times10^{-1}\,\check{d}_{ZX} - 1.2\,\check{g}_{YZ} - 1.6\,\check{g}_{YX} - 1.5\,\check{H}_{YT}\right)^2} \lesssim 8.0 \times 10^{-22}\,\mathrm{GeV}.
\end{aligned}
\tag{4.44}
$$

Search for annual variations of the anomaly frequency therefore allows bounds on different coefficient combinations not accessible in sidereal variations analysis or

136

4. Testing Lorentz symmetry with muon $(g-2)$ experiments

muon/antimuons comparison analysis. In Table 4.12 we estimate the sensitivity to individual Sun-frame μ^+ coefficients for Fermilab and J-PARC. As expected, both experiments have competitive sensitivity to the minimal coefficients.

Table 4.12: Estimated sensitivity to real or imaginary parts of spherical Sun-frame μ^+ coefficients.

Sun-frame coefficient	Fermilab	J-PARC
$\check{b}_T$	$7.1 \times 10^{-23}\,\text{GeV}$	$5.3 \times 10^{-22}\,\text{GeV}$
$\check{g}_T$	$7.1 \times 10^{-23}\,\text{GeV}$	$5.7 \times 10^{-22}\,\text{GeV}$
$\check{H}_{XT}$	$5.6 \times 10^{-22}\,\text{GeV}$	$5.7 \times 10^{-22}\,\text{GeV}$
$\check{H}_{YT}$	$5.3 \times 10^{-22}\,\text{GeV}$	$5.3 \times 10^{-22}\,\text{GeV}$
$\check{d}_+$	$1.3 \times 10^{-22}\,\text{GeV}$	$8.7 \times 10^{-22}\,\text{GeV}$
$\check{d}_Q$	$1.3 \times 10^{-22}\,\text{GeV}$	$9.6 \times 10^{-22}\,\text{GeV}$
$\check{g}_{XY}$	$3.2 \times 10^{-22}\,\text{GeV}$	$3.1 \times 10^{-22}\,\text{GeV}$
$\check{d}_{ZX}$	$7.7 \times 10^{-21}\,\text{GeV}$	$1.1 \times 10^{-21}\,\text{GeV}$
$\check{g}_{YX}$	$6.7 \times 10^{-22}\,\text{GeV}$	$5.0 \times 10^{-22}\,\text{GeV}$
$\check{g}_{YZ}$	$5.3 \times 10^{-22}\,\text{GeV}$	$6.7 \times 10^{-22}\,\text{GeV}$

Muons

All results of the previous section are for μ^+ coefficients, but results for μ^- coefficients could be readily obtained by means of a CPT transformation, changing the sign of the CPT odd *fundamental* coefficients b_ν and $g_{\kappa\lambda\nu}$. For instance, see the definition of $\check{b}_3^\pm$ in (4.24), $\check{b}_3^\mp \xrightarrow{\text{CPT}} \check{b}_3^\pm = \pm\frac{1}{\gamma}(b_3^\pm + mg_{120}^\pm) + H_{12}^\pm + md_{30}^\pm \pm \frac{3}{2}\gamma(1 - \frac{1}{\gamma^2})m\,g_{120}^{M\pm}$.

Alternatively, we can approach the results for muons using the haček definitions of (4.40). As mentioned before, they were defined to be exactly the same for μ^+ and μ^-, without any sign change. As a consequence, in what follows we obtain expressions for μ^- that at first seem to be unrelated by a CPT transformation to the corresponding ones for μ^+, but we emphasize they are definitely the CPT transformation of each

137

other as it can be explicitly verified when they are written in terms of fundamental coefficients instead of haček ones.

Following the above considerations, analogously to the antimuon discussion, in the laboratory frame, muon $(g-2)$ experiments are sensitive to the combination

$$\check{b}_3 \equiv \tfrac{1}{\gamma}\left(b_3 + mg_{120}\right) + \tfrac{3}{2}\gamma\left(1 - \tfrac{1}{\gamma^2}\right)mg_{120}^M - md_{30} - H_{12} \tag{4.45}$$

because $\delta\omega_a^- = 2\check{b}_3$. Comparing to (4.24), we emphasize we have once more changed our notations to match the ones of Ref. [10]. Expression (4.24) and (4.45) are related by $\check{b}_3 = -\check{b}_3^-$. In the *Sun-frame*, the above expression is given by

$$
\begin{aligned}
\check{b}_3 =\ & \cos\chi\,\check{b}_Z - \beta_L \sin\chi\left(\tfrac{2\gamma}{(\gamma+1)^2}\check{d}_{XY} - \tfrac{11\gamma^2-10\gamma-1}{2(\gamma+1)(2\gamma-1)}\check{g}_{ZX} - \tfrac{3\gamma^2+2\gamma-5}{2(\gamma+1)(2\gamma-1)}\check{g}_{ZY} - \tfrac{2\gamma}{\gamma+1}\check{H}_{ZT}\right) \\
& + \beta_\oplus \cos\chi\cos\Omega_\oplus T\Big[\cos\eta\left(\tfrac{\gamma^2-4\gamma+3}{(\gamma+1)(2\gamma-1)}\check{g}_{XY} + \tfrac{2\gamma}{(\gamma+1)}\check{H}_{XT}\right) \\
& \qquad - \sin\eta\left(-\tfrac{8\gamma^4-11\gamma^2+3}{\gamma(3\gamma^2-1)}\check{b}_T + \tfrac{8\gamma^4-8\gamma^2+2}{\gamma(3\gamma^2-1)}\check{g}_T - \tfrac{2\gamma(\gamma^2+1)}{3\gamma^2-1}\check{d}_+ + \tfrac{2\gamma^3}{3\gamma^2-1}\check{d}_Q\right)\Big] \\
& + \beta_\oplus \cos\chi\sin\Omega_\oplus T\Big[\left(-\tfrac{4\gamma}{(\gamma+1)^2}\check{d}_{ZX} + \tfrac{2(\gamma-1)}{\gamma+1}\check{g}_{YZ} - \tfrac{3\gamma^2-2\gamma-1}{(\gamma+1)(2\gamma-1)}\check{g}_{YX} + \tfrac{2\gamma}{\gamma+1}\check{H}_{YT}\right)\Big] \\
& + \cos\Omega t\Big\{\sin\chi\,\check{b}_X - \beta_L\cos\chi\left(\tfrac{7\gamma^2-4\gamma-3}{(\gamma+1)(2\gamma-1)}\check{g}_{XY} + \tfrac{2\gamma}{\gamma+1}\check{H}_{XT}\right) \\
& \quad + \beta_\oplus \sin\chi\cos\Omega_\oplus T\Big[\cos\eta\left(\tfrac{4\gamma}{(\gamma+1)^2}\check{d}_{XY} - \tfrac{2(\gamma-1)}{\gamma+1}\check{g}_{ZX} - \tfrac{3\gamma^2+2\gamma-5}{(\gamma+1)(2\gamma-1)}\check{g}_{ZY} - \tfrac{2\gamma}{\gamma+1}\check{H}_{ZT}\right) \\
& \qquad + \sin\eta\left(\tfrac{7\gamma^2-4\gamma-3}{(\gamma+1)(2\gamma-1)}\check{g}_{YZ} + \tfrac{2\gamma}{\gamma+1}\check{H}_{YT}\right)\Big] \\
& \quad - \beta_\oplus \sin\chi\sin\Omega_\oplus T\left(\tfrac{21\gamma^6+6\gamma^5-9\gamma^4+12\gamma^3-21\gamma^2-2\gamma+9}{4\gamma(\gamma+1)^2(3\gamma^2-1)}\check{b}_T + \tfrac{2\gamma}{(\gamma+1)^2}\check{d}_- + \tfrac{2(3\gamma^2-5)}{(\gamma+1)^2}\check{g}_c\right. \\
& \qquad \left. - \tfrac{21\gamma^6+6\gamma^5+3\gamma^4+36\gamma^3-13\gamma^2-10\gamma+5}{4\gamma(\gamma+1)^2(3\gamma^2-1)}\check{g}_T + \tfrac{4\gamma}{3\gamma^2-1}\check{d}_+ - \tfrac{\gamma}{3\gamma^2-1}\check{d}_Q\right)\Big\} \\
& + \sin\Omega t\Big\{\sin\chi\,\check{b}_Y + \beta_L\cos\chi\left(\tfrac{4\gamma}{(\gamma+1)^2}\check{d}_{ZX} - \tfrac{2(\gamma-1)}{\gamma+1}\check{g}_{YZ} - \tfrac{3\gamma^2+2\gamma-5}{(\gamma+1)(2\gamma-1)}\check{g}_{YX} - \tfrac{2\gamma}{\gamma+1}\check{H}_{YT}\right) \\
& \quad + \beta_\oplus \sin\chi\cos\Omega_\oplus T\Big[\cos\eta\left(\tfrac{9\gamma^5(\gamma-2)-5\gamma^4-4\gamma^3-9\gamma^2+6\gamma+5}{4\gamma(\gamma+1)^2(3\gamma^2-1)}\check{b}_T - \tfrac{2\gamma}{(\gamma+1)^2}\check{d}_- + \tfrac{2(3\gamma^2-1)}{(\gamma+1)^2}\check{g}_c\right. \\
& \qquad \left. - \tfrac{9\gamma^5(\gamma-2)+7\gamma^4+20\gamma^3-\gamma^2-2\gamma+1}{4\gamma(\gamma+1)^2(3\gamma^2-1)}\check{g}_T + \tfrac{4\gamma}{3\gamma^2-1}\check{d}_+ - \tfrac{\gamma}{3\gamma^2-1}\check{d}_Q\right) \\
& \qquad + \sin\eta\left(\tfrac{4\gamma}{(\gamma+1)^2}\check{d}_{YZ} - \tfrac{2(\gamma-1)}{\gamma+1}\check{g}_{XY} + \tfrac{3\gamma^2-2\gamma-1}{(\gamma+1)(2\gamma-1)}\check{g}_{XZ} - \tfrac{2\gamma}{\gamma+1}\check{H}_{XT}\right) \Big] \\
& \quad - \beta_\oplus \sin\chi\sin\Omega_\oplus T\Big[\left(\tfrac{7\gamma^2-4\gamma-3}{(\gamma+1)(2\gamma-1)}\check{g}_{ZX} + \tfrac{2\gamma}{\gamma+1}\check{H}_{ZT}\right)\Big]\Big\} \\
& - \cos 2\Omega t\Big[\beta_L\sin\chi\left(\tfrac{2\gamma}{(\gamma+1)^2}\check{d}_{XY} + \tfrac{3\gamma^2+2\gamma-5}{2(\gamma+1)(2\gamma-1)}(\check{g}_{ZX}-\check{g}_{ZY})\right)\Big]
\end{aligned}
$$

$$+ \sin 2\Omega t \left[\beta_L \sin\chi \left(\tfrac{3\gamma^3(\gamma+6)-10\gamma-3}{4\gamma(\gamma+1)^2}\check{b}_T + \tfrac{2\gamma}{(\gamma+1)^2}\check{d}_- - \tfrac{2(3\gamma^2-1)}{(\gamma+1)^2}\check{g}_c - \tfrac{3\gamma^3(\gamma+6)-10\gamma-3}{4\gamma(\gamma+1)^2}\check{g}_T \right) \right],$$

$$(4.46)$$

where the haček coefficients are given by (4.40).

Interpretation of (4.46) is identical to the analogous expression (4.39) for antimuons. We again highlight interesting combinations proportional to $\cos\Omega t \cos\Omega_\oplus T$, $\cos\Omega t \sin\Omega_\oplus T$, $\sin\Omega t \cos\Omega_\oplus T$, and $\sin\Omega t \sin\Omega_\oplus T$ bringing up one-sidereal variations with slow annual modulation, respectively given by

(i) $\quad \cos\eta \left(\tfrac{4\gamma}{(\gamma+1)^2}\check{d}_{XY} - \tfrac{2(\gamma-1)}{\gamma+1}\check{g}_{ZX} - \tfrac{3\gamma^2+2\gamma-5}{(\gamma+1)(2\gamma-1)}\check{g}_{ZY} - \tfrac{2\gamma}{\gamma+1}\check{H}_{ZT} \right)$

$$+ \sin\eta \left(\tfrac{7\gamma^2-4\gamma-3}{(\gamma+1)(2\gamma-1)}\check{g}_{YZ} + \tfrac{2\gamma}{\gamma+1}\check{H}_{YT} \right),$$

(ii) $\quad \tfrac{21\gamma^6+6\gamma^5-9\gamma^4+12\gamma^3-21\gamma^2-2\gamma+9}{4\gamma(\gamma+1)^2(3\gamma^2-1)}\check{b}_T + \tfrac{2\gamma}{(\gamma+1)^2}\check{d}_- + \tfrac{2(3\gamma^2-5)}{(\gamma+1)^2}\check{g}_c$

$$- \tfrac{21\gamma^6+6\gamma^5+3\gamma^4+36\gamma^3-13\gamma^2-10\gamma+5}{4\gamma(\gamma+1)^2(3\gamma^2-1)}\check{g}_T + \tfrac{4\gamma}{3\gamma^2-1}\check{d}_+ - \tfrac{\gamma}{3\gamma^2-1}\check{d}_Q,$$

(iii) $\quad \cos\eta \left(\tfrac{9\gamma^5(\gamma-2)-5\gamma^4-4\gamma^3-9\gamma^2+6\gamma+5}{4\gamma(\gamma+1)^2(3\gamma^2-1)}\check{b}_T - \tfrac{2\gamma}{(\gamma+1)^2}\check{d}_- + \tfrac{2(3\gamma^2-1)}{(\gamma+1)^2}\check{g}_c \right.$

$$\left. - \tfrac{9\gamma^5(\gamma-2)+7\gamma^4+20\gamma^3-\gamma^2-2\gamma+1}{4\gamma(\gamma+1)^2(3\gamma^2-1)}\check{g}_T + \tfrac{4\gamma}{3\gamma^2-1}\check{d}_+ - \tfrac{\gamma}{3\gamma^2-1}\check{d}_Q \right)$$

$$+ \sin\eta \left(\tfrac{4\gamma}{(\gamma+1)^2}\check{d}_{YZ} - \tfrac{2(\gamma-1)}{\gamma+1}\check{g}_{XY} + \tfrac{3\gamma^2-2\gamma-1}{(\gamma+1)(2\gamma-1)}\check{g}_{XZ} - \tfrac{2\gamma}{\gamma+1}\check{H}_{XT} \right),$$

(iv) $\quad \tfrac{7\gamma^2-4\gamma-3}{(\gamma+1)(2\gamma-1)}\check{g}_{ZX} + \tfrac{2\gamma}{\gamma+1}\check{H}_{ZT}.$ $\hfill (4.47)$

Terms with pure annual variations are the ones of the second, third, and fourth lines,

$$\check{b}_3 \supset \beta_\oplus \cos\chi \cos\Omega_\oplus T \left[\cos\eta \left(\tfrac{\gamma^2-4\gamma+3}{(\gamma+1)(2\gamma-1)}\check{g}_{XY} + \tfrac{2\gamma}{(\gamma+1)}\check{H}_{XT} \right) \right.$$

$$\left. - \sin\eta \left(-\tfrac{8\gamma^4-11\gamma^2+3}{\gamma(3\gamma^2-1)}\check{b}_T + \tfrac{8\gamma^4-8\gamma^2+2}{\gamma(3\gamma^2-1)}\check{g}_T - \tfrac{2\gamma(\gamma^2+1)}{3\gamma^2-1}\check{d}_+ + \tfrac{2\gamma^3}{3\gamma^2-1}\check{d}_Q \right) \right]$$

$$+ \beta_\oplus \cos\chi \sin\Omega_\oplus T \left[\left(-\tfrac{4\gamma}{(\gamma+1)^2}\check{d}_{ZX} + \tfrac{2(\gamma-1)}{\gamma+1}\check{g}_{YZ} - \tfrac{3\gamma^2-2\gamma-1}{(\gamma+1)(2\gamma-1)}\check{g}_{YX} + \tfrac{2\gamma}{\gamma+1}\check{H}_{YT} \right) \right].$$

$$(4.48)$$

4. Testing Lorentz symmetry with muon $(g-2)$ experiments

Considering upcoming $(g-2)$ experiments, we predict an attainable bound of

$$
\sqrt{\left(0.39\breve{g}_{XY} + 1.8\breve{H}_{XT} + 31\breve{b}_T - 31\breve{g}_T + 7.8\breve{d}_+ - 7.8\breve{d}_Q\right)^2 \cdots}
$$
$$
\overline{\cdots + \left(0.13\breve{d}_{ZX} - 1.9\breve{g}_{YZ} + 1.4\breve{g}_{YX} - 1.9\breve{H}_{YT}\right)^2} \lesssim 1.0 \times 10^{-21}\,\text{GeV}
$$

$$(4.49)$$

for the Fermilab experiment, and

$$
\sqrt{\left(2.7 \times 10^{-3}\,\breve{g}_{XY} + 1.4\,\breve{H}_{XT} + 2.9\,\breve{b}_T - 3.0\,\breve{g}_T + 9.3 \times 10^{-1}\,\breve{d}_+ - 8.4 \times 10^{-1}\breve{d}_Q\right)^2 \cdots}
$$
$$
\overline{\cdots + \left(7.5 \times 10^{-1}\breve{d}_{ZX} - 1.0\,\breve{g}_{YZ} + 1.0\,\breve{g}_{YX} - 1.5\,\breve{H}_{YT}\right)^2} \lesssim 8.0 \times 10^{-22}\,\text{GeV},
$$

$$(4.50)$$

for the J-PARC one. Estimates of the sensitivity to individual Sun-frame μ^- coefficients for Fermilab and J-PARC are given in Table 4.13.

Table 4.13: Estimated sensitivity to real or imaginary parts of spherical Sun-frame μ^- coefficients.

Sun-frame coefficient	Fermilab	J-PARC
$\breve{b}_T$	$3.2 \times 10^{-23}\,\text{GeV}$	$2.8 \times 10^{-22}\,\text{GeV}$
$\breve{g}_T$	$3.2 \times 10^{-23}\,\text{GeV}$	$2.7 \times 10^{-22}\,\text{GeV}$
$\breve{H}_{XT}$	$5.5 \times 10^{-22}\,\text{GeV}$	$5.7 \times 10^{-22}\,\text{GeV}$
$\breve{H}_{YT}$	$5.3 \times 10^{-22}\,\text{GeV}$	$5.3 \times 10^{-22}\,\text{GeV}$
$\breve{d}_+$	$1.3 \times 10^{-22}\,\text{GeV}$	$8.6 \times 10^{-22}\,\text{GeV}$
$\breve{d}_Q$	$1.3 \times 10^{-22}\,\text{GeV}$	$9.5 \times 10^{-22}\,\text{GeV}$
$\breve{g}_{XY}$	$2.6 \times 10^{-21}\,\text{GeV}$	$3.0 \times 10^{-19}\,\text{GeV}$
$\breve{d}_{ZX}$	$7.7 \times 10^{-21}\,\text{GeV}$	$1.1 \times 10^{-21}\,\text{GeV}$
$\breve{g}_{YX}$	$7.1 \times 10^{-22}\,\text{GeV}$	$8.0 \times 10^{-22}\,\text{GeV}$
$\breve{g}_{YZ}$	$5.3 \times 10^{-22}\,\text{GeV}$	$8.0 \times 10^{-22}\,\text{GeV}$

4.4 Summary

In this chapter, Lorentz violation was investigated in the context of muon $(g-2)$ experiments. Our framework was based on the Lorentz-violating QED extension for operators of arbitrary mass dimension — whereas they were restricted to mass dimension less than five in previous chapters. Our formalism was then adapted to spherical coordinates, where spherical Lorentz-violating coefficients are described by more compact and simpler notation then Cartesian ones. This approach allows for very clean results in the sense of what is effectively observable in the experiment.

After a brief overview of muon $(g-2)$ experiments, we have sorted out which observable signals coming from Lorentz violation can be expected in such experiments. Fairly clean effects of Lorentz violation can be looked for by analysing the so called anomaly frequency ω_a, which is the difference between the muon spin precession frequency and its cyclotron frequency, and is one of the key quantities measured in muon $(g-2)$ experiments. The high precision to which ω_a can be measured is very suitable in the search of diminute violations of Lorentz symmetry, and although no significant deviation from Lorentz invariance have been detected in the already concluded BNL Muon $(g-2)$ experiment, it allowed us to place stringent upper bounds on coefficients controlling Lorentz violation by means of available data for antimuon/muon anomaly frequency difference and searches for sidereal variations of this quantity. Using the estimated precision of upcoming Fermilab and J-PARC $(g-2)$ experiments we also predict their sensitivity to Lorentz-violating signals.

As our main result, we derived the correction to the anomaly frequency due to Lorentz violation. Our expression can be written in quite compact form and is valid for Lorentz-violating operators of arbitrarily high dimensions. Such expression was used to constrain coefficients for Lorentz violation using CERN's and BNL's data. These bounds are related to signals of Lorentz symmetry breaking predicted by our model, as discussed below. In the literature, these are the first bounds on such coefficients of the nonminimal muon sector. Additionally, we estimated the sensitivity to Lorentz-violation for the upcoming $(g-2)$ experiments.

4. Testing Lorentz symmetry with muon $(g-2)$ experiments

Differences between particles and antiparticles are characteristic signals of Lorentz noninvariance. By comparing the anomaly frequency of muons and antimuons measured in the BNL experiment, we have written explicit bounds on dimension four to dimension ten CPT odd coefficients. Our general expression for differences between muon and antimuons also allows for extra constraints on CPT even coefficient combinations, which can be obtained comparing data from two experiments in different locations, and using data from the CERN and BNL experiments we presented new bounds on such coefficients as well. We predict data from upcoming Fermilab and J-PARC experiments may improve those bounds by roughly a factor of five, or even greater for comparisons from different experiments.

Sidereal variations of the anomaly frequency are also predicted by our model. A reanalysis of the BNL data was performed in the past by other authors and no significant Lorentz violation due to one-sidereal variations was found for minimal coefficients. Here we provided the adequate framework for the search for sidereal variations associated with nonminimal coefficients as well. We used bounds on signals within one-sidereal variation — initially intented to constrain minimal coefficients — to provide new constraints on nonminimal ones as well, explicitly written for coefficients with dimension up to eight. Considering the expected precision of the Fermilab and J-PARC experiments, we have also written the estimated sensitivity to Lorentz violation coming from nonminimal coefficients.

Similarly, annual variations can be expected due to Lorentz violation. No such analysis was ever done for data from any muon $(g-2)$ experiment, and we provided the characteristic signals to be search for as well as the coefficient combinations that would create such signals — for practical reasons, in this case we have limited ourselves to minimal coefficients. Estimated sensitivity of future experiments to such signals was also provided, where we expect Fermilab and J-PARC experiments to achieve competitive sensitivities.

Conclusions and Perspectives

More than a hundred years have passed since the development of Special Relativity, and so far Lorentz symmetry of the known physical laws stands strong on solid experimental grounds. Nevertheless, our desire for a long sought consistent quantum description of gravity leads us to question the very basic building blocks of our description of Nature by devising theoretical frameworks and high precision experiments to test such principles. If even minuscule violations of Lorentz symmetry were ever found, a drastic change of paradigm would occur, infusing our knowledge with fresh air and possibly helping us on the search for more fundamental theories describing the physics of particles and fields.

In this thesis, we have studied different aspects of a single-fermion Lorentz-violating extension of quantum electrodynamics, based on the framework of the Standard Model Extension. We investigated first matters of renormalizability of the minimal QED extension, and secondly we considered the nonminimal extension in the context of muon $(g - 2)$ experiments. Although not expected, we found intersecting points between both studies.

Aiming for an analysis to all orders in perturbation theory, renormalizability was investigated using the algebraic renormalization approach leading to a natural emphasis on the search for quantum gauge anomalies. It was found that new potentially anomalous structures are induced because of Lorentz violation. Important is the fact these are not *necessarily* anomalies, but *candidate* anomalies. In practice, we found conventional gauge identities — for instance, the Ward-Takahashi identity — are no longer automatically satisfied once they are extended by Lorentz-violating contributions, each of these carrying so-called anomaly coefficients. The value of each of these

coefficients tells about the true anomaly content of the model. If they vanish to all orders, gauge identities recover the conventional structure and there is no anomaly. It turns out, we verified all anomaly coefficients indeed vanish to one-loop order. Additionally, by arguments based on behavior under discrete symmetries and a generalized version of the Furry theorem, we suggested gauge identities related to the transversality of the vacuum polarization and current conservation at each vertex of the three-photon triangular diagram are non-anomalous to all orders. Nevertheless, there remains the question as to whether or not anomaly coefficients related to the Ward-Takahashi identity — the only other potentially anomalous identity — develop nonvanishing values under multiloop corrections. On the other hand, we found more restricted models, where C or PT invariance are enforced, are definitely free of anomalies to all orders — revealing the previously overlooked importance of discrete symmetries in guaranteeing the absence of anomalies of a model.

Proof of renormalizability to all orders, if no anomaly is found, follows in the algebraic approach once is found a consistent set of renormalization conditions fixing free parameters introduced by renormalization. Analysis of this last point is better done by explicit calculation of finite radiative corrections coming from divergent diagrams, as Lorentz violation may introduce unexpected features inaccessible by the algebraic approach only. Indeed, in the form of preliminary results, investigation of the fermion-self energy revealed coefficients $c_S^{\mu\nu}$, $d_S^{\mu\nu}$, $g_M^{\kappa\lambda\mu}$, and $(k_F)_{\mu\rho\nu}{}^{\rho}$ generate contributions which fail to be properly renormalized once the corresponding introduced free parameters apparently cannot be consistently fixed by renormalization conditions. Mention should be made of the possibility that this result comes out from an inadequate choice of renormalization conditions. Nevertheless, we also mention other conditions were tried but the conclusion remained the same.

Additional preliminary results suggest radiative corrections modify the free propagation of fermions — an effect absent in conventional QED — as finite Lorentz-violating corrections radiatively induce field operators of dimension higher than four modifying the tree-level action. Because of the dimensionality of such induced operators, there are extra factors of momentum divided by the fermion mass, revealing the

possibility that Lorentz-violating radiative contributions can be as relevant as tree-level ones in specific experiments. In particular, that would be the case for tests of Lorentz symmetry with electrons of energy $\gtrsim 70\,\text{MeV}$ — which is a typical energy for such tests — or muons of energy $\gtrsim 1.4\,\text{GeV}$ — we point out muon $(g-2)$ experiments are performed at $3.09\,\text{GeV}$, making them ideal for such investigation. In such situations, it is possible that coefficient bounds derived from radiative corrections can be at least as strong as bounds derived by tree-level analysis.

We emphasize the above two points we have discussed are based on preliminary results and are under ongoing investigation, and raising interesting questions, both theoretical and experimental.

This thesis' last work was devoted to application of the nonminimal Lorentz-violating QED extension to muon $(g-2)$ experiments. Such experiments are suitable as tests of Lorentz invariance as they can achieve high precision measurements and are very sensible to physics of higher energy scales. In particular, we predicted signatures of Lorentz violation in the muon anomaly frequency — currently measured to about 0.5 part per million — using a powerful formalism which allows consideration of contributions coming from fermion operators of arbitrary dimension. The first signature we mention is the difference between the anomaly frequency of μ^+ and μ^-, which we showed is caused not only by CPT violation, but also by CPT invariant Lorentz-violating contributions as well. Using data from CERN's and BNL's muon $(g-2)$ experiments, we derived the first explicit bounds on several azimuthally symmetric coefficients associated to operators with dimension up to ten. The other Lorentz violation signatures we propose for experimental search are sidereal and annual variations of the anomaly frequency. The Muon $(g-2)$ Collaboration searched for signals within one sidereal variation assuming this effect as due to minimal coefficients only, and here we found nonminimal coefficients can also generate such signals and, therefore, the null result found at the BNL also provides new bounds on nonminimal coefficients. We also found searches within higher number of sidereal variations are important as these are typical signals from nonmininal coefficients. Additionally, annual variation of the anomaly frequency have never been searched for and we provided the whole set of min-

imal coefficient combinations that can be accessed in this experiment. For both cases, we estimated the sensitivity for Lorentz violation of upcoming Fermilab and J-PARC muon $(g-2)$ experiments.

Appendix A: Transformation between frames

In this Appendix, we present some definitions and results for transformations between rotating Earth-based laboratory frames and nonrotating Sun-centered frames — see, for instance, Refs. [9,10,24,109]. As discussed in Chapter 4, the motivation to perform such transformations is twofold: (i) the laboratory frame is noninertial and moving to inertial frames reveals the time-dependence of Lorentz-violating signals, and (ii) it allows comparison among different experiments.

It is important to define two cases:

1) When a nonrotating Earth-centered frame can be approximated as an inertial frame, which is a reasonable simplification when investigating signals within days or few weeks — in this time span, Earth's rotation axis precession can also be neglected once its period is about 26.000 years. In this case, only Earth's rotational motion is considered.

2) When signals are investigated within months or year-long time span, and Earth's noninertial orbital motion need to be considered. In this case a nonrotating Sun-centered frame is more adequate.

Naturally, even the Sun-frame is not really inertial because of its motion around the center of the galaxy, but it takes about 230 million years for it to complete a full orbit, thus it is a reasonable approximation to consider this frame as an inertial one within a time span of thousands of years.

Let us consider a nonrotating Earth-based frame $\{X, Y, Z\}$ to be taken as centered on Earth, as depicted in Fig. 4.6. Orientation of the Z axis can be suitably

Appendix A: Transformation between frames

chosen so as to simplify searches for rotation violations in Earth-based laboratories. Therefore, to define the orientation of the axes, we note that an equinox occurs twice a year, when the equatorial plane of Earth passes through the center of the Sun. Defining Earth's rotation axis as having declination $90°$, the vernal equinox point can be defined as having right ascension $0°$ and declination $0°$. Now we define the Z axis as coinciding with Earth's rotation axis at the vernal equinox of year 2000, X and Y axes lying in Earth's equatorial plane, with X pointing to the vernal equinox point of the celestial sphere, and Y completing the right-handed coordinate system at right ascension $90°$ and declination $0°$.
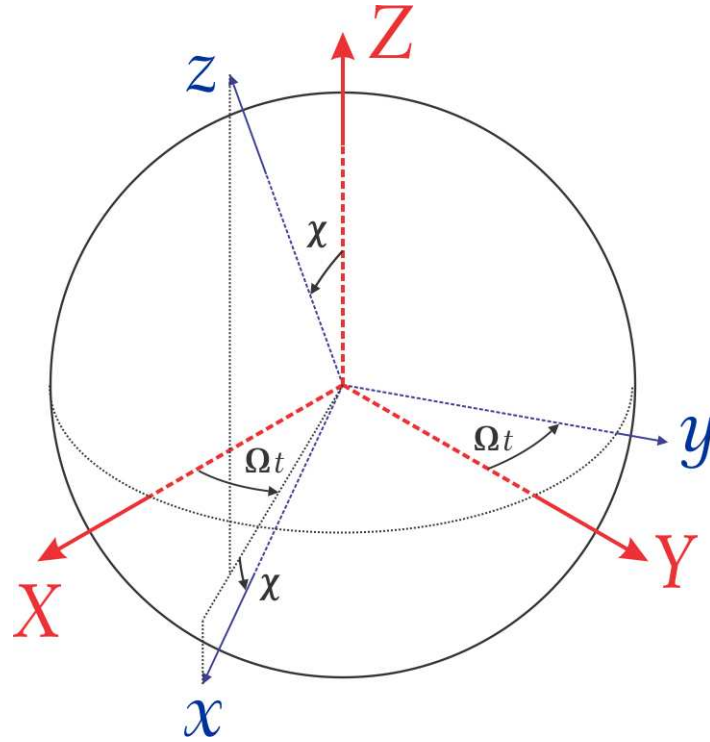

Figure 4.6: Rotating earth-based laboratory frame $\{x, y, z\}$ (translated to the center of Earth, in the picture) and nonrotating Earth-centered frame $\{X, Y, Z\}$.

The position of a laboratory at the surface of the Earth is described by its colatitude χ — defined as the complementary angle of the latitude — and the angle Ωt, where $\Omega = 2\pi/23\,\mathrm{h}\,56\mathrm{min}$ is Earth's sidereal frequency as measured by t. Coordinates $\{x, y, z\}$ of the laboratory frame can be defined with z passing through Earth's center, x perpendicular to z and contained in the plane spanned by $\hat{z} \cdot \hat{Z}$, and $\hat{y} \equiv \hat{z} \times \hat{x}$ always

Appendix A: Transformation between frames

lying in the equatorial plane — see Fig. 4.6, where the $\{x, y, z\}$ laboratory frame was translated to the origin of the $\{X, Y, Z\}$ nonrotating frame.

A nonrotating Sun-centered frame, as depicted in Fig. 4.7, can be defined precisely as above by means of a simple translation of the $\{X, Y, Z\}$ coordinate system to the center of the Sun, where $\Omega_\oplus = 2\pi/(365.26\,\text{days})$ is Earth's orbital frequency, with T measured by a clock at the origin, setting $T = 0$ as the vernal equinox of the year 2000. Thefore Earth is in the negative X axis at $T = 0$ and crosses the XY plane on a descending trajectory — note T and t differ by a constant value. At last, $\eta \approx 23.5°$ is the tilt angle of Earth's orbital plane with respect to its equatorial plane.
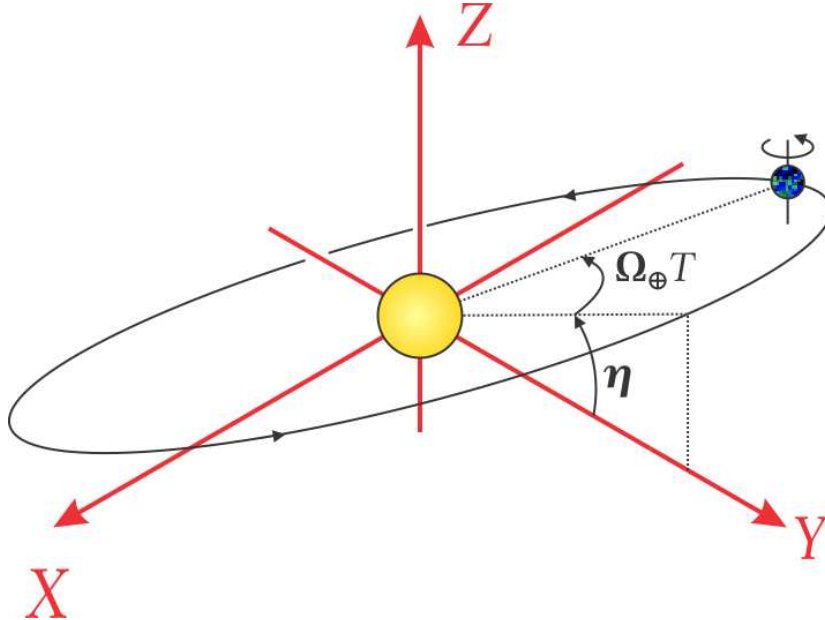

Figure 4.7: Nonrotating Sun-centered frame $\{X, Y, Z\}$, obtained as a translation from the nonrotating Earth-centered frame.

From the above definitions, it is evident the construction of a nonrotating Sun-centered frame is suitable for both cases mentioned before. The approximation as to whether or not Earth can be taken as an inertial frame effectively plays a role when we make a *coordinate transformation* from the Earth-based laboratory $\{x, y, z\}$ frame to the Sun-centered frame $\{X, Y, Z\}$. The transformations for both cases are presented below.

Appendix A: Transformation between frames

Case 1: Earth's orbital motion can be neglected

As discussed before, in this case, only Earth's rotational motion is relevant. For a fully relativistic treatment, the transformation relating the nonrotating Earth-centered frame and the rotating laboratory frame could be obtained by means of an *instantaneous* boost, but since Earth's rotational speed $\beta_L \sim 10^{-6}$ can be neglected, a nonrelativistic approach is enough. Additionally, we approximate Earth's orbit to a circle. In this sense, the transformation can be constructed, for instance, by two spatial rotations, one with respect to the Z axis and parameterized by Ωt, followed by another one around the Y axis parameterized by χ, and an additional translation setting the frame at the center of the Sun, thus we can still say this transformation relates a laboratory-based frame to a Sun-centered frame, although it is limited to time scales where Earth's motion around the Sun may be neglected. The resulting transformation is given by

$$
R^{\mu\nu} = \begin{pmatrix} 1 & 0 & 0 & 0 \\ \hline 0 & & & \\ 0 & & \mathcal{R}^{jJ} & \\ 0 & & & \end{pmatrix}, \quad \text{where} \quad \mathcal{R}^{jJ} = \begin{pmatrix} \cos\chi\cos\Omega t & \cos\chi\sin\Omega t & -\sin\chi \\ -\sin\Omega t & \cos\Omega t & 0 \\ \sin\chi\cos\Omega t & \sin\chi\sin\Omega t & \cos\chi \end{pmatrix},
$$

$$(A.1)$$

where $j = \{x, y, z\} = \{1, 2, 3\}$ are indices in the laboratory frame and $J = \{X, Y, Z\}$ are indices in the Sun-frame.

The transformation matrix (A.1) is suitable for *cartesian* coefficients. For instance, the coefficient $\check{b}_3$ of definition (4.24) transforms as

$$
\check{b}_3 = \mathcal{R}_{3J}\check{b}_J = \check{b}_Z \cos\chi + \left(\check{b}_X \cos\Omega t + \check{b}_Y \sin\Omega t\right) \sin\chi. \tag{A.2}
$$

This expression clearly reveals the time-dependence of Lorentz-violating signals on sidereal time scales, as discussed in Sec. 4.3.4.

On the other hand, cartesian coefficients with several indices — nonminimal coefficients, for instance — become hard to handle under the transformation (A.1). In

Appendix A: Transformation between frames

this case, it is convenient to decompose then in spin-weighted spherical harmonics, as described in Sec. 4.3.1. In this case, coefficients in the laboratory frame and in the Sun-centered frame are related by [24]

$$\mathcal{C}_{jm}^{(\text{lab})} = \sum_{m'} e^{im'\Omega t} d_{mm'}^{(j)}(-\chi) \mathcal{C}_{jm'}^{(\text{Sun})}, \qquad (A.3)$$

where $d_{mm'}^{(j)}(\theta)$ is the "little" Wigner matrix,

$$d_{mm'}^{(j)}(\theta) = \sum_{k} (-1)^{k+m+m'} \frac{\sqrt{(j+m)!(j-m)!(j+m')!(j-m')!}}{(j-m-k)!(m-m'+k)!(j+m'-k)!k!}$$
$$\times \left(\cos\frac{\theta}{2}\right)^{2j} \left(\tan\frac{\theta}{2}\right)^{2k+m-m'}, \qquad (A.4)$$

for all values of k such that the factorials are non-negative. For a derivation of this result, see Section V A of Ref. [24].

Case 2: Earth's orbital motion is taken into account

In this case, Earth's orbital motion around the Sun is also considered along with its rotational motion. The transformation from the Sun-centered frame to the rotating laboratory frame can be obtained in two steps: (i) an *instantaneous* boost from the nonrotating Sun-centered frame to a Sun-orbiting nonspinning frame at the surface of the Earth — with surface velocity, as measured in the Sun-centered frame depicted in Fig. 4.7, given by

$$\vec{\beta} = \beta_{\oplus} \begin{pmatrix} \sin\Omega_{\oplus}T \\ -\cos\eta\cos\Omega_{\oplus}T \\ -\sin\eta\cos\Omega_{\oplus}T \end{pmatrix} + \beta_L \begin{pmatrix} -\sin\Omega t \\ \cos\Omega t \\ 0 \end{pmatrix}, \qquad (A.5)$$

where $\beta_{\oplus}$ is Earth's orbital speed — and (ii) a rotation to the Sun-orbiting spinning Earth-based laboratory frame, as done before. A reasonable approximation is to keep contributions only up to leading order in $\beta_{\oplus} \sim 10^{-4}$ and $\beta_L \sim 10^{-6}$, and for this reason the boost will only mix temporal and spatial components, changing the first row and column of (A.1), but will not introduce extra spatial rotations. Finally, the

Appendix A: Transformation between frames

transformation from the nonrotating Sun-centered frame to the rotating Earth-based laboratory frame is given by

$$
\Lambda^{\mu\nu} = \begin{pmatrix} 1 & \Lambda_{0X} & \Lambda_{0Y} & \Lambda_{0Z} \\ \Lambda_{1T} & & & \\ \Lambda_{2T} & & \mathcal{R}^{jJ} & \\ \Lambda_{3T} & & & \end{pmatrix}, \tag{A.6}
$$

where $\mathcal{R}^{jJ}$ is given by (A.1), and

$$
\begin{aligned}
\Lambda_{0X} &= \beta_{\oplus} \sin \Omega_{\oplus} T - \beta_L \sin \Omega t, \\
\Lambda_{0Y} &= - \beta_{\oplus} \cos \eta \cos \Omega_{\oplus} T + \beta_L \cos \Omega t, \\
\Lambda_{0Z} &= - \beta_{\oplus} \sin \eta \cos \Omega_{\oplus} T, \\
\Lambda_{1T} &= \beta_{\oplus} \sin \Omega_{\oplus} T - \beta_L \sin \Omega t, \\
\Lambda_{2T} &= - \beta_{\oplus} \cos \eta \cos \Omega_{\oplus} T + \beta_L \cos \Omega t, \\
\Lambda_{3T} &= - \beta_{\oplus} \sin \eta \cos \Omega_{\oplus} T,
\end{aligned} \tag{A.7}
$$

are the contributions from the boost. Naturally, in the limit $\beta_{\oplus} \to 0$ we recover Case 1 discussed before. Application of this transformation is done in Sec. (4.3.5), revealing Lorentz-violating signals to be searched for in time scales within months or years.

Bibliography

[1] O. W. Greenberg, Phys. Rev. Lett. **89**, 231602 (2002); arXiv:hep-ph/0309309v1 (2003).

[2] G.W. Bennett et al. Muon $(g-2)$ Collaboration, Phys. Rev. Lett. **100**, 091602 (2008).

[3] D. Colladay and V.A. Kostelecký, Phys. Rev. D **55**, 6760 (1997).

[4] D. Colladay and V.A. Kostelecký, Phys. Rev. D **58**, 116002 (1998).

[5] V.A. Kostelecký, Phys. Rev. D **69**, 105009 (2004).

[6] V.A. Kostelecký and S. Samuel, Phys. Rev. D **39**, 683 (1989).

[7] V.A. Kostelecký and R. Potting, Nucl. Phys. B **359**, 545 (1991).

[8] V.A. Kostelecký and R. Potting, Phys. Rev. D **51**, 3923 (1995).

[9] V.A. Kostelecký and M. Mewes, Phys. Rev. D **66**, 056005 (2002).

[10] *Data Tables for Lorentz and CPT Violation, 2014 edition*, V.A. Kostelecký and N. Russell, arXiv:0801.0287v7, updated version of V. A. Kostelecký and N. Russell, Rev. Mod. Phys. **83**, 11 (2011).

[11] O.M. Del Cima, J.M. Fonseca, D.H.T. Franco, A.H. Gomes, and O. Piguet, Phys. Rev. D **85**, 065023 (2012).

[12] D.H.T. Franco and A.H. Gomes, J. Phys. A **46**, 04540 (2013).

References

[13] A.H. Gomes, V.A. Kostelecký, and A.J. Vargas, arXiv:1407.7748 (submitted to Physical Review D).

[14] Personal website of V.A. Kostelecký with introductory questions and answers on Lorentz symmetry violation along with several up-to-date references, `http://www.physics.indiana.edu/~kostelec/faq.html`.

[15] R. Bluhm, Lect. Notes Phys. **702**, 191 (2006).

[16] R. Lehnert, *Quantum Theory and Symmetries IV*, Heron Press, Sofia, 2006.

[17] V.A. Kostelecký, Phys. Lett. B **701**, 137 (2011).

[18] V.A. Kostelecký, N. Russell , R. Tso, Phys. Lett. B **716**, 470 (2012).

[19] R. Bluhm and V.A. Kostelecký, Phys. Rev. D **71**, 065008 (2005).

[20] V.A. Kostelecký and R. Potting, Int. J. Mod. Phys. D **14**, 2341 (2005).

[21] R. Bluhm, S.-H. Fung, and V.A. Kostelecký, Phys. Rev. D **77**, 065020 (2008).

[22] V.A. Kostelecký and R. Potting, Phys. Rev. D **79**, 065018 (2009).

[23] V.A. Kostelecký and M. Mewes, Phys. Rev. D **69**, 016005 (2004).

[24] V.A. Kostelecký and M. Mewes, Phys. Rev. D **80**, 015020 (2009).

[25] V.A. Kostelecký and M. Mewes, Phys. Rev. D **88**, 096006 (2013).

[26] S.M. Carroll, J.A. Harvey, V.A. Kosteleck, C.D. Lane, and T. Okamoto, Phys. Rev. Lett. **87**, 141601 (2001).

[27] V.A. Kosteleck, R. Lehnert, and M.J. Perry, Phys. Rev. D **68**, 123511 (2003).

[28] O. Bertolami, R. Lehnert, R. Potting, and A. Ribeiro, Phys. Rev. D **69**, 083513 (2004).

[29] A. Ferrero and B. Altschul, Phys. Rev. D **80**, 125010 (2009).

[30] V.A. Kostelecký and R. Lehnert, Phys. Rev. D **63**, 065008 (2001).

References

[31] C. Adam and F.R. Klinkhamer, Nucl. Phys. B **607**, 247 (2001).

[32] A.P. Baêta Scarpelli, H. Belich, J.L. Boldo, and J.A. Helaÿel-Neto, Phys. Rev. D **67**, 085021 (2003).

[33] R. Casana, M.M. Ferreira Jr., A.R. Gomes, and P.R.D. Pinheiro, Phys. Rev. D **80**, 125040 (2009).

[34] R. Casana, M.M. Ferreira Jr., A.R. Gomes, and F.E.P. dos Santos, Phys. Rev. D **82**, 125006 (2010).

[35] A.P. Baêta Scarpelli, and J.A. Helaÿel-Neto, Phys. Rev. D **73**, 105020 (2006).

[36] R. Lehnert, J. Math. Phys. **45**, 3399 (2004).

[37] D. Colladay, P. McDonald, and D. Mullins, J. Phys. A **43**, 275202 (2010).

[38] M. Cambiaso, R. Lehnert, and R. Potting, Phys. Rev. D **85**, 085023 (2012).

[39] R. Potting, Phys. Rev. D **85**, 045033 (2012).

[40] V.A. Kostelecký, C.D. Lane, and A.G.M. Pickering, Phys. Rev. D **65**, 056006 (2002).

[41] G. de Berredo-Peixoto, I.L. Shapiro, Phys. Lett. B **642**, 153 (2006).

[42] M. Cambiaso, R. Lehnert, and R. Potting, arXiv:hep-th/1401.7317 (2014).

[43] D. Colladay and P. McDonald, Phys. Rev. D **75**, 105002 (2007); **77**, 085006 (2008); **79**, 125019 (2009).

[44] A. Ferrero and B. Altschul, Physical Rev. D **84**, 065030 (2011).

[45] D. Mattingly, Living Rev. Rel. **8**, 5 (2005).

[46] *CPT and Lorentz Symmetry I-V*, edited by V. A. Kostelecky, World Scientific, Singapore, 1999-2011.

[47] R. Jackiw and V.A. Kostelecký, Phys. Rev. Lett. **82**, 3572 (1999).

References

[48] M. Pérez-Victoria, Phys. Rev. Lett. **83**, 2518 (1999).

[49] C. Adam and F.R. Klinkhamer, Phys. Lett. B **513**, 245 (2001).

[50] G. Bonneau, L.C. Costa, and J.L. Tomazelli, Int. J. Theor. Phys. **47**, 1764 (2008).

[51] O. Piguet and S.P. Sorella, *Algebraic Renormalization*, Lect. Notes Phys. M **28**, Springer-Verlag, Berlin, 1995.

[52] S.L. Adler, Phys. Rev. **177**, 2426 (1969).

[53] W.A. Bardeen, Phys. Rev. **184**, 1848 (1969).

[54] J.S. Bell and R. Jackiw, Nuovo Cimento **60**, 47 (1969).

[55] S.L. Adler and W.A. Bardeen, Phys. Rev. **182**, 1517 (1969).

[56] J.H. Lowenstein, Commun. Math. Phys. **4**, 2281 (1971); **24**, 1 (1971).

[57] Y-M.P. Lam, Phys. Rev. D **6**, 2145 (1972); **7**, 2943 (1973).

[58] T.E. Clark and J.H. Lowenstein, Nucl. Phys. B **113**, 109 (1976).

[59] O. Piguet and A. Rouet, Phys. Rep. **76**, 1 (1981).

[60] P. Breitenlohner and D. Maison, Commun. Math. Phys. **52**, 11 (1977) 11; **52**, 39 (1977); **52**, 55 (1977).

[61] F. Brennecke and M. Dütsch, Rev. Math. Phys. **20**, 119 (2008).

[62] F. Brennecke and M. Dütsch, *The Quantum Action Principle in the Framework of Causal Perturbation Theory*, in *Quantum Field Theory - Competitive Models*, Birkhäuser, 2009.

[63] M. Dütsch, *The Master Ward Identity: A Universal Formulation of Classical Symmetries. Can they be realized in perturbative Quantum Field Theory?*, in `http://wwwthep.physik.uni-mainz.de/~scheck/Hessbg02.html` (Conference held at Hesselberg Academy, Germany, 2002).

References

[64] V.P. Nair, *Quantum Field Theory: A Modern Perspective*, Springer, New York, 2005.

[65] S. Coleman and S.L. Glashow, Phys. Rev. D **59**, 116008 (1999).

[66] B. Altschul, Phys. Rev. D **70**, 101701 (2004).

[67] B. Altschul, Phys. Rev. D **73**, 036005 (2006).

[68] W.F. Chen and G. Kunstatter, Phys. Rev. D **62**, 10529 (2000).

[69] C.D. Carone, M. Sher, and M. Vanderhaeghen, Phys. Rev. D **74**, 077901 (2006).

[70] J. Furtado and T. Mariz, arXiv:hep-ph/1401.0492 (2014).

[71] V.A. Kostelecký and A.G.M. Pickering, Phys. Rev. Lett. **91**, 031801 (2003).

[72] G. Leibbrandt, Rev. Mod. Phys. **47**, 849 (1975).

[73] G. 't Hooft and M. Veltman, Nucl. Phys. B **44**, 189 (1972).

[74] D. Colladay and V.A. Kostelecký, Phys. Lett. B **511**, 209 (2001).

[75] D. Colladay and P. McDonald, J. Math. Phys. **43**, 3554 (2002).

[76] B. Altschul, J. Phys. A **39**, 13757 (2006).

[77] A. Fittante and N. Russell, J. Phys. G: Nucl. Part. Phys. **39**, 125004 (2012).

[78] M.A. Hohensee, R. Lehnert, D.F. Phillips, and R.L. Walsworth, Phys. Rev. D **80**, 036010 (2009).

[79] M.E. Peskin and D.V. Schroeder, *An Introduction to Quantum Field Theory*, Addison-Wesley, 1995.

[80] This package is available for free at `http://www.feyncalc.org`, where its documentation for use can be found.

[81] C. Itzykson and J.B. Zuber, "Quantum Field Theory", Dover, New york, (2005).

References

[82] B.F. Hatfield, "*Quantum Field Theory of Point Particles and Strings*", Addison-Wesley, Frontier in Physics, 1992.

[83] G.W. Bennett et al. Muon $(g-2)$ Collaboration, Phys. Rev. D **73**, 072003 (2006).

[84] New Muon $(g-2)$ Collaboration, Fermilab Proposal 0989 (2009), `http://lss.fnal.gov/archive/test-proposal/0000/fermilab-proposal-0989.pdf`.

[85] J-PARC $(g-2)$ Collaboration, J-PARC-PAC2009-12 (2009), `http://j-parc.jp/researcher/Hadron/en/pac_1001/pdf/KEK_J-PARC-PAC2009-12.pdf`.

[86] K. Hagiwara, R. Liao, A.D. Martin, D. Nomura, and T. Teubner, J. Phys. G **38**, 085003 (2011).

[87] G. Venanzoni, Journal of Physics: Conference Series **349**, 012008 (2012).

[88] R. Bluhm, V.A. Kostelecký, and C.D. Lane, Phys. Rev. Lett. **84**, 1098 (2000).

[89] M. Deile *et al.*, arXiv:hep-ex/0110044 (2001).

[90] S. Eidelman, and M. Passera, Mod. Phys. Lett. A. 22, 159 (2007).

[91] A. Pich, arXiv:hep-ph/1310.7922 (2013).

[92] K. Melnikov and A. Vainshtein, *Theory of the Muon Anomalous Magnetic Moment*, Springer, 2006.

[93] F. Jegerlehner, *The Anomalous Magnetic Moment of the Muon*, Springer, 2007.

[94] S.G. Karshenboim, Lect. Notes Phys. **745** (2008).

[95] G.W. Bennet *et al.* (Muon $(g-2)$ Collaboration), Phys. Rev. D **73**, 072003 (2006).

[96] J. Schwinger, Phys. Rev. **73**, 416 (1948).

[97] R. Bluhm, V.A. Kostelecký, and N. Russell, Phys. Rev. D. **57**, 3932 (1998).

[98] J. Bailey *et al.* (CERN-Mainz-Daresbury Collaboration), Nucl. Phys. B **150**, 1 (1979).

References

[99] Muon ($g-2$) Collaboration, The E821 Technical Design Report (1995), `http://www.g-2.bnl.gov/publications/tdr/index.html`

[100] M. Deile *et al.* (Muon ($g-2$) Collaboration), Nucl. Phys. B **116**, 215 (2003).

[101] W. Liu *et al.*, Phys. Rev. Lett. **82**, 711 (1999).

[102] M. Davier, S. Eidelman, A. Höcker, and Z. Zhang, Eur. Phys. J. C **31**, 503 (2003).

[103] K. Hagiwara, A.D. Martin, D. Nomura, and T. Teubner, Phys. Lett. B **557**, 69 (2003); Phys. Rev. D **69**, 093003 (2004).

[104] C. Amsler *et al.* (Particle Data Group), Phys. Lett. B667 (2008) 1.

[105] B.L. Roberts, Chinese Phys. C **34**, 741 (2010).

[106] P.J. Mohr, B.N. Taylor and D.B. Newell (CODATA 2006), Rev. Mod. Phys. **80**, 633 (2008).

[107] V.A. Kostelecký and N. Russell, Phys. Lett. B. **693**, 443 (2010).

[108] V.A. Kostelecký and M. Mewes, Phys. Rev. D **80**, 015020 (2009).

[109] V.A. Kostelecký and C.D. Lane, Phys. Rev. D **60**, 116010 (1999).

[110] R. Bluhm, V.A. Kostelecký, C.D. Lane, and N. Russell, Phys. Rev. Lett. **88**, 090801 (2002).

[111] R. Bluhm, V.A. Kostelecký, C.D. Lane, and N. Russell, Phys. Rev. D **68**, 125008 (2003).